



UNIVERSIDADE D
COIMBRA

Filipa Almeida Martins de Matos Gonçalves Dinis

**DEVELOPMENT OF BIOCOMPATIBLE POLYESTERS
BASED FORMULATIONS FOR MICROSTEREO-
THERMAL-LITHOGRAPHY**

**Doctoral thesis in Chemical Engineering, supervised by Professor Doctor
Jorge Fernando Jordão Coelho and Professor Doctor Paulo Jorge da Silva
Bártolo, submitted to the Chemical Engineering Department, Faculty of
Science and Technology, University of Coimbra**

Coimbra, 2021

Filipa Almeida Martins de Matos Gonçalves Dinis

Development of biocompatible polyesters based formulations for microstereo-thermal-lithography

Thesis submitted to the Faculty of Sciences and Technology of the University of Coimbra, to obtain the Degree of Doctor in Chemical Engineering

Advisors:

Prof. Dr. Jorge Fernando Jordão Coelho
Prof. Dr. Paulo Jorge da Silva Bártolo

Host institutions

University of Coimbra

Financing

Portuguese Foundation for Science and Technology (FCT)
Doctoral degree grant: BD/71113/2010

Coimbra

2021



UNIVERSIDADE DE COIMBRA



Governo da República Portuguesa



UNIÃO EUROPEIA
Fundo Social Europeu

To my family

*“Recomeça...
Se puderes
Sem angústia
E sem pressa
E os passos que deres,
Nesse caminho duro
Do futuro
Dá-os em liberdade.
Enquanto não alcances
Não descanses.
De nenhum fruto queiras só metade.”*

Miguel Torga

ACKNOWLEDGMENTS

Expresso os meus mais sinceros agradecimentos a todos aqueles que de algum modo contribuíram e me acompanharam ao longo deste percurso da minha vida.

Em primeiro lugar gostaria de agradecer ao meu orientador Professor Doutor Jorge Coelho pela oportunidade que me foi dada, pelo apoio e orientação constantes ao longo deste trabalho, mesmo nas alturas em que os resultados tardavam em aparecer!

Ao meu co-orientador Professor Doutor Paulo Bártolo, pelas reuniões produtivas e descontraídas, pelas ideias e pela partilha de conhecimento, numa altura tão fundamental para o desenvolvimento do presente trabalho.

Ao Professor Doutor Arménio Serra, por me ter acompanhado ao longo deste processo, pela sua inesgotável disponibilidade para me ensinar, pelo seu espírito crítico e discussões construtivas que resultaram muitas vezes em mudança de estratégia de trabalho e na transposição de inúmeros obstáculos.

À Ana Fonseca, pois a sua ajuda preciosa foi fundamental para o arranque deste trabalho. Pelo seu incentivo, boa disposição, pelas discussões e troca de ideias que me acompanharam até à reta final.

Um agradecimento especial ao Professor Doutor Henrique Faneca, e à sua equipa do CNC, e em especial à Rose Cordeiro, pela disponibilidade, amizade e ensaios de viabilidade celular, fundamentais para o presente trabalho.

Ao Doutor Marco Domingos e Doutor António Glória, por toda a ajuda nos ensaios de citotoxicidade e testes mecânicos.

À Professora Paula Piedade, pela sua boa disposição e pelas análises de AFM.

À Professora Graça Rasteiro, pela sua disponibilidade e por me ter fornecido as bases para poder realizar os ensaios de reologia.

Queria também deixar um agradecimento ao Professor Peter Dubruel e a sua equipa da Universidade de Ghent, pelo apoio nos ensaios de tratamento por plasma dos meus materiais.

Não poderia deixar de agradecer ao Professor Doutor Abel Ferreira, em grande parte responsável pela minha iniciação no meio académico, por todo o conhecimento e ajuda nos meus primeiros anos na investigação.

Aos meus colegas do CDRSP, Tatiana, Juliana e Rúben, por toda a ajuda e companheirismo ao longo desta minha jornada, por me ensinarem a manusear o equipamento de litografia, nomeadamente no seu processo de “montagem-desmontagem”.

A todos os meus colegas do Departamento de Engenharia Química, pelos momentos bem passados no laboratório e fora dele, pelo convívio e boa disposição, por tornarem esta caminhada muito mais fácil de percorrer.

À Fundação para a Ciência e Tecnologia pelo financiamento do presente doutoramento (SFRH / BD / 71113 / 2010).

A todos os meus amigos e em especial à Sofia e Maria, Daniel e Pedro, e aos pequenos João, Gonçalo, Mariana e afilhados Miguel e Madalena, por estarem sempre presentes, mesmo que à distância. Pela vossa amizade, boa disposição e por todas as aventuras que vivemos juntos.

Às minhas irmãs Joana e Catarina, que são sem sombra de dúvida um dos meus suportes. Mesmo à distância, estiveram sempre presentes. São e serão sempre um dos meus pilares: *“For when three sisters love each other with such sincere affection, the one does not experience sorrow, pain or affliction of any kind, but the other’s heart wishes to relieve, and vibrates in tenderness...like a well-organized musical instrument”*.

Ao Sérgio Dinis, por ter estado sempre ao meu lado, e pelo seu apoio incondicional mesmo nas alturas mais adversas. Obrigada por lavares a loiça e tomares conta dos miúdos (de vez em quando!).

Aos meus filhos Afonso, Alice e André, pelo despertar à realidade sobre o que é acima de tudo mais importante na vida.

À minha mãe Cristina. *I am because you were.*

Aos meus avós Dulce e Norberto. A vós vos devo tudo o que sou hoje.

ABSTRACT

The goal of the present PhD work was the development of new biobased unsaturated polyesters (UPs) to be applied in additive manufacturing technologies, such as microstereo-thermal-lithography (μ STLG), aiming to produce 3D scaffolds for biomedical applications. UPs are widely used in industrial fields, however their excellent thermomechanical properties and tunability make them excellent candidates for tissue engineering applications. UPs were produced by step-growth polycondensation, using several glycols and diacids of sustainable resources, such as succinic acid (SuCA) and sebacic acid (SeBA). Fumaric acid (FA) was used as the source of double bonds to promote posterior crosslinking reactions with vinylic monomers.

In a first approach, the synthesis of UPs using renewable monomers was performed. The properties of the polyesters were extensively studied, namely thermal and mechanical properties, and the final products compared with a commercial resin named Crystic 272, which has been successfully tested on μ STLG. To understand the polyesters properties, the study of the ratio between diacids and glycols as well as the type of monomers used was performed. By carefully selecting the monomers and the ratio between diacids and glycols it is possible to control the final properties of the polymers. The produced oligomers, characterized by low molecular weights and obtained from aliphatic monomers and natural based diacids, showed high thermal stability, with T_{on} higher than 330 °C. Thermal stability remains constant even with the replacement of isophthalic acid by aliphatic diacids. To achieve the proper viscosity to be applied in μ STLG experiments, 2-hydroxyethyl methacrylate (HEMA) and styrene (St) were used as the crosslinking agents. The results were very promising, with the production of two layered scaffolds based on bio resins. Preliminary cell viability tests showed that the synthesized polyesters are biocompatible.

The choice of the crosslinking agent also plays a determinant role in the properties of the final unsaturated polyester resins (UPRs). Although St is one of the most used unsaturated monomer (UM) to promote the formation of 3D networks, a more friendly UM is desired. Therefore, the prepared biobased UPs were crosslinked with different vinylic monomers, such as HEMA and *N*-vinyl-2-pyrrolidinone (NVP). Since the final viscosity of the formulations is a crucial parameter, determining the applicability on the μ STLG, the viscosity of the formulations was measured and HEMA was selected as the proper monomer due to its low viscosity and biocompatible character. Photo and thermal polymerization studies were performed to evaluate the properties of the final biobased UPRs. The thermal crosslinked polyesters showed low gel content with variable water contact angles (WCA) with hydrophilic character.

Morphology and roughness of the polymers were also studied since these parameters strongly influence the cell adhesion. Posteriorly, a full characterization of the UPRs, cytotoxicity and cell adhesion tests were performed. After 48 h of incubation, for the μ STLG UPRs, 50-60% of the cells were viable, but both thermal and μ STLG scaffolds presented high levels of acidity.

Alongside with the synthesis and processing of the polyesters, new formulations were tested. Due to the low incorporation of the diacids observed in the previous formulations, new syntheses were performed in two distinct steps, which also resulted in a reduction of the time of the polycondensation reaction. The formulations based on SuCA, diethylene glycol (DEG) and other renewable sources (UP7 to UP11s formulations) were prepared in a two-step bulk polycondensation reaction. Glutaric acid (GA) and isosorbide (IS) were some of the chosen renewable sources for the development of the new UPs formulations. Afterwards, the UPs were crosslinked with HEMA. Overall, the developed formulation showed better reaction times, and had the desired properties for the intended final application. GA also proved to be an interesting diacid to be used in the preparation of new UPs for biomedical areas, with high water solubility, high thermal stability and low T_g .

Several problems arise concerning the viability of the materials regarding their use in the biomedical field. The UPs showed surface acidity and to overcome this issue, several strategies were attempted to eliminate the scaffolds acidity. Reflux treatment with ethanol and oxygen plasma were some of the protocols used to change the polyesters surface. The simplest technique, reflux with ethanol, demonstrated to be adequate in the elimination of surface acidity. Results obtained from plasma treatments suggested that they are not effective to solve the acidity problem and enhance biocompatible character of the polyesters. The μ STLG scaffolds Scf6 and Scf7, based on formulations UP6 and UP7, respectively, were subjected to reflux and showed cell viabilities around 100% after 48 h.

The use of renewable sources to obtain fully biobased UPs was accomplished within this PhD work, and the final materials reveal to be strong candidates to be used in the fabrication of 3D scaffolds by μ STLG. The materials exhibit low viscosity, good thermo-mechanical properties, similar to commercial products, high hydrophilicity and cell viability. Ultimately, these polymers can bring new advances and opportunities for the use of these unsaturated polyesters in the preparation of tailored scaffolds for specific uses.

RESUMO

O objetivo do presente trabalho de doutoramento consistiu no desenvolvimento de poliésteres insaturados para aplicação em técnicas de prototipagem rápida, nomeadamente em microestereo-termo-litografia (μ STLG). Os materiais desenvolvidos são deste modo processados tendo em vista o desenvolvimento de scaffolds para aplicações biomédicas.

Os poliésteres insaturados, regra geral, são extensivamente utilizados em aplicações industriais, contudo as suas propriedades revelam-se de extrema utilidade em áreas como a engenharia de tecidos. A possibilidade de manipular as propriedades destes materiais consoante a aplicação final pretendida torna-os bastante atrativos para o desenvolvimento de scaffolds. Os poliésteres insaturados foram obtidos por policondensação de massa, tendo sido utilizados vários glicóis e diácidos de base natural, tais como o ácido succínico (SuCA) e sebácico (SeBA). O ácido fumárico (FA) foi usado em todas as reações desenvolvidas como a fonte de ligações duplas, de modo a promover a posterior reticulação com monómeros vinílicos.

Numa primeira abordagem, a síntese de poliésteres insaturados tendo como materiais de partida monómeros de base natural foi executada. O estudo das propriedades destes poliésteres foi realizado, nomeadamente no que diz respeito às suas propriedades térmicas e mecânicas, e os produtos comparados com uma resina comercial, Crystic 272, previamente testada, com sucesso, no equipamento de μ STLG. O estudo das propriedades dos poliésteres, a razão entre diácidos e glicóis bem como o tipo de monómeros usados foi fundamental para a compreensão das características dos poliésteres. Uma seleção cuidada dos monómeros e da razão entre diácidos e dióis permite controlar a estrutura final dos polímeros. Os oligómeros obtidos, de baixos pesos moleculares, com base em monómeros alifáticos e diácidos de base natural, mostraram elevada estabilidade térmica, com T_{on} superiores a 330 °C. A substituição do ácido isoftálico, presente na resina comercial, por ácidos alifáticos, não resultou na perda de estabilidade térmica. Os materiais obtidos foram processados por μ STLG, usando 2-hidroxietil metacrilato (HEMA) e estireno (St) como agentes reticulantes, conferindo assim uma viscosidade adequada ao processamento dos scaffolds. Os resultados foram bastante promissores, tendo-se fabricado scaffolds constituídos por duas camadas de resina de carácter bio. Resultados preliminares de viabilidade celular revelaram que os poliésteres sintetizados não apresentaram citotoxicidade.

A escolha dos agentes de reticulação determina em grande parte as propriedades finais dos poliésteres insaturados reticulados (UPRs). Embora o St seja dos monómeros insaturados

(UMs) mais utilizados para a formação de redes reticuladas 3D, a sua substituição por um composto de carácter bio é desejável. Por conseguinte, os poliésteres insaturados foram posteriormente reticulados com diferentes monómeros vinílicos, tais como o HEMA e N-Vinil-2-pirrolidona (NVP). Uma vez que a viscosidade final das formulações é um parâmetro crucial para a sua aplicação na μ STLG, as viscosidades das formulações desenvolvidas foram determinadas, tendo-se selecionado o HEMA devido à baixa viscosidade conferida ao poliéster, bem como ao seu carácter biocompatível. Estudos de foto reticulação e reticulação térmica foram desenvolvidos de modo a avaliar as propriedades finais das resinas de carácter bio. Os poliésteres reticulados termicamente revelaram baixo teor gel, com ângulos de contacto variáveis, apresentando na sua maioria um carácter hidrofílico. A morfologia das resinas, bem como a determinação da rugosidade, foram analisadas, uma vez que estes parâmetros influenciam a adesão das células na superfície polimérica. Após uma completa caracterização das resinas de poliéster insaturado, testes de citotoxicidade e de adesão celular foram realizados. As amostras preparadas por μ STLG demonstraram viabilidades na ordem dos 50-60% após 48 horas, tendo-se, no entanto, comprovado a acidez dos materiais, tanto dos scaffolds processados por μ STLG como dos UPs preparados por reticulação térmica.

Em paralelo à síntese e processamento dos poliésteres, a otimização do processo de policondensação de massa foi efetuada. Tendo-se registado anteriormente a baixa incorporação dos ácidos, as sínteses foram realizadas em dois passos distintos, verificando-se a diminuição do tempo de reação de policondensação. As formulações desenvolvidas à base de SuCA, dietilenoglicol (DEG) e outras fontes de origem renovável (formulações UP7 a UP11s) foram preparadas por policondensação em massa. O ácido glutárico (GA) e o isosorbide (IS) foram algumas das matérias-primas de fontes renováveis selecionadas para a síntese das novas formulações que, posteriormente, foram reticulados com HEMA. De um modo geral, verificou-se que as novas formulações possuíam as propriedades desejadas tendo em vista a aplicação final pretendida. O GA mostrou ser um diácido interessante para ser usado na preparação de novos UPs para aplicação biomédica, apresentando elevada solubilidade, estabilidade térmica e baixo T_g .

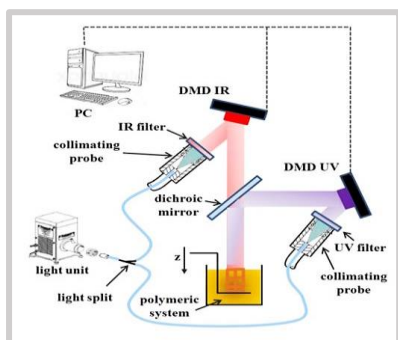
Vários problemas surgiram no que diz respeito à viabilidade dos materiais para aplicação biomédica. A maioria dos UPs sintetizados apresentava uma acidez elevada, que em última instância daria origem à morte celular. De modo a contornar esta limitação, uma série de tratamentos foram efetuados, com o intuito de remover a acidez da superfície dos scaffolds. Tratamento por refluxo com etanol e tratamento por plasma com oxigénio, foram algumas das estratégias usadas para modificação da superfície dos poliésteres. O tratamento mais simples, por refluxo, revelou-se extremamente eficaz na eliminação da acidez dos UPs. Ao

passo que o tratamento por plasma não foi eficiente para resolver o problema da acidez. Os materiais processados por μ STLG, Scf6 e Scf7, tratados com refluxo de etanol por 3 h, demonstraram viabilidades superiores a 100 % após 48 h.

O desenvolvimento de UPs e UPRs à base de matérias-primas renováveis foi realizado com sucesso, tendo sido demonstrado que são excelentes candidatos para a fabricação de scaffolds tridimensionais por μ STLG. Propriedades tais como baixa viscosidade, performance térmica e mecânica semelhantes às exibidas pelos produtos comerciais, elevada hidrofiliabilidade, viabilidade e adesão celular caracterizam os polímeros obtidos, reforçando a sua potencialidade em áreas como a engenharia de tecidos.

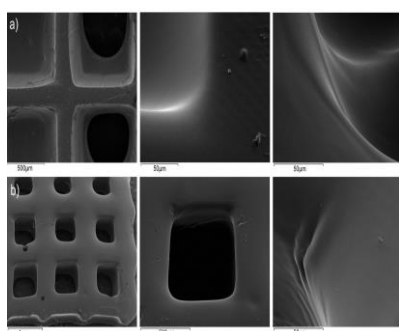
THESIS LAYOUT

Chapter I – The Potential of Unsaturated Polyesters in Biomedicine and Tissue Engineering: Synthesis, Structure-Properties Relationships and Additive Manufacturing



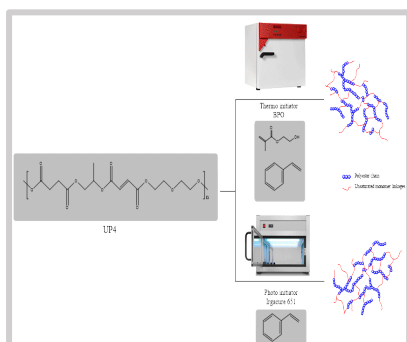
This PhD thesis focuses the development of polymeric materials suitable to be used in microstereo-thermal-lithography (μ STLG). An overview of the potential of unsaturated polyesters (UPs) and unsaturated polyester resins (UPRs), their growing development into biomedical fields and some highlights about AM technologies and applications is herein presented.

Chapter II – 3D Printing of New Biobased Unsaturated Polyesters by Microstereo-thermal-lithography



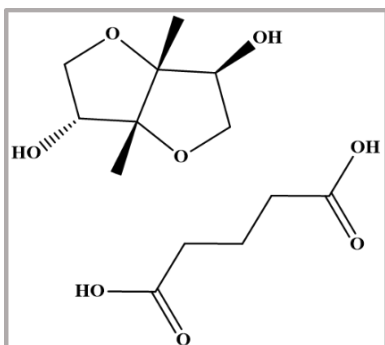
The synthesis of new biobased UPs aiming to mimic some of the properties of a commercial product are described in this chapter. New biobased UPs were prepared by bulk polycondensation and posteriorly accurate 3D scaffolds were produced by μ STLG. The new 3D scaffolds proved to be biocompatible and suitable for AM technologies.

Chapter III – Novel Biobased Unsaturated Polyester Resins prepared by Thermal crosslinking and μ STLG



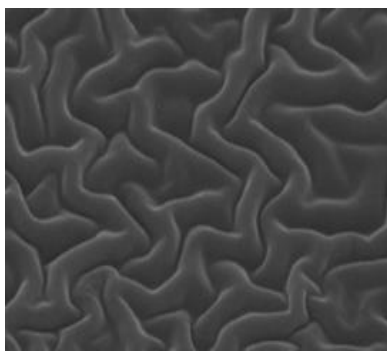
The crosslinking studies of the new biobased UPs are discussed in this chapter. The morphology, topography, swelling behavior and contact angles of the final structures were analyzed, along with the evaluation of their cell viabilities. The materials processed by μ STLG presented higher cellular viability when compared with the thermally crosslinked UPs. The impact of the crosslinking strategy in the final properties of the materials is also discussed.

Chapter IV – Fully Biobased Unsaturated Polyesters from Renewable Resources: Synthesis, Characterization and HEMA Crosslinking



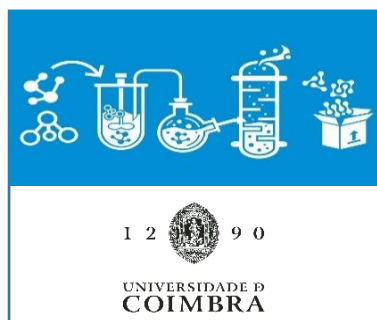
New synthesis on fully biobased UPs were performed *via* bulk polycondensation with the purpose of enhance the properties of the UPRs. For that purpose, different diacids (glutaric acid) and diols (isosorbide) were used. The new formulations were fully characterized and crosslinked with HEMA. The thermal and mechanical properties of UPs and UPRs were determined, validating the potential of these renewable polyester's resins.

Chapter V – A Preliminary Study: Strategies to Improve the Biological Performance of μ STLG Scaffolds



Chapter V describes some of important problems faced in the development of the biocompatible UPRs, *e.g.*, acidity of the final resins. To overcome such issue, several approaches were tested, from simple reflux treatments to O₂ plasma surface modifications. Concerning the reduction of the acid character of the polymeric structures, EtOH reflux exhibited the best results, followed by O₂ plasma treatment.

Chapter VI – Concluding Remarks



A critical evaluation of the work performed, highlighting the strengths, weaknesses alongside with some recommendations for further research lines is herein presented.

LIST OF ACRONYMS

AA	adipic acid
AcA	acrylic acid
AESO	acrylated epoxidized soybean oil
AFM	atomic force microscopy
AIBN	α,α' -azoisobutyronitrile
AM	additive manufacturing
ATR-FTIR	Attenuated Total Reflectance-Fourier Transform Infrared Spectroscopy
AV	acid value
BM	4,4-bismaleimidodiphenylmethane
BMP	butyl-3-mercapto propionate
BPO	benzoyl peroxide
BOD	biochemical oxygen demand
CA	<i>Candida Antarctica</i>
CAD	computer-aided design
CALB	Lipase B from <i>Candida Antarctica</i>
CAM	computer aided manufacturing
CDM	1,4-cyclohexanedimethanol
CDRSP	Centre for Rapid and Sustainable Product Development
CHD	cyclohexanediol
CHDM	1,4-cyclohexanedimethanol
CTNB	carboxy terminated nitrile rubber
CQ	camphorquinone
DACC	3,4-diacetoxycinnamoyl chloride
DAHs	dianhydrohexitols
DCC	dicyclohexylcarbodiimide
DEG	diethylene glycol
DHCA	3,4-dihydroxycinnamic acid
DHO	6,7-dihydro-2(5H)-oxepinone
DMAMEA	dimethylamino methyl ethylacrylate
DMAP	dimethylaminopyridine
DMD	2,2-dimethyl-1,3-propanediol
DMEM	Dulbecco's modified Eagle's medium
DMEM-HG	Dulbecco's modified Eagle's medium-high glucose

DMF	dimethylformamide
DMI	dimethyl itaconate
DMTA	dynamic mechanical thermal analysis
DN	double network
DSC	differential scanning calorimetry
EDAC	1-ethyl-3-(3-dimethylaminopropyl) carbodiimide hydrochloride
EG	ethylene glycol
EO	ethylene oxide
EtOH	ethanol
EVA	ethylene vinyl acetate
FA	fumaric acid
FAME	fatty acid methyl ester
FBS	fetal bovine serum
FU	diethyl fumarate
FUPR	fluorinated modified unsaturated polyester resin
GA	glutaric acid
GFP	green fluorescence protein
GL	diethyl <i>trans</i> -glutaconate
GI	globalide
GPC	gel permeation chromatography
HA	hyaluronic acid
HDA	10-hydroxycaproic acid
HDI	6-hexamethylene diisocyanate
HDT	heat deflection temperature
HEMA	2-hydroxyethyl methacrylate
hFOB1.19	human fetal osteoblasts cell line
HMA	<i>trans</i> - β -hydromuconic acid
HM	diethyl <i>trans</i> - β -hydromuconate
HPR	hydroxyl-ended hyperbranched polyester resin
HTNR	hydroxyl terminated natural rubber
HTPB	hydroxyl terminated polybutadiene
IA	isophthalic acid
ITA	itaconic acid
IFM	infinite focus microscopy
IM	isomannide
IS	isosorbide

IT	diethyl itaconate
MA	maleic anhydride
MALDI-TOF	matrix-assisted laser desorption/ionization – time of flight
mCPBA	m-chloroperbenzoic acid
MEKP	methyl ethyl ketone peroxide
MES	2-(<i>N</i> -morpholino) ethanesulfonic acid sodium salt
MH	6-mercapto-1-hexanol
MM	<i>Mucor miehei</i>
MMA	methyl methacrylate
MPD	2-methyl-1,3-propanediol
MPDO	2-methyl-1,5-pentanediol
nACA	<i>N</i> -acetylcysteamine
NMR	nuclear magnetic spectroscopy
NPG	neopentylglycol
NVP	<i>N</i> -vinylpyrrolidone
OMIS	oligo(isosorbide maleate)
PBF	poly(butylene fumarate)
PBS	phosphate buffered saline solution
PBSI	poly(butylene succinate-co-itaconate)
PC	<i>Pseudomonas cepacia</i>
PCL	poly(ϵ -caprolactone)
PCLF	poly(ϵ -caprolactone-co-fumarate)
PCL-PFPE-PCL	poly(ϵ -caprolactone)-perfluoropolyether- poly(ϵ -caprolactone)
PD	1,2-propanediol
PEFS	poly(ethylene fumarate-co-sebacate)
PEG	poly(ethylene glycol)
PEGF	poly(ethylene glycol-co-fumarate)
PEGF-co-PHMCF	poly(ethylene glycol fumarate-co-hexamethylene carbonate- fumarate)
PET	poly(ethylene terephthalate)
P(FA-GLY-BA)	poly(fumaric acid-glycol-brassylic acid)
P(FA-GLY-DDDA)	poly(fumaric acid-glycol-dodecanedioic acid)
P(FA-GLY-PA)	poly(fumaric acid-glycol-pentadecanedioic acid)
P(FA-GLY-SA)	poly(fumaric acid-glycol-sebacic acid)
P(FA-GLY-TA)	poly(fumaric acid-glycol-tetradecanedioic acid)
PG	propylene glycol
PGA	poly(glycolic acid)
PGI	polyglobalide

PhA	phthalic anhydride
PHEMA	poly(2-hydroxyethyl methacrylate)
PHFS	poly(hydroquinone fumarate- <i>co</i> -sebacate)
PHMCA	poly(hexamethylene carbonate) diacrylate
PHV	poly(hydroxy valerate)
PHMCF	poly(hexamethylene carbonate-fumarate)
PRFS	poly(resorcinol fumarate- <i>co</i> -sebacate)
PLA	poly(lactic acid)
PLLA	poly(L-lactic acid)
PLGA	poly(lactic- <i>co</i> -glycolic acid)
P(MA-GLY-SA)	poly(maleic anhydride-glycol-sebacic acid)
PMMA	poly(methyl methacrylate)
PO	propylene oxide
PPF	polypropylene fumarate
PPFS	poly(propylene fumarate- <i>co</i> -sebacate)
PPS	poly(1,2-propylene succinate)
PSAGE	poly(3-allyloxy-1,2-propylene succinate)
PTSA	<i>p</i> -toluenesulfonic acid monohydrate
PVA	polyvinyl acetate
PU	polyurethane
RP	rapid prototyping
ROP	ring opening polymerization
SuCA	succinic acid
SeBA	sebacic acid
SEC	size exclusion chromatography
SEM	scanning electron microscopy
SLA	stereolithography
SN	single network
Sorb	Sorbitol
SPD	(<i>S</i>)-(+)-1,2-propanediol
SRB	sulforhodamine B colorimetric assay
St	styrene
TC	tamoxifen citrate
TDI	toluene diisocyanate
TE	tissue engineering
TEG	triethylene glycol
TFE	2,2,2-trifluoroethanol

TGA	thermogravimetric analysis
THF	tetrahydrofuran
THPA	cyclohex-4-ene-dicarboxylic anhydride
TMP	trimethylolpropane
TMPTA	trimethylolpropane triacrylate
TMS	tetramethylsilane
TPA	terephthalic acid
UM	unsaturated monomer
UPs	unsaturated polyesters
UPHR	unsaturated hyperbranched polyester resin
UPRs	unsaturated polyester resins
WCA	water contact angles
ϵ -CL	ϵ -caprolactone
μ STLG	microstereo-thermal-lithography
1,3PG	1,3-propanediol

NOMENCLATURE

\bar{D}	Polydispersity
E	Modulus of Elasticity or Young's Modulus (Pa)
E'	Elastic Modulus
E''	Loss Modulus
M_n	Number-Average Molecular Weight ($\text{g}\cdot\text{mol}^{-1}$)
M_w	Weight-Average Molecular Weight ($\text{g}\cdot\text{mol}^{-1}$)
R_a	Arithmetic average of the roughness profile
S_a	Arithmetic average of 3D roughness
T_{on}	Onset Temperature ($^{\circ}\text{C}$)
T_g	Glass Transition Temperature ($^{\circ}\text{C}$)
T_m	Melting Temperature ($^{\circ}\text{C}$)
$T_{5\%}$	Temperature for 5% of Mass Loss ($^{\circ}\text{C}$)
$T_{10\%}$	Temperature for 10% of Mass Loss ($^{\circ}\text{C}$)
α, β, γ	Thermal Transitions
σ	Stress (Pa)
ε	Strain (mm)
η	Viscosity ($\text{Pa}\cdot\text{s}$)

Table of Contents

Acknowledgments.....	IX
Abstract	XI
Resumo	XIII
Thesis Layout	XVII
List of Acronyms	XIX
Nomenclature	XXV
Table of Contents.....	XXVII
List of Figures	XXIX
List of Tables	XXXV
Motivations, research significance and impact	XXXVII
Chapter I	1
Chapter II	65
Chapter III	95
Chapter IV.....	119
Chapter V	149
Chapter VI.....	175

LIST OF FIGURES

CHAPTER I

Figure 1. Path for the development of UPRs: (A) Polycondensation reaction, and (B) cure reaction.	5
Figure 2. A) Schematic diagram showing the possible reactions in the styrene-unsaturated polyester copolymerization. B) Formation of microgel particles through the growth of free radicals: (I) growth of free radicals; (II) formation of microgel particles.	6
Figure 3. Structures of the crosslinkers: (A) styrene, (B) BM, and (C) BM-styrene.	9
Figure 4. Monomers used for the preparation of durene based polyesters (A), and structure of the UPs (B).....	11
Figure 5. UPs synthesis through interfacial polycondensation technique.....	12
Figure 6. Scheme of preparation in two steps of amine glycol modifiers for UP resin, i.e. 3,6-diaza-3,6-diphenyloctane-1,8-diol (R=-(CH ₂) ₂ -; R ₁ =-H), 4,7-diaza-4,7-diphenyldecane-2,9-diol (R=-(CH ₂) ₂ -; R ₁ =-CH ₃) and 3,10-diaza-3,10-diphenyldodecane-1,12-diol (R=-(CH ₂) ₆ -; R ₁ =-H).	14
Figure 7. Structures of the amine glycols bearing s-triazine rings: (A) 2-[N,N-bis(2-hydroxyethyl)amine]-4,6-dimethoxy-1,3,5-triazine; (B) 2,4-[N,N-bis(2-hydroxyethyl)amine]-6-methoxy-1,3,5-triazine; (C) 2,4,6-tris[N,N-bis(2-hydroxyethyl)amine]-1,3,5-triazine; (D) 2-[N-phenyl-(2-hydroxyethyl)amine]-4,6-dimethoxy-1,3,5-triazine; (E) 2,4-bis[N-phenyl-(2-hydroxyethyl)amine]-6-methoxy-1,3,5-triazine; and (F) 2,4,6-tris[N-phenyl-(2-hydroxyethyl)amine]-1,3,5-triazine.	14
Figure 8. Polyesterification of the monohydroxyethyl esters of maleic acids with boric acid-pyridine mixture as mild catalyst.....	15
Figure 9. ROP of DHO to give the poly(DHO).....	15
Figure 10. Metal-mediated reaction of UP via functionalization of maleic or fumaric diesters, followed by oxidative homo-coupling of the introduced alkyne moieties.....	16
Figure 11. Crosslinking reaction between the UP and a polynitrone, leading to a 3D network.	17
Figure 12. Structures of: (A) unsaturated oligoester; and (B) unsaturated epoxyoligoester, using EG as the diol.....	17
Figure 13. Chain extension reaction of PPS-diol and PBF-diol mediated by HDI.	18
Figure 14. Synthesis of HMA homopolymers, HMA-adipic acid copolymers and of HMA and diethylene glycol poly(ester ether)s.	20
Figure 15. Structures of the synthesized diesters, diethyl adipate, diethyl fumarate, diethyl itaconate, diethyl trans-glutaconate and diethyl trans- β -hydromuconate used for further transesterification reaction with isosorbide or isomannide.	20
Figure 16. Preparation of the UPs by the two-step solution polycondensation.	21
Figure 17. Structures of the N-alkylated dinitrones based on IS.....	23
Figure 18. Scheme of the synthesis of poly (DHCA-HDA) and photoreaction of the DHCA moiety promoted by UV irradiation.	24
Figure 19. Photoreaction scheme of DACA-PLLA by UV irradiation at $\lambda > 280$ nm.	24
Figure 20. Structure of the fluorescent dye.	25

Figure 21. ROP of globalide and thiol-ene reaction of PGI with MH, BMP and nACA.	26
Figure 22. Structures of the derivatives prepared using Michael addition reactions.	27
Figure 23. Polymer-functionalization via ruthenium-catalyzed olefin-metathesis (A), and via thiol-ene addition reaction (B).	28
Figure 24. Representation of the SN (A), and of the DN (B).	29
Figure 25. Alcoholysis reaction to yield a polyol based on vegetable oils.	30
Figure 26. Reaction of PEG with fumaric acid in the presence of DMAP/DCC.	33
Figure 27. Synthesis of: (A) PCLF, PEGF, and (B) PEGF-co-PCLF.	33
Figure 28. Synthesis of: (A) PHMCF macromers, and (B) respective networks.	35
Figure 29. Branched polyesters obtained by thermal polyesterification (A) and the photocurable polymer achieved by enzymatic polymerization (B) using CALB as catalyst.	36
Figure 30. (A) Unsaturated dicarboxylic monomers synthesized for the preparation of new unsaturated aliphatic polyesters, (B) overall strategy for the synthesis of polyesters, and (C) synthesis strategy for polyester thermoset elastomer.	37
Figure 31. Illustration of the four main steps in scaffold-based TE strategy. 1) Cell harvesting and in vitro expansion; 2) cell seeding in porous scaffolds; 3) in vitro dynamic cell culture using bioreactors; 4) scaffold+cell construct implantation.	38
Figure 32. Schematic representation of the main steps required to produce TE scaffolds using AM techniques.	40
Figure 33. 3D CAD and physical models produced via melt extrusion. (A) 3D CAD model of breast implant; (B) 3D CAD model of humerus bone; (C) 3D CAD model of human ear; (D) 3D physical model of breast implant; (E) 3D physical model of humerus bone; (F) 3D physical model of human ear. ...	41
Figure 34. Constructs with embedded cells. (A) PEG-co-PDP copolymer hydrogels with HUVECs encapsulated cells prepared via stereolithography (SLA). (B) gelatin/alginate/fibrinogen containing adipose-derived stem cells (in pink) and hepatocytes in gelatin/alginate/chitosan (white).	42
Figure 35. Methodology for indirect fabrication of TE scaffolds.	42
Figure 36. Conventional stereolithography: Mask-based method (A); Direct or laser writing method (B).	43
Figure 37. Schematic representation of SLA system.	44
Figure 38. Schematic illustration of the SLA process to produce micrometric resolution constructs containing cells.	45
Figure 39. Schematic illustration of the fabrication method used to create patterns of acryl-fibronectin on PEGDA hydrogels produced by SLA.	46
Figure 40. Integral micro-SLA system developed by CDRSP researchers.	47
Figure 41. PHEMA 3D scaffold produced via SLA.	47
Figure 42. Structures of the UPs developed by Gonçalves and co-workers that were used in the development of scaffolds by micro-SLA.	48
Figure 43. SEM pictures of the scaffolds obtained by micro-SLA a) scaffolds based on UP5/St, with different curing times and b) scaffold based on UP4/HEMA formulation.	48
Figure 44. Irradiation process in stereo-thermal-lithography.	49

Figure 45. Schematic representation of the stereo-thermal-lithographic process with rotating multi-vat system which allows the production of multi-material constructs.	50
Figure 46. A typical setup for multi-photon polymerization.	51
Figure 47. Typical set-up for nano-stereolithographic process.	51

CHAPTER II

Scheme 1. Schematic illustration of the relationship between the polycondensation of bio products and the AM technologies in Tissue Engineering.....	69
Figure 1. Monomers structure used in the synthesis of the unsaturated polyesters.....	73
Figure 2. Rheological behavior of the UPs in styrene (37%) (A) and the biobased UPs after 6 months (B).....	75
Figure 3. ATR-FTIR spectra for a) UP1 to UP3 and b) UP4 to UP6.	76
Figure 4. ¹ H NMR spectra of unsaturated polyesters based on isophthalic acid, UP1 to UP3, where (s) correspond to the solvent peaks of THF- d8.....	77
Figure 5. ¹ H NMR spectra of UP4 to UP6, where (s) correspond to the solvent peaks of THF- d8. .	78
Figure 6. MALDI-TOF-MS in the linear mode (using DHB as matrix) of UP5 from m/z 400 to 1600 and the different observed populations from A to E.....	79
Figure 7. A. TG curves of the synthesized UPs obtained at a heating rate of 10°C·min ⁻¹ and B. detailed view within the mass loss range up to 10%.	81
Figure 8. Loss function (tanδ) versus temperature for the synthesized UPs.	82
Figure 9. Effect of different UPR on cell viability. The statistical analysis (one-way ANOVA) indicates that there is not a significant difference between the different conditions.	84
Figure 10. SEM pictures of the scaffolds obtained by μSTLG a) Scf5 based on UP5/Styrene, with different curing times and b) Scf4, based on UP4/HEMA formulation.	85
Figure 11. IFM images of 3D scaffolds: A. Scf4/HEMA (60 seconds, 1 layer), B. Scf5/HEMA (28.5 seconds, 2 layers) and C. Scf6/HEMA (28.5 sec, 1 layer).....	85
Figure S1. ATR-FTIR spectra for the developed UPs.....	90
Figure S2. ATR-FTIR spectra of UP4 and respective diacid monomers.	90
Figure S3. ATR-FTIR spectra of UP4 and respective glycol monomers.	91
Figure S4. MDSC curves for the developed UPs. The polymers were tested in the temperature range -90 to 50 °C.	91

CHAPTER III

- Figure 1.** Viscosity *versus* shear rate for the UP4, UP5 and UP6 formulations using A. AcA, B. NVP and C. HEMA as the UMs. 102
- Figure 2.** Dynamic water contact angles of UPRs crosslinked with HEMA determined by the sessile drop method and respective standard deviations. 104
- Figure 3.** TG curves obtained at a heating rate of $10^{\circ}\text{C}\cdot\text{min}^{-1}$ of the UPRs thermal crosslinked with BPO 1% (w/w), using 37% (w/w) of HEMA. 105
- Figure 4.** E' and $\tan \delta$ traces for biobased UPRs at 1 Hz. 106
- Figure 5.** Scanning electron micrographs using microscopy (MEV)/EDS, JEOL, model JSM-5310, at an accelerating voltage of 10 kV of UPR4 (A), UPR5 (B) and UPR6 (C) photo-crosslinked with HEMA (37 % (w/w)) in the μSTLG . The magnifications used were 2000x for A, 200x for B and 200x for C. 108
- Figure 6.** AFM images of UPRs thermally crosslinked with HEMA (37 % w/w). The images at the left correspond to the phase image while the images at our right are topographic images. 109
- Figure 7.** Effect of thermal and photo crosslinked materials on 3T3-L1 cell viability. The data are expressed as percentage of cell viability with respect to the control corresponding to untreated cells (mean \pm SD, obtained from triplicates). The results are representative of at least three independent experiments. The statistical analysis (one-way ANOVA) indicates that there is not a significant difference between the different conditions. 111

CHAPTER IV

- Figure 1.A.** Chemical structure of the new diacid and glycol used in bulk polycondensation reactions and B. Synthesis of isosorbide from starch..... 122
- Figure 2.** Chemical structure of the synthesized bio unsaturated polyesters UP7 to UP11s. 128
- Figure 3.** ATR-FTIR spectra of the synthesized UPs. 128
- Figure 4.** ^1H NMR spectra of the biobased UP7 and UP8, where (s) correspond to the solvent peaks of THF- d_8 129
- Figure 5.** ^1H NMR spectra of UP9.1 and UP10, where (s) correspond to the solvent peaks of THF- d_8 130
- Figure 6.** ^1H NMR spectra of UP11.1 where (s) correspond to the solvent peaks of THF- d_8 131
- Figure 7.** MALDI-TOF-MS in the linear mode (using DHB as matrix) of A. UP7 and B. UP8, from m/z 400 to 1600. For UP7, the black values identify the (SA+DEG+FA-2*H₂O) n formulation, the red values correspond to formulation (SA) n + (DEG) p+ (FA) m – (H₂O) y, the blue values for (SA) n + (DEG) p – (H₂O) y and green values for (FA) m + (DEG) p – (H₂O) y. For UP8, the black values identify the (GA+DEG+FA-2*H₂O) n formulation, the red values correspond to formulation (GA) n + (DEG) p+ (FA) m – (H₂O) y, the blue values for (GA + DEG - H₂O) n, green values for (GA) n + (DEG) p – (H₂O) y and orange values for (FA) m + (DEG) p – (H₂O) y. 132
- Figure 8.** Thermal gravimetric curves of the synthesized UPs, with a heating rate of $5^{\circ}\text{C}\cdot\text{min}^{-1}$, in the range of 25°C to 600°C 135

Figure 9. Dynamic water contact angles of UPRs crosslinked with HEMA determined by the sessile drop method and respective standard deviations.	138
Figure 10. Thermogravimetric curves and respective derivatives of the selected bio UPRs crosslinked with HEMA.....	139
Figure 11. DMTA traces of the selected biobased UPRs in terms of E' and $\tan \delta$	140
Figure 12. Pictures of biobased UPR8/HEMA and its flexible behavior.	141
Figure S1. ^1H NMR spectrum of biobased UP9.2, where (s) correspond to the solvent peaks of THF-d ₈	146
Figure S2. ^1H NMR spectrum of biobased UP11.2 where (s) correspond to the solvent peaks of THF-d ₈	146
Figure S3. Loss function ($\tan\delta$) versus temperature for the synthesized bio-UPs.....	147
Figure S4. DSC curves from the second heating cycle, for the developed bio-UPs. The polymers were tested in the temperature range -80 to 50 °C.....	147

CHAPTER V

Scheme 1. Generic scheme of biological surface modification.....	151
Scheme 2. Schematic representation of the electrospinning apparatus used in the present work. A power supply, a syringe pump and a collector plate constitute the equipment.	154
Figure 1.A. The μSTLG scaffolds used in the SRB assay. B. Images of the scaffolds incubated with cells after SRB assay.	157
Figure 2. Scanning electron micrographs of the scaffolds Scf6 and Scf7 before (A) and after (B and C) immersion in DMEM medium, using microscopy (MEV)/EDS, JEOL, model JSM-5310, at an accelerating voltage of 10 kV. The magnifications used were 2000x for the controls (A, A'); for scaffolds Scf6, 35x (B) and 2000x (C); and for Scf7, 350x (B') and 2000x (C').....	158
Figure 3. Screening of Scf6 and Scf7 and respective changes on pH medium after A. Reflux with EtOH and B. Lysine-ethyl-ester treatment, after 24 h and 48 h.	160
Figure 4. Scanning electron micrographs of the 3D scaffolds, with electrospun fibers of gelatin type A (7.5% w/v, in TFE), B (7.5% w/v, TFE) and HA (1.5% w/v, DMF/H ₂ O) at the surface. The magnifications used for the Scf5 modified with gelatin B were 35x, 500x and 1000x; for the modification with gelatin A, 35x, 1000x and 5000x and for Scf5 with HA fibers, 50x, 500x and 1000x.	162
Figure 5. Screening of Scf6 and Scf7 covered with gelatin type B fibers and respective changes on pH medium.	163
Figure 6. Scanning electron micrographs for the processed Scf6 and Scf7 before (control, A and E) (with magnifications of 15000x) and after modification by O ₂ plasma and posterior grafting with styrene (magnifications of 1000x (B, F), 2000x (C, G) and 15000x (D, H)).....	163
Figure 7. Screening of Scf6 and Scf7 and respective changes on pH medium after O ₂ plasma treatment after A. 24 h and B. 48 h.	164
Scheme 3. Schematic representation of the strategies followed for the reduction of acidity of the scaffolds and some preliminary results obtained. These preliminary assays were based on surface	

modifications by EtOH reflux, O₂ plasma and electrospinning. The modified scaffolds were placed into a 48-well plate with 300 µL per well of the cell culture medium and their acidity was visually evaluated at 24 h and 48 h by change of cell culture medium color. Scanning electron micrographs of some of the modification used are also displayed. 165

Figure 8. A. Differences in the cell culture medium colour after 24 h of incubation with different scaffolds. **B.** Effect of different 3D scaffolds on 3T3-L1 cell viability. The data are expressed as percentage of cell viability with respect to the control corresponding to untreated cells (mean ± SD, obtained from triplicates). The results are representative of at least three independent experiments. The statistical analysis (one-way ANOVA) indicates that there is not a significant difference between the different conditions. 166

Figure 9. Photo activated localization microscopy images of 3T3-L1 cells on the top of the scaffolds. Cells in absence of any material were used as control (**A**) and cell adhesion was detected on Scf6 (HEMA) surface (**B**). Images were captured by microscopy PALM MicroBeam equipment (Zeiss, Göttingen, Germany) with LD Plan-Neofluar 40x/0.6 Korr objective at excitation wavelength of 395 nm for GFP (green). 167

Figure S1. Scanning electron micrographs of the 3D scaffolds, with electrospun fibers of gelatin type B (7.5% w/v, TFE) at the surface. The magnifications used with gelatin B were 2000x and 5000x. .. 171

Figure S2. Scanning electron micrographs for the processed Scf6 and Scf7 after modification by O₂ plasma and posterior grafting with styrene (magnifications of 1500x (A), 5000x (B) and 15000x (C, D) for treated Scf6 and Scf. 171

Figure S3. Fluorescence microscopy images of 3T3-L1 fibroblast cells on the biobased UPR6 (HEMA) discs (B) by fluorescence microscopy. Cells in absence of any material were used as control (A). Cell nuclei were stained by Hoechst 333258. Control cells were seeded directly to the well. Images were captured by microscopy PALM MicroBeam equipment (Zeiss, Göttingen, Germany) with LD Plan-Neofluar 40x/0.6 Korr objective at excitation wavelength of 445 nm for Hoechst (blue). 172

LIST OF TABLES

CHAPTER II

Table 1. Synthesis conditions and properties of the UPs synthesized from dicarboxylic acids (IA, SuCA, AA and SeBA) and diethylene glycol (DEG), propylene glycol (PG) and fumaric acid (FA) as double bond provider.	74
Table 2. Viscosity data of UPs and UPs in 37% (w/w) of styrene at 100 sec ⁻¹ and 25°C.	75
Table 3. Relationship between m/z and the chemical structure of UP5.	80
Table 4. TGA of UPs (Tx%: temperature at x% mass loss; Ton: extrapolated onset temperature)...	81
Table 5. Glass transition temperatures obtained from DMTA and MDSC techniques.	82
Table 6. Surface roughness of some of the developed 3D scaffolds.	86
Table S1. MALDI-TOF possible combinations, from A to E, for UP5.	92

CHAPTER III

Table 1. Viscosity values for the different formulations with 37% (w/w) of UMs, at 25 °C and at a shear rate of 100 sec ⁻¹	103
Table 2. Gel content for the bio UPRs prepared with 37% (w/w) of HEMA and St at a final curing temperature of 80 °C.	104
Table 3. Degradation temperature (T _{x%}) and onset temperature (T _{on}) for the biobased UPRs.	106
Table 4. Data obtained from DMTA analysis for UPRs. T _g : glass transition temperature; E'37 °C: modulus at 37 °C.	106
Table 5. Results from tensile tests for the bio UPRs crosslinked with HEMA for 24 h: Young's modulus (E), maximum stress (σ _{max}) and maximum strain (ε _{max}), reported as mean value ± standard deviation.	107
Table 6. AFM results for the UPRs thermally crosslinked with HEMA.	110
Table S1. Results of TGA and DMTA for the biobased UPRs/St.	116
Table S2. Results from tensile tests for the bio UPs crosslinked with styrene: modulus (E), maximum stress (σ _{max}) and maximum strain (ε _{max}), reported as mean value ± standard deviation.	116

CHAPTER IV

Table 1. Synthesis conditions and properties of the UPs prepared from dicarboxylic acids (succinic acid (SA), glutaric acid (GA)) and diethylene glycol (DEG), propylene glycol (PG), 1,3-propanediol (1,3 PG) and fumaric acid (FA) as double bond provider.	127
---	-----

Table 2. Initial and final molar ratio of the biobased UPs.	131
Table 3. Relationship between m/z and the chemical structure of UP7 and UP8.	133
Table 4. Degradation temperatures ($T_{x\%}$) and onset temperature (T_{on}) of the UPs, obtained from TGA curves.	136
Table 5. Glass transition temperatures, T_g , obtained from DMTA and MDSC techniques.	137
Table 6. Degradation temperatures ($T_{x\%}$) and onset temperature (T_{on}) of the selected bio UPRs, obtained from TGA curves.	140
Table 7. Thermomechanical parameters of the prepared bio UPRs obtained from DMTA. T_g : glass transition temperature; $E'_{37\text{ }^\circ\text{C}}$: elastic modulus at 37 $^\circ\text{C}$; $E''_{37\text{ }^\circ\text{C}}$: loss modulus at 37 $^\circ\text{C}$	141
Table 8. Results from UPRs tensile tests: modulus (E), maximum stress (σ_{max}) and maximum strain (ϵ_{max}), reported as mean value \pm standard deviation. The UPRs were crosslinked with HEMA. ...	142

CHAPTER V

Table 1. Scaffolds fabricated by μ STLG and corresponding polyesters formulation.	153
Table 2. Type of μ STLG scaffolds and respective treatments performed.	159
Table 3. Composition of the formulations and electrospinning conditions used in the electrospinning method and scaffolds used for this study.	161

MOTIVATIONS, RESEARCH SIGNIFICANCE AND IMPACT

Recently, important efforts have been made to develop new and innovative unsaturated polyesters (UPs) for a wide range of applications - mostly industrial ones. The crosslinking of UPs with a reactive diluent, usually styrene (St), generates rigid and insoluble resins called unsaturated polyester resins (UPRs). These are vastly used in glass-fiber-reinforced composite materials on automotive, construction and marine industries. Nowadays a lot of attention is being given to the development of sustainable UPs, with the replacement of the fossil based monomers by more eco-friendly alternatives. This growing source for alternatives to the conventional UPRs can be directly related with the depletion of fossil fuels but also to the increase of global pollution and consequently emission of greenhouse gases. Besides economic and environmental concerns, the use of these biobased sources will provide important properties to the UPRs, such as biocompatibility and degradability, which, combined with the UPRs already excellent properties, makes them suitable candidates in tissue engineering (TE) fields.

In TE field, the production of 3D scaffolds is of huge importance, being stereolithography (SLA) one of the most used methods to produce high quality models. However, SLA requires fast curing resins, being most of the available ones toxic, therefore limiting its use in biomedical areas.

This PhD project focused on the development of new biocompatible UPs suitable to prepare biocompatible 3D scaffolds for TE applications, using microstereo-thermo-lithography (μ STLG). A UP appropriate for μ STLG, should fulfil several characteristics, such as: biocompatibility, fast curing process (in few seconds) and low viscosity. These requirements make the development of full, or even only partial biobased UPRs a very challenging task, because the bio UPs must also meet the properties of conventional petroleum-based materials, regarding their mechanical strength, thermal stability, processability and compatibility.

Driven by the current lack of acceptable materials for SLA on the TE area, the development of new biobased UPRs that overcome these limitations is of great interest, aiming to produce biobased 3D scaffolds with high quality and accuracy. Towards this objective, it is necessary to understand the chemistry behind the polyester preparation as well as its structure *versus* property relationship of UPs. In order to develop a new biobased UP that could resemble the curing behavior of commercial resins, successfully tested on the μ STLG equipment, this project started by reproducing a commercial UP. This step was then followed by the introduction of renewable sources to UPs formulations. By varying the type and amount of

monomers, it was possible to fine tune the UPs properties, allowing to meet the requirements to produce 3D biobased scaffolds. Posteriorly, the synthesized UPs were crosslinked with Styrene (St) (for comparison purposes) and 2-hydroxyethyl methacrylate (HEMA). HEMA ultimately revealed as the preferred UM to develop 3D scaffolds, which have presented high cell viabilities. These new UPRs, developed in the context of this PhD work, can establish an evolution milestone not only in areas such as TE and other similar biomedical fields, but also in industrial applications.

CHAPTER I

The Potential of Unsaturated Polyesters in Biomedicine and Tissue Engineering: Synthesis, Structure-Properties Relationships and Additive Manufacturing

1. POLYESTERS	3
2. UPS AND UPRS: FROM SYNTHESIS TO BIOMEDICAL APPLICATIONS	4
2.1 THE CHEMISTRY OF UPRS.....	4
2.2 STRATEGIES TO TAILOR AND IMPROVE THE PROPERTIES OF THE UPS AND UPRS	7
2.3 ALTERNATIVE CROSSLINKING METHODS FOR THE UPS	16
2.4 UPS AND UPRS FROM RENEWABLE MONOMERS	18
2.5 UPS AND UPRS DIRECTED TO BIOMEDICAL APPLICATIONS.....	30
3. SCAFFOLD-BASED TISSUE ENGINEERING.....	37
3.1 MANUFACTURING TECHNOLOGIES.....	39
3.1.1 <i>Conventional technologies</i>	39
3.1.2 <i>Non-conventional technologies (Additive Manufacturing)</i>	40
3.1.3 <i>Stereolithographic processes</i>	43
Microstereolithography	46
Stereo-Thermal-Lithography	49
Two-Photon-Initiated Polymerization	50
4. CONCLUSIONS AND OUTLOOK.....	52
5. REFERENCES	53

Adapted from: Gonçalves, F. A. M. M.; Fonseca, A. C.; Domingos, M.; Gloria, A.; Serra, A. C.; Coelho, J. F. J. The potential of unsaturated polyesters in biomedicine and tissue engineering: Synthesis, structure-properties relationships and additive manufacturing. *Progress in Polymer Science* **2017**, *68*, 1-34.

1. Polyesters

The history of polyesters dates back to the 1930's when Carothers reacted aliphatic diols with aliphatic diacids and established the relationships between the structure and properties of the obtained polymer. The results were not very promising since the polyesters obtained had low melting points, were very prone to hydrolysis, and no practical applications were found for the synthesized polymers. The search for polyesters with better properties continued and, in 1941, Whinfield and Dickson, from Calico Printers Association, reported the synthesis of high melting and fiber forming polyesters from the reaction of terephthalic acid (TPA) and aliphatic glycols [1, 2]. The polyester that resulted from this work was poly(ethylene terephthalate) (PET), that is still today one of the most produced and used polymers worldwide.

Nowadays, polyesters constitute one of the most important and versatile classes of polymers, being suitable to be used in a variety of applications (e.g., automotive industry, plastics industry, biomedical field, among others) [2]. Polyesters are prepared through a polycondensation process, where a dihydroxy compound (or a mixture of dihydroxy compounds) reacts with anhydrides or dicarboxylic acids [2]. To achieve high reaction conversions and polyesters with high molecular weight the generated by-product, water, needs to be continuously removed from the reaction medium. For such purpose, a stream of nitrogen and vacuum can be used or, alternatively, the removal of water can be done with the help of solvents that are able to form azeotropes with water (e.g., xylene or toluene).

The use of catalysts is also common in the field of polyesterification. The most used are metal based catalysts (e.g., $\text{Sn}(\text{Oct})_2$, ZnCl_2), and organic acids (e.g., *p*-toluene sulfonic acid, PTSA). The use of enzymes as catalysts has also been reported [3]. Ring opening polymerization (ROP) is another method that can be used to prepare polyesters. Typically, with this synthetic method it is possible to obtain polyesters with high molecular weight and low polydispersity (\mathcal{D}) [4]. Polyesters can be divided into different classes (e.g., aromatic or aliphatic) depending on the type of monomers used. Two classes that result from this division are the saturated polyesters and the unsaturated polyesters (UPs). Examples of saturated polyesters are poly(ϵ -caprolactone) (PCL), poly(L-lactic acid) (PLLA), poly(glycolic acid) (PGA), as well as their copolymers. These polyesters found a broad range of applications in the biomedical field due to their biodegradability and biocompatibility. Some of the applications include scaffolds for tissue engineering [5], sutures [6] and drug delivery systems [7]. Nevertheless, there is still a need to develop materials with more specific properties, for example, in terms of solubility, crystallinity, reactivity, among others [8]. Overall, these materials are hydrophobic and

with few reactive groups along the backbone, thus limiting their applicability and further functionalization.

Regarding the UPs, these are characterized by their low-molecular weight and high polydispersity values (\mathcal{D}). The unsaturations present in the polymer backbone allow the UPs to be used in cure reactions via radical polymerization reactions, in the presence of an unsaturated monomer (UM), usually styrene, leading to thermosetting polyesters, known as unsaturated polyester resins (UPRs). Maleic anhydride (MA) and fumaric acid (FA) are the most used commercial monomers for introducing unsaturations in the polyester chain. The UP properties can be easily tuned by using different types of diols and diacids or even by changing the reactant ratio [9]. The properties of the UPRs depend not only on their molecular composition but also on the extent of the cure reaction, which means that it is very important to understand the reactions occurring during the curing and its implications in the process [10]. Although UPRs were developed in the 1930's, they still today widely used in a variety of applications closely related with the industry (*e.g.*, construction and automotive). Nevertheless, in the last years, efforts have been made to prepare UPRs more directed to biomedical applications [11-13]. In this case UPs are very attractive candidates mainly due to their unsaturations, providing further functionalization sites [14] and enabling the fabrication of complex 3D structures via Additive Manufacturing (AM) processes [12]. This chapter intends to give a broad overview about the synthesis and preparation of UPRs, in particular the relationship between structure and properties as well as the latest developments regarding their application in the biomedical field. AM processes used to produce scaffolds are reviewed with special focus on stereolithography (SLA).

2. UPs and UPRs: From synthesis to biomedical applications

2.1 The chemistry of UPRs

The transformation of UPs into a structural material requires the addition of another component, the UM, commonly named as diluent and generally used in weight percentages ranging from 30 to 40 % [4]. The generic process to obtain UPRs is divided in two main steps: the synthesis of the UPs and the curing reaction (Figure 1).

The Potential of Unsaturated Polyesters in Biomedicine and Tissue Engineering

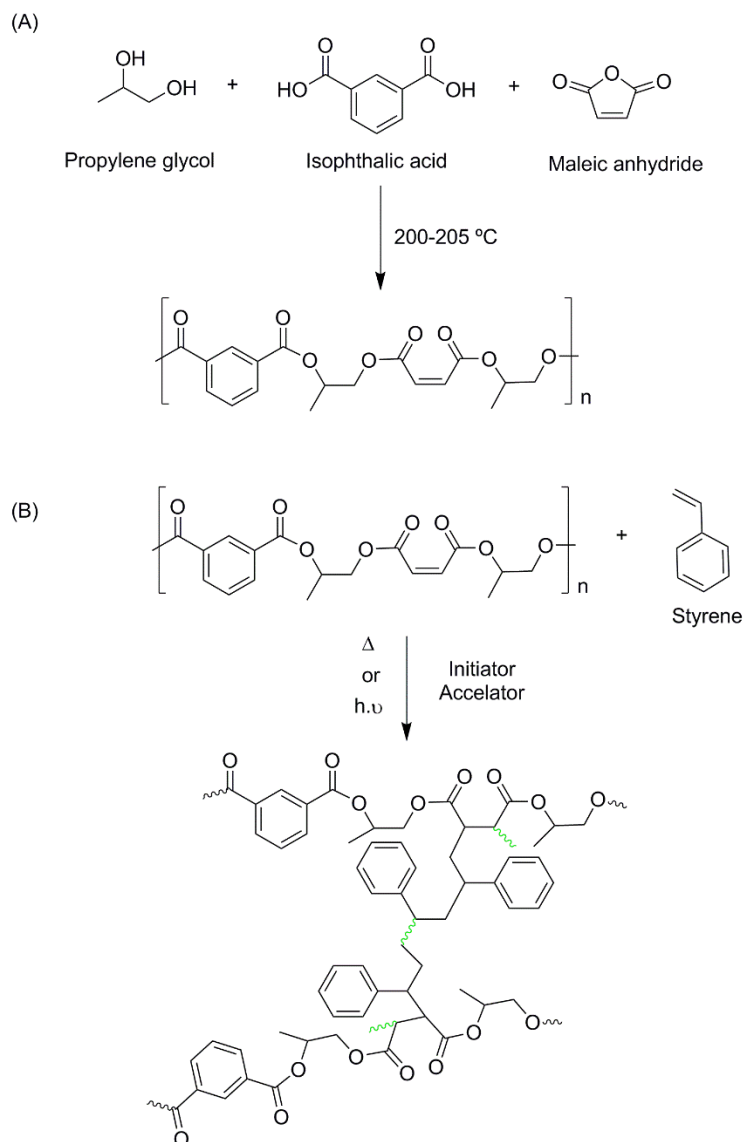


Figure 1. Path for the development of UPRs: (A) Polycondensation reaction, and (B) cure reaction.

The UM is added to the UP for two main purposes: (1) to reduce the viscosity of the system (aiding the resins processing) and (2) to create an efficient crosslink network with the double bonds available in the UP backbone. Styrene is the most commonly used UM, but others, like dimethacrylates, alkyl methacrylates vinyl esters, and divinylbenzene can also be used [4, 15]. Due to the radical nature of the curing process, the addition of a radical initiator to the formulation is needed. The most employed initiators are the organic peroxides, namely ketone peroxides, alkyl hydroperoxides, diacyl or dialkyl peroxides [15]. Another important component of the formulation is the accelerator or promoter, a compound able to reduce the activation energy involved in the initiator decomposition, leading to the reduction of the temperature required for crosslinking. Vanadium or cobalt salts and tertiary amines (e.g., *N,N*-diethylaniline, *N,N*-

dimethylaniline, or *N,N*-dimethyl-*p*-toluidine) are the most commonly used accelerators [15]. Inhibitors, like hydroquinone or *t*-butyl hydroquinone, can also be used to avoid unwanted radical polymerization during the polycondensation (due to the high reaction temperatures), mixture with UM, handling and storage. The amount of inhibitor, however, should be carefully adjusted to avoid further slowdown of the crosslinking reaction [4]. When the UPR formulation is exposed to heating and/or radiation, the crosslinking reaction starts by the formation of free radicals from initiators. The first radicals formed are trapped by any inhibitor in the mixture until its full consumption. At this stage, the radical crosslinking reactions starts, forming long chain molecules through the connection of vinyl monomers, by intermolecular and intramolecular reactions (Figure 2A). These long chain molecules are predisposed to form spherical structures called microgels (Figure 2B). These gels can be defined as crosslinking dense structures, where several pendant groups (from UM) are confined to the interior of these structures [16]. This fact can result in the lowering of the final conversion, due to a chain segmental immobility in the crosslinked network. In the case of the reaction between UP and UM, previous studies demonstrated that gelation begins at an early stage of nearly 3-5% of conversion, which means that the reaction might be diffusion-controlled over almost its entire course [17]. Thus, the formation of microgel particles is a key feature of the UM-UP copolymerization. Yang and Lee [18] observed similar results in sheet molding compounds and in polyurethane-polyester interpenetrating polymer networks.

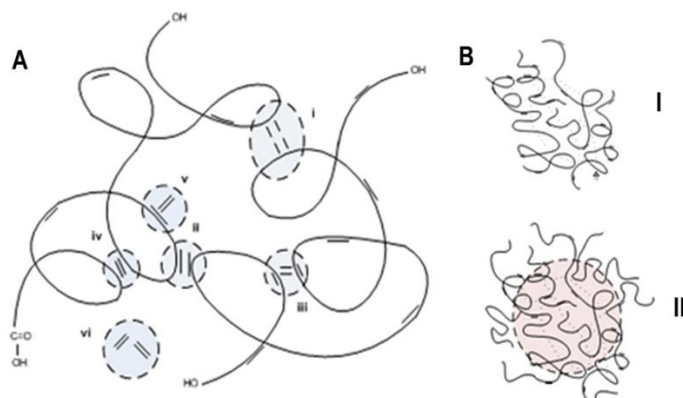


Figure 2. **A.** Schematic diagram showing the possible reactions in the styrene-unsaturated polyester copolymerization. **B.** Formation of microgel particles through the growth of free radicals: (I) growth of free radicals; (II) formation of microgel particles, adapted from [18].

The curing process and the reaction kinetics are very complex due to the simultaneous occurrence of different reactions: UM-UP copolymerization, homopolymerization of UM and UP homopolymerization. The importance of each reaction can be adjusted

depending on the formulation used and the curing conditions [19]. As shown in Figure 2A, these three processes can be divided into four possible reactions:

- (1) Intermolecular crosslinking with or without linking between the UM (reaction I and II);
- (2) Intramolecular crosslinking with or without linking through UM (reactions III and IV);
- (3) Branching on the polyester molecule by UM (reaction V);
- (4) UM homopolymerization (reaction VI).

The reaction (1) results in a macroscopic network formation through the connection of adjacent polyester molecules; reaction (2) increases the crosslinking density but does not contribute to the macroscopic network formation; the other side reactions (3) and (4) may increase the polymer coil size, however their impact on the network formation is residual [18]. All these reactions affect the curing kinetics, but only the first two contribute to network formation.

Usually, the course of the UPRs cure is followed by differential scanning calorimetry (DSC) analysis [20-26].

2.2 Strategies to tailor and improve the properties of the UPs and UPRs

Due to their excellent properties, easy synthesis, high versatility and low cost, UPRs applications continue to expand globally at robust rates. These type of materials had a leading role in the improvement of fiberglass reinforced products, for example in building materials for boats and cars [2], as they are a very inexpensive and useful solution [10, 15]. UPRs are widely employed as adhesives and coatings but also in the building and electrical industries, among others [27]. Apart from the advantages, UPRs also present some disadvantages, such as their high flammability, low impact strength and poor toughness, which *a priori* can be mitigated by changing the UPR formulations. These changes can be performed in the structure of the UP, in the amounts or types of UM, or even in the initiator systems used.

Sanchez and co-workers [28] have studied the influence of styrene concentration in the final properties of the UPs using a commercial UPR, RESAPOL 10-203. The results provided by the dynamic mechanical thermal analysis (DMTA) showed a broadening of the $\tan \delta$ peak as the concentration of styrene increased (from 6 %wt to 58 %wt). This fact was attributed to the existence of microenvironments that differ in their composition and crosslinking density. Above 18 wt% of styrene, two distinct transitions were observed and ascribed to the presence of two different and immiscible phases within the crosslinked network: an UP-rich phase and a polystyrene-rich phase. An increase in the

T_g values was also reported for higher contents of styrene. The sample with 38 %wt of styrene was found to be the most thermally stable.

It is known that when the UPs are prepared with only one diol, namely ethylene glycol (EG) or diethylene glycol (DEG), a limited solubility in styrene is observed. Nevertheless, Matynia and co-workers [29] managed to synthesize styrene soluble UPs making use of only one diol, EG, and two acid anhydrides, viz. MA and phthalic anhydride (PhA). The synthesized UPs were end-capped with isopropyl alcohol or monoesters from the used anhydrides, which enhanced their solubility in styrene. The increase in the amount of double bonds yields UPRs with high reactivity, high crosslinking density and higher mechanical stability. The UPRs obtained from the UPs end-capped with the monoesters showed better thermal stability and higher heat deflection temperatures than those end-capped with isopropyl alcohol.

The enhancement of toughness and impact resistance is a very important issue in the UPRs' field. One possible approach to achieve this goal encompasses the preparation of block copolymers of UPs incorporating rubber segments that are subsequently used in the preparation of UPRs. Cherian and Tachil [30] prepared copolymers of UP with hydroxyl terminated polybutadiene (HTPB), carboxy terminated nitrile rubber (CTBN) and also hydroxyl terminated natural rubber (HTNR). The polycondensation was carried out in two stages, leading to UPs containing alternating rigid and soft segments. The UPs were then crosslinked with styrene, in the presence of methyl ethyl ketone peroxide (MEKP), as initiator, and cobalt naphthenate, as accelerator. The mechanical properties of the UPRs were evaluated and the results showed that CTBN is the most promising in improving the mechanical properties of the UPRs because the toughness and the impact strength were significantly enhanced, without jeopardizing extensively the remaining properties. Another approach was studied by the same researchers [31], in which poly(ethylene glycol) (PEG) segments were incorporated in the UP structure. The mechanical properties of the ensuing UPRs (35 %wt styrene) were evaluated and the influence of the incorporation of PEG in the UP structure was accessed. The results showed that the use of UPs with PEG segments of molecular weights *ca.* 200 g/mol resulted in UPRs with enhanced flexibility, fracture toughness and impact resistance. Following the same rationale, Cherian and co-workers [32] reported the use of polyurethane (PU) prepolymers as a mean to improve the mechanical properties of the UPRs. The prepolymers were prepared by reacting toluene diisocyanate (TDI) with different polyols (HTNR, hydroxyl-terminated polybutadiene (HTPB), PEG and castor oil), and subsequently added in varying amounts (up to 10 %wt) to the UP to be crosslinked in the presence of styrene. The results showed that the HTNR-PU prepolymer was the most effective in improving the mechanical properties of the UPRs.

An increase of 20 % in the tensile strength was observed, while the toughness was shown to increase 188 %. Very important, the DMTA of the modified UPRs showed only one $\tan \delta$ peak, indicating that the PU prepolymers are miscible with the UPR. In another approach, Rosa and Felisberti [33] incorporated poly(organosiloxane) segments in the UP network to increase their flexibility.

The mechanical properties of UPRs have also shown to be improved by the addition of bismaleimides [34, 35], which are a class of compounds with two maleimide groups that are connected by a nitrogen atom via a linker and are used as crosslinking agents in the polymer field. These molecules are known for their high thermal stability, strength, and fire resistance, among other interesting properties. Gawdzik and co-workers [35] proposed the modification of a commercial UP (D-1103) with 4,4-bismaleimidodiphenylmethane (BM). The authors reported that the addition of the BM accelerated the curing reaction, resulting in UPRs with high T_g values (ca. 180 °C vs 70 °C for the unmodified ones) and high hardness. It was also shown that BM can react with the UP at high temperatures, without any chemical initiator. When styrene is added to the system, different reactions can take place, namely UP-BM crosslinking, UP-styrene crosslinking, or even UP-(BM-styrene sequences) crosslinking. Figure 3 illustrates the structures of the UP and of the crosslinkers.

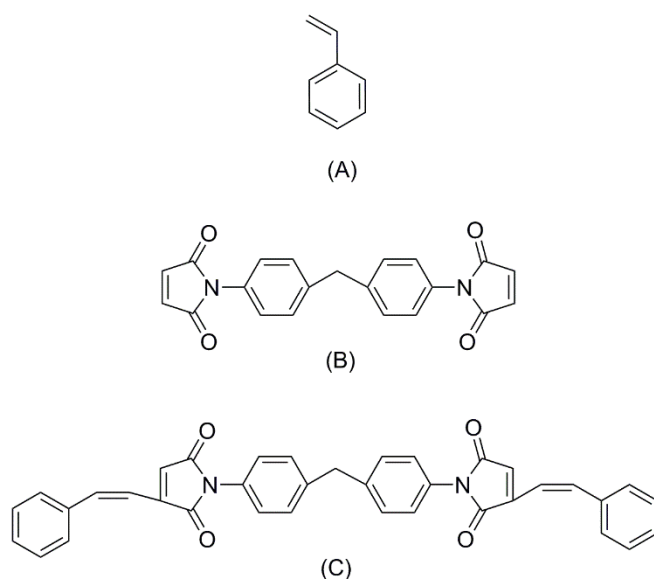


Figure 3. Structures of the crosslinkers: (A) styrene, (B) BM, and (C) BM-styrene, adapted from [35].

In a very interesting approach, Cherian and Tachil [36] studied how the addition sequence of the reactants in the UPs preparation influenced the final properties of the UPRs. The authors used five different sequences of reactants addition and found out that reacting first PhA with the whole amount of propylene glycol (PG), with the

subsequent addition of MA was the most promising sequence. This procedure led to shorter reaction times, and the resulting UPs yield UPRs with enhanced elongation at break and toughness.

Fluorinated polymers, in turn, have shown to be suitable to improve both the mechanical properties and surface properties of the UPRs, as demonstrated by Messori and co-workers [37]. The authors reported the modification of an UPR by blending it with poly(ϵ -caprolactone)-perfluoropolyether- poly(ϵ -caprolactone) (PCL-PFPE-PCL) triblock copolymers. The fluorinated modified UPR (FUPR) showed a surface enrichment in fluorine segments and, as expected, a decrease in the water diffusion coefficient value. The morphology of the FUPR has shown to be strongly dependent on the molecular weight and the PFPE/ PCL ratio. It was also found that a plasticization effect occurred with an increase in the molecular weight of the triblock copolymer and in the PCL length. The absorbed energy at break was observed to be enhanced when the PFPE/PCL ratio was 2/10.

In another work, Nebioglu and co-workers [38] studied the effect of the amount of both multifunctional UM and internal and terminal unsaturation in the network structure and in the mechanical properties of the resulting UPRs. Acrylate-terminated UPs were obtained from the reaction of MA, adipic acid (AA), neopentyl glycol (NPG), and trimethylolpropane (TMP), and their end-chains were modified with acrylic acid (AcA). The UPRs were obtained from the photopolymerization of the UPs in the presence of trimethylolpropane triacrylate (TMPTA) as UM, and Irgacure 184 as photoinitiator. The DMTA showed that both high concentrations of TMPTA and high internal unsaturation led to phase separation in the cured UPRs. It was also observed a broadening of the $\tan \delta$ curve, revealing the heterogeneity of the sample, as the amount of TMPTA increased. Surprisingly, the increase in the amount of internal and terminal unsaturations was not translated in an improvement of the crosslinking density. The authors attributed this result to the fact that a higher unsaturation concentration causes more microgelation, resulting in a higher amount of trapped free radicals inside the microgels, with consequent reduction in the crosslinking density. The microgels were also responsible for a decrease in the fracture toughness properties and on the reverse impact resistance. In a subsequent work, the authors [39] used the same type of UPs to obtain UV-cured films and studied how the extent of microgelation affected the viscoelastic, fracture and tensile properties of the films. The results demonstrated that when the microgelation occurred in a low extent, the microgels acted as micro-support units enhancing the mechanical properties. However, for high extent of microgelation, a phase separation occurred jeopardizing the mechanical properties of the films.

Another very important aspect in the field of UPRs is related with their thermal stability. Some strategies regarding the improvement of this property have been presented in literature. Tawfik [40] developed different UPs based on durene derivatives, *viz.* 3,6-bis(methoxymethyl)durene and 3,6-bis(benzyloxymethyl)durene, that were obtained from the 3,6-bis(chloromethyl)durene (Figure 4A). The other monomers used in the preparation of the UPs were PhA, MA and succinic acid (SuCA) as well as different glycols, such as PG, triethylene glycol (TEG), and cyclohexane diol (CHD). The UPs were able to cure with styrene, at room temperature, in the presence of cobalt naphthenate and MEKP as accelerator and initiator, respectively. From the thermogravimetric analysis (TGA) and DSC studies, the authors found that the UPR prepared from UP V (see Figure 4B) was the resin with the highest thermal stability. Additionally, both this UPR and that obtained from UP III (see Figure 4B) showed flame-retardant properties.

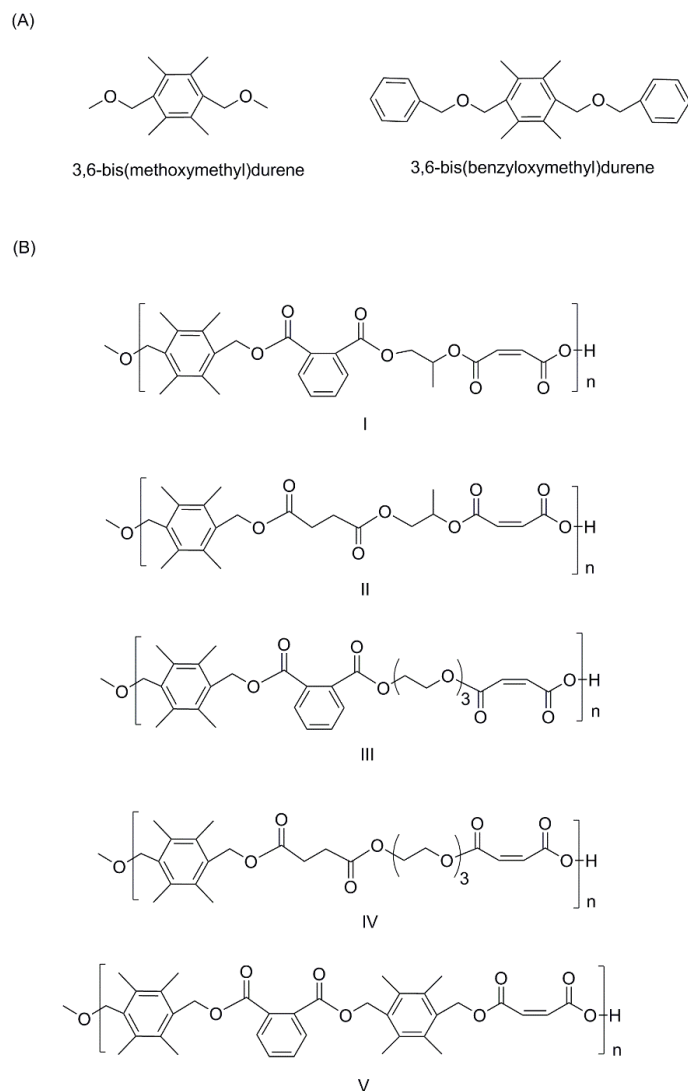


Figure 4. Monomers used for the preparation of durene based polyesters (A), and structure of the UPs (B), adapted from [40].

In a different approach, Tibilleti and co-workers [41] improved the thermal stability and fire behavior of UPRs through the introduction of nanometric alumina oxide and submicron alumina trihydrate.

Alskas and co-workers [42] developed thermally stable UPs containing a cyclopentapyrazoline moiety in the main chain. The cyclopentapyrazoline moiety is known to enhance the thermal stability of the materials, their solubility and can also provide the materials with photoconductivity. The method for the preparation of the UPs was based on an interfacial polymerization between diols bearing the cyclopentapyrazoline moiety, namely 3-*p*-hydroxyphenyl-6-*p*-hydroxybenzylidene cyclopentapyrazoline and 3-anillyl-7-vanillylidene cyclopentapyrazoline, and different diacyl chlorides, *viz.* adipoyl, sebacoyl, isophthaloyl, and terephthaloyl dichlorides (Figure 5).

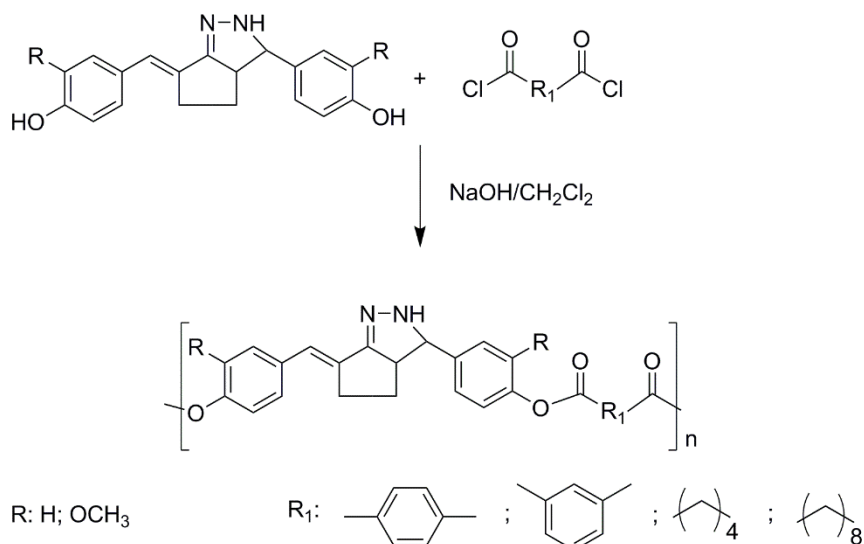


Figure 5. UPs synthesis through interfacial polycondensation technique, adapted from [42].

The UPs presented T_g values ranging from 103 °C to 208 °C, being soluble in a variety of organic solvents. Thermal analysis showed that these aromatic based polyesters were more thermally stable than the aliphatic counterparts. It should be stressed, that this new UP also showed electrical conductivity when doped with iodine. Unfortunately, no data regarding the cure reaction of this UP to yield the UPRs was reported by the authors.

The synthesis of modified UPs to enable the control of product viscosity was performed by Chiu and co-workers [43]. The authors grafted thermally breakable functional groups based on diketogluconic acid onto the UPs backbone and the results showed that these moieties were crucial to control the viscosity during the moulding process.

In another work related with the viscosity control, Zhang and co-workers [44] developed new unsaturated hyperbranched polyester resin (UHPR) based on the reaction between maleic monoisooctyl alcohol ester and a hydroxyl-ended hyperbranched polyester resin (HPR). The hydroxyl ended HPR was prepared from PhA and TMP. The UHPR showed a viscosity below 10,000 cP, at room temperature, being suitable to be used in the field of coatings.

It is known that UPRs can have large volume shrinkage during the polymerization, which leads to sink mark formation, surface waviness, warpage, poor dimension accuracy, or internal crack. This particular aspect can pose several issues to the application of these materials in AM processes. Shenoy and co-workers [45] reported a study on the effect of the addition of ethylene vinyl acetate (EVA) (partially depolymerized and presenting different degrees of branching) on the mechanical, thermal, chemical and shrinkage properties of UPRs. The authors concluded that the addition of 0.5 % wt EVA (with a high degree of branching) led to an improvement in the flexural and tensile properties, without deleterious effects in the heat deflection temperature (HDT) and impact properties. A decrease in the percentage of shrinkage of ca. 2% was observed for the system containing 0.5 % wt EVA. Further increase in the EVA percentage led to a decrease in the volume shrinkage, but a notorious worsening of the remaining properties was observed. It is known that the increase of the crosslinking density results in a decrease of shrinkage behavior. This phenomenon will not be fully discussed here, although it assumes a great importance in industrial fields and has been intensively investigated [46-48].

Another important aspect in the UPRs field is related with the initiator systems that are used. As mentioned before, tertiary amines are widely used as accelerators, but often the formulations containing these compounds have a reduced shelf-life. A possible strategy to overcome this issue is to incorporate the amine in the UP structure [49-52]. For such purpose, Duliban [49] developed novel amine modifiers with hydroxyl terminal groups to be incorporated in the UPs. The amines were prepared from the reaction of ethylene oxide (EO) or propylene oxide (PO) with *N,N'*-diphenylethane-1,2-diamine or from the reaction of EO with *N,N'*-diphenylhexane-1,6-diamine (Figure 6). The amine modifiers were used to partially replace PG (up to 2 % mol) in a UP composed by MA, PhA, PG and DEG. The UPs were cured in the presence of benzoyl peroxide (BPO), the most used initiator in amine-curing systems, or alternatively in the presence of the initiator methyl ketone hydroperoxide and the accelerator cobalt(II) octanoate. The results obtained from the cure reactions showed a reduction of the gelation time in both curing systems when 2 %wt of the modifier was used. The best result, in terms of gelation time and storage stability, was obtained for the UP containing 1 % wt of the modifier 3,6-

diaza-3,6-diphenyloctane-1,8-diol. The addition of benzyltriethylammonium chloride to the cobalt curing system was also performed to improve the storage stability of the resins. However, the stabilizer reduced the resins reactivity.

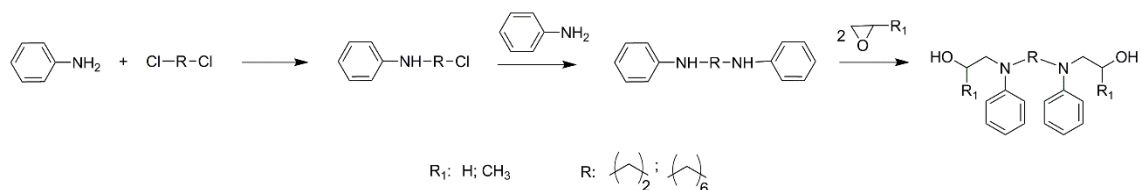


Figure 6. Scheme of preparation in two steps of amine glycol modifiers for UP resin, i.e. 3,6-diaza-3,6-diphenyloctane-1,8-diol ($R=-(\text{CH}_2)_2-$; $R_1=-\text{H}$), 4,7-diaza-4,7-diphenyldecane-2,9-diol ($R=-(\text{CH}_2)_2-$; $R_1=-\text{CH}_3$) and 3,10-diaza-3,10-diphenyldodecane-1,12-diol ($R=-(\text{CH}_2)_6-$; $R_1=-\text{H}$), adapted from [49].

In the same line of research, Kucharski and co-workers [52] prepared diols bearing tertiary amine groups, from the reaction of *N,N*-dimethyl-*p*-phenylenediamine with EO or PO. The results showed that when the amine diols are incorporated in the UP structure, a reduction in the gelation time of the respective UPRs is observed. Nevertheless, the UPRs stability is also compromised exhibiting a significant reduction. Related works by Duliban [50, 51] show that amine diols (or triols) bearing *s*-triazine rings (Figure 7), when introduced in the structures of the UPs, are also effective in reducing the gelation times of the respective UPRs.

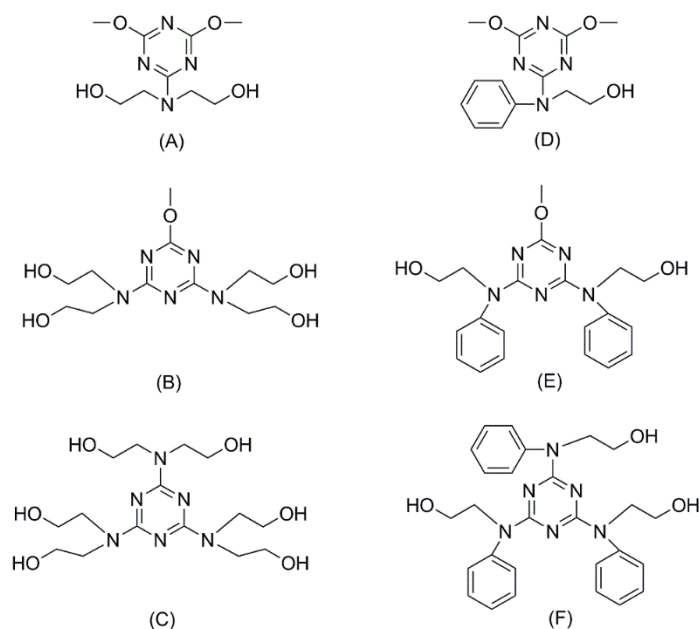


Figure 7. Structures of the amine glycols bearing *s*-triazine rings: (A) 2-[*N,N*-bis(2-hydroxyethyl)amine]-4,6-dimethoxy-1,3,5-triazine; (B) 2,4-[*N,N*-bis(2-hydroxyethyl)amine]-6-methoxy-1,3,5-triazine; (C) 2,4,6-tris[*N,N*-bis(2-hydroxyethyl)amine]-1,3,5-triazine; (D) 2-[*N*-phenyl(2-hydroxyethyl)amine]-4,6-dimethoxy-1,3,5-triazine; (E) 2,4-bis[*N*-phenyl(2-hydroxyethyl)amine]-6-methoxy-1,3,5-triazine; and (F) 2,4,6-tris[*N*-phenyl(2-hydroxyethyl)amine]-1,3,5-triazine [50, 51].

The catalyst of polycondensation to prepare the UPs can also be modified as a route to improve the efficiency of the reaction. In this sense, Alemdar and co-workers [53] proposed a boric acid-pyridine mixture as a mild catalyst for the preparation of UPs, from hydroxyethyl esters *in-situ* generated from cyclic anhydrides (maleic, succinic and phthalic anhydrides) (Figure 8). The UPs, with molecular weights ranging from 1650 to 1950 g/mol, were obtained after 4h of reaction. This reaction time can be seen as a great advantage since it opens the possibility of avoiding side-reactions (e.g., branching or crosslinking from the reaction of hydroxyl groups with the double bonds). It was also found that the UPs easily bind to sodium bisulfite to give sulfonated derivatives that have an amphiphilic nature.

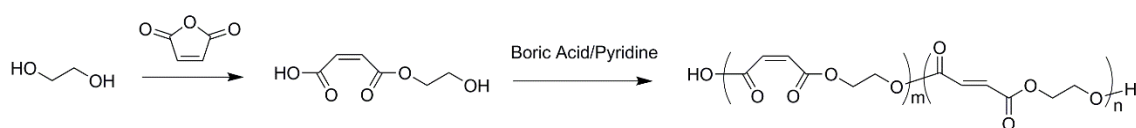


Figure 8. Polyesterification of the monohydroxyethyl esters of maleic acids with boric acid-pyridine mixture as mild catalyst, adapted from [53].

In another work, Lou and co-workers [54] demonstrated that it is possible to obtain UPs with a controlled structure and tailorable properties by ROP. The homopolymerization of 6,7-dihydro-2(5*H*)-oxepinone (DHO) and its copolymerization with ϵ -caprolactone (ϵ -CL) [40] were initiated by aluminium isopropoxide [$\text{Al}(\text{O}^i\text{Pr})_3$], in toluene, at room temperature (Figure 9).

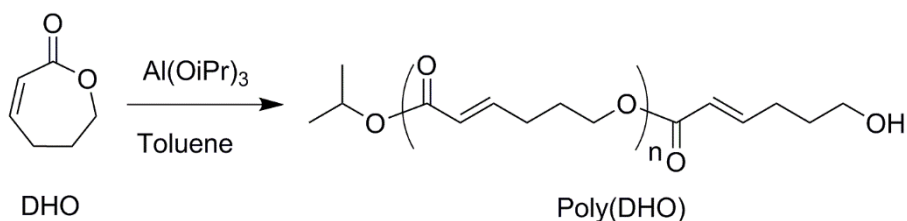


Figure 9. ROP of DHO to give the poly(DHO), adapted from [54].

The poly(DHO) was obtained with the predicted molecular weight, with a narrow molecular weight distribution, and with T_g and T_m of -50°C and 35°C , respectively. The copolymers DHO with ϵ -CL were also prepared in a controlled manner. From this experiment, it was also possible to observe that an increase in the DHO amount in the random copolymer increases the T_g and decreases the T_m , in comparison with PCL.

2.3 Alternative crosslinking methods for the UPs

Commonly, the UPRs are obtained from the cure reaction between the UP and the UM. Due to its low cost and availability, styrene is often used as UM. Additionally, styrene is known to provide UPRs with excellent mechanical properties. However, this UM has high volatility, and during the cure process it is released to the atmosphere. Thus, in the recent years, significant efforts have been devoted to find alternative UMs capable to overcome this problem. Possible strategies encompass the use of UMs with boiling temperatures higher than styrene [55, 56], the reduction of styrene content in the formulation and, more interesting, the introduction of different moieties in the UP structure to allow the further crosslinking in the absence of UM. It should be noted, that in this subsection the described strategies are exclusively related with fossil based UPRs. The strategies focused on the development of self-crosslinkable biobased UPs will be presented in the following section of this chapter.

In a very interesting contribution, Straub and co-workers [57] developed alternative crosslinking methods for UPs avoiding the use of styrene. The strategy proposed was based on the use of maleic or fumaric diesters functionalized with triple bonds, followed by oxidative metal mediated homo-coupling of the introduced alkyne moieties (Figure 10). The authors discovered that the combination of Pd/Cu and air is a very effective system for the catalytic oxidative homo-coupling of alkynes, leading to the crosslinking of UPs chains.

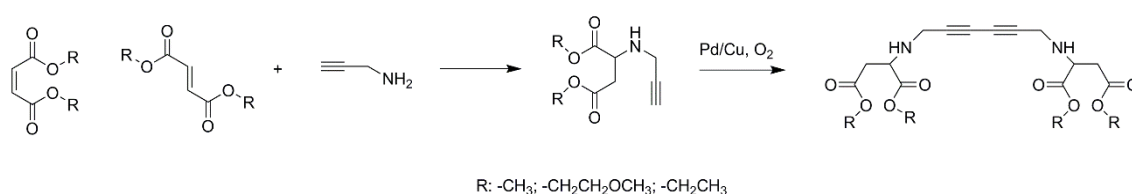


Figure 10. Metal-mediated reaction of UP via functionalization of maleic or fumaric diesters, followed by oxidative homo-coupling of the introduced alkyne moieties, adapted from [57].

In turn, Cinar and co-workers [58] proposed the use of bis(nitrone)s as crosslinkers for UPs bearing maleate and fumarate groups. The nitrones are known to easily undergo 1,3-cycloadditions with double bonds. The crosslinking reaction successfully occurred at 120 °C, for 30 min, in the absence of catalysts (Figure 11). Unfortunately, no data regarding the properties of the UPRs were presented by the authors.

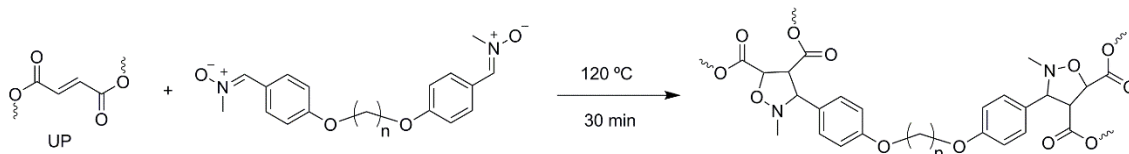


Figure 11. Crosslinking reaction between the UP and a polynitrene, leading to a 3D network, adapted from [58].

Worzakowska [27] reported the synthesis of UPs through polycondensation of cyclohex-4-ene-dicarboxylic anhydride (THPA), MA and different diols (1,4-butanediol, 1,6-hexanediol and EG), as well their selective epoxidation with peracetic acid in mild conditions (Figure 12) [59], to yield unsaturated epoxyoligoesters. It should be noted that in this method only the double bonds in the cyclohexenyl ring were converted in epoxy groups, leaving the remaining C=C bonds (from the maleate units) unmodified. The ensuing polymers have the ability of being crosslinked in the presence of UMs or by polyaddition reactions with suitable curing agents. Interestingly, the resins obtained from the cure of unsaturated epoxyoligoesters in the presence of 20 %wt styrene (usually, the percentage of styrene is about 37 %wt), and using BPO as initiator, revealed a better thermal stability and increased viscoelastic properties in comparison to those obtained from the unmodified UP. The properties were further improved when THPA was added to the curing system. In this case the crosslinked network resulted from two types of reaction: (i) copolymerization of the C=C double bonds in the polyester and the UM, and (ii) polyaddition of epoxy groups to anhydride groups, forming additional diester segments. The length of the diol has demonstrated an important influence in the final properties of the resins; shorter diols led to resins with better properties than those obtained with larger diols.

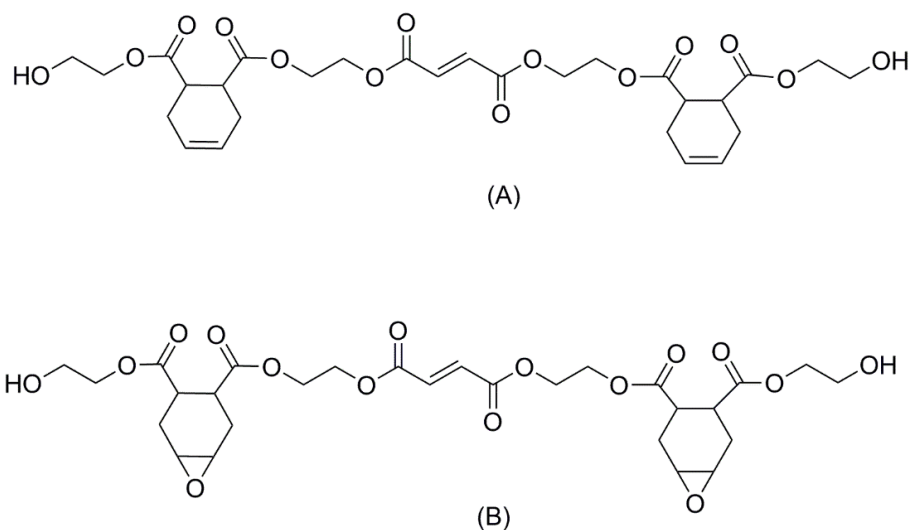


Figure 12. Structures of: (A) unsaturated oligoester; and (B) unsaturated epoxyoligoester, using EG as the diol.

2.4 UPs and UPRs from renewable monomers

A field that is nowadays attracting considerable attention from the scientific community is the preparation of polymers from renewable resources [60, 61]. In the last years, many contributions regarding the use of renewable monomers (e.g., FA, ITA, sebacic acid (SeBA), dianhydrohexitols (DAHs), 1,3-propanediol (1,3PG) [11, 12, 62-64], or vegetable oils [65-67]) in the preparation of UPs and, ultimately, UPRs have been reported. For a better understanding, the first part of this subsection will be devoted to the preparation of biobased UPs, where some approaches regarding the crosslinking reactions of these polymers in the absence of UM will be presented; the second part will be focused on the development of biobased UPRs, resulting from the crosslinking reaction of biobased UPs with UMs.

Takenouchi and co-workers [68] prepared a set of UPs based on different anhydrides (succinic, methylsuccinic, maleic and citraconic), FA, and EG and studied the effect of the geometric configuration (*E*- and *Z*-) of the double bonds in their biodegradation properties. Enzymatic degradation tests were carried out at controlled temperature (37 °C) in the presence of *Rizopous delemar* lipase. Additional degradation tests were carried out with an activated sludge (25 °C) and the values of the biochemical oxygen demand (BOD) registered. The overall results showed that the UPs with the double bonds in the *E*-configuration are more prone to degradation, when compared to those that have the double bonds in the *Z*-configuration. It was also found that the methyl group as a pendent chain contributes to a decrease in the biodegradability of the samples.

Zheng and co-workers [69] synthesized multiblock copolymers based on poly (butylene fumarate) (PBF) and poly (1,2-propylene succinate) (PPS), by the chain extension reaction of PBF diol and PPS diol with 1,6-hexamethylene diisocyanate (HDI) (Figure 13). The main purpose of this work was to increase the biodegradability of PBF by introduction of PPS moieties.

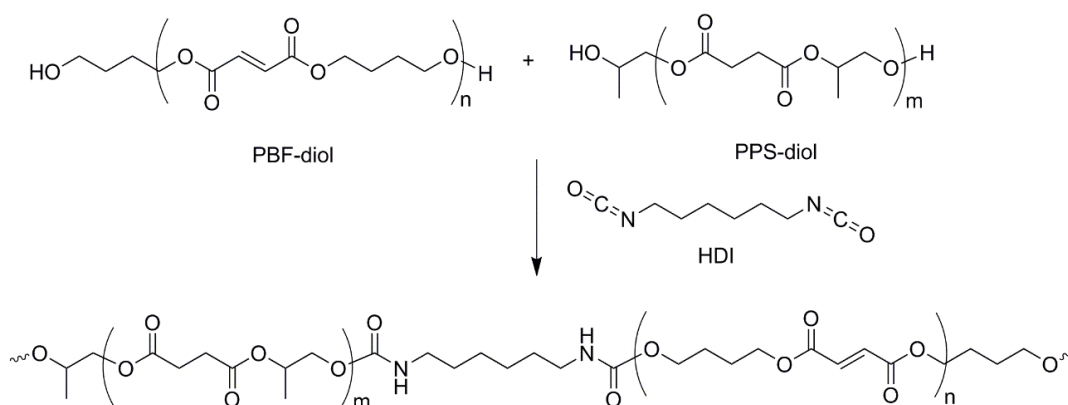


Figure 13. Chain extension reaction of PPS-diol and PBF-diol mediated by HDI.

The results showed that the biodegradability of PBF was enhanced by the copolymerization of PPS. For contents above 20 %wt, the effect was more notorious. Also, the introduction of PPS led to materials with higher impact strength and less crystallinity when compared with PBF.

Najafi and Sarbolouki [70] prepared partially water-soluble UPs through the reaction of two linear unsaturated aromatic oligoesters, *viz.* poly(hydroquinone fumarate-co-sebacate) (PHFS) and poly(resorcinol fumarate-co-sebacate) (PRFS), and PEG. Both diblock (PHFS-co-PEG and PRFS-co-PEG) and triblock copolymers (PEG-co-PHFS-co-PEG and PEG-co-PRFS-co-PEG) were prepared and their thermal properties were assessed. It was found that both the diblock and triblock copolymers were thermally more stable than the unsaturated oligoesters. The DSC analysis showed that the block copolymers had one exothermic transition, corresponding to the melt of the PEG segment. The same authors [71] also reported the preparation of diblock and triblock copolymers from poly(propylene fumarate-co-sebacate) (PPFS), poly(ethylene fumarate-co-sebacate) (PEFS), and PEG. Similarly to what was previously reported, the copolymerization of the unsaturated oligoesters with PEG results in an increase of the thermal stability. The *in vitro* hydrolytic degradation (pH=7.4, 37 °C) was evaluated and the ¹H NMR analysis revealed that the fumarate ester bond cleaves faster than the ester sebacate bonds.

Jasinska and Koning [72] also reported the preparation of water-soluble UPs making use of PEG, isosorbide (IS), and MA. The bulk polycondensation, catalyzed by titanium(IV) *n*-butoxide was the chosen synthesis method. The results have demonstrated that these UPs presented branched structures resulting from the reaction of the double bonds with the –OH groups of the PEG or IS moieties. The thermal properties of the UPs were evaluated, and the results showed that the T_g was dependent on the amount of PEG in the structure; for higher contents of PEG, lower T_g were observed. The UPs were thermally stable up to temperatures of 255 °C ($T_{5\%}$). The authors suggested that these UPs could be suitable for coating applications.

Although the polycondensation reaction catalyzed by metals is the common method used in the industry and in most academic reports dealing with the preparation of UPs, in the last years the enzyme-catalyzed polycondensation has gained increasing importance.

Olson and Shears [8] prepared unsaturated aliphatic polyesters by polycondensation of *trans*- β -hydromuconic acid (HMA) with several diols (C₄ to C₁₀, and DEG) using enzyme (Lipase B from *Candida Antarctica* (CALB)) and metal-based catalysts (Figure 14). The use of AA as the second diacid was also tested. HMA was the selected unsaturated diacid because it is not prone to the side reactions commonly associated with FA. The UPs prepared from this monomer usually present higher molecular weights. The UPs

resulting from the reaction of HMA with the different diols were obtained in high yields, with molecular weights between 2500 to 10500 g/mol, and \bar{D} below 2. The highest molecular weight was obtained from the enzyme catalyzed reaction of HMA with the C₈ diol. The UP also showed to be thermally stable up to temperatures of approximately 320 °C. When AA was used as comonomer, the enzyme catalyzed reaction has also shown to be effective in producing UPs with higher molecular weights when compared with those obtained from the metal-catalyzed reaction, for the same reaction time (13000 g/mol vs 11600 g/mol). The T_m of all the prepared UPs was found to be dependent on the length of the diol, being higher when diols with longer aliphatic chains were used. Another UP, from DEG and HMA, was also prepared, being liquid at ambient temperature with a T_g of -40 °C.

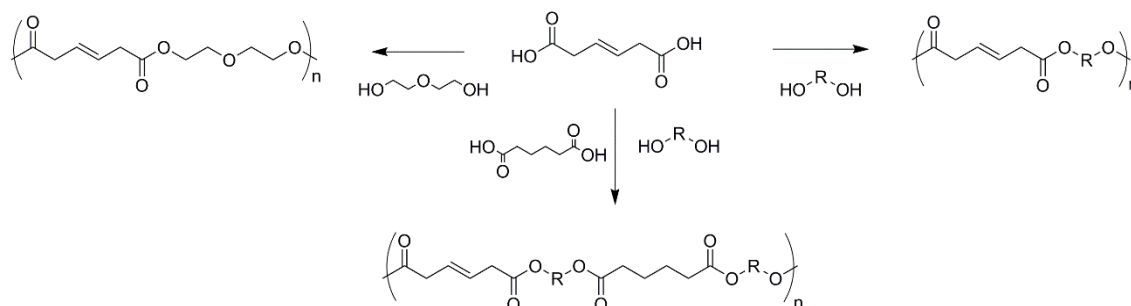


Figure 14. Synthesis of HMA homopolymers, HMA-adipic acid copolymers and of HMA and diethylene glycol poly(ester ether)s adapted from [8].

In another contribution, Naves and co-workers [73] reported the polycondensation of IS or isomannide (IM) with diethyl adipate and different unsaturated diesters, *viz.* diethyl fumarate (FU), diethyl itaconate (IT), diethyl *trans*-glutaconate (GL) and diethyl *trans*- β -hydromuconate (HM) (Figure 15), using CALB as catalyst.

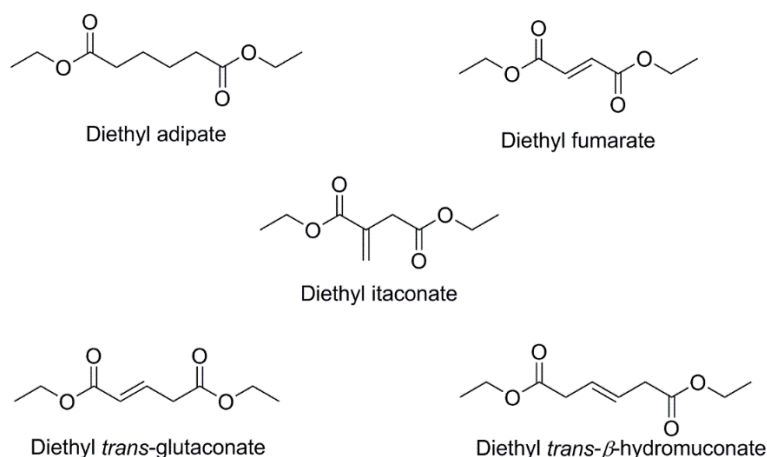


Figure 15. Structures of the synthesized diesters, diethyl adipate, diethyl fumarate, diethyl itaconate, diethyl *trans*-glutaconate and diethyl *trans*- β -hydromuconate used for further transesterification reaction with isosorbide or isomannide.

The UPs based on IM showed higher molecular weights, but lower isolated yields, than their IS based counterparts. The UP with the highest molecular weight was obtained when FU was used as the unsaturated diacid; a decrease in the UPs' molecular weight was observed for increasing chain lengths of the unsaturated diacid. The same method of synthesis was used with less sterically hindered diols, namely 1,4-butanediol and 1,6-hexanediol, and it was found that the molecular weights obtained were very close to that presented by the UPs prepared from IS and IM. The matrix-assisted laser desorption/ionization-time of flight (MALDI-TOF) analysis showed unequivocally the presence of the double bonds, making the materials good candidates to be used in crosslinking reactions.

Jiang and co-workers [63] synthesized biobased UPs by the polymerization of diethyl succinate, dimethyl itaconate and 1,4-butanediol in solution, by a two-stage method (Figure 16), in the presence of CALB.

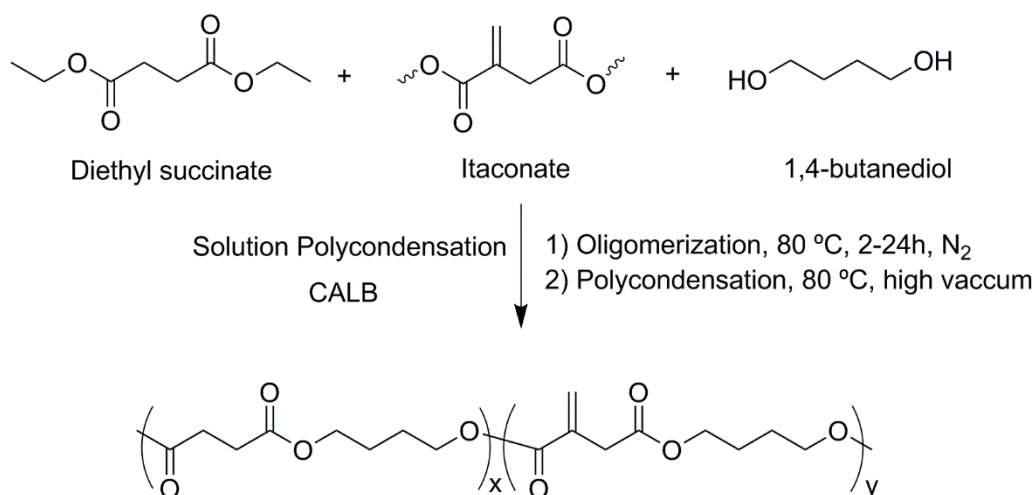


Figure 16. Preparation of the UPs by the two-step solution polycondensation, adapted from [63].

The use of diphenyl ether as the solvent allowed the preparation of UPs with higher molecular weight, when compared to that obtained with the other used solvents (diglyme and dodecane). The best result in terms of molecular weight (ca. 13000 g/mol) and yield (90%) was obtained for the UP prepared with a molar feed amount of IT of 15 %. The NMR analysis showed that the amount of double bonds can be easily changed by using different amounts of dimethyl itaconate (up to 35 % mol). The results provided by the thermal analysis showed that the amount of dimethyl itaconate had no significant influence on the T_g (a variation of 3°C was observed) nor on the thermal stability. In turn,

the T_m revealed an almost linear decrease, with the increasing amount of dimethyl itaconate (from ca. 115 °C to 70 °C).

The same research group [64] reported the enzymatic synthesis, using the same enzyme, of poly(butylene succinate-co-itaconate) (PBSI) making use of three different methods: two-stage melt polymerization, azeotropic polymerization using cyclohexane/toluene as solvent, and two-stage solution polymerization in diphenyl ether. The authors reported that when the dialkyl esters (dimethyl itaconate and diethyl succinate) were replaced by the respective dicarboxylic acids (ITA and SuCA) only oligomeric species were obtained. When using dialkyl esters, the best results in terms of molecular weight and yields were obtained with the azeotropic distillation method. In this case, it was possible to use molar feed amounts of dimethyl itaconate up to 50 %. As previously noted [63], a decrease in the crystallinity of the UP was observed with increasing amounts of the itaconate moieties. The UPs were crosslinked via a hot press method, in the presence of dicumyl peroxide. The resulting crosslinked materials have shown to be brittle, presenting high tensile strain and low rupture strain.

Very recently, Jiang and co-workers [62] enlarged the library of biobased UPs, making use of the two-stage enzymatic polycondensation (catalyzed by CALB) previously reported [63, 64]. The authors prepared various polyesters using 1,4-butanediol, dimethyl itaconate and diacid ethyl esters with different chain lengths. The results showed CALB presents the highest specificity for diethyl adipate, among all the tested diacid ethyl esters. The thermal properties showed to be dependent on the length of the diacid ethyl ester used. The UV curing reaction was performed using Irgacure 184 and the thermomechanical properties (T_g , Young modulus', tensile stress, and rupture strain) of the cured film could be easily adjusted and tuned by controlling the amount of itaconate moieties in the UPs structure.

Another work, reported by Tsujimoto and co-workers [74], used enzymatic polymerization between divinyl esters and glycerol in the presence of unsaturated fatty acids to develop biodegradable crosslinking polyesters. In this study different lipases were tested as catalyst, namely, *Candida Antarctica* (CA), *Mucor miehei* (MM), and *Pseudomonas cepacia* (PC). The comparison between the activity of the three lipases, revealed that CA lipase was the best in promoting the polycondensation. The UPs were able to be crosslinked in the absence of UM, using two methods: (i) catalytic oxidation in air, using cobalt naphthenate, and (ii) thermal treatment (150 °C, 2 h). The film obtained from the UP made from divinyl sebacate and linoleic acid was subjected to the BOD test in an activated sludge. The results highlight the gradual degradation of the film, and after 42 days the percentage of biodegradation of the film was 45%. The same enzymatic polymerization was used to synthesize polyesters based on divinyl sebacate, glycerol

and unsaturated fatty acids or epoxidized fatty acids [75]. The polyesters bearing the unsaturated polyesters were further epoxidized in the presence of CA lipase. This work showed that the enzymatic polymerization can be carried out using both unsaturated or epoxidized moieties. The crosslinking reaction was carried out as previously presented [74] and the biodegradability of the films (assessed by the BOD test) showed a percentage of biodegradation near 50%, after 50 days of test.

Recently, Goerz and Ritter [76] crosslinked biobased UPs made from IA, IS and SA in the presence of *N*-alkylated dinitrones based on IS (Figure 17). The results obtained showed that the new dinitrones were very effective in promoting the crosslinking of the biobased UPs via a 1,3-dipolar cycloaddition.

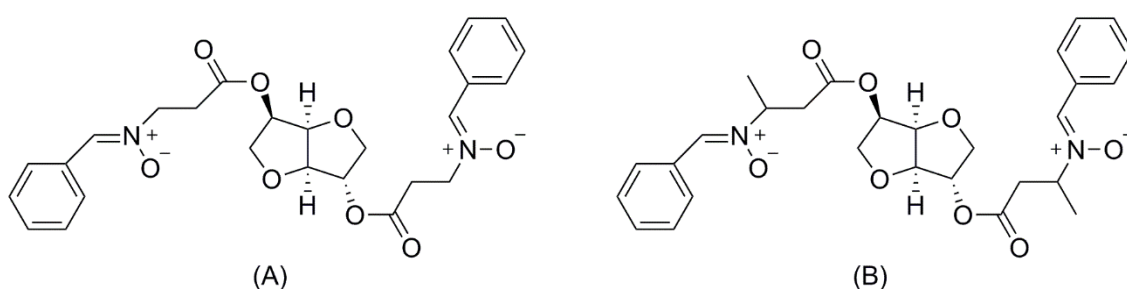


Figure 17. Structures of the *N*-alkylated dinitrones based on IS, adapted from [76].

Another important class of renewable monomers that has been used in the development of UPs are the cinnamic acid derivatives. These compounds can undergo [2+2] cycloaddition reactions under UV irradiation ($\lambda > 260$ nm), forming photoreversible crosslinks. Thus, the polymers comprising these derivatives in their structure are photoresponsive [77, 78]. Dong and co-workers [79] developed new biodegradable polyesters by the polycondensation reaction of 3,4-dihydroxycinnamic acid (DHCA), obtained from lignin, and 10-hydroxycaproic acid (HDA), obtained from the castor oil (Figure 18). The authors evaluated how the properties of the UPs were affected by the amount of each monomer in the polymer chain. An increase in the amount of HDA led to more flexible materials and was also shown to improve the elongation at break of the UPs. The UPs were further crosslinked by UV irradiation ($\lambda > 320$ nm) and their mechanical properties were also studied. The crosslinked UPs showed improved tensile strength, but low elongation at break. The *in vitro* hydrolytic degradation tests revealed that the UPs were able to be degraded. Surprisingly, the degradation rate was higher for the crosslinked UPs.

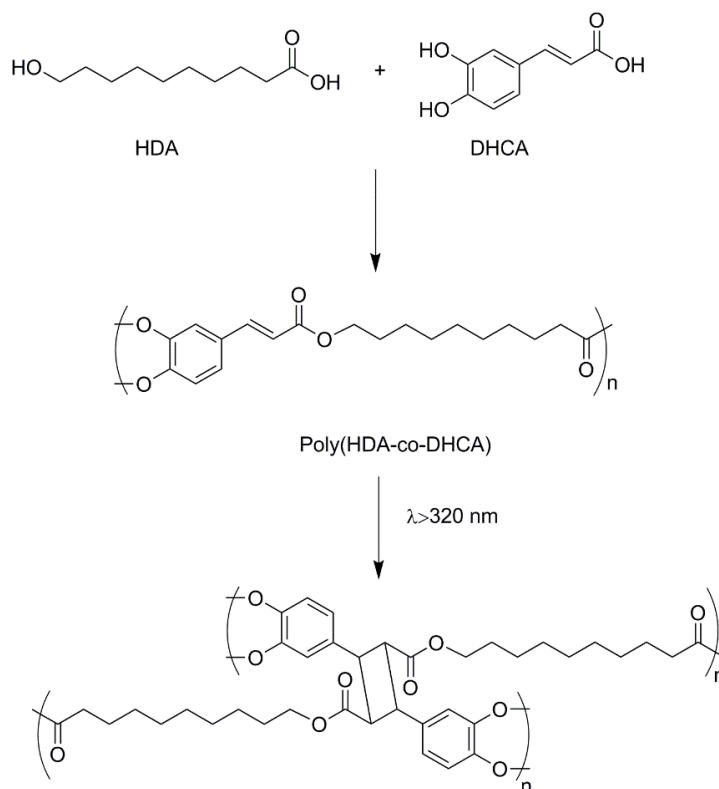


Figure 18. Scheme of the synthesis of poly (DHCA-HDA) and photoreaction of the DHCA moiety promoted by UV irradiation, adapted from [79].

The preparation of copolymers based on cinnamic acid derivatives and PLLA [80-82] has also been reported, and different approaches have been used. In a very interesting report, Thi and co-workers [81] used the -OH terminal group of PLLA to attach 3,4-diacetoxycinnamoyl chloride (DACC), to yield DACC-PLLA. The ensuing polymers showed excellent thermal stability when compared to neat PLLA (an increase of about 100 °C in the thermal stability was observed). Also, the DACC-PLLAs revealed the ability to undergo [2+2] cycloaddition reactions when irradiated with UV light with $\lambda > 280$ nm (Figure 19).

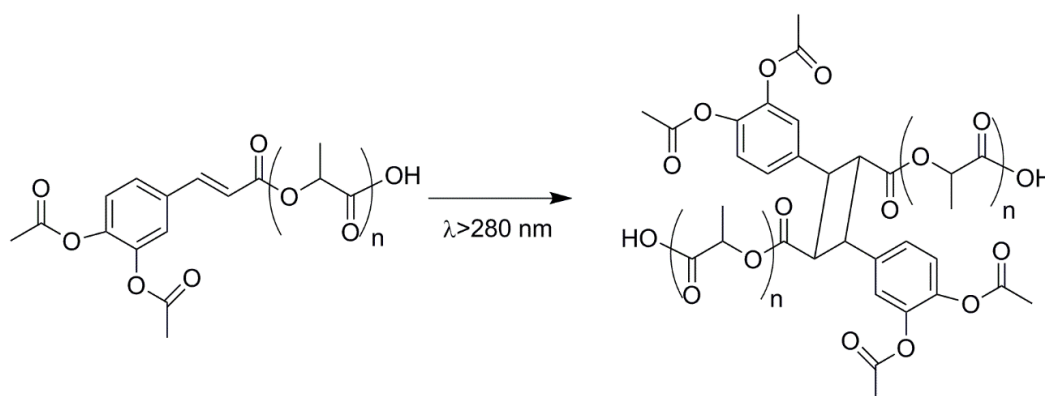


Figure 19. Photoreaction scheme of DACC-PLLA by UV irradiation at $\lambda > 280$ nm, adapted from [81].

The properties of UPs can also be tailored through the manipulation of their double. One of the strategies to accomplish such modifications is based on the so called *click-chemistry*. In this context, Ates and co-workers [84] proposed the functionalization of polyesters using thiol-ene click reactions on UPs that were obtained from the ROP of unsaturated macrolactone globalide (GI), derived from non-toxic fatty acids. The ROP of globalide was promoted by the use CALB and then polyglobalide (PGI) was functionalized with compounds, *viz.* 6-mercapto-1-hexanol (MH), butyl-3-mercaptopropionate (BMP) and N-acetylcysteamine (nACA) (Figure 21).

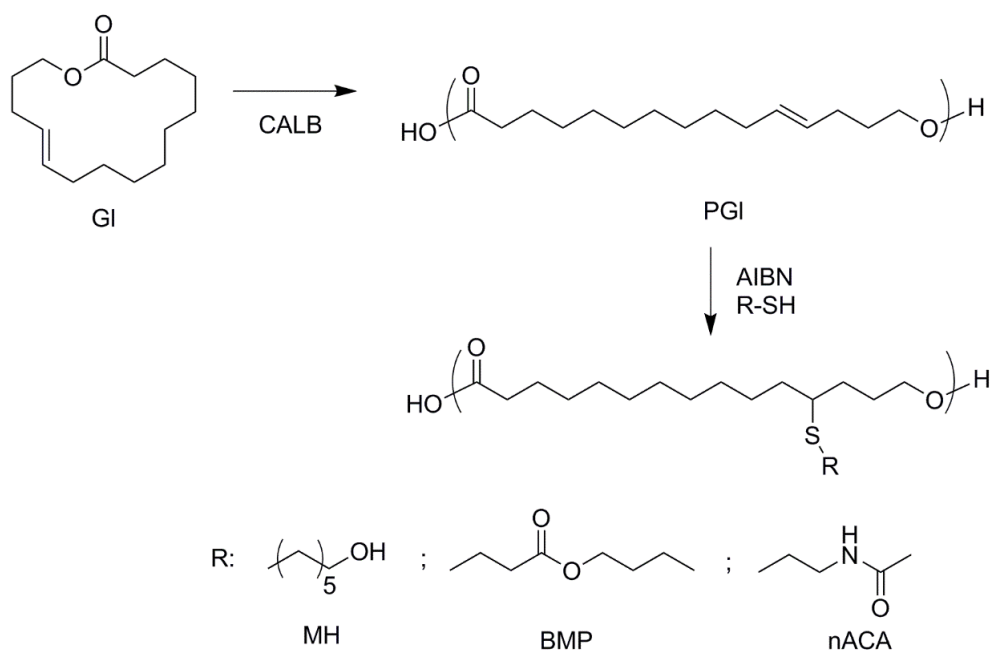


Figure 21. ROP of globalide and thiol-ene reaction of PGI with MH, BMP and nACA, adapted from [84].

The different moieties used were able to introduce diverse chemical groups in the side chain of the UP. The use of MH led to the obtainment of an UP with $-\text{OH}$ pendent groups. In the case of BMP and nACA, the authors foresaw the possibility of obtaining UPs with $-\text{COOH}$ or $-\text{NH}_2$ groups, respectively. Additionally, the authors believe that this approach could be very useful in preparing a vast range of polymeric materials with potential application in the biomedical field.

Chanda and Ramakrishnan [14], demonstrated that it is possible to modify the double bonds of the UPs bearing itaconate moieties using Michael addition reactions. Different UPs were prepared *via* bulk transesterification of dibutyl itaconate with different diols, *viz.* 1,12-dodecanediol, 1,20-icosanediol, 1,4-cyclohexane dimethanol (CDM) and PEG, in the presence of dibutyltin dilaurate. The ^1H NMR analysis of the obtained UPs showed that the double bonds remained intact after the reaction, enabling a further

functionalization, with different thiols and amines (Figure 22). The ^1H NMR analysis of the products suggested a quantitative functionalization.

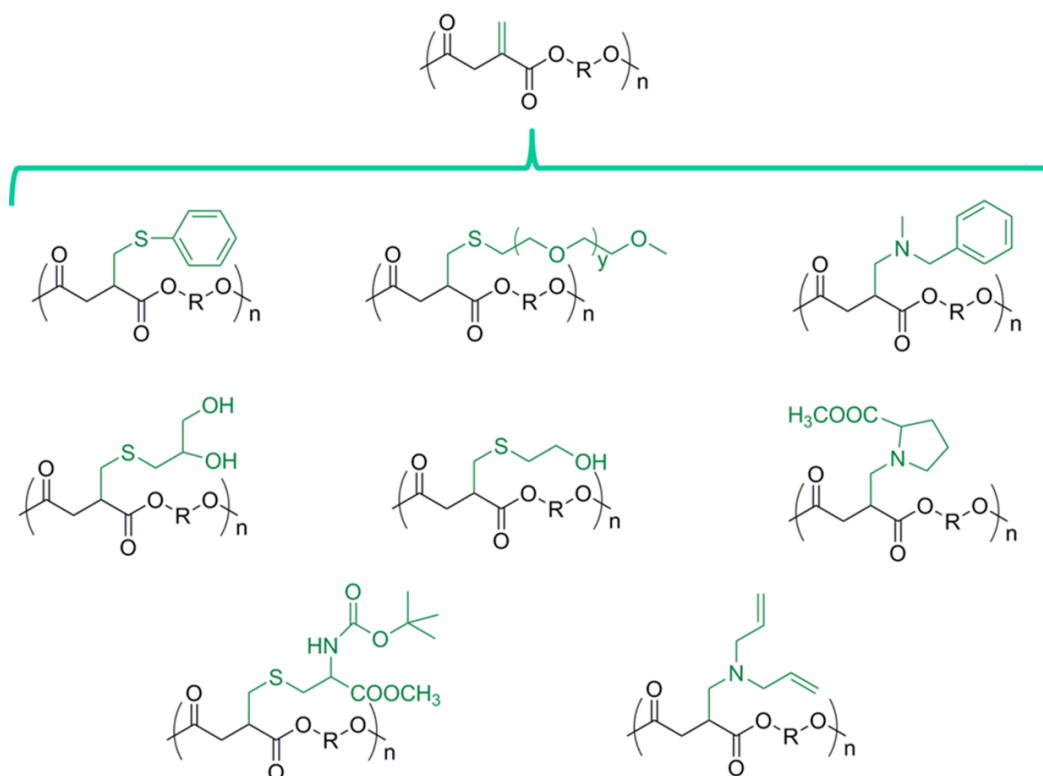


Figure 22. Structures of the derivatives prepared using Michael addition reactions, adapted from [14].

Another type of modification that has been used is related with the epoxidation of the UPs double bonds, as already seen in Section 2.3. Roumanet and co-workers [85] synthesized oleic acid based UPs *via* bulk polycondensation of 1,18-(Z)-octadec-9-enedioic acid (D18:1) with different glycols (1,3PG, 1,8-octanediol, 1,9-nonanediol, 1,10-decanediol, 1,12-dodecanediol). UPs with molecular weights ranging from 7000 to 20000 g/mol were obtained, with T_m ranging from 21 °C to 45 °C, being the lowest and highest value registered for the UPs with 1,6-hexanediol and 1,12-dodecanediol in the structure, respectively. The double bonds of the UP were then modified with epoxy groups through the reaction of the UP with *m*-chloroperbenzoic acid (mCPBA). The crosslinking reaction was then performed (by the formation of ether bridges), using UV light (photocrosslinking) and an iodonium salt as the photoinitiator. Transparent and highly cured films (< 5% of extractables) were obtained. The films were subjected to enzymatic degradation (pH=7.4, 37 °C) in the presence of *Rhizopus Arrhizus* lipase. Results showed no significant degradation after 8 weeks which could be attributed to the highly hydrophobic nature of the films.

Kolb and Meier reported some interesting data related to the modification of saturated fatty acid methyl esters (FAMEs) [86] and proposed new methodologies for the modification of polyesters bearing pendant double bonds (Figure 23) [87] *via* cross-metathesis with acrylates or *via* thiol-ene coupling modifications. The results proved that the methods used were efficient to introduce new functional groups on the structure of the polyester that could be used to tune their thermophysical properties.

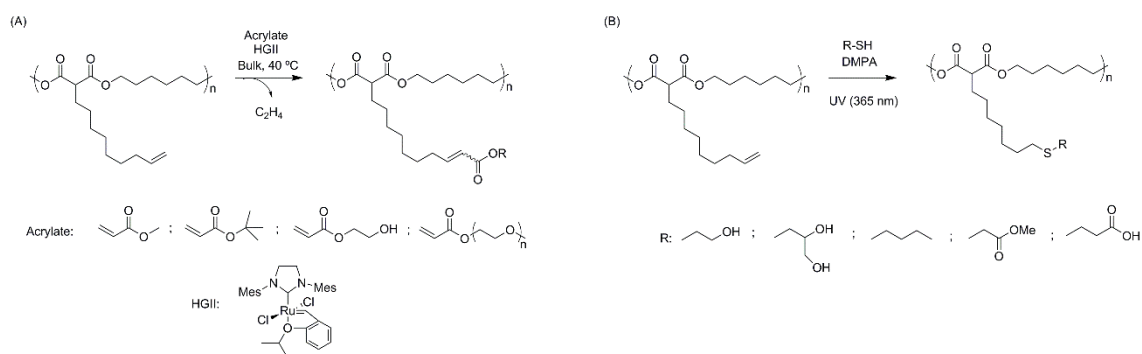


Figure 23. Polymer-functionalization via ruthenium-catalyzed olefin-metathesis (A), and *via* thiol-ene addition reaction (B), adapted from [87].

Regarding the development of partially biobased UPRs, Olson and co-workers [88] prepared unsaturated poly(ester ether)s, using the methodology previously presented by the same research group [8], and used the ensuing polymers in the preparation of biodegradable elastomers. The unsaturated polymers were thermally crosslinked in the presence of BPO and *N*-vinylpyrrolidone (NVP) as UM, to yield elastomeric films. Additionally, the materials were also fabricated into more complex forms with micropatterned surfaces making use of the lithography techniques. Overall, the results indicated that, depending on their composition, the crosslinked structures can be obtained with different *in vitro* degradation profiles (from 30 days to 6 months) and also with a vast range of mechanical properties (Young modulus' ranged from 0.2 to 20 MPa). In another contribution, Tang and Takasu [89] developed UPRs bearing itaconate and maleate moieties through bulk polycondensation of MA and itaconic anhydride with 3-methyl-1,5-pentanediol, in the presence of bis(nonafluorobutanesulfonyl)imide, under mild conditions (60 °C, 12 h, vacuum). The preparation of UPRs from the UPRs encompassed two steps. First, a diamine was added to a mixture containing the UPR, methyl methacrylate (MMA) and a UV-initiator. By means of Michael addition reaction, in particular through the reaction of the maleate units in the UPR with the diamine, it was possible to obtain a single gel network (SN). Interestingly, it was found that the itaconate moieties did not participate in this reaction. Next, the mixture was subjected to UV irradiation, and the reaction of the itaconate moieties with MMA led to the formation of

the UPR (DN gel) (Figure 24). It was found that the ensuing UPR had high mechanical strength and exhibited shape memory properties. The authors suggested that this material could be useful in different areas but did not reference any specific application.

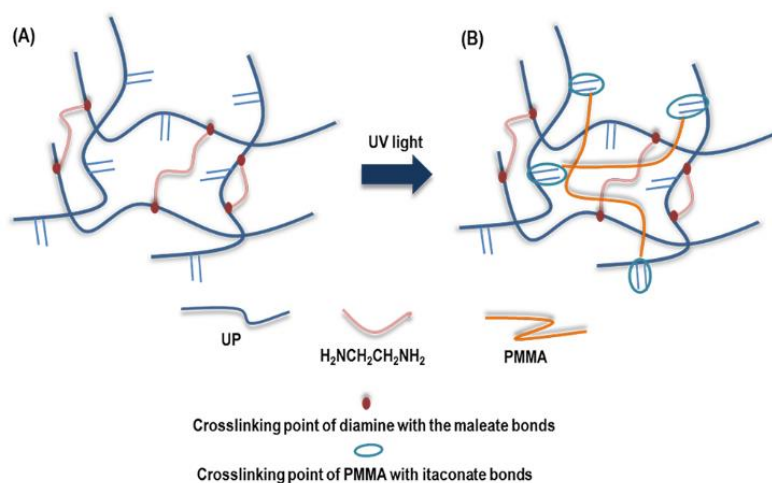


Figure 24. Representation of the SN (A), and of the DN (B), adapted from [89].

Jasinska and Koning [90] prepared UPs from IS, SuCA and MA *via* thermal polycondensation in the presence of titanium(IV) *n*-butoxide [72]. The UPs showed a slightly branched structure that could result from the reaction of IS hydroxyl groups with the double bonds. The UPs, however, showed good thermal stability ($T_{5\%}$ above 260 °C) and high T_g values (52 to 76 °C). The UPs were further crosslinked in the presence of 2-butanone peroxide as initiator and cobalt (II) 2-ethylhexanoate as accelerator; styrene was replaced for less toxic monomers, *viz.* 2-hydroxyethyl methacrylate (HEMA), NVP, methacrylamide and AcA. UPRs with high T_g (60 to 103 °C) were obtained and it was found that those were thermally stable up to 200 °C.

In another work, UPs with ‘high green content’, making use of different biobased monomers (e.g., ITA, FA, IS, SeBA) were prepared by Fonseca and co-workers [11] and crosslinked with HEMA. The UPs were prepared through bulk polycondensation in the absence of catalysts. The cure reaction was carried out at 80 °C, using BPO as initiator. It was found that when IA was used as the unsaturated diacid, UPs with branched structures were obtained, as inferred by the high values of \bar{D} (>4). The UPRs presented high gel contents (>70 %), being the highest values obtained for the formulations with higher amounts of HEMA. The DMTA showed the existence of two transitions, indicating the presence of different domains within the UPR structure. Swelling tests were also carried out, and it was found that 20% was the maximum value attained, indicating that the UPRs have a highly hydrophobic nature. Additionally, the *in vitro* degradation tests (pH=7.4, 37 °C) showed that the UPRs are hardly degraded under the tested conditions. The maximum weight loss was 9%, after 50 days.

In the last years, the use of vegetable oils, or their derivatives, in the preparation of new UPs and UPRs has gained significant interest in the scientific community. The oils were used both as monomers in the preparation of the UPs [65, 66, 91, 92] or in blends with commercial UPRs to increase their biobased content [67, 93]. To be used as monomers in the UPs synthesis, the vegetable oils primarily undergo an alcoholysis reaction (Figure 25) with glycerol [65, 66, 91, 92], to yield a monoglyceride that is subsequently used in the polycondensation reactions.

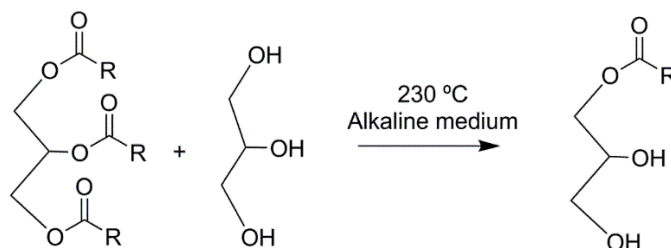


Figure 25. Alcoholysis reaction to yield a polyol based on vegetable oils.

In a study by Mahmoud and co-workers [66], palm oil (PO) based UPRs were prepared and characterized. The PO based monoglyceride was made to react with MA, in the presence of 2-methylimidazole. The ensuing UP was then mixed with styrene (30 %wt) and UV-crosslinked, using Irgacure 184 as the photoinitiator. The results showed that the UPRs prepared from the UPs with 3 eq. of MA relatively to the monoglyceride showed the highest value of gel content and the best mechanical performance (high values of tensile strength and toughness). In another interesting contribution, UPs made from glycerol, 1,4-butanediol and IA were prepared and were mixed with acrylated epoxidized soybean oil and water, in order to obtain stable waterborne dispersions [94]. The dispersions were then photocrosslinked in the presence of Irgacure 2959 and triethanolamine, as the initiator and accelerator, respectively. The authors tested the potential of the material to be used as a coating and the overall results showed that the crosslinked UPs presented excellent adhesion, high flexibility, and improved solvent resistance.

2.5 UPs and UPRs directed to biomedical applications

The double bonds in the UPs structure, as previously discussed, can be easily modified using different approaches. This particularity is very advantageous in the biomedical context because it enables the attachment of specific moieties that could enhance the properties of the final material. The fact that some UPs can be crosslinked in the absence

of UMs is also very promising since the use of hazardous UMs is avoided. Nevertheless, and as it will be described in this section, efforts have been made to produce UPRs with less toxic monomers or with macromers based on biocompatible materials. This subsection aims to present the most relevant works related with the use of UPs and UPRs in biomedical applications (e.g., tissue engineering or drug delivery systems).

Kharas and co-workers reported the synthesis of fumarate-based UP to be used in bioresorbable bone cement composites, replacing poly(methyl methacrylate) (PMMA), which is currently used in clinical practice [95]. The UPs were prepared by polycondensation of diethyl fumarate and different diols, namely 1,2-propanediol (PD), (S)-(+)-1,2-propanediol (SPD), 2-methyl-1,3-propanediol (MPD) and 2,2-dimethyl-1,3-propanediol (DMD). Different catalysts, namely PTSA, AlCl_3 , TiCl_4 , $\text{Ti}(\text{OC}_4\text{H}_9)_4$, and ZnCl_2 , were also tested. The results suggested the possibility of controlling the UP structure and the extent of the side reactions by choosing the proper catalyst. For instance, the polycondensation of the monomers in the presence of PTSA led to branched UPs due to the occurrence of side reactions (between the hydroxyl groups and the double bonds), whereas in the presence of metallic catalysts an UP with a more regular structure and with high amounts of double bonds was obtained. After the polycondensation, the UPs were mixed with NVP, BPO and inorganic filler, $\text{CaSO}_4 \cdot 2\text{H}_2\text{O}$, and cured to obtain a composite able to be used as a bone replacement material. The results showed that the composite presenting higher compressive strength and modulus was the one obtained based on the UP synthesized from PD in the presence of ZnCl_2 . This fact was ascribed to the higher content of double bonds of this UP, that led to a more crosslinked composite, and also to the unbranched nature of the glycol used. The *in vitro* degradation tests (pH=7.4, 37 °C) revealed that both the UPs obtained from branched glycols and the unbranched UPs (based on the polycondensation in the presence of metallic catalysts) are less susceptible to hydrolysis. Regarding the composites, it was found that those are less susceptible to hydrolysis than the corresponding uncrosslinked UPs. Nevertheless, the mass loss tendency observed, was the same both for composites and their uncrosslinked counterparts.

Recently, Śmiga-Matuszowicz and co-workers [13] also reported a work in the field of UPRs as bone substitutes. The authors prepared porous scaffolds from the crosslinking reaction of poly(3-allyloxy-1,2-propylene succinate) (PSAGE) with oligo(isosorbide maleate) (OMIS) and a small amount of MMA, in the presence of BPO and *N,N'*-dimethyl-*p*-toluidine, as the initiator and accelerator, respectively. The foaming system used comprised calcium carbonate and L-LA or pyruvic acid. The results showed that the maximum temperature observed during the crosslinking reaction was 43 °C, and the crosslinked porous structure was able to be formed within 15 minutes. It was found that

the scaffolds exhibited mechanical properties (e.g., compressive modulus and strength) similar to the trabecular bone. The *in vitro* cytotoxicity tests carried out with human fetal osteoblasts (hFOB1.19) cell line revealed that, after 24 h, the percentage of viable cells was between 77 and 99 %. Upon incubation in a phosphate buffered saline solution (pH=7.4, 37 °C) it was found that the porous scaffolds lose 40% of their initial weight after 26 weeks of degradation. Additionally, the scanning electron microscopy (SEM) analysis revealed that, after 3 hours of incubation, a crystal layer resembling apatite was formed at the surface of the scaffold. Considering the obtained results, the authors suggested that these materials can be used as fillers for bone voids.

Guo and co-workers [96] developed new UPs *viz.* poly(fumaric acid-glycol-dodecanedioic acid) (P(FA-GLY-DDDA)) copolymers, poly(fumaric acid-glycol-brassylic acid) (P(FA-GLY-BA)) copolymers, poly(fumaric acid-glycol-tetradecanedioic acid) (P(FA-GLY-TA)) copolymers and poly(fumaric acid-glycol-pentadecanedioic acid) (P(FA-GLY-PA)) copolymers. These were prepared in high yields by melt polycondensation of the corresponding monomers. The UPs were subsequently mixed with MMA, a dimer acid, and with BPO-triethylamine system, and it was found that the ensuing formulation was able to gel at temperatures close to human body temperatures. In terms of application in the biomedical field, the gels obtained from P(FA-GLY-BA) have shown to be the most promising, considering its degradation profile (pH=7.4, 37 °C), its lack of toxicity when implanted in mice, and the release profile of hydrophilic drugs. Additionally, it was also found that the gels obtained from this UP (with a specific molar composition of 1.75FA/2.20 GLY/0.25BA) when used to encapsulate adriamycin hydrochloride were able to enhance the anti-tumor efficacy of the drug, as revealed by the *in vivo* tests carried out on mice bearing Sarcoma-180 tumor. In a subsequent work, Guo and co-workers [97] reported the use of poly(fumaric acid-glycol-sebacic acid) (P(FA-GLY-SA)) copolymers and poly(maleic anhydride-glycol-sebacic acid) (P(MA-GLY-SA)) for the same purpose. The gels of both UPs have shown to be biocompatible and suitable for applications related with the drug delivery for cancer therapy.

Doulabi and co-workers [98] developed poly(ethylene glycol-co-fumarate) (PEGF) macromers to be used in the preparation of hydrogels. The macromers were prepared from PEG (1000 g/mol and 4000 g/mol) and fumaric acid, at 50 °C, in the presence of the system dicyclohexylcarbodiimide (DCC)/dimethylaminopyridine (DMAP) as the condensation promoter (Figure 26). The crystallinity and T_m were shown to be higher for the macromers prepared from PEG with high molecular weight.

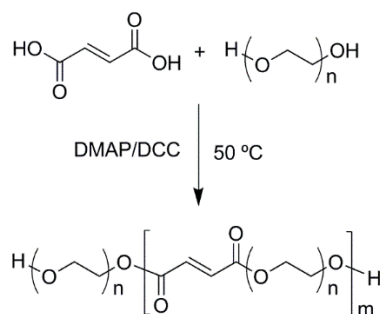


Figure 26. Reaction of PEG with fumaric acid in the presence of DMAP/DCC, adapted from [98].

The hydrogels were prepared in the presence of a crosslinking agent, NVP, using a water-soluble redox system comprising ammonium persulphate/*N, N, N', N'*-tetramethylethylenediamine as initiator. It was found that the gelation time to produce the hydrogels decreased with the increase in the PEG molecular weight. The swelling capacity was also higher for the hydrogels prepared from the macromers with PEG of high molecular weight.

In a different approach, Wang and co-workers [99] prepared a set of self-crosslinkable and biodegradable UPs from poly(ϵ -caprolactone-*co*-fumarate) (PCLF), poly(ethylene glycol-*co*-fumarate) (PEGF) and their copolymer PEGF-*co*-PCLF. The PCLF and PEGF were prepared from the reaction of the PCL-diol or PEG with fumaryl chloride, in the presence of K₂CO₃, as the proton scavenger. The copolymer was prepared in the same way, making use of the PCLF and PEGF macrodiols previously obtained (Figure 27).

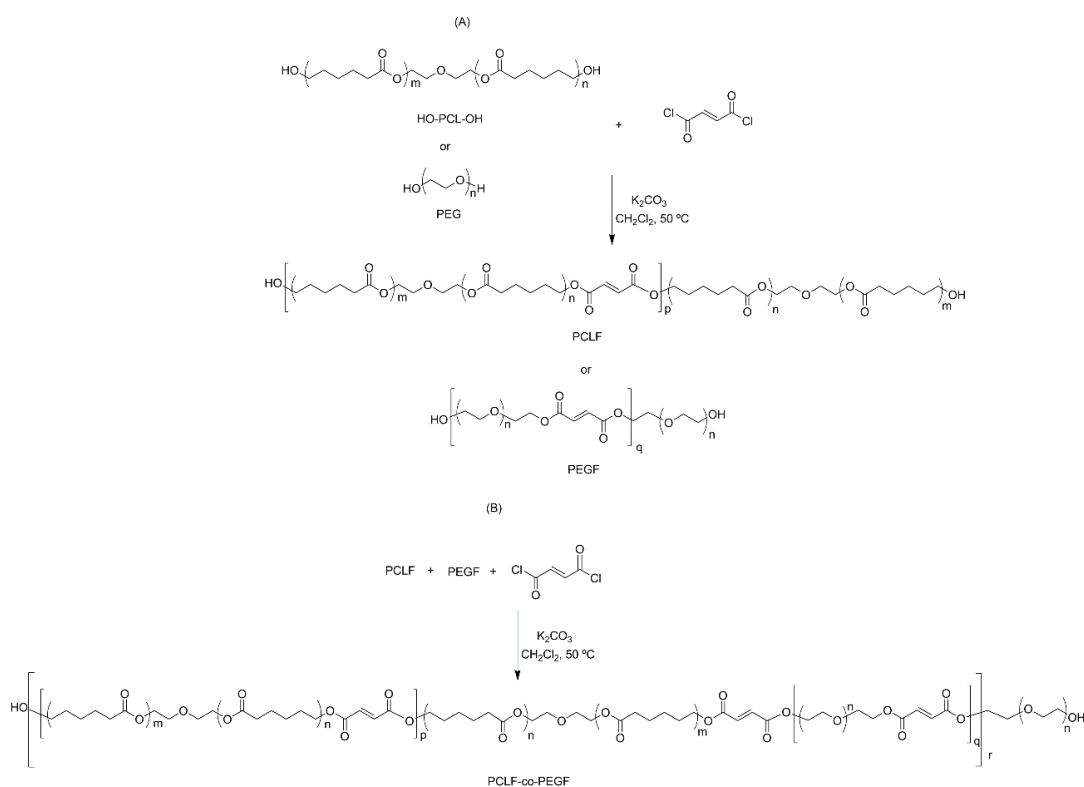


Figure 27. Synthesis of: (A) PCLF, PEGF, and (B) PEGF-*co*-PCLF, adapted from [99].

The prepared UPs were able to be thermally or photocrosslinked, without the addition of a crosslinking agent. The authors suggested that these UP could be useful in the preparation of diverse materials for biomedical applications.

PCLF was used by Sharifi and co-workers [100] in the development of an *in situ* forming drug delivery system for tamoxifen citrate (TC), an anti-cancer drug. The networks were prepared *via* photocrosslinking using camphorquinone (CQ) and dimethyl-*p*-toluidine as the initiator and accelerator, respectively, and NVP as the crosslinking agent. Increasing the NVP content up to 16 %wt, led to an increase in the gel yield and a decrease in the swelling capacity. Above this value, the increment of the NVP concentration in the formulation did not translate in an increase of the gel yield, remaining some of the monomer unreacted. The *in vitro* cytotoxicity tests carried out on MCF-7 and L929 cell lines showed that the PCLF based networks containing 10 %wt NVP had no adverse effects on the cells. However, when PCLF/10%NVP networks were loaded with TC, it was observed that 40-60% of the cells were killed after 72 h of incubation.

In another approach, Sharifi and co-workers [101] synthesized novel self-crosslinkable and biodegradable polymers, namely poly(hexamethylene carbonate-fumarate) (PHMCF) and poly(hexamethylene carbonate) diacrylate (PHMCA), and their amphiphilic copolymers with PEG, poly(ethylene glycol fumarate-co-hexamethylene carbonate-fumarate) (PEGF-co-PHMCF). The synthetic route to obtain polymers was similar to that proposed by Wang and co-workers [99], but, in this case, instead of K_2CO_3 , propylene oxide was used as the proton scavenger (Figure 28). The developed materials were able to be photocrosslinked, without the addition of a crosslinker or accelerator, and in the presence of camphorquinone (CQ). The *in vitro* cytotoxicity tests showed that the materials did not evoke any cytotoxic effect. The optimization of the photocuring parameters of PHMCF were reported by Mohtaram and co-workers [102]. The photocrosslinking reaction was studied in the presence of CQ (0.5 to 1.5 %wt) and also in the presence of CQ and an amine accelerator, *viz.* dimethylamino methyl ethylacrylate (DMAMEA) (0.5 to 1.5 %wt). The PHMCF has shown to be able to be photocrosslinked with a high degree of conversion (ca. 75 %), in the presence of CQ (1 % wt) and without DMAMEA. The network obtained from this specific photocrosslinking reaction showed the lowest swelling ratio and a total absence of cytotoxicity.

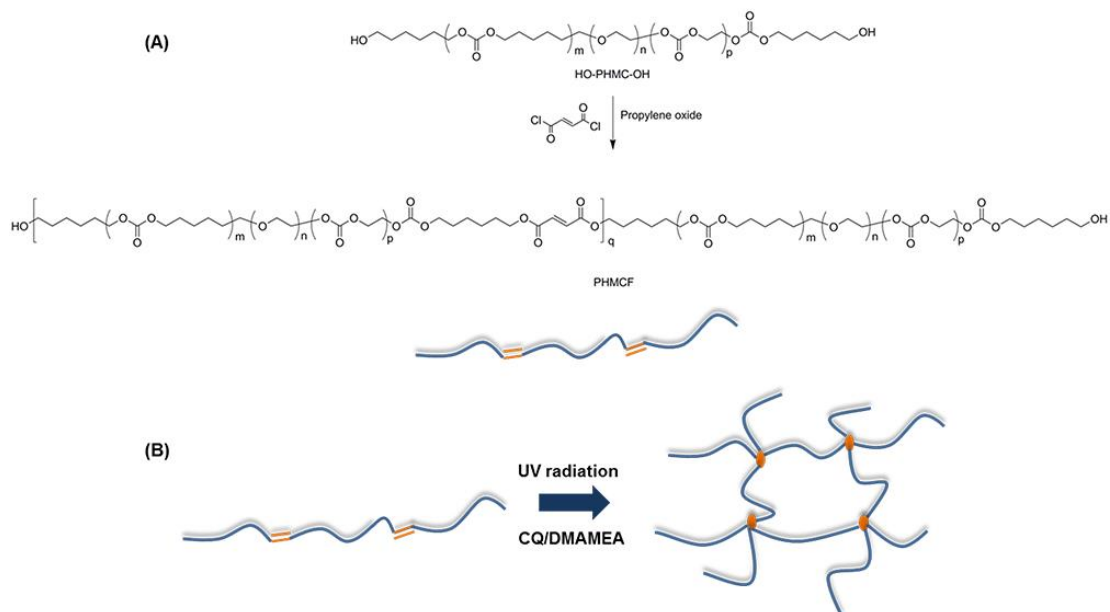


Figure 28. Synthesis of: (A) PHMCF macromers, and (B) respective networks, adapted from [102].

UPs based on itaconic acid (ITA), and the corresponding diester (dimethyl itaconate, DMI), AA, SuCA, and different diols, *viz.* sorbitol (Sorb), TMP, 1,4-cyclohexanedimethanol (CHDM), PEG and 3-methyl-1,5-pentanediol (MPDO) were prepared by Barret and co-workers [103]. Thermal and enzymatic polycondensation (mediated CALB) were used as the polymerization methods with IA and DMI, respectively. Both branched and linear UPs were prepared (Figure 29); the first ones were prepared from the copolymerization of ITA with AA and TMP and from the copolymerization of SuCA Sorb, whereas the second ones resulted from the copolycondensation of DMI with CHDM, PEG and MPDO. The UPs were then photocrosslinked using 2,2-diethoxyacetophenone as the photoinitiator, and poly(ethylene glycol) methyl ether methacrylate (475 g/mol), or 2-(methacryloyloxy)ethyl acetoacetate as the UM. It was shown that the thermomechanical properties can be easily tuned by the choice of the monomers, being the best results obtained for the network based on the UP synthesized from DMI, AA, and MPDO. The materials have also shown to have low cytotoxicity, making them good candidates to be used in biomedical applications. Moreover, the suitability of the UPs to be used in imprint lithographic techniques was also shown.

Chapter I

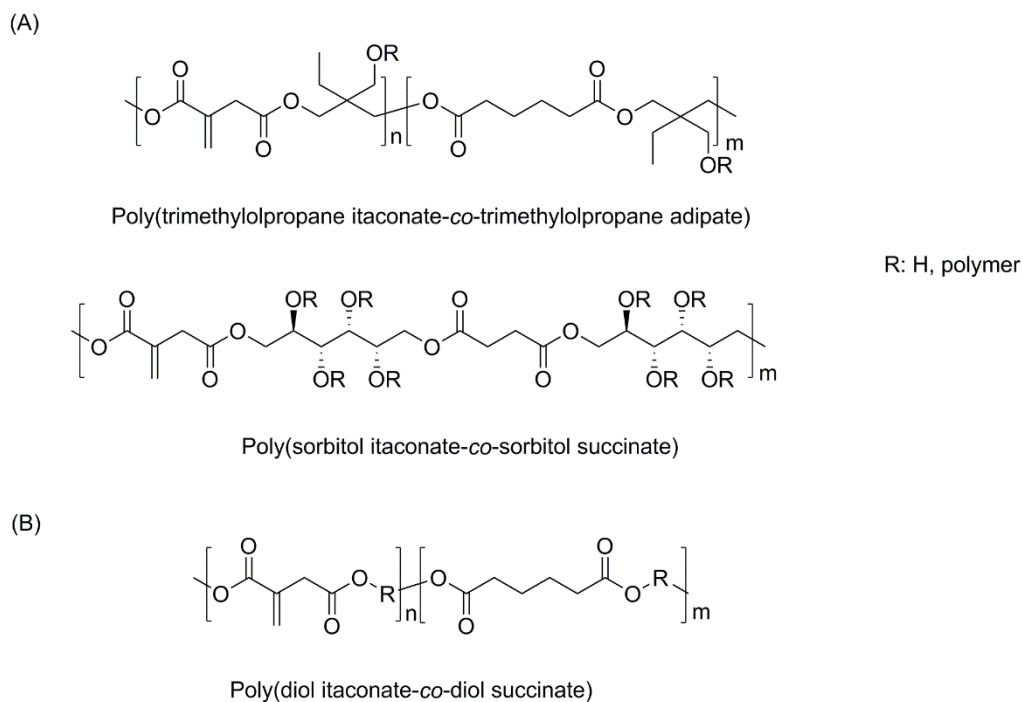


Figure 29. Branched polyesters obtained by thermal polyesterification (A) and the photocurable polymer achieved by enzymatic polymerization (B) using CALB as catalyst.

In another approach, Brown and co-workers [104] reported the synthesis of aliphatic UPs with potential application in the biomedical field making use of a new dicarboxylic acids and anhydrides (Figure 30A), obtained from the Diels-Alder reaction of FA and MA with several dienes. This synthetic route allowed to afford new monomers with diverse functionalities, *viz.* ether and amine, that were preserved in the UP structure, after the polycondensation reaction with 1,8-octanediol, in the presence of $\text{Sn}(\text{Oct})_2$ (Figure 29B). All the UPs were amorphous, with T_g ranging from -30 to -15 °C. The UPs were liquid at room temperature, and were able to self-crosslink in the presence of α,α' -azoisobutyronitrile (AIBN), at 130 °C (Figure 30C), yielding degradable elastomeric materials. These structures were evaluated in terms of their *in vitro* cytotoxicity, and the results showed that only the elastomer prepared from the UP containing the anhydride III (Figure 30A) evoked a cytotoxic response. The remaining elastomers have shown to be non-cytotoxic.

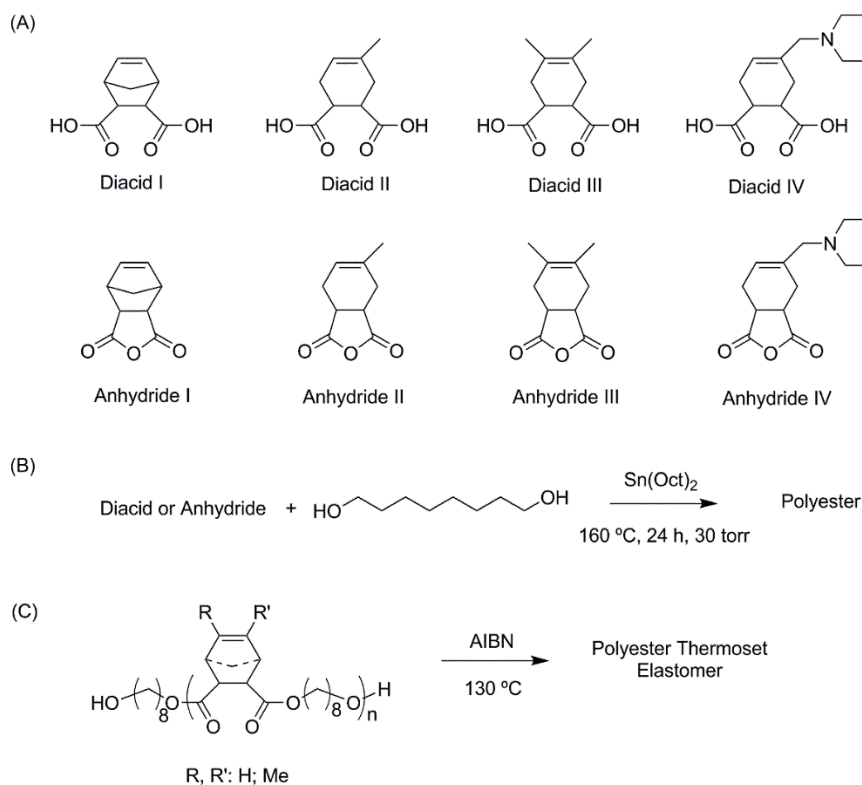


Figure 30. (A) Unsaturated dicarboxylic monomers synthesized for the preparation of new unsaturated aliphatic polyesters, (B) overall strategy for the synthesis of polyesters, and (C) synthesis strategy for polyester thermoset elastomer, adapted from [104].

The previous sections of this manuscript described the different strategies available in the literature to afford UPs and UPRs with tunable properties (e.g., thermomechanical, biodegradability, etc.) for biomedical applications. Despite their huge potential, the design and production of 3D scaffolds using these materials remains very limited due to the processing techniques employed. The introduction of AM in the field of Tissue Engineering (TE) opens the possibility to generate 3D matrices with complex shapes, reproducible internal/external architectures, interconnected network of pores and multiple materials. In the next sections of this contribution, the rationale behind TE and AM processes is presented with especial emphasis in stereolithographic systems.

3. Scaffold-based tissue engineering

Tissue engineering (TE) represents an emerging multidisciplinary scientific field where principles of biology, medicine, materials and engineering are combined with the aim of developing artificial bio-implants for the regeneration/repair of damaged tissues and organs. The most common strategy in TE (scaffold based TE strategy) comprises the combined use of cells and scaffolds to promote and enhance the healing process of the native tissues (Figure 31).

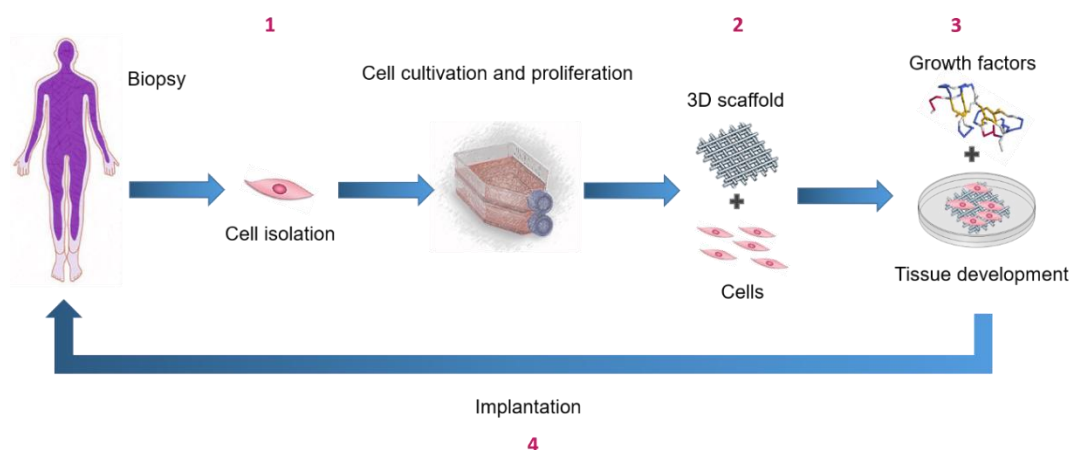


Figure 31. Illustration of the four main steps in scaffold based TE strategy. 1) Cell harvesting and *in vitro* expansion; 2) cell seeding in porous scaffolds; 3) *in vitro* dynamic cell culture using bioreactors; 4) scaffold+cell construct implantation.

Most of cell lines used in TE are anchorage dependent, which means they will need a support template. For this reason, scaffolds play a major role in TE acting as a temporary biomechanical support to accommodate cells and promote the guided regeneration of the neo tissue [105]. The capacity of scaffolds to retain and deliver cells and biological molecules, promote the adequate diffusion of cell nutrients, oxygen and vascularization are fundamental aspects inherent to the regeneration process of tissues [106-111]. Due to the multi-functionality of human tissues, it becomes very complex, if not impossible, to define which are the parameters of an ideal scaffold, even for a single tissue [112]. These considerations are complex and include chemical, morphological, mechanical and biological aspects, as well their time dependence. Despite this complexity, there seems to be a general agreement on which are the essential requirements for a TE scaffold [106-108, 110]:

- **Biocompatibility:** The material, pre- and post-processing, must interact positively with the biological environment without triggering any adverse host tissue response [113-115];
- **Biodegradability:** The degradation rate of the scaffolds must be controlled and should ideally match the regeneration rate of the native tissue. The degradation products must not be toxic for cells [116-118];
- **Porosity, micro and macro-structure:** Ideally, the scaffolds should be highly porous to enhance cell adhesion and proliferation as well neo vascularisation. Adequate porosity is also required in order to enhance the biomechanical coupling between the native tissue and implant [119, 120];
- **Pore size and geometry:** Pore size and geometry are strongly related with the adhesion, proliferation and differentiation of cells. According to the literature it is

possible to find different pore sizes and geometries according to different cell lines [121-123];

- *Mechanical Resistance:* Scaffolds must be able to withstand mechanical stresses both *in vitro* as *in vivo*. During the regeneration process of the neo tissue the scaffolds should gradually transfer the loads to the neo tissue hence promoting the correct healing mechanism;
- *External macro geometry:* The adequate biomechanical coupling between the scaffold and the tissue can only be achieved if the scaffold possesses an appropriate external dimension and geometry that lead to the correct distribution of stresses and the scaffold/tissue interface [106, 107, 110, 115, 116];
- *Easily manufactured and sterilized:* the scaffolds should be manufactured rapidly with high precision and reproducibility. Chemical or physical sterilization processes should be employed to easily sterilize the structures.
- *Adequate surface topography:* Surface topography is of outmost importance during the adhesion, proliferation and differentiation of cells. The scale, shape and orientation of the topography may have an effective control on the viability and phenotype expression of cells [124-126].

The mechanical, chemical and biological behavior of scaffolds are determined both by the intrinsic properties of the biomaterials as well the manufacturing processes used for their fabrication. In this sense, different technologies have been developed with the aim of producing scaffolds with optimized properties for TE applications.

3.1 Manufacturing Technologies

Currently, it is possible to identify and classify the existing technologies into two major groups: conventional and non-conventional technologies.

3.1.1 Conventional technologies

Since the early days of TE, conventional technologies have been extensively used and with relative success in the fabrication of scaffolds. These methodologies include [106, 127-130]:

- Salt leaching;
- Lyophilisation;
- Supercritical fluids;
- Moulding;
- Electrospinning;

These processes are generally quite simple from an implementation point of view enabling the production of highly porous structures. Despite this simplicity, they do not allow for a perfect control over the pore size, geometry and spatial distribution, leading to the generation of 3D structures with limited or inexistent pore channel interconnectivity. Besides the abovementioned limitations of these so-called conventional techniques, the use of toxic organic solvents and long fabrication times are other drawbacks that must be considered. Therefore, additive fabrication techniques are gaining increasing importance in the fabrication of 3D structures with customised external shape and predefined internal morphology, allowing good control of pore size and distribution.

3.1.2 Non-conventional technologies (Additive Manufacturing)

Non-conventional or Additive Manufacturing (AM) technologies represent a group of techniques recently introduced in the medical field. Besides the high reproducibility and elevated capacity to quickly produce very complex 3D shapes, these techniques enable the fabrication of scaffolds with good control over pore size and distribution increasing the vascularisation and mass transport of oxygen and nutrients throughout the scaffold [131-133]. The rationale behind AM technologies is based on the use of two-dimensional data (2D) obtained from the slicing process of 3D models created *via* CAD (Computer Aided Manufacturing) systems to physically reproduce 3D objects in a layer-by-layer fashion [134]. Figure 32 illustrates the main steps required to produce TE scaffolds using AM techniques.

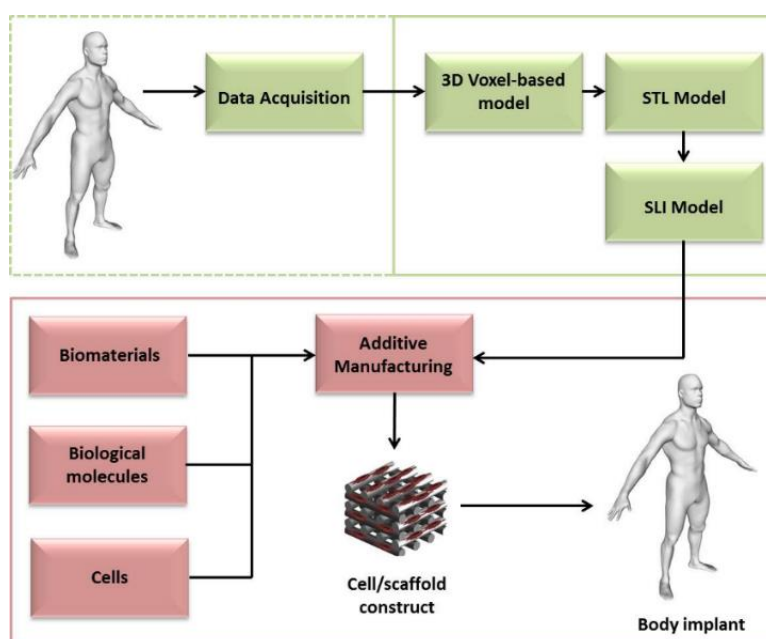


Figure 32. Schematic representation of the main steps required to produce TE scaffolds using AM techniques, adapted from [135-140].

The first stage requires the generation of the 3D solid model to be produced. This model can either be obtained directly from 3D CAD software, imported from 3D scanners or from medical imaging data (computed tomography, magnetic resonance, ultra sounds, etc.) [135].

The CAD model is then tessellated into an STL model. This operation consists on the approximation of the model surfaces through a mesh of triangular elements. Finally, the STL model is mathematically sliced into layers of homogeneous thickness (SLI file) and sent for production in one of the available AM techniques. The main advantages of AM techniques rely on the capacity of the systems to physically reproduce very complex 3D objects with relatively high speed and employing a wide range of materials. Through the combination of AM techniques with imaging data it is possible to produce personalized structures with optimal internal/external geometries, which will enhance the biomechanical coupling between the implant and the native tissue at the site of the defect. Figure 33 illustrates some customized implants produced *via* AM techniques.

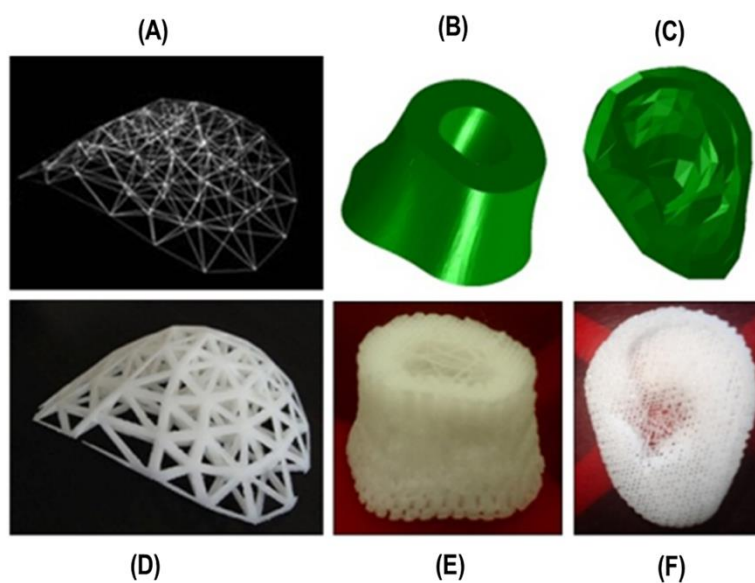


Figure 33. 3D CAD and physical models produced *via* melt extrusion. (A) 3D CAD model of breast implant; (B) 3D CAD model of humerus bone; (C) 3D CAD model of human ear; (D) 3D physical model of breast implant; (E) 3D physical model of humerus bone; (F) 3D physical model of human ear [141].

Some of these processes can operate at room temperature, with relatively low mechanical work hence enabling the production of 3D hydrogel-based constructs with embedded cells (Figure 34).

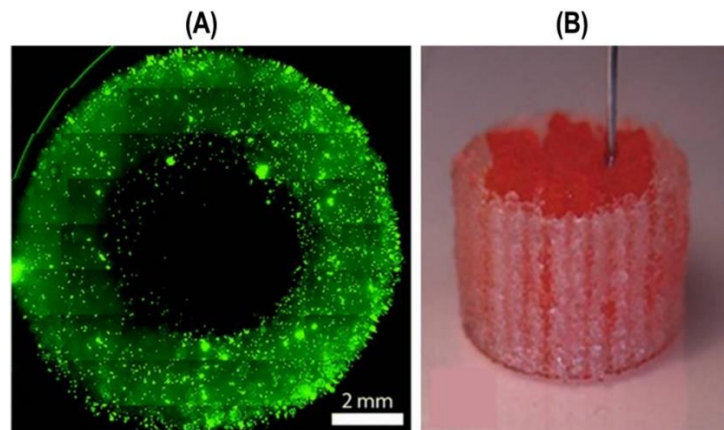


Figure 34. Constructs with embedded cells. (A) PEG-co-PDP copolymer hydrogels with HUVECs encapsulated cells prepared via stereolithography (SLA). (B) gelatin/alginate/fibrinogen containing adipose-derived stem cells (in pink) and hepatocytes in gelatin/alginate/chitosan (white) [142, 143].

Depending on the application, AM techniques allow for the direct or indirect production of 3D scaffolds. The last, requires the generation of a lost mould where the biomaterial can be deposited and give shape to the scaffold (Figure 35). The existing or under development AM techniques employed in TE comprise:

- Stereolithographic processes;
- Sintering processes;
- Extrusion;
- Inkjet Printing;

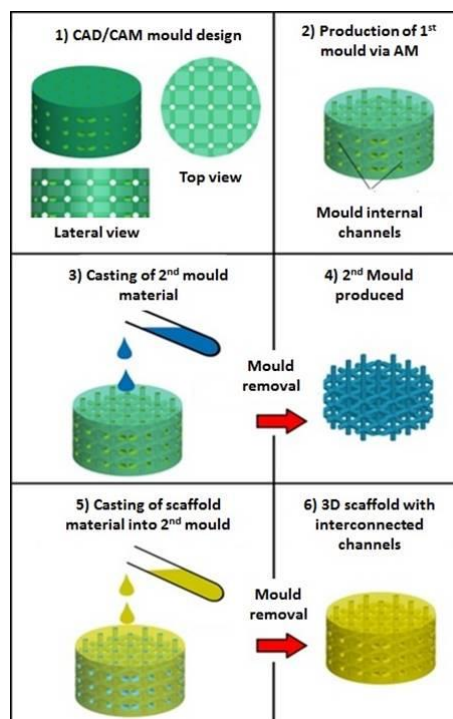


Figure 35. Methodology for indirect fabrication of TE scaffolds, adapted from [144].

The next section revises the main stereolithographic processes, principles and applications, as well recent advances in micro and multi material systems to produce TE scaffolds.

3.1.3 Stereolithographic processes

The AM stereolithographic processes, initially proposed by Hull and Pomerantz, involve the selective solidification of photosensitive resins [145, 146]. Currently, stereolithographic processes comprise two distinct irradiation methods (Figure 36):

- Mask irradiation;
- Direct irradiation;

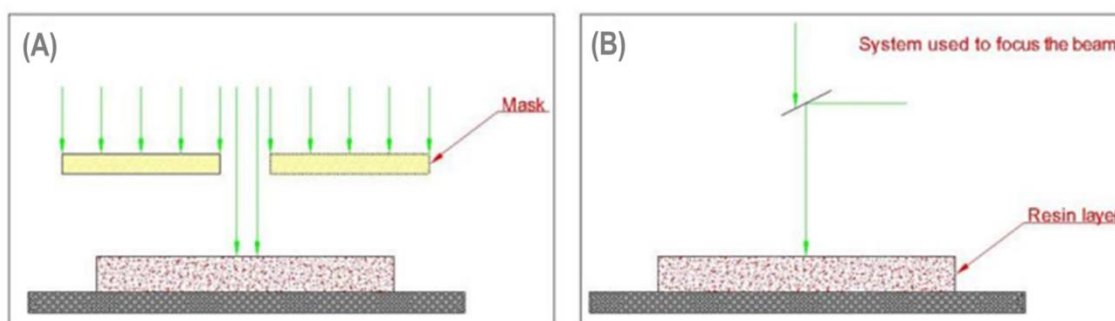


Figure 36. Conventional stereolithography: Mask-based method (A); Direct or laser writing method (B), adapted from [147].

In the first method, each layer of the polymer is solidified *via* exposure to UV radiation, generated by a lamp and transmitted through a mask with transparent areas corresponding to the section of the model to be fabricated. This strategy can also be designated as integrative fabrication method as each layer is produced in full at once [147]. In the second method, also called vector photo-fabrication, a laser is employed to polymerize, point by point each layer of the polymer hence defining the cross section of the 3D object. The direct irradiation system is composed of a vat containing a photosensitive polymer, a movable platform where the model is built, a laser irradiating UV light and a dynamic optical system to direct the laser along the polymeric layer (Figure 37). After the construction of each layer, the platform lowers inside the vat containing the polymer promoting the deposition of a non-crosslinked polymeric film upon which the next layer will be generated.

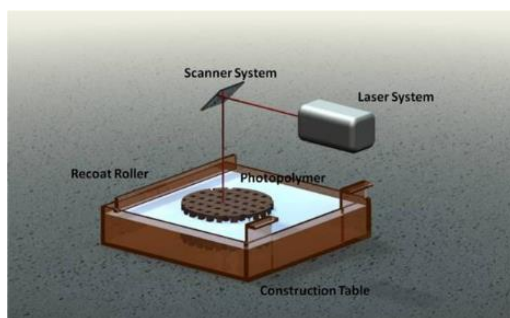


Figure 37. Schematic representation of SLA system [141].

The methods described above comprise polymerization mechanisms (solidification or cure of liquid resins) through the absorption of a single radiation photon. However, there are processes based on the use of femtosecond laser emitting IR, where the polymeric system is solidified through a reaction ignited by the absorption of two radiation photons. This process is designated two-photon polymerization and enables the curing process to occur inside the polymeric system with nanometric resolution.

Independently from the adopted stereolithographic strategy, two main events occur during the curing reaction, namely gelation and vitrification.

During the curing process, an increase in the T_g of the material may be observed, as a consequence of the increase in the molecular weight and cross-linking density. Generally, it is expected that by increasing the extent of cure, molecular weight and cross-linking will increase, thus removing free chain ends and reducing polymer chain motions [148]. Consequently, the specific volume should decrease with increasing the extent of cure [148], and it might be expected an increase in density and modulus of the material as the conversion increases [147, 149]. The kinetics of the curing process is strongly affected by temperature, light intensity, and resin composition. As reported in the literature [147, 150-152], photoinitiated curing processes are characterized by high initiation rates. Accordingly, volume shrinkage is much slower than the rate of chemical reaction and the system cannot be in volume equilibrium. For this reason, a temporary excess of free volume is generated, thus increasing the mobility of the reactive species in the system. This effect induces higher reaction rates and conversions. Hence, the higher the temperature, light intensity, or initiator concentration, the higher the rate of gel formation which leads to higher conversion [147].

A wide range of materials can be used to produce 3D structures *via* conventional SLA such as agarose, dextran, PEG, polyvinyl acetate (PVA), poly(2-hydroxyethyl methacrylate) (PHEMA), etc. In this case the photo initiators must possess low cytotoxicity, enabling the polymerization of polymeric suspensions containing cells.

Liu and Bhatia [153] have developed a mask irradiation process to produce cell laden constructs with micrometric resolution. In this process, the polymeric solution containing the cells is deposited in the working platform using a syringe (Figure 38).

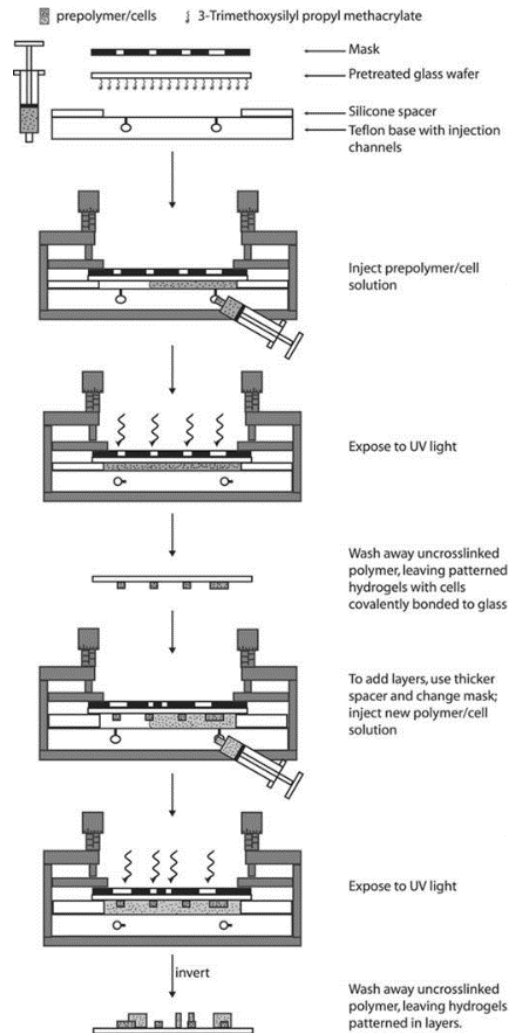


Figure 38. Schematic illustration of the SLA process to produce micrometric resolution constructs containing cells [153].

Chan and co-workers [154] have developed a method to promote cell alignment on three-dimensional hydrogel-based constructs through the combination of micro-contact printing and stereolithography (Figure 39). Fibronectin was initially modified with acrylate groups and then used to pattern glass coverslips with acryl-fibronectin *via* micro patterning technique. Generated patterns were transferred to hydrogels produced *via* SLA and cell alignment investigated using NIH/3T3 mouse embryonic fibroblasts.

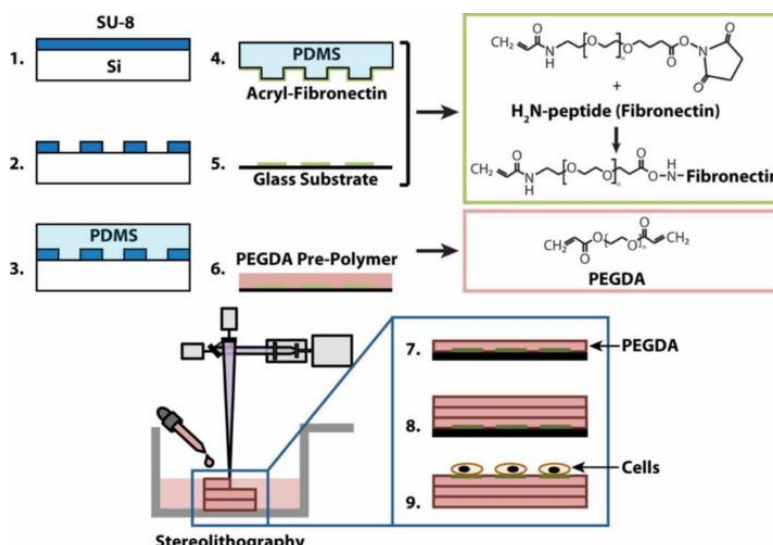


Figure 39. Schematic illustration of the fabrication method used to create patterns of acryl-fibronectin on PEGDA hydrogels produced by SLA [154].

Microstereolithography

Microstereolithography has evolved from conventional stereolithography process and possesses the same operating principles. High resolution 3D objects are built by superimposition of layers, each being produced by a light-induced photopolymerization of a liquid resin [132, 145, 155].

Since 1993 different strategies have been adopted to improve both the vertical (along the building axis) and lateral (in-plane) resolution of the stereolithography process, thus resulting in the development of several machines that can be classified into three categories:

- 1) Scanning microstereolithography systems, which are based on a vector-by-vector tracing of every layer of the object with a light beam;
- 2) Integral microstereolithography processes, which are based on the projection of the image of the layer to be built on the surface of the resin with a high resolution;
- 3) Sub-micron microstereolithography systems, allowing the polymerization of the layers which compose the structure directly inside the reactive medium. The improvement of the resolution is basically related to the reduction of the light-material interaction [156].

All microstereolithography machines are based on the use of a liquid resin that should possess specific characteristics, since it is directly related to the resolution of the object that will be manufactured. One important development in this area was the development of a novel integral SLA system by researchers from the Centre for Rapid and Sustainable Product Development (CDRSP), Portugal. This system comprises a light source

consisting on a 200 Watts mercury lamp with 3 fundamental peaks of irradiation (320-390 nm with radiation intensity of 17 Watts/cm², 390-450 nm with radiation intensity of 20 Watts/cm² and 280-320 nm with radiation intensity of 7 Watts/cm²), a shutter for the radiation on/off, a set of filters and collimating lenses which guarantee the adequate selection of the wave length, a UV radiation DMD (*Digital Micro-Mirror Device* DMD 0.7 XGA 12° DDR, 1024x768 pixel of 14 μm dimension) which enables the micro definition of each cross section to be built, a reduction Zeiss lens (10X maximum reduction) and building moveable platform with a resin vat (Figure 40).

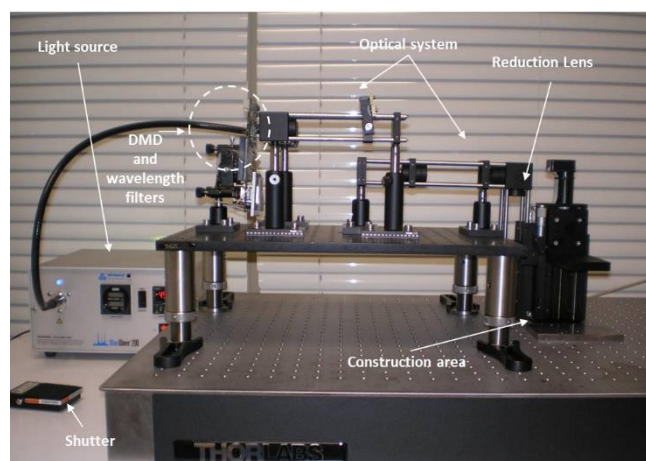


Figure 40. Integral micro-SLA system developed by CDRSP researchers.

This system allows to produce hydrogel-based constructs for TE applications (Figure 41). The structures are formed by physical or covalent reticulation of a liquid polymeric solution transforming it into a solid hydrogel.

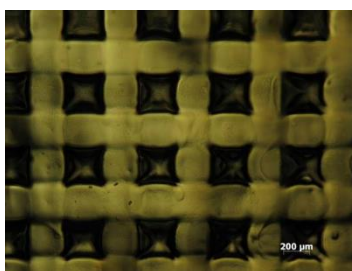


Figure 41. PHEMA 3D scaffold produced *via* SLA.

In the TE field, micro-stereolithography has been used, for example, to produce customized PPF/diethyl fumarate photopolymer 3D scaffolds incorporating BMP-2 loaded poly(lactic-co-glycolic acid) (PLGA) microspheres [157]. In this case, PLGA microspheres were incorporated into a 3D scaffold which was fabricated through a microstereolithography system with a suspension of microspheres and a PPF/DEF photopolymer. The *in vitro* release profiles were assessed, and it was demonstrated that

the produced microsphere-containing 3D scaffold was able to gradually release the growth factor. The biological performance of such multifunctional structures was analysed, confirming that scaffolds produced by micro-stereolithography were superior to traditional structures obtained using particulate leaching/gas foaming method.

Knowing the potential of UPs and UPRs as materials for AM due to the possibility of fine tuning their properties as described in previous sections, our research group developed new bio UPs to be applied in SLA [12]. In this work, the different biobased UPs (Figure 42) were used to prepare scaffolds by micro-SLA, using HEMA as UM and Irgacure 651 as photoinitiator.

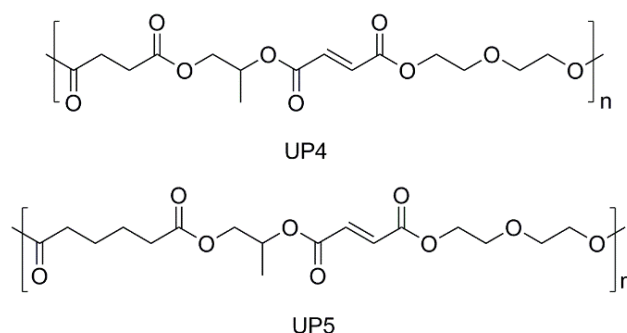


Figure 42. Structures of the UPs developed by Gonçalves and co-workers [12] that were used in the development of scaffolds by micro-SLA.

The obtained structures presented very accurate external geometries (Figure 43), well defined internal pores and nano scale surface roughness, which is very important to promote cell adhesion and proliferation.

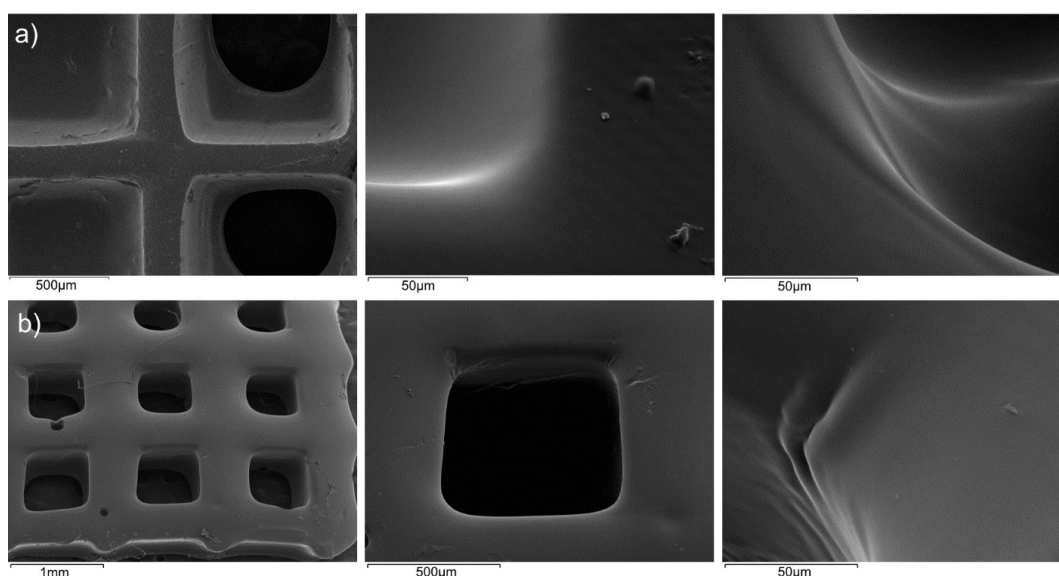


Figure 43. SEM pictures of the scaffolds obtained by micro-SLA a) scaffolds based on UP5/St, with different curing times and b) scaffold based on UP4/HEMA formulation [12].

Stereo-Thermal-Lithography

To manufacture multi-material functionally graded components, researchers from the CDRSP, Portugal have developed a new stereolithographic fabrication process, which is known as stereo-thermal-lithography [147, 158]. This fabrication process uses UV radiation and thermal energy produced by IR radiation to initiate the polymerization reaction in a medium which contains both photo- and thermal-initiators (Figure 44) [147, 158].

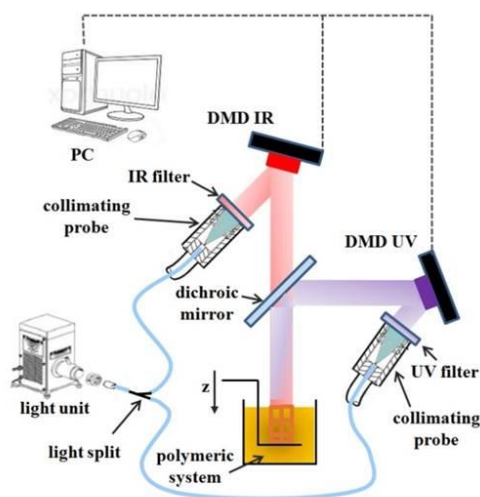


Figure 44. Irradiation process in stereo-thermal-lithography, adapted from [147].

The concentrations of these initiators must be properly selected and the curing process starts when there is a specific combination of thermal and UV radiation energy [147, 158]. The amount of each initiator must be low for inhibiting that the polymerization starts by only one of these two effects.

In this fabrication process, temperature is used to produce both radicals through the thermal decomposition of the initiators, simultaneously increasing the initiation and reaction rate of the photoinitiated curing reaction. Consequently, the extent of cure increases and no post-cure should be needed, thus producing high quality models [147]. If compared to conventional stereolithography, stereo-thermal-lithography presents several advantages such as a more efficient generation of radicals, the use of small concentrations of two different types of initiator which enables the radiation to penetrate deeper into the material, an increase in the reaction rate and fractional conversion values due to the specific combination of UV radiation and temperature, an improvement of the accuracy of the produced models as a consequence of a more localized curing reaction, and a more tunable system [147].

In particular, the overall system may be divided into four subsystems:

- Subsystem A employs UV radiation to solidify a liquid resin containing a specific amount of photoinitiator. It corresponds to an approach which is similar to conventional stereolithography.
- Subsystem B uses thermal energy produced by infrared radiation for solidifying a liquid resin which contains a specific amount of thermal initiator.
- Subsystem C employs both heat produced by infrared radiation and ultraviolet radiation in order to solidify a liquid resin which contains a certain amount of photoinitiator.
- Subsystem D uses both heat produced using infrared radiation and ultraviolet radiation to solidify a liquid resin containing a certain amount of thermal initiator and photoinitiator [147].

Furthermore, the system also contains a rotating multi vat allowing the production of multi-material structures (Figure 45).

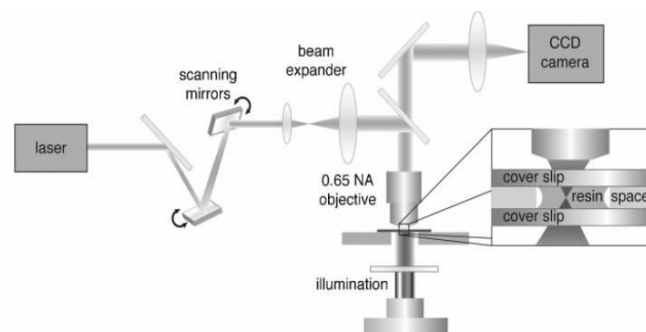


Figure 45. Schematic representation of the stereo-thermal-lithographic process with rotating multi-vat system which allows the production of multi-material constructs (Adapted from [141, 147]).

This should represent an important advancement in developing multi-material functional graded scaffolds for tissue engineering, multi-material microscopic engineering prototypes through nanostructures for different applications in several fields, biomedical components, as well as functional metallic or ceramic parts [147].

Two-Photon-Initiated Polymerization

Two-photon-initiated polymerization may be considered as a useful stereolithographic strategy to fabricate micro/nanoscale structures. Basically, femtosecond laser pulses are focused into the volume of a liquid resin transparent to the infrared radiation without using photomasks (Figure 46) [147, 159-167].

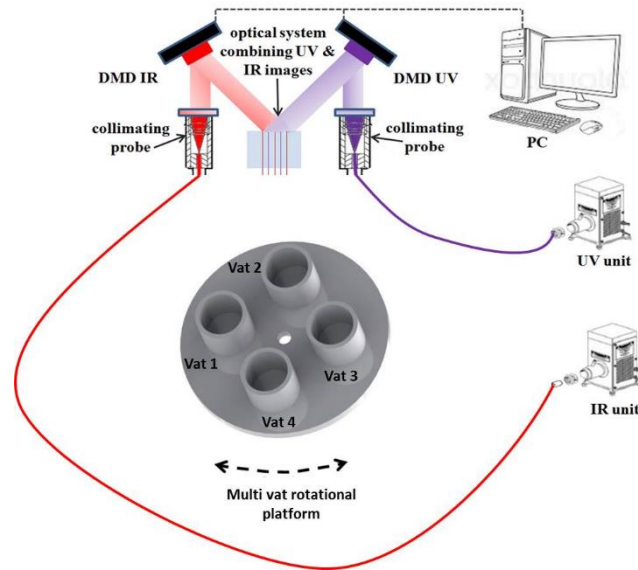


Figure 46. A typical setup for multi-photon polymerization [168].

In this fabrication process, the reactive molecule should be able to simultaneously absorb two photons instead of one as it is excited to a higher singlet state. The process allows a submicron 3D resolution, also allowing 3D fabrication at greater depth and ultra-high speed [147]. Regarding the fabrication of 2D and 3D microstructures with two-photon polymerization, a nano-stereolithography system was also developed (Figure 47) [147, 164].

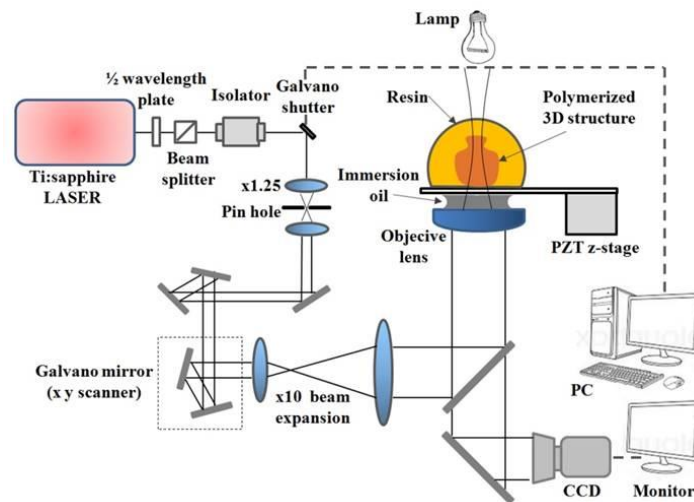


Figure 47. Typical set-up for nano-stereolithographic process, adapted from [147, 164].

It involves the use of a mode-locked Ti:sapphire laser as the light source, providing a wavelength of 780 nm and a pulse width of less than 100 fs at a repetition rate of 80 MHz [102, 169]. The beam is scanned across the focal plane by employing a set of two Galvano-mirrors characterized by a resolution of approximately 2.5 nm per step, and along the vertical axis using a piezoelectric stage. The laser is closely focused into a

volume of photocurable resin with an objective lens. In order to obtain exposure times less than 1 ms, a Galvano-shutter combined with a pin-holed plate is applied [164]. A control program is used to control the shutter, scanner, and piezoelectric stage. A high magnification CCD camera is also employed to monitor the fabrication process [164]. The contour scanning method and the raster scanning method have been considered to produce micro-objects with two-photon polymerization. In the contour scanning method, the contour profile of the microstructure is traced by the laser beam, whilst in the raster scanning method all of the cubic volume containing the microstructure is scanned. The contour scanning method improves the fabrication efficiency, requiring less processing time [164]. In the nanostereolithography process, according to the scanning paths one sliced layer of the 3D microstructure is solidified. After translating the position of the beam spot along the z-axis, another layer is produced. The 3D structure is sequentially produced with this method [164]. Two-photon polymerization using resins which contain conventional initiators have been reported in the literature, even if such polymeric systems exhibit low photosensitivity [147, 166, 170]. Commonly used materials are inorganic–organic hybrid materials whose properties can be suitably tailored benefiting from a combination of the characteristics of their constituents, polymers and inorganic glasses [171, 172].

To sum up, stereolithographic processes present significant advantages to produce TE scaffolds, namely high dimensional accuracy, capability to generate very complex geometries, possibility to use multiple materials and ability to operate at room temperature (or above) for the encapsulation of cells and biological molecules. Significant advances are expected in the next few years with the integration of different technologies into a single hybrid system capable of replicating the nano, micro and macro features of the tissues, introducing biomimetic functional gradients and improving the overall regeneration process.

4. Conclusions and Outlook

Recently, the development of new UP based materials have received enormous interest for biomedical applications, particularly in the development of tailor made 3D structures. These polymers can be successfully used in additive manufacturing due to several important features: biocompatibility, easy synthesis, functional side groups, large availability and fast UV/Vis curing. Although, important developments have been made over the last years regarding the synthesis of UP, their full use in AM requires important research efforts to overcome some existing issues. On this matter, the full absence of toxicity compounds used during the synthesis, the exclusive use of compounds that are

authorized by regulatory agencies, the stringent control over the characteristics of the UP for effective AM (e.g., viscosity), the fine adjustment of the mechanical properties of the final 3D scaffolds for specific applications, the optimization of cell attachment, growth and proliferation are of the utmost importance.

More than ever, the technologies involving the synthesis of these new polymers and the design/conception of the AM equipment require a combined knowledge and articulated efforts to generate complex well defined scaffolds. These synergic research efforts are expected to allow the preparation of advanced scaffolds materials over the coming years with increasing levels of complexity. These materials will also be essential to better understand the mechanism of interaction between the body and the implants, opening avenues for effective solutions that can be translated to clinical practice.

5. References

1. Odian G. *Principles of Polymerization*. New Jersey: John Wiley & Sons, Inc.; 2004.
2. Rogers ME, Long TE. *Synthetic methods in step-growth polymers*. New Jersey: John Wiley & Sons, Inc.; 2003.
3. Varma IK, Albertsson A-C, Rajkhowa R, Srivastava RK. *Enzyme catalyzed synthesis of polyesters*. *Prog Polym Sci*. 2005;30:949-81.
4. Scheirs J, Long TE. *Modern Polyesters: Chemistry and Technology of Polyesters and Copolyesters*. Chichester: John Wiley & Sons, Inc.; 2003.
5. Doulabi ASH, Mirzadeh H, Imani M, Sharifi S, Atai M, Mehdipour-Ataei S. *Synthesis and preparation of biodegradable and visible light crosslinkable unsaturated fumarate-based networks for biomedical applications*. *Polym Adv Technol*. 2008;19:1199-208.
6. Taylor MS, Shalaby SW. Sutures. In: Ratner BD, Hoffman AS, Schoen FJ, Lemons JE, editors. *Biomaterials Science: An Introduction to Materials in Medicine*. Oxford: Academic Press; 2012.
7. Fonseca AC, Ferreira P, Cordeiro RA, Mendonça PV, Góis JR, Gil MH, et al. *Drug delivery systems for predictive medicine: Polymers as tools for advanced applications*. In: Mozaffari MS, editor. *New Strategies to Advance Pre/Diabetes Care: Integrative Approach by PPPM, Advances in Predictive, Preventive and Personalised Medicine 3*. Dordrecht: Springer Science+Business Media; 2013.
8. Olson DA, Sheares VV. *Preparation of unsaturated linear aliphatic polyesters using condensation polymerization*. *Macromolecules*. 2006;39:2808-14.
9. Stevens MP. *Polymer chemistry: an introduction*. 3rd ed. New York: Oxford University Press, Inc.; 1999.
10. Dholakiya B. *Unsaturated polyester resin for specialty applications*. In: Saleh HE-D, editor. <http://www.intechopen.com/books/polyester/unsaturated-polyester-resin-for-specialty-applications>: InTech; 2012.

Chapter I

11. Fonseca AC, Lopes IM, Coelho JFJ, Serra AC. *Synthesis of unsaturated polyesters based on renewable monomers: Structure/properties relationship and crosslinking with 2-hydroxyethyl methacrylate*. React Funct Polym. 2015;97:1-11.
12. Gonçalves FAMM, Costa CSMF, Fabela IGP, Simões PN, Farinha D, Faneca H, et al. *3D printing of new biobased unsaturated polyesters by microstereo-thermal-lithography*. Biofabrication. 2014;6:035024.
13. Śmiga-Matuszowicz M, Janicki B, Jaszcz K, Łukaszczyk J, Kaczmarek M, Lesiak M, et al. *Novel bioactive polyester scaffolds prepared from unsaturated resins based on isosorbide and succinic acid*. Mater Sci Eng, C. 2014;45:64-71.
14. Chanda S, Ramakrishnan S. *Poly(alkylene itaconate)s - an interesting class of polyesters with periodically located exo-chain double bonds susceptible to Michael addition*. Polym Chem. 2015;6:2108-14.
15. Fink JK. *Unsaturated Polyester Resins. Reactive Polymers: Fundamentals and Applications*. New York: William Andrew Publishing; 2005.
16. Dusek K, Duskov-Smrckova M. *Network structure formation during crosslinking of organic coating systems*. Prog Polym Sci. 2000;25:1215-60.
17. Lu MG, Shim MJ, Kim SW. *Curing behavior of an unsaturated polyester system analyzed by Avrami equation*. Thermochemica Acta. 1998;323:37-42.
18. Yang YS, Lee LJ. *Microstructure formation in the cure of unsaturated polyester resins* Polymer. 1988;29:1793-800.
19. Penczek P, Czub P, Pielichowski J. *Unsaturated polyester resins: Chemistry and technology*. Crosslinking in Materials Science. Berlin: Springer-Verlag Berlin; 2005. p. 1-95.
20. Martin JL. *Kinetic analysis of two DSC peaks in the curing of an unsaturated polyester resin catalyzed with methylethylketone peroxide and cobalt octoate*. Polym Eng Sci. 2007;47:62-70.
21. Hsu CP, Lee LJ. *Structure formation during the copolymerization of styrene and unsaturated polyester resin*. Polymer. 1991;32:2263-71.
22. Hong C, Wang X, Pan Z, Zhang Y. *Curing thermodynamics and kinetics of unsaturated polyester resin with different chain length of saturated aliphatic binary carboxylic acid*. J Therm Anal Calorim. 2015;122:427-36.
23. Morel M, Lacoste J, Baba M. *Photo-DSC I: A new tool to study the semi-crystalline polymer accelerated photo-ageing*. Polymer. 2005;46:9274-82.
24. Lee SS, Luciani A, Månson J-AE. *A rheological characterisation technique for fast UV-curable systems*. Prog Org Coat. 2000;38:193-7.
25. Claesson H, Malmström E, Johansson M, Hult A, Doyle M, Månson J-AE. *Rheological behaviour during UV-curing of a star-branched polyester*. Prog Org Coat. 2002;44:63-7.
26. Castell P, Wouters M, Fischer H, de With G. *Kinetic studies of a UV-curable powder coating using photo-DSC, real-time FTIR and rheology*. J Coat Technol Res. 2007;4:411-23.
27. Worzakowska M. *Chemical modification of unsaturated polyesters influence of polyester's structure on thermal and viscoelastic properties of low styrene content copolymers*. J Appl Polym Sci. 2009;114:720-31.
28. Sanchez EMS, Zavaglia CAC, Felisberti MI. *Unsaturated polyester resins: influence of the styrene concentration on the miscibility and mechanical properties*. Polymer. 2000;41:765-9.

29. Matynia T, Worzakowska M, Tamawski W. Synthesis of unsaturated polyesters of increased solubility in styrene. *J Appl Polym Sci.* 2006;101:3143-50.
30. Cherian AB, Thachil ET. Block copolymers of unsaturated polyesters and functional elastomers. *J Appl Polym Sci.* 2004;94:1956-64.
31. Cherian AB, Thachil ET. Modification of unsaturated polyesters using polyethylene glycol. *Plast, Rubber Compos.* 2007;36:128-33.
32. Cherian AB, Abraham BT, Thachil ET. Modification of unsaturated polyester resin by polyurethane prepolymers. *J Appl Polym Sci.* 2006;100:449-56.
33. Rosa VM, Felisberti MI. Unsaturated polyester resin modified with poly(organosiloxanes). I. Preparation, dynamic mechanical properties, and impact resistance. *J Appl Polym Sci.* 2001;81:3272-9.
34. Abbate M, Martuscelli E, Musto P, Ragosta G. A polymer network of unsaturated polyester and bismaleimide resins: Yielding and fracture behaviour. *Die Angewandte Makromolekulare Chemie.* 1996;241:11-29.
35. Gawdzik B, Matynia T, Chmielewska E. Modification of unsaturated polyester resin with bismaleimide. *J Appl Polym Sci.* 2001;82:2003-7.
36. Cherian B, Thachil ET. Synthesis of unsaturated polyester resin - Effect of sequence of addition of reactants. *Polym-Plast Technol Eng.* 2005;44:931-8.
37. Messori M, Toselli M, Pilati F, Tonelli C. Unsaturated polyester resins modified with poly(epsilon-caprolactone)-perfluoropolyethers block copolymers. *Polymer.* 2001;42:9877-85.
38. Nebioglu A, Soucek MD. Investigation of the properties of UV-curing acrylate-terminated unsaturated polyester coatings by utilizing an experimental design methodology. *J Coat Technol Res.* 2007;4:425-33.
39. Nebioglu A, Soucek MD. Microgel formation and thermo-mechanical properties of UV-curing unsaturated polyester acrylates. *J Appl Polym Sci.* 2008;107:2364-74.
40. Tawfik SY. Preparation and characterization of some new unsaturated polyesters based on 3,6-bis(methoxymethyl)durene. *J Appl Polym Sci.* 2001;81:3388-98.
41. Tibiletti L, Longuet C, Ferry L, Coutelen P, Mas A, Robin J-J, et al. Thermal degradation and fire behaviour of unsaturated polyesters filled with metallic oxides. *Polym Degrad Stab.* 2011;96:67-75.
42. Alskas IA, El-Gnidi BA, Azam F. Synthesis and characterization of new unsaturated polyesters containing cyclopentapyrazoline moiety in the main chain. *J Appl Polym Sci.* 2010;115:3727-36.
43. Chiu Y-Y, Saito R, James Lee L. Modification of unsaturated polyester resins for viscosity control. *Polymer.* 1996;37:2179-90.
44. Zhang D, Wang J, Li T, Zhang A, Jia D. Synthesis and characterization of a novel low-viscosity unsaturated hyperbranched polyester resin. *Chem Eng Technol.* 2011;34:119-26.
45. Shenoy MA, D'Mello D, Patil M. Effect of the addition of depolymerised ethylene vinyl acetate on the mechanical, thermal, chemical and shrinkage properties of cured unsaturated polyester resins. *Polym Int.* 2010;59:867-74.
46. Huang Y-J, Liang C-M. Volume shrinkage characteristics in the cure of low-shrink unsaturated polyester resins. *Polymer.* 1996;37:401-12.

Chapter I

47. Saito R, Kan W-MJ, James Lee L. Thickening behaviour and shrinkage control of low profile unsaturated polyester resins. *Polymer*. 1996;37:3567-76.
48. Cao X, Lee LJ. Control of shrinkage and residual styrene of unsaturated polyester resins cured at low temperatures: I. Effect of curing agents. *Polymer*. 2003;44:1893-902.
49. Duliban J. *Novel amine modifiers for unsaturated polyester resins*. *Macromol Mater Eng*. 2001;286:624-33.
50. Duliban J. *Amine modifiers with an s-triazine ring for unsaturated polyester resins, 1*. *Macromol Mater Eng*. 2006;291:137-47.
51. Duliban J. *Amine modifiers with an s-triazine ring for unsaturated polyester resins, 2*. *Macromol Mater Eng*. 2007;292:1126-39.
52. Kucharski M, Duliban J, Chmiel-Szukiewicz E. *Novel amine preaccelerators for polyester resins*. *J Appl Polym Sci*. 2003;89:2973-6.
53. Alemdar N, Erciyes AT, Bicak N. *Preparation of unsaturated polyesters using boric acid as mild catalyst and their sulfonated derivatives as new family of degradable polymer surfactants*. *Polymer*. 2010;51:5044-50.
54. Lou X, Detrembleur C, Lecomte P, Jerome R. *Living ring-opening (co)polymerization of 6,7-dihydro-2(5H)-oxepinone into unsaturated aliphatic polyesters*. *Macromolecules*. 2001;34:5806-11.
55. Cousinet S, Ghadban A, Fleury E, Lortie F, Pascault J-P, Portinha D. *Toward replacement of styrene by bio-based methacrylates in unsaturated polyester resins*. *Eur Polym J*. 2015;67:539-50.
56. La Scala JJ, Sands JM, Orlicki JA, Robinette EJ, Palmese GR. *Fatty acid-based monomers as styrene replacements for liquid molding resins*. *Polymer*. 2004;45:7729-37.
57. Straub T, Brunner M, Koskinen AMP. *Model studies towards alternative cross-linking of unsaturated polyesters*. *Lett Org Chem*. 2005;2:74-6.
58. Cinar H, Tabatabai M, Ritter H. *Bis(nitrone) as crosslinking agent for unsaturated polyesters via 1,3-dipolaric cycloaddition*. *Polym Int*. 2012;61:692-5.
59. Worzakowska M. *Synthesis and characterization of the new unsaturated epoxyoligoester suitable for further modification*. *J Appl Polym Sci*. 2008;109:2973-8.
60. Vilela C, Sousa AF, Fonseca AC, Serra AC, Coelho JFJ, Freire CSR, et al. *The quest for sustainable polyesters - insights into the future*. *Polym Chem*. 2014;5:3119-41.
61. Farmer T, Castle R, Clark J, Macquarrie D. *Synthesis of unsaturated polyester resins from various bio-derived platform molecules*. *Int J Mol Sci*. 2015;16:14912.
62. Jiang Y, Woortman AJJ, Alberda van Ekenstein GOR, Loos K. *Environmentally benign synthesis of saturated and unsaturated aliphatic polyesters via enzymatic polymerization of biobased monomers derived from renewable resources*. *Polym Chem*. 2015;6:5451-63.
63. Jiang Y, Woortman A, van Ekenstein G, Loos K. *Enzyme-catalyzed synthesis of unsaturated aliphatic polyesters based on green monomers from renewable resources*. *Biomolecules*. 2013;3:461-80.
64. Jiang Y, van Ekenstein GORA, Woortman AJJ, Loos K. *Fully biobased unsaturated aliphatic polyesters from renewable resources: Enzymatic synthesis, characterization, and properties*. *Macromol Chem Phys*. 2014;215:2185-97.
65. Lai C-M, Rozman HD, Tay G-S. *Palm oil-based unsaturated polyester: Activation energy and swelling properties*. *Polym Eng Sci*. 2013;53:1138-45.

66. Mahmoud AH, Tay GS, Rozman HD. *A preliminary study on ultraviolet radiation-cured unsaturated polyester resin based on palm oil*. Polym-Plast Technol Eng. 2011;50:573-80.
67. Miyagawa H, Mohanty AK, Burgueño R, Drzal LT, Misra M. *Development of biobased unsaturated polyester containing functionalized linseed oil*. Ind Eng Chem Res. 2006;45:1014-8.
68. Takenouchi S, Takasu A, Inai Y, Hirabayashi T. *Effects of geometric structure in unsaturated aliphatic polyesters on their biodegradability*. Polym J. 2001;33:746-53.
69. Zheng L, Wang Z, Li C, Zhang D, Xiao Y. *Novel unsaturated aliphatic polyesters: Synthesis, characterization, and properties of multiblock copolymers composing of poly(butylene fumarate) and poly(1,2-propylene succinate)*. Ind Eng Chem Res. 2012;51:14107-14.
70. Najafi F, Sarbolouki MN. *Synthesis and characterization of block copolymers from aromatic diols, fumaric acid, sebacic acid and PEG*. J Appl Polym Sci. 2003;90:2358-63.
71. Najafi F, Sarbolouki MN. *Synthesis and characterization of biodegradable block copolymers of poly(propylene fumarate-co-sebacate)-copoly(ethylene glycol) and poly(ethylene fumarate-co-sebacate)-co-poly(ethylene glycol)*. J Appl Polym Sci. 2004;92:295-300.
72. Jasinska L, Koning CE. *Waterborne polyesters partially based on renewable resources*. J Polym Sci, Part A: Polym Chem. 2010;48:5907-15.
73. Naves AF, Fernandes HTC, Immich APS, Catalani LH. *Enzymatic syntheses of unsaturated polyesters based on isosorbide and isomannide*. J Polym Sci, Part A: Polym Chem. 2013;51:3881-91.
74. Tsujimoto T, Uyama H, Kobayashi S. *Enzymatic synthesis and curing of biodegradable crosslinkable polyesters*. Macromolecular Bioscience. 2002;2:329-35.
75. Uyama H, Kuwabara M, Tsujimoto T, Kobayashi S. *Enzymatic synthesis and curing of biodegradable epoxide-containing polyesters from renewable resources*. Biomacromolecules. 2003;4:211-5.
76. Goerz O, Ritter H. *N-Alkylated dinitrones from isosorbide as cross-linkers for unsaturated bio-based polyesters*. Beilstein J Org Chem. 2014;10:902-9.
77. Jiang HY, Kelch S, Lendlein A. *Polymers move in response to light*. Adv Mater. 2006;18:1471-5.
78. Lendlein A, Jiang H, Junger O, Langer R. *Light-induced shape-memory polymers*. Nature. 2005;434:879-82.
79. Dong W, Ren J, Lin L, Shi D, Ni Z, Chen M. *Novel photocrosslinkable and biodegradable polyester from bio-renewable resource*. Polym Degrad Stab. 2012;97:578-83.
80. Matsusaki M, Kishida A, Stainton N, Ansell CWG, Akashi M. *Synthesis and characterization of novel biodegradable polymers composed of hydroxycinnamic acid and D,L-lactic acid*. J Appl Polym Sci. 2001;82:2357-64.
81. Hang Thi T, Matsusaki M, Akashi M. *Thermally stable and photoreactive polylactides by the terminal conjugation of bio-based caffeic acid*. Chem Commun. 2008:3918-20.
82. Nagata M, Inaki K. *Synthesis and characterization of photocrosslinkable poly(l-lactide)s with a pendent cinnamate group*. Eur Polym J. 2009;45:1111-7.
83. Kim YB, Kim HK, Choi HC, Hong JW. *Photocuring of a thiol-ene system based on an unsaturated polyester*. J Appl Polym Sci. 2005;95:342-50.

Chapter I

84. Ates Z, Thornton PD, Heise A. *Side-chain functionalisation of unsaturated polyesters from ring-opening polymerisation of macrolactones by thiol-ene click chemistry*. Polym Chem. 2011;2:309-12.
85. Roumanet P-J, Laflèche F, Jarroux N, Raoul Y, Claude S, Guégan P. *Novel aliphatic polyesters from an oleic acid based monomer. Synthesis, epoxidation, cross-linking and biodegradation*. Eur Polym J. 2013;49:813-22.
86. Kolb N, Meier MAR. *Monomers and their polymers derived from saturated fatty acid methyl esters and dimethyl carbonate*. Green Chem. 2012;14:2429-35.
87. Kolb N, Meier MAR. *Grafting onto a renewable unsaturated polyester via thiol-ene chemistry and cross-metathesis*. Eur Polym J. 2013;49:843-52.
88. Olson DA, Gratton SEA, DeSimone JM, Sheares VV. *Amorphous linear aliphatic polyesters for the facile preparation of tunable rapidly degrading elastomeric devices and delivery vectors*. J Am Chem Soc. 2006;128:13625-33.
89. Tang T, Takasu A. *Facile synthesis of unsaturated polyester-based double-network gels via chemoselective cross-linking using Michael addition and subsequent UV-initiated radical polymerization*. RSC Adv. 2015;5:819-29.
90. Jasinska L, Koning CE. *Unsaturated, biobased polyesters and their cross-linking via radical copolymerization*. J Polym Sci, Part A: Polym Chem. 2010;48:2885-95.
91. Li J, Qin Y, Zhao L. *Mechanical Properties of UP Resin from Soybean Oil Applied Mechanics and Materials*. 2011;55-57:443-6.
92. Qin Y, Jia JR, Zhao L, Huang ZX, Zhao SW, Zhang GW, et al. *Synthesis and characterization of soybean oil based unsaturated polyester resin*. Adv Mater Res. 2011;393-395:349-53
93. Miyagawa H, Mohanty AK, Burgueno R, Drzal LT, Misra M. *Novel biobased resins from blends of functionalized soybean oil and unsaturated polyester resin*. J Polym Sci, Part B: Polym Phys. 2007;45:698-704.
94. Dai J, Ma S, Wu Y, Zhu J, Liu X. *High bio-based content waterborne UV-curable coatings with excellent adhesion and flexibility*. Prog Org Coat. 2015;87:197-203.
95. Kharas GB, Kamenetsky M, Simantirakis J, Beinlich KC, Rizzo AMT, Caywood GA, et al. *Synthesis and characterization of fumarate-based polyesters for use in bioresorbable bone cement composites*. J Appl Polym Sci. 1997;66:1123-37.
96. Guo W-x, Huang K-x, Tang R, Xu H-b. *Synthesis, characterization of novel injectable drug carriers and the antitumor efficacy in mice bearing Sarcoma-180 tumor*. J Controlled Release. 2005;107:513-22.
97. Guo W-x, Shi Z-l, Liang K, Liu Y-l, Chen X-h, Li W. *New unsaturated polyesters as injectable drug carriers*. Polym Degrad Stab. 2007;92:407-13.
98. Doulabi ASH, Sharifi S, Imani M, Mirzadeh H. *Synthesis and characterization of biodegradable in situ forming hydrogels via direct polycondensation of poly(ethylene glycol) and fumaric acid*. Iran Polym J. 2008;17:125-33.
99. Wang SF, Lu LC, Gruetzmacher JA, Currier BL, Yaszemski MJ. *Synthesis and characterizations of biodegradable and crosslinkable poly(epsilon-caprolactone fumarate), poly(ethylene glycol fumarate), and their amphiphilic copolymer*. Biomaterials. 2006;27:832-41.
100. Sharifi S, Mirzadeh H, Imani M, Rong Z, Jamshidi A, Shokrgozar M, et al. *Injectable in situ forming drug delivery system based on poly(epsilon-caprolactone fumarate) for*

- tamoxifen citrate delivery: Gelation characteristics, in vitro drug release and anti-cancer evaluation.* Acta Biomater. 2009;5:1966-78.
101. Sharifi S, Imani M, Mirzadeh H, Atai M, Ziaee F, Bakhshi R. *Synthesis, characterization, and biocompatibility of novel injectable, biodegradable, and in situ crosslinkable polycarbonate-based macromers.* J Biomed Mater Res, Part A. 2009;90A:830-43.
 102. N. K. Mohtaram, Mohammad Imani, Sharifi S, Mobedi H, Atai M. *Novel, biocompatible and photo crosslinkable polymeric networks based on unsaturated polyesters: Optimization of the network properties* In: Jos Vander Sloten PV, Marc Nyssen and Jens Hauelsen, editor. ECIFMBE 2008. Belgium: Springer; 2008. p. 2182-5.
 103. Barrett DG, Merkel TJ, Luft JC, Yousaf MN. *One-step syntheses of photocurable polyesters based on a renewable resource.* Macromolecules. 2010;43:9660-7.
 104. Brown AH, Sheares VV. *Amorphous unsaturated aliphatic polyesters derived from dicarboxylic monomers synthesized by Diels-Alder chemistry.* Macromolecules. 2007;40:4848-53.
 105. Landers R, Pfister A, Hubner U, John H, Schmelzeisen R, Mulhaupt R. *Fabrication of soft tissue engineering scaffolds by means of rapid prototyping techniques.* J Mater Sci. 2002;37:3107-16.
 106. Bártolo PJ, Almeida H, Rezende R, Laoui T, Bidanda B. *Advanced processes to fabricate scaffolds for tissue engineering.* In: Bidanda B, Bártolo PJ, editors. Virtual prototyping & bio manufacturing in medical applications. New York: Springer; 2008. p. 149-70.
 107. Bártolo PJ, Chua CK, Almeida HA, Chou SM, Lim ASC. *Biomanufacturing for tissue engineering: Present and future trends.* Virtual Phys Prototyping. 2009;4:203-16.
 108. Holtorf H, Jansen J, Mikos A. *Modulation of cell differentiation in bone tissue engineering constructs cultured in a bioreactor.* In: Fisher J, editor. Tissue Engineering: Springer US; 2007. p. 225-41.
 109. Samuel RE, Lee CR, Ghivizzani SC, Evans CH, Yannas IV, Olsen BR, et al. *Delivery of Plasmid DNA to Articular Chondrocytes via Novel Collagen–Glycosaminoglycan Matrices.* Hum Gene Ther. 2002;13:791-802.
 110. Matsumoto T, Mooney D. *Cell Instructive Polymers.* In: Lee K, Kaplan D, editors. Tissue Engineering I: Springer Berlin Heidelberg; 2006. p. 113-37.
 111. Sanz-Herrera JA, García-Aznar JM, Doblaré M. *On scaffold designing for bone regeneration: A computational multiscale approach.* Acta Biomater. 2009;5:219-29.
 112. Hutmacher DW, Schantz JT, Lam CXF, Tan KC, Lim TC. *State of the art and future directions of scaffold-based bone engineering from a biomaterials perspective.* J Tissue Eng Regen Med. 2007;1:245-60.
 113. Anderson JM. *Inflammatory response to implants.* ASAIO Trans. 1988;34:101-7.
 114. Anderson JM. *Mechanisms of inflammation and infection with implanted devices.* Cardiovascular Pathology. 1993;2:33-41.
 115. Anderson JM. Chapter II. 8 - *Biocompatibility of Tissue Engineered Implants.* In: Mikos CWPG, Langer LVMS, editors. Frontiers in Tissue Engineering. Oxford: Pergamon; 1998. p. 152-65.
 116. Gilbert TW, Stewart-Akers AM, Badylak SF. *A quantitative method for evaluating the degradation of biologic scaffold materials.* Biomaterials. 2007;28:147-50.
 117. Sung H-J, Meredith C, Johnson C, Galis ZS. *The effect of scaffold degradation rate on three-dimensional cell growth and angiogenesis.* Biomaterials. 2004;25:5735-42.

Chapter I

118. Domingos M, Chiellini F, Cometa S, De Giglio E, Grillo-Fernandes E, Bártolo P, et al. *Evaluation of in vitro degradation of PCL scaffolds fabricated via BioExtrusion*. Part 1: Influence of the degradation environment. *Virtual Phys Prototyping*. 2010;5:65-73.
119. Kuboki Y, Takita H, Kobayashi D, Tsuruga E, Inoue M, Murata M, et al. *BMP-Induced osteogenesis on the surface of hydroxyapatite with geometrically feasible and nonfeasible structures: Topology of osteogenesis*. *J Biomed Mater Res*. 1998;39:190-9.
120. Story BJ, Wagner WR, Gaisser DM, Cook SD, Rust-Dawicki AM. *In vivo performance of a modified CSTi dental implant coating*. *Int J Oral Maxillofac Implants*. 1998;13:749-57.
121. Oh SH, Park IK, Kim JM, Lee JH. *In vitro and in vivo characteristics of PCL scaffolds with pore size gradient fabricated by a centrifugation method*. *Biomaterials*. 2007;28:1664-71.
122. Yang S, Leong KF, Du Z, Chua CK. *The design of scaffolds for use in tissue engineering. Part I. Traditional factors*. *Tissue Eng*. 2001;7:679-89.
123. Wang H, Pieper J, Péters F, van Blitterswijk CA, Lamme EN. *Synthetic scaffold morphology controls human dermal connective tissue formation*. *J Biomed Mater Res, Part A*. 2005;74A:523-32.
124. Stevens MM, George JH. *Exploring and engineering the cell surface interface*. *Science*. 2005;310:1135-8.
125. Price RL, Ellison K, Haberstroh KM, Webster TJ. *Nanometer surface roughness increases select osteoblast adhesion on carbon nanofiber compacts*. *J Biomed Mater Res, Part A*. 2004;70:129-38.
126. Curtis ASG, Gadegaard N, Dalby MJ, Riehle MO, Wilkinson CDW, Aitchison G. *Cells react to nanoscale order and symmetry in their surroundings*. *NanoBioscience, IEEE Transactions on*. 2004;3:61-5.
127. Reignier J, Huneault MA. *Preparation of interconnected poly(ϵ -caprolactone) porous scaffolds by a combination of polymer and salt particulate leaching*. *Polymer*. 2006;47:4703-17.
128. Gomes ME, Reis RL. *Biodegradable polymers and composites in biomedical applications: from catgut to tissue engineering. Part 2 Systems for temporary replacement and advanced tissue regeneration*. *Int Mater Rev*. 2004;49:274-85.
129. Ho M-H, Kuo P-Y, Hsieh H-J, Hsien T-Y, Hou L-T, Lai J-Y, et al. *Preparation of porous scaffolds by using freeze-extraction and freeze-gelation methods*. *Biomaterials*. 2004;25:129-38.
130. Whang K, Thomas CH, Healy KE, Nuber G. *A novel method to fabricate bioabsorbable scaffolds*. *Polymer*. 1995;36:837-42.
131. Hoque ME, Huttmacher DW, Feng W, Li S, Huang MH, Vert M, et al. *Fabrication using a rapid prototyping system and in vitro characterization of PEG-PCL-PLA scaffolds for tissue engineering*. *J Biomater Sci, Polym Ed*. 2005;16:1595-610.
132. Woodruff MA, Huttmacher DW. *The return of a forgotten polymer—Polycaprolactone in the 21st century*. *Prog Polym Sci*. 2010;35:1217-56.
133. Peltola SM, Melchels FPW, Grijpma DW, Kellomäki M. *A review of rapid prototyping techniques for tissue engineering purposes*. *Ann Med*. 2008;40:268-80.
134. Bártolo PJ. *Optical approaches to macroscopic and microscopic engineering*: PhD Thesis, University of Reading; 2001.
135. Bártolo PJ, Mendes, A. and Jardini, A. *Bio-prototyping*. In: Press W, editor. *Design and Nature II – comparing design in nature with science and engineering*. Southampton2004.

136. Ritman EL. *Micro-computed tomography-Current status and developments* Annu Rev Biomed Eng. 2004;6:185-208.
137. Potter HG, Nestor BJ, Sofka CM, Ho ST, Peters LE, Salvati EA. *Magnetic resonance imaging after total hip arthroplasty: evaluation of periprosthetic soft tissue.* J Bone Joint Surg Am. 2004;1947-54.
138. Fenster A, Downey DB. *3-D ultrasound imaging: a review.* Engineering in Medicine and Biology Magazine, IEEE. 1996;15:41-51.
139. McElroy DP, MacDonald LR, Beekman FJ, Yuchuan W, Patt BE, Iwanczyk JS, et al. *Performance evaluation of A-SPECT: a high resolution desktop pinhole SPECT system for imaging small animals.* Nuclear Science, IEEE Transactions on. 2002;49:2139-47.
140. Edinger M, Cao Ya, Hornig YS, Jenkins DE, Verneris MR, Bachmann MH, et al. *Advancing animal models of neoplasia through in vivo bioluminescence imaging.* Eur J Cancer.38:2128-36.
141. Melchels FPW, Domingos MAN, Klein TJ, Malda J, Bartolo PJ, Hutmacher DW. *Additive manufacturing of tissues and organs.* Prog Polym Sci. 2012;37:1079-104.
142. Arcaute K, Mann B, Wicker R. *Stereolithography of three-dimensional bioactive poly(ethylene glycol) constructs with encapsulated cells.* Ann Biomed Eng. 2006;34:1429-41.
143. Elomaa L, Pan C-C, Shanjani Y, Malkovskiy A, Seppala JV, Yang Y. *Three-dimensional fabrication of cell-laden biodegradable poly(ethylene glycol-co-depsipeptide) hydrogels by visible light stereolithography.* J Mater Chem B. 2015;3:8348-58.
144. He J, Li D, Liu Y, Gong H, Lu B. *Indirect fabrication of microstructured chitosan-gelatin scaffolds using rapid prototyping.* Virtual Phys Prototyping. 2008;3:159-66.
145. Hull CW. *Method for production of three-dimensional objects by stereolithography.* US 4929402 A. USA. 1990.
146. Pomerantz I, Gilad S, Dollberg Y, Ben-Ezra B, Sheinman Y, Barequet G, et al. *Three dimensional modeling apparatus.* US 5386500 A, USA. 1995.
147. Bártoło PJ. *Stereolithography Processes.* In: Springer, editor. Stereolithography: Materials, Processes and Applications. New York: Springer; 2011. p. 1-36.
148. Pang KP, Gillham JK. *Anomalous behavior of cured epoxy resins: Density at room temperature versus time and temperature of cure.* J Appl Polym Sci. 1989;37:1969-91.
149. Ferry JD. *Viscoelastic Properties of Polymers.* New York: John Wiley & Sons; 1980.
150. Simon SL, Gillham JK. *Conversion-temperature-property diagram for a liquid dicyanate ester/high-Tg polycyanurate thermosetting system.* J Appl Polym Sci. 1994;51:1741-52.
151. Fouassier J-P. *Photoinitiation, photopolymerization, and photocuring: Fundamentals and Applications.* Munich: Carl Hanser Verlag GmbH & Co 1995.
152. Decker C. *New developments in UV-curable acrylic monomers.* In: Fouassier J-P, editor. Radiation curing in polymer science and technology. London: Kluwer Academic Publishers; 1993.
153. Liu V, Bhatia S. *Three-Dimensional Photopatterning of Hydrogels Containing Living Cells.* Biomed Microdevices. 2002;4:257-66.
154. Chan V, Collens MB, Jeong JH, Park K, Kong H, Bashir R. *Directed cell growth and alignment on protein-patterned 3D hydrogels with stereolithography.* Virtual Phys Prototyping. 2012;7:219-28.

Chapter I

155. Andre JC, Mehaute AL, Witte OD. *Dispositif pour realiser un modele de piece industrielle*. French Patent 84411241. France. 1984.
156. Bertsch A, Renaud P. Microstereolithography. In: Bártolo PJ, editor. *Stereolithography: Materials, Processes and Applications*. Berlin: Springer Science & Business Media,; 2011.
157. Lee JW, Kang KS, Lee SH, Kim J-Y, Lee B-K, Cho D-W. *Bone regeneration using a microstereolithography-produced customized poly(propylene fumarate)/diethyl fumarate photopolymer 3D scaffold incorporating BMP-2 loaded PLGA microspheres*. *Biomaterials*. 2011;32:744-52.
158. Bartolo PJ, Mitchell G. *Stereo-thermal-lithography: a new principle for rapid prototyping*. *Rapid Prototyping Journal*. 2003;9:150-6.
- 159] Stratakis E, Ranella A, Farsari M, Fotakis C. *Laser-based micro/nanoengineering for biological applications*. *Prog Quantum Electron*. 2009;33:127-63.
160. Yan Y-X, Tao X-T, Sun Y-H, Xu G-B, Wang C-K, Yang J-X, et al. *Two new asymmetrical two-photon photopolymerization initiators: Synthesis, characterization and nonlinear optical properties*. *Opt Mater*. 2005;27:1787-92.
161. Schafer KJ, Hales JM, Balu M, Belfield KD, Van Stryland EW, Hagan DJ. *Two-photon absorption cross-sections of common photoinitiators*. *J Photochem Photobiol, A*. 2004;162:497-502.
162. Kawata S, Sun H-B. *Two-photon photopolymerization as a tool for making micro-devices*. *Appl Surf Sci*. 2003;208–209:153-8.
163. Miwa M, Juodkazis S, Kawakami T, Matsuo S, Misawa H. *Femtosecond two-photon stereo-lithography*. *Appl Phys A*. 2001;73:561-6.
164. Lee K-S, Yang D-Y, Park SH, Kim RH. *Recent developments in the use of two-photon polymerization in precise 2D and 3D microfabrications*. *Polym Adv Technol*. 2006;17:72-82.
165. Lim TW, Park SH, Yang D-Y. *Contour offset algorithm for precise patterning in two-photon polymerization*. *Microelectron Eng*. 2005;77:382-8.
166. Wu S, Serbin J, Gu M. *Two-photon polymerisation for three-dimensional micro-fabrication*. *J Photochem Photobiol, A*. 2006;181:1-11.
167. Zhou M, Yang HF, Kong JJ, Yan F, Cai L. *Study on the microfabrication technique by femtosecond laser two-photon photopolymerization*. *J Mater Process Technol*. 2008;200:158-62.
168. Tayalia P, Mendonca CR, Baldacchini T, Mooney DJ, Mazur E. *3D Cell-Migration Studies using Two-Photon Engineered Polymer Scaffolds*. *Adv Mater*. 2008;20:4494-8.
169. Landers R, Hübner U, Schmelzeisen R, Mülhaupt R. *Rapid prototyping of scaffolds derived from thermoreversible hydrogels and tailored for applications in tissue engineering*. *Biomaterials*. 2002;23:4437-47.
170. Belfield KD, Schafer KJ, Liu Y, Liu J, Ren X, Stryland EWV. *Multiphoton-absorbing organic materials for microfabrication, emerging optical applications and non-destructive three-dimensional imaging*. *J Phys Org Chem*. 2000;13:837-49.
171. Schlie S, Ngezahayo A, Ovsianikov A, Fabian T, Kolb H-A, Haferkamp H, et al. *Three-dimensional cell growth on Structures Fabricated from ORMOCER® by Two-Photon Polymerization Technique*. *J Biomater Appl*. 2007;22:275-87.

172. Doraiswamy A, Jin C, Narayan RJ, Mageswaran P, Mente P, Modi R, et al. *Two photon induced polymerization of organic–inorganic hybrid biomaterials for microstructured medical devices*. Acta Biomater. 2006;2:267-75.

CHAPTER II

3D Printing of New Biobased Unsaturated Polyesters by Microstereo-thermal-lithography

1. ABSTRACT	67
2. INTRODUCTION	67
3. MATERIALS AND METHODS.....	69
3.1 MATERIALS	69
3.2 SYNTHESIS OF UNSATURATED POLYESTERS BY BULK POLYCONDENSATION.....	69
3.3 SPECTROSCOPIC ANALYSIS	70
3.4 THERMAL ANALYSIS OF UPS	70
3.5 SIZE EXCLUSION CHROMATOGRAPHY ANALYSIS.....	70
3.6 MALDI-TOF MASS SPECTROMETRY	71
3.7 VISCOSITY MEASUREMENTS.....	71
3.8 CELL VIABILITY ASSAYS.....	71
3.9 SCAFFOLDS FABRICATION	72
3.10 SCAFFOLDS MORPHOLOGY.....	72
4. RESULTS AND DISCUSSION.....	73
4.1 UNSATURATED POLYESTERS BY POLYCONDENSATION OF BIOBASED DICARBOXYLIC ACIDS	73
4.2 CHEMICAL CHARACTERIZATION OF UNSATURATED POLYESTERS	76
4.3 THERMAL AND MECHANICAL ANALYSIS OF UNSATURATED POLYESTERS	80
4.4 CELL VIABILITY	83
4.5 SCAFFOLDS FABRICATION AND CHARACTERIZATION.....	84
5. CONCLUSIONS	86
6. REFERENCES	87
SUPPLEMENTARY INFORMATION.....	90

Adapted from: Gonçalves, F. A. M. M., C. S. M. F. Costa, I. G. P. Fabela, D. Farinha, H. Faneca, P. N. Simões, A. C. Serra, P. J. Bártolo and J. F. J. Coelho (2014). "3D printing of new biobased unsaturated polyesters by microstereo-thermal-lithography." *Biofabrication* **6**(3): 035024.

1. Abstract

New micro 3D scaffolds using biobased unsaturated polyesters (UPs) were prepared by microstereo-thermal-lithography (μ STLG). This advanced processing technique offers indubitable advantages over traditional printing methods. UPs were synthesized by bulk polycondensation between biobased aliphatic diacids (succinic, adipic and sebacic acid) and two different glycols, propylene glycol (PG) and diethylene glycol, (DEG) using fumaric acid (FA) as the source of double bonds. The chemical structures of the new oligomers were confirmed by ^1H NMR, ATR-FTIR and MALDI-TOF. The thermal and mechanical properties of the UPs were evaluated to determine the influence of the diacid/glycol ratio and the type of diacid in polyesters properties. In addition, an extensive thermal characterization of the polyesters is reported. The accuracy and roughness of the 3D structures were evaluated by scanning electron microscopy (SEM) and Infinite Focus Microscope (IFM), revealing a suitable roughness for cell attachment. The data presented in this work opens the possibility for the use of bio UPs in additive manufacturing (AM) technologies as a route to prepare biodegradable tailor-made scaffolds that have potential applications in tissue engineering area.

2. Introduction

Stereolithography (SL) is an additive manufacturing (AM) technique [1], which allows the fabrication of three-dimensional models from a computer-aided design (CAD) [2]. This technology produces multi-layered materials through a selective photo-initiated cure reaction of specific polymers, providing very accurate and precise scaffold architectures [3]. Microstereo-thermal-lithography (μ STLG) is an improved SL technology that was developed by Paulo Bártolo and co-workers [4], where thermal and optical parameters are simultaneously used to produce 3D structures. The μ STLG presents several advantages when compared with the conventional stereolithography: i) the generation of radicals in polymer matrix is more efficient; ii) small concentrations of the two types of initiator (thermal and photo) can be used; iii) the combination of UV radiation and heat increases the reaction rate and the fractional conversion values; iv) the curing reaction is more localized, resulting in more accurate models and v) the system has more tunability [5]. One big issue associated with this advanced technique is related with the lack of proper biocompatible and photocurable polymers [6]. To overcome such problem, this work was focused on the development of suitable unsaturated polyester resins (UPRs) to be used in μ STLG. The materials need to fulfil some critical requirements: i) fast curing process; ii) low viscosity; iii) and biocompatibility if the final scaffolds are intended to be used in

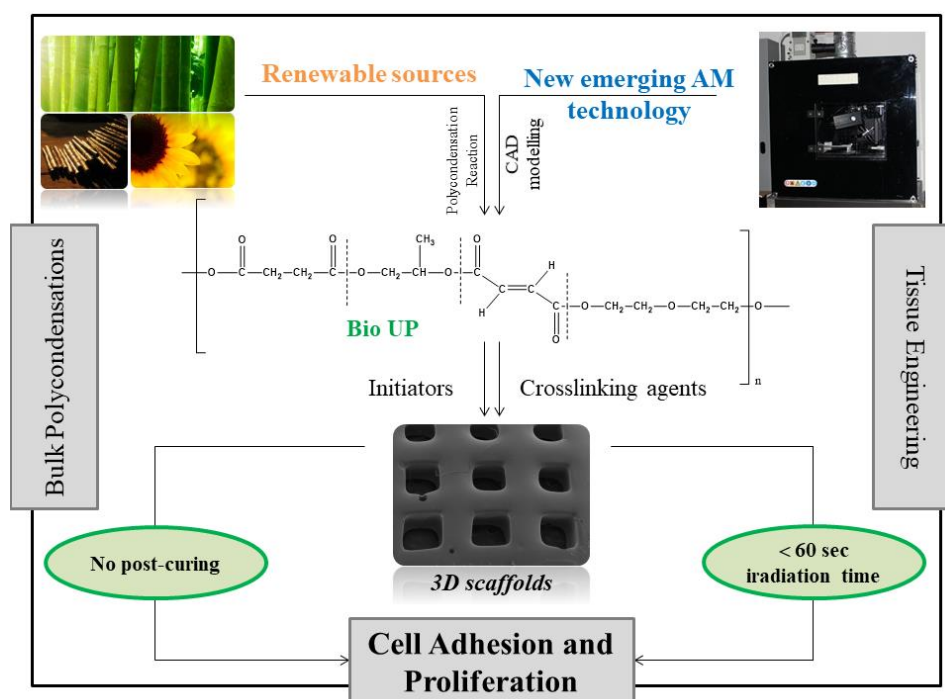
Chapter II

biomedical applications. The UPs are versatile materials with wide industrial use, such as: glass-fiber-reinforcement composite materials or paint constituent for different applications as the automotive, construction and marine industries [7, 8]. These oligomeric structures are easily prepared and involve the use of non-expensive monomers. Therefore, these materials could be an effective and convenient technical solution [9]. UPs are characterized by having low molecular weights, and are generally obtained by polycondensation of 1,2-diols with saturated and unsaturated anhydrides or diacids [10]. Using UPs, it is possible to obtain a three-dimensional network structure by crosslinking the unsaturated bonds of the polyester structure with a vinyl monomer, typically styrene (St), originating crosslinked polyester resins (UPRs) with important industrial applications [8]. Other chemical modifications (e.g. oxidation of UPs, leading to unsaturated epoxy polyesters) are also possible to improve their mechanical properties [11-13].

Nowadays, a growing attention is being paid to environmental and sustainability issues involving the preferential use of biobased monomers to reduce the CO₂ footprint. This concern is particularly relevant in polymeric materials that primarily use monomers derived from fossil resources. In addition, UPs based materials are receiving particular attention in the biomedical areas considering their potential biodegradability [14]. On this matter, the selection of monomers is crucial since UP properties can be fine-tuned by changing the structure of the diacid or the dihydroxy compounds. For instance, it is known that an increase in the propylene glycol (PG) content in the UP formulation increases the UP hardness [15]. Also, the presence of aromatic rings in the polyester structure enhances the rigidity of the resin. The opposite effect occurs by increasing the content of aliphatic acids, leading to more flexible polyesters. Other studies related to the UPs synthesis are focused on the influence of the glycols nature or the St concentration in the final properties of the crosslinked polyesters [11, 16, 17]. In industrial applications isophthalic acid (IA) and PG are the most common used reagents [10]. Several authors have already reported the synthesis of UPs using the succinic acid (SuCA) [18, 19], adipic acid (AA) [20, 21] sebacic acid (SeBA) [14, 22] and other biobased materials [23]. In our work, to the best of our knowledge, the formulations here described have never been reported and characterized. The biobased UPRs were synthesized *via* bulk polycondensation using the previously described diacids (SuCA, AA and SeBA) with the purpose of replacing IA, while fumaric acid (FA) was used as the source of double bonds for further crosslinking reactions, instead of maleic anhydride (MA), which is widely reported in the literature due to its low cost and high reactivity [19, 24, 25]. However, the use of MA is responsible for the occurrence of *cis-trans* isomerism in the final materials [26, 27]. PG and diethylene

3D Printing of New Biobased Unsaturated Polyesters by Microstereo-thermal-lithography

glycol (DEG) were the selected glycols. The biobased UPs were used to prepared 3D scaffolds by μ STLG, using at this stage only the UV irradiation (Scheme 1).



Scheme 1. Schematic illustration of the relationship between the polycondensation of bio products and the AM technologies in Tissue Engineering.

3. Materials and Methods

3.1 Materials

Fumaric acid (FA, 99%), isophthalic acid (IA, 99%), succinic acid (SuCA, 99%), adipic acid (AA, 99.6%), sebacic acid (SeBA, 94.5%), diethylene glycol (DEG, 99%), propylene glycol (PG, 99%), and potassium hydroxide (90%) were purchased from Sigma-Aldrich Chemical Company and used as received. Hydroquinone (99%) was purchased from Analar, ethanol (96%) from Panreac, Deuterated tetrahydrofuran-D (THF- d_6 , 99.5%) from Eurisotop and phenolphthalein (99%) from Nidel-de-Haën. Styrene (St, >99%) and 2-hydroxyethyl methacrylate (HEMA, 97%) were also purchased from Sigma-Aldrich. All chemicals were used as received.

3.2 Synthesis of Unsaturated Polyesters by Bulk Polycondensation

The UPs were prepared by bulk polycondensation. The diacid, the source of double bonds, glycols and hydroquinone (0.02 % of the total weight) were charged into a four-necked glass reactor, equipped with a mechanical stirrer, a nitrogen inlet and a condenser

Chapter II

connected to a receiver flask. The reactor was first heated at 190 °C–200 °C, and then the temperature during reaction was raised to 220 °C. The polycondensation was carried out at least for 14 h. The end of the reaction was determined by monitoring the acid value (AV), (according to ASTM 109-01).

3.3 Spectroscopic analysis

Attenuated total reflection-FTIR (ATR-FTIR) spectroscopic analysis was carried out with a JASCO FT-IR 4100. ¹H NMR spectra were obtained at room temperature on a Varian Unity 600 MHz Spectrometer using a 3 mm broadband NMR probe, in deuterated tetrahydrofuran (THF-*d*₈). Tetramethylsilane (TMS) was used as internal reference.

3.4 Thermal analysis of UPs

The thermal stability of UPs was evaluated in the range of *ca.* 25 – 600 °C, in a TA Instruments Q500 thermogravimetric analyzer (thermobalance sensitivity: 0.1 µg) at a heating rate of 10 °C·min⁻¹ and under a dry nitrogen purge flow of 100 mL·min⁻¹. The Modulated Differential Scanning Calorimetry) (MDSC) studies, were performed within a temperature interval ranging from -90 to 50 °C, in a TA Q100 instrument at a heating rate of 2 °C·min⁻¹ in the temperature modulated mode, and under a nitrogen flow of 50 mL·min⁻¹. Dynamic mechanical thermal analysis (DMTA) were performed in Tritec 2000 DMA equipment at a heating rate of 5 °C·min⁻¹, in the temperature range from -150 °C to 300 °C, with a multifrequency mode (1 and 10 Hz). The polyesters were placed into stainless steel pockets. The pocket was clamped directly into the DMTA using a single cantilever configuration.

3.5 Size exclusion chromatography analysis

The chromatographic parameters of the samples were determined using high-performance gel permeation chromatography (HPSEC; Viscotek TDAmix) with a differential viscometer (DV), right-angle laser-light scattering (RALLS, Viscotek), low-angle laser-light scattering (LALLS, Viscotek), and refractive-index (RI) detectors. The column set consisted of a PL 10 mm guard column (50 × 7.5 mm²) followed by one Viscotek T200 column (6 µm), one MIXED-E PLgel column (3 µm), and one MIXED-C PLgel column (5 µm). HPLC dual piston pump was set with a flow rate of 1 mL·min⁻¹. The eluent (THF) was previously filtered through a 0.2 µm filter. The system was also equipped with an on-line degasser. The tests were done at 30 °C using an Elder CH-150 heater. Before the injection (100 µL), the samples were filtered through a polytetrafluoroethylene (PTFE) membrane with 0.2 µm pore. The system was calibrated with narrow PS standards.

3D Printing of New Biobased Unsaturated Polyesters by Microstereo-thermal-lithography

Number average (M_n), weight average (M_w) and dispersity (\mathcal{D}) of the synthesized polymers were determined by conventional calibration (OmniSEC software version 4.6.1.354).

3.6 MALDI-TOF Mass Spectrometry

The biobased UPs were analyzed by matrix-assisted laser desorption/ionization-time of flight mass spectrometry (MALDI-TOF MS). The dried-droplet sample preparation technique was used, applying 2 μL of 2,5-dihydroxybenzoic acid (DHB) matrix solution (20 $\text{mg}\cdot\text{mL}^{-1}$ in THF) directly on a MTP AnchorChip™ 800/384 TF MALDI target (Bruker Daltonik, Bremen Germany), and, before drying the matrix solution, 2 μL of sample (20 $\text{mg}\cdot\text{mL}^{-1}$ in THF) were added and allowed to dry at room temperature. External mass calibration was performed with a calibration standard (Bruker Daltonik, Bremen Germany) for the range m/z 700–3000 (9 mass calibrant points): 0.5 mL of calibrant solution and DHB matrix previously mixed in an eppendorf tube (1:2, v/v) were applied directly on the target and allowed to dry at room temperature. Mass spectra were recorded using an Autoflex III smart beam MALDI-TOF mass spectrometer Bruker Daltonik (Bremen, Germany), operating in linear positive ion mode. Ions formed upon irradiation by a smart beam nitrogen laser (337nm) using an accelerating potential of 20kV and a frequency of 200 Hz. Each mass spectrum was produced by averaging 2000 laser shots collected across the whole sample spot surface by rastering in the range m/z 400–3000. The laser irradiance was set to 45–50% arbitrary units according to the corresponding threshold required for the applied matrix system. Low molecular ion gating was set to 400 Da to remove the ions below this value arising from the matrix and their clusters or other unknown contaminants. All spectra were acquired and treated using the flexControl 3.0 and flexAnalysis 3.0 softwares (Bruker Daltonik), respectively.

3.7 Viscosity measurements

A controlled stress rheometer, Haake, model RS1, was used to measure the viscosity. The geometry used was a plate/plate system PP20 (titanium for the rotating part and stainless steel for the stationary part). The UPs were dissolved in 37 % (w/w) of St and measured under certain conditions. The biobased polyesters were also studied at 25°C. All measurements were made in triplicate.

3.8 Cell viability assays

For cell viability tests the UPs were crosslinked with St: once the UP synthesis was finished the temperature was decreased to 80°C–100 °C and the reaction mixture was discharged

Chapter II

to a vessel containing the right amount of St (37 % (w/w)). The mixture was continuously stirred and warmed until the total dissolution of the UP. After, the UPs were photo polymerized in a UV chamber, in the presence of 2 to 5% (w/w) of the photo initiator Irgacure 651 and using a UV light (253.7 nm) for a period time not exceeding 15 minutes, at room temperature.

The cytotoxicity of the different photo polymerized products were evaluated in the 3T3-L1 cell line by an extraction test according to ISO 10993-5 Standard [28]. 3T3-L1 cells, seeded in 48-well culture plates, were incubated with extraction fluid for 24 h, and the cell viability was assessed by a modified *Alamar Blue* assay [29]. This assay measures the redox capacity of the cells due to the production of metabolites as a result of cell growth. Briefly, following cells incubation during 24 h with the extraction medium, the medium of each well was replaced with 0.3 ml of DMEM-HG containing 10 % (v/v) of *Alamar Blue* (0.1 mg/mL in PBS) and, after 1 h of incubation at 37 °C, 170 µL of the supernatant was collected from each well and transferred to 96-well plates. Then, absorbance at 570 and 600 nm was immediately measured in a SPECTRAmax PLUS 384 spectrophotometer (Molecular Devices, Union City, CA).

3.9 Scaffolds Fabrication

3-D scaffolds were prepared by means of µSTLG. The µSTLG can create scaffolds with specific geometries, varying in shape and thickness. The UPs and the corresponding UM were loaded into the reservoir and were exposed to the UV light, in a period between 25 and 60 seconds. µSTLG system uses a mercury lamp of 350 W as a light source. Optical fibers, projection and focal lenses irradiate a UV-DMD and an IR-DMD [4, 30]. A dichroic mirror captures the images projected on DMD (1024 x 768 pixels, 14 mm in size), combining them into a single image that is transferred to the reactive resin (monomer or oligomers). The equipment also includes a multi-vat system. The vertical displacement of the platform is secured by a uniaxial MYCOSIS Translation Stage VT-80. This positioning system allows vertical increments of 1 µm, at a speed ranging between 0.001 and 20 mm/s.

3.10 Scaffolds Morphology

The morphologies of the processed scaffolds were observed by means of scanning electron microscopy (SEM) (MEV)/EDS, JEOL, model JSM-5310, at an accelerating voltage of 10 kV. The topography of the scaffolds surface was observed by an Optical Microscopy 3d micro, Alicona, IFM G4 3.5 EN.

4. Results and Discussion

4.1 Unsaturated Polyesters by Polycondensation of Biobased Dicarboxylic Acids

UPs were prepared through a bulk polycondensation reaction between biobased dicarboxylic acids, two glycols and an unsaturated acid monomer in different relative ratios. The selection of the diacid monomers was based on their linear chain structure. SuCA plays an important role in Krebs cycle, occurring naturally in plant and animal tissues, while SeBA is a derivative of vegetable oils (e.g. castor oil) [31]. AA is one of the most used acids at industrial scale in different applications, such as medicine and food industries. These three monomers are among the most common diacids used in polyester synthesis [32] and can be considered interesting candidates to substitute phthalic acids [33]. The formulations were developed to fulfil two important requirements: the incorporation of biobased monomers and the preparation of low molecular weight structures with internal double bonds for further crosslinking (Figure 1).

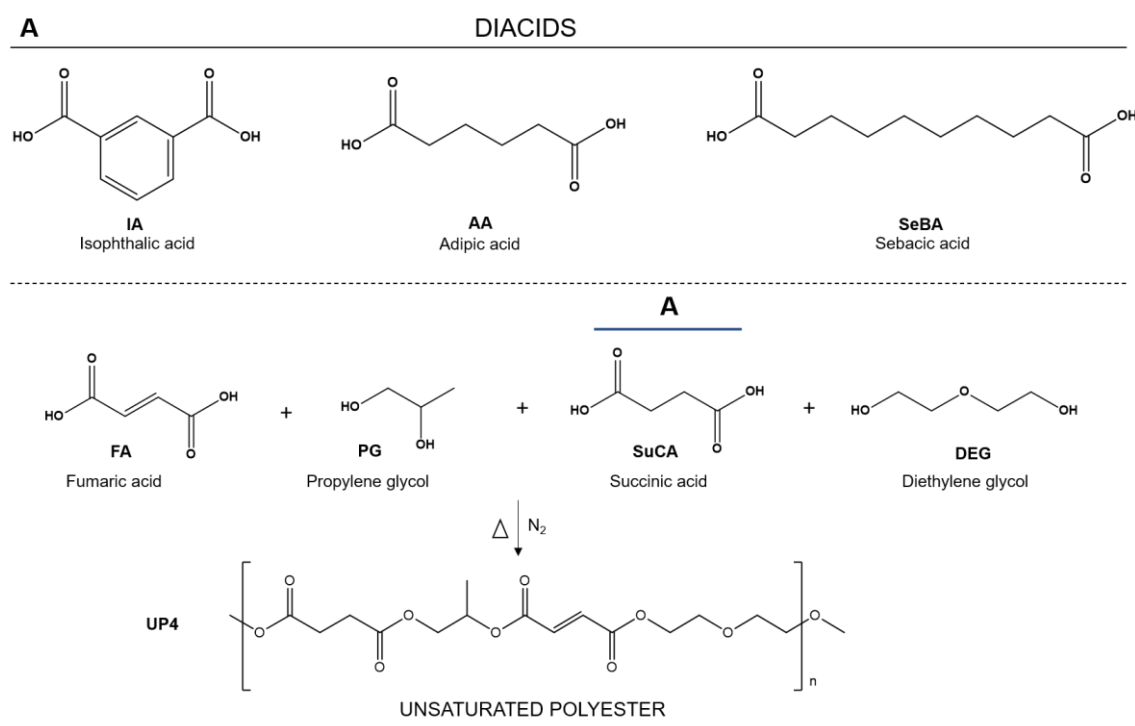


Figure 1. Monomers structure used in the synthesis of the unsaturated polyesters.

The results of polycondensation reactions formulations are presented in Table 1. For comparison purpose, UPs based on IA were prepared with different ratios between the IA and the glycols, to evaluate the results of increasing the number of aromatic rings, as well as the influence of decreasing the percentage of glycols in the final properties of the UPs (UP1, UP2 and UP3). For formulations UP4 to UP6 the main objective was to determine

the effect of the replacement of the IA by aliphatic biobased diacids with different chain lengths. In this case, it is expected a polymer structure with higher flexibility compared to the counterpart using IA [34]. As expected, the molecular weight of the obtained oligomers is small (between 604 and 1221) with \bar{D} higher than 2 [10].

Table 1. Synthesis conditions and properties of the UPs synthesized from dicarboxylic acids (IA, SuCA, AA and SeBA) and diethylene glycol (DEG), propylene glycol (PG) and fumaric acid (FA) as double bond provider.

UPs	Initial Molar ratio (%)	AV (mg KOH/g) ^a	M _w	M _n	\bar{D} ^b	Final Molar ratio (%) ^c	Acids/Alcohols Final Molar Ratio
UP1	IA/FA/PG/DEG 24 /22 /25 /29	29.0	2768	951	2.91	33/19/20/28	52/48
UP2	IA/FA/PG/DEG 16 /30 /25 /29	40.0	1988	604	3.29	28/24/20/28	52/48
UP3	IA/FA/PG/DEG 25 /40 /15 /20	28.0	-	-	-	35/26/18/21	71/29
UP4	SuCA/FA/PG/DEG 24 /22 /25 /29	41.0	3639	1138	3.20	34/11/40/15	45/55
UP5	AA/FA/PG/DEG 24 /22 /25 /29	21.4	3081	1221	2.52	13/13/57/17	26/74
UP6	SeBA/FA/PG/DEG 24 /22 /25 /29	43.3	4700	928	5.10	18/16/46/20	34/66

^aAV, acid value; ^b \bar{D} , polydispersity, was determined by SEC, using conventional calibration with polystyrene standards and THF as eluent; ^c Monomers molar percentages from ¹H NMR spectra.

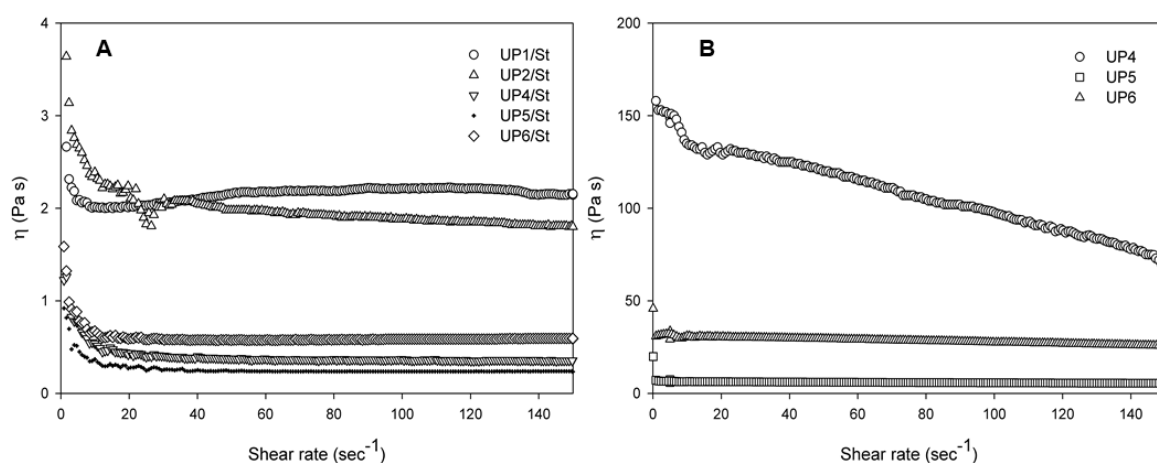
According to Table 1, there are significant differences between the initial and the final molar ratio of the UPs. For UP1, UP2 and UP3 a high amount of acids in the final polymer was detected, which could be explained by some losses of the glycols during the polycondensation reaction. By the contrary, for the biobased UPs, a high percentage of glycols is observed, mainly of PG.

The viscosities of the polyesters after dissolution in styrene (UP/St) were determined and are presented in Table 2 and Figure 2A. The viscosity values of UPs based on alkylic carboxylic acids were substantially low (between 0.24 and 0.58 Pa·s), when compared with those based in IA. This can be ascribed to the higher mobility of the polymeric chains which incorporate long chain alkylic backbone. The determination of the viscosity for UP3 was prevented by the extremely high hardness of the polyester, which may be related to the high concentration of carbon-carbon bonds in the polymer backbone and the possibility of the occurrence of some crosslinking reactions during polymerization reaction (Table 1).

Table 2. Viscosity data of UPs and UPs in 37% (w/w) of styrene at 100 sec⁻¹ and 25°C.

Polyesters	η (UP/St) (Pa·s), 37 sec ⁻¹	η (UPs) (Pa·s), 100sec ⁻¹
UP1	2.09	-
UP2	2.08	-
UP3	-	-
UP4	0.38	125.00
UP5	0.24	6.16
UP6	0.58	29.90

Regarding only the UPs stability, UP viscosities were determined after a period of 6 months. The biobased UPs showed an increase of the viscosity over time. This characteristic suggested that UPs present some rheological instability, probably due to the occurrence of some gelation processes. Such behaviour has been already reported by other authors, [24] being characterized by a change of the state of the material, i.e. a liquid-to-rubber transition and is associated to non-reversible events [5].

**Figure 2.** Rheological behavior of the UPs in St (37%) (A) and the biobased UPs after 6 months (B).

The rheological curves of the polyesters determined six months after the synthesis are presented in Figure 2B. It was possible to observe that UPs showed a constant value of viscosity, except for UP4 – in this case the observed viscosity was unexpectedly high. Additionally, the viscosity of UP4 decreased sharply with the increase of shear rate. Although this result can be expected for polymers due to a pseudo plastic behaviour [35], the abrupt decrease in UP4 was not expected. There is not enough information on the literature regarding the rheological behaviour of unsaturated polyesters or an extensive study of its stability. However, studies concerning the rheology of cured resins are widely reported [36-38].

4.2 Chemical Characterization of Unsaturated Polyesters

The structure of the UPs was analysed by ATR- FTIR and ^1H NMR. Figure 3 shows strong bands ascribed to the carbonyl stretching group characteristic of the polyesters, at ca. $1750\text{--}1725\text{ cm}^{-1}$ [39].

The OH band at $3600\text{--}3200\text{ cm}^{-1}$ is absent for the different UPs. The characteristic adsorption bands of double bonds are assigned to the C=C stretching vibration present at $1680\text{--}1600\text{ cm}^{-1}$ [40]. These double bonds are associated to FA, present in the different formulations. Also, the group frequency $3095\text{--}3075\text{ cm}^{-1}$ from the pendant =C-H stretch was detected (see Figure S1 to S3 in SI). UP1 and UP3 show additional bands in the $1615\text{--}1580\text{ cm}^{-1}$ and $1510\text{--}1450\text{ cm}^{-1}$ regions, characteristic of the aromatic ring from the IA [39]. A distinct peak at 725 cm^{-1} was observed for UPs containing IA and it is assigned to the aromatic C-H out-of-plane bending vibrations. The peaks in the characteristic region $1150\text{--}1050\text{ cm}^{-1}$ observed in all cases can be ascribed to the C-O group.

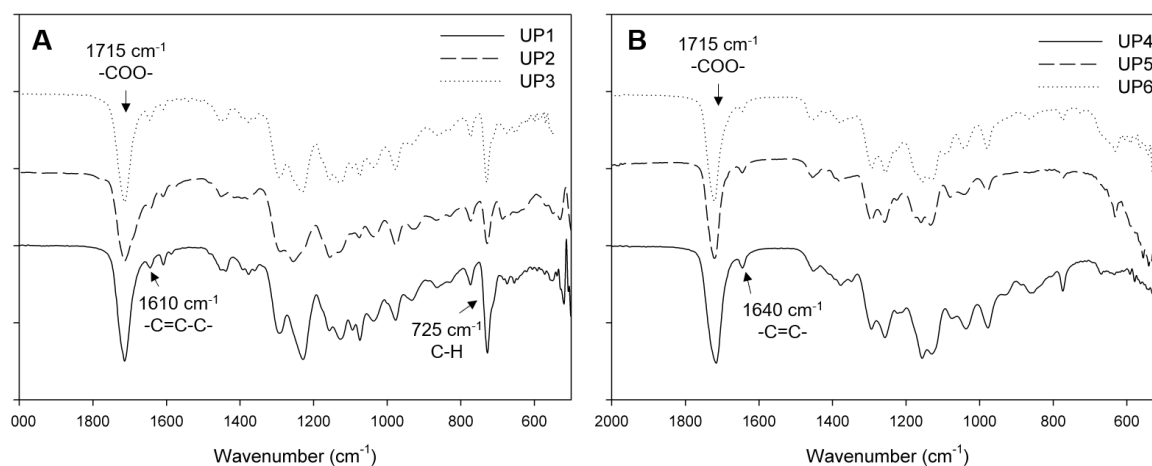


Figure 3. ATR-FTIR spectra for UP1 to UP3 (A) and UP4 to UP6 (B).

Figure 4 shows the ^1H NMR spectra of the UPs based on IA. The spectrum of UP1 exhibits three distinct peaks (**a**) at 8.63, 8.19 and 7.57 ppm, which are assigned to the aromatic ring protons. The protons characteristics of the double bonds of fumaric acid (**b**) are located between 6.50 and 7.0 ppm. The CH_3 signals (**c**) of PG are located between 1.03 and 1.47 ppm, while the CH signal (**d**) of PG was found at around 5.25 and 5.54 ppm. The CH_2 signals (**e**) of both glycols are located between 3.71 and 4.45 ppm. The proximity of the (**e**) peaks due to glycols, which appear almost overlapped, avoids a straightforward analysis. The glycol content was determined from the signal of the methyl proton of PG (**c**) and the CH_2 signals of DEG and PG (**e**).

3D Printing of New Biobased Unsaturated Polyesters by Microstereo-thermal-lithography

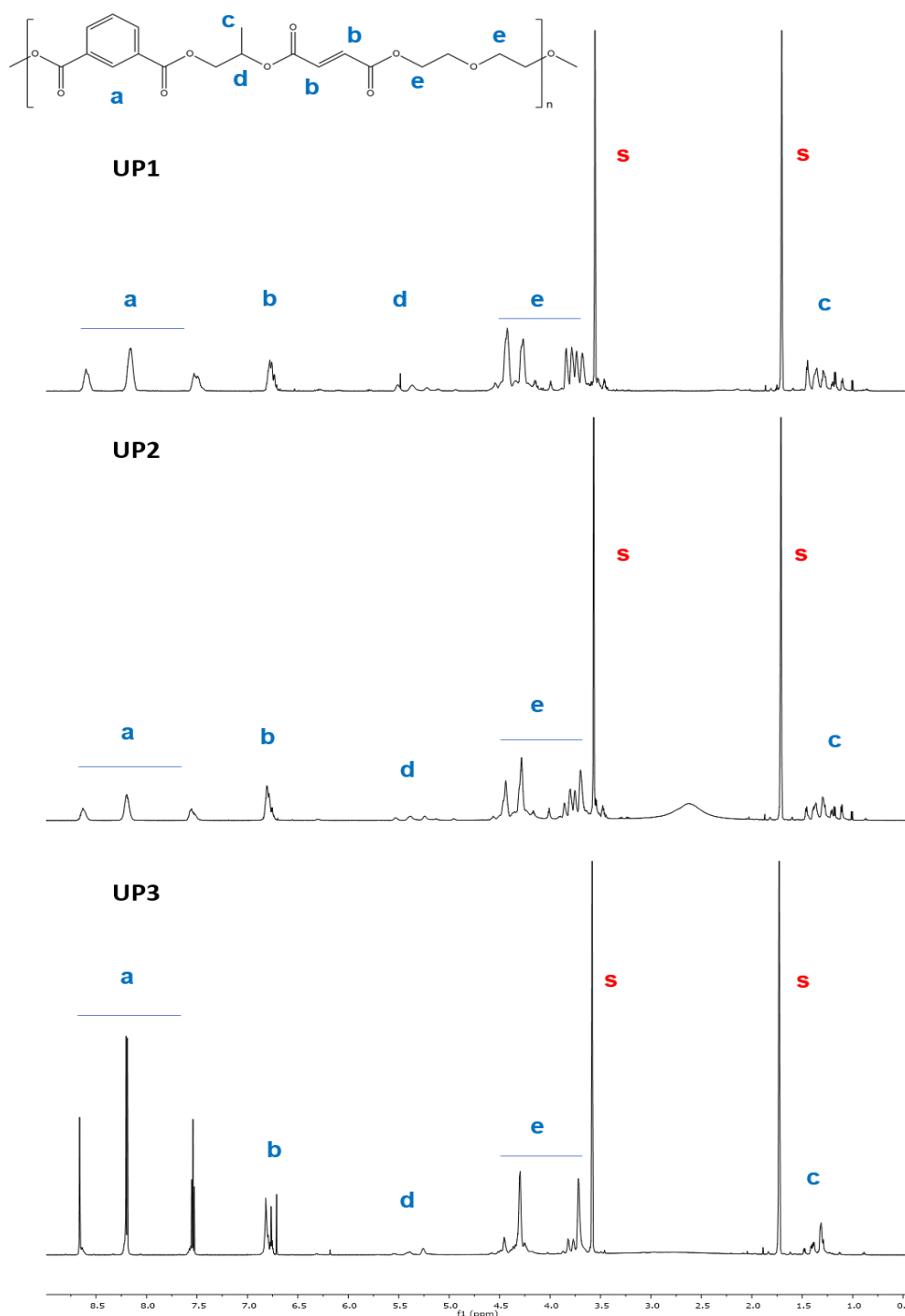


Figure 4. ¹H NMR spectra of unsaturated polyesters based on isophthalic acid, UP1 to UP3, where (s) correspond to the solvent peaks of THF- *d*₈.

Figure 5 shows the ¹H NMR spectra of UP4 to UP6. Besides the signals corresponding to FA, PG and DEG parts in UP4 to UP6, which are easily identified, on the UP4 spectrum the signal at 2.58 ppm (**f**) corresponds to the CH₂ of SuCA. On the other hand, UP5 shows two peaks, $\delta = 2.30$ ppm (**g**) and $\delta = 1.68$ ppm (**h**) assigned to the CH₂ bonds of the AA. In UP6 spectra three peaks at $\delta = 2.27$ (**i**) ppm, $\delta = 1.58$ ppm (**j**) and $\delta = 1.31$ ppm (**k**) correspond

Chapter II

to the CH₂ of SeBA [40]. Relative integration of (**K**) protons and (**i**) + (**j**) protons confirm this assumption.

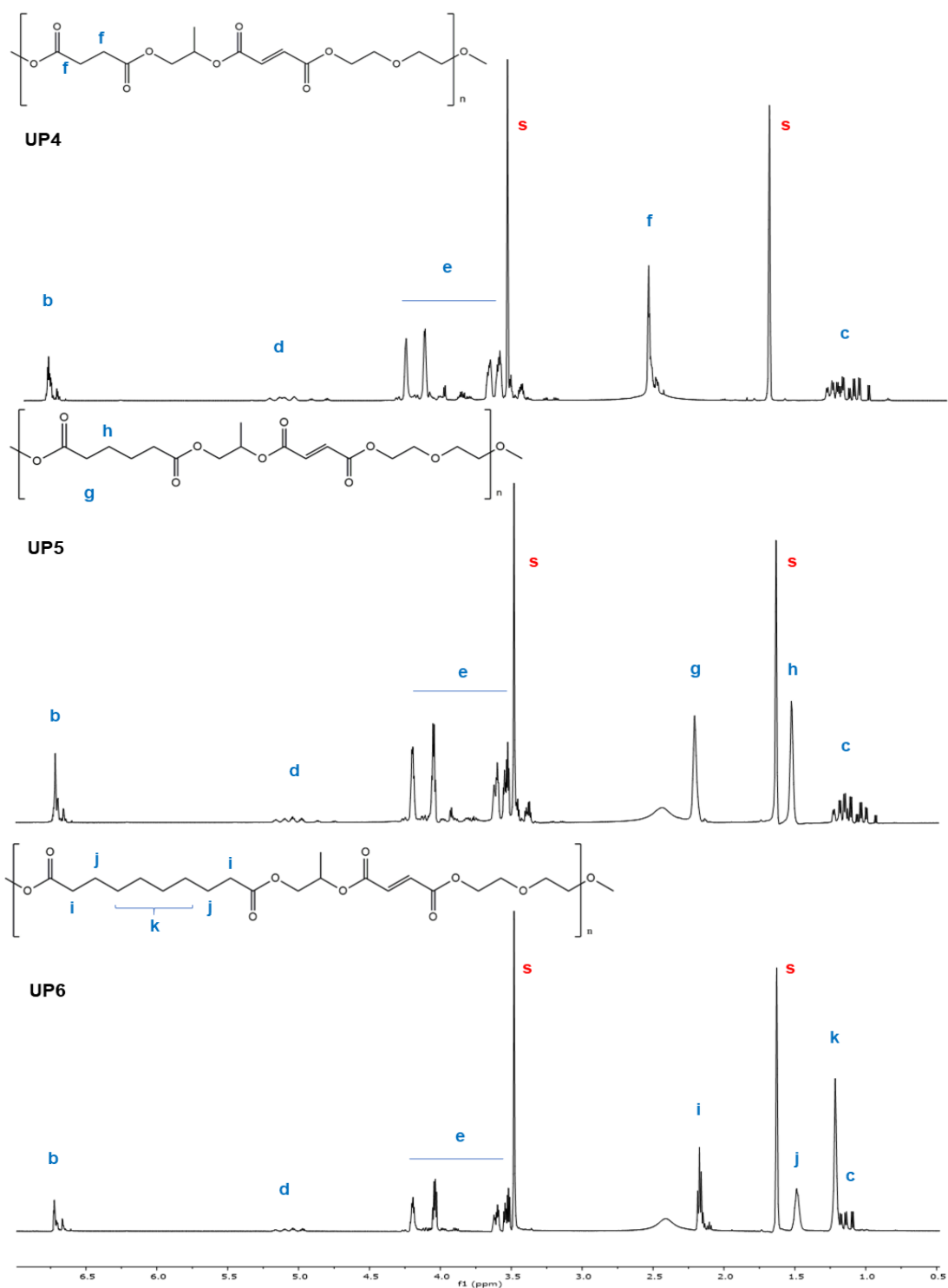


Figure 5. ¹H NMR spectra of UP4 to UP6, where (s) correspond to the solvent peaks of THF- *d*₈. From the integration of the ¹H NMR signals it was possible to determine the relative molar amount of the monomers that are incorporated in the polymer structure (see Table 1).

3D Printing of New Biobased Unsaturated Polyesters by Microstereo-thermal-lithography

Regarding the glycol's quantification, a higher amount of PG is observed in the final UP for the formulations having biobased acids rather than for the formulation using IA. This result suggests that alkylic diacids reacts preferentially with this glycol rather than IA.

The structures of UPs were also confirmed by MALDI-TOF-MS. As an example, the mass spectrum obtained for UP5 from 400 to 2000 m/z is showed in Figure 6. The spectrum presents five different polymer populations indicated in letter from A to E. For some MALDI signals, it is possible to assign the monomer composition of the different oligomers as showed in Table 3 with two degrees of polymerization (DP=2 and DP=3). Some of the observed polyesters m/z values were associated with the Na⁺ or K⁺ cations. Likewise, UP4 and UP6 revealed m/z values in the range of 500 to 1500 and 500 to 2000, respectively.

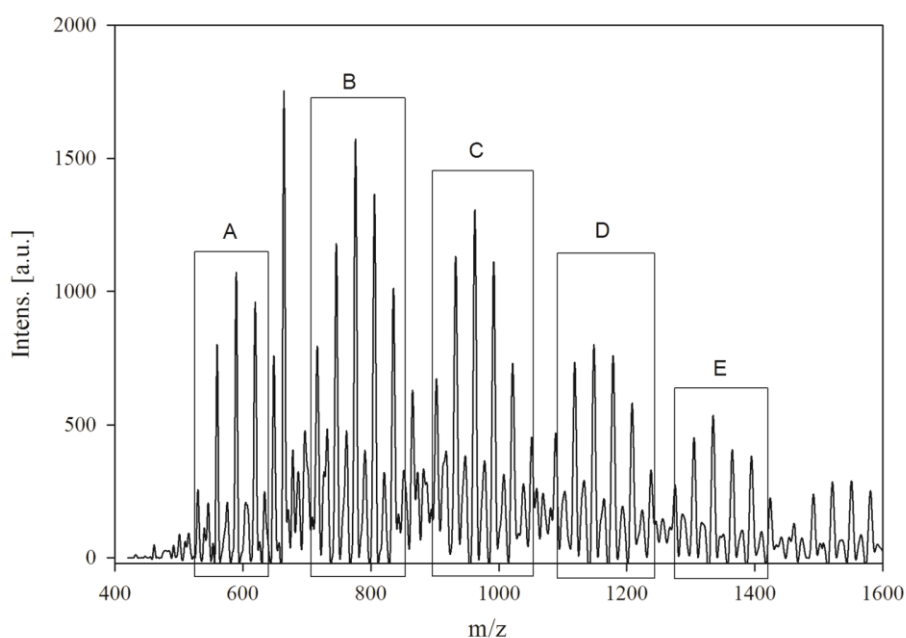


Figure 6. MALDI-TOF-MS in the linear mode (using DHB as matrix) of UP5 from m/z 400 to 1600 and the different observed populations from A to E.

The qualitative information collected suggest that the observed mass of UP5 (Table 3) was identified on the B and D groups, where the B population showed the peaks with the highest intensities. Also, in the MALDI-TOF spectrum of UP5 a repeating unit was identified, differing from 30 Da. This value can correspond to the difference between FA (116.07 g·mol⁻¹) and AA (146.14 g·mol⁻¹) units or between DEG (106.12 g·mol⁻¹) and PG (76.09 g·mol⁻¹) units. Based on the MALDI-TOF data, it can be suggested that other combinations of monomers were obtained besides the structure presented in Table 3.

Table 3. Relationship between m/z and the chemical structure of UP5.

UP5 structure		
Observed mass	Calculated mass	n=
805.54	803.830	2 + [Na ⁺]
1193.65	1194.251	3 + [Na ⁺]
820.80	819.941	2 + [K ⁺]
1208.31	1210.362	3 + [K ⁺]

It was also possible to confirm the existence of several combinations of monomers present in the other polyester structures (see Table S1). Between the five populations observed (A-E) almost all the peaks were ascribed to a specific formulation, e.g. $(AA)_n+(FA)_m+(PG)_p-(H_2O)_y$ or $(AA)_n+(FA)_m+(DEG)_q-(H_2O)_y$. The differences between near peaks are usually due to the number of the monomer in the formulation – n , m , p and q . The formation of other oligomers is expected due to the nature of the step growth polymerization.

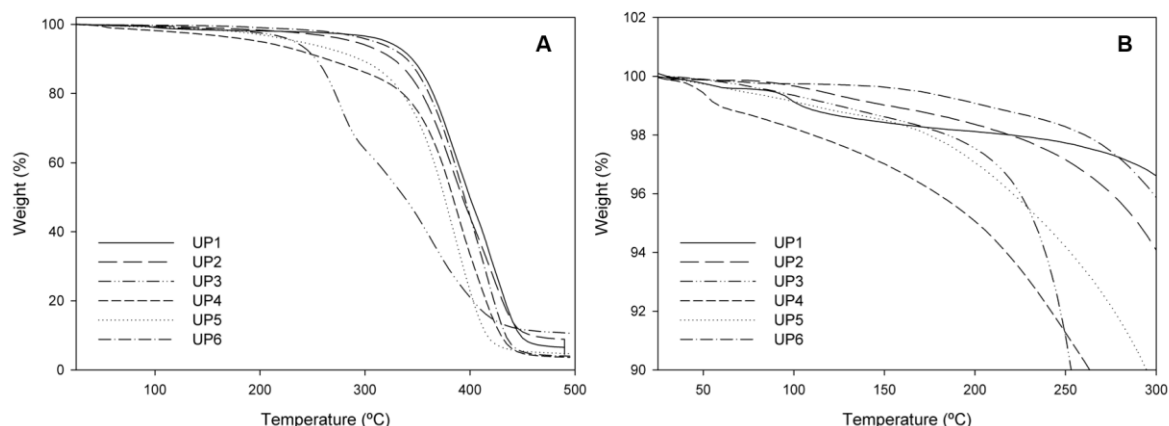
4.3 Thermal and Mechanical Analysis of Unsaturated Polyesters

Figure 7 and Table 4 present the data obtained from the thermogravimetric analysis. Comparing UP1 to UP2 and UP3 profiles, it is possible to observe that changing the percentages of the components in the formulation led to minor differences in the thermal decomposition. The differences between UP1 and UP2 thermal profiles were not relevant – only a slight decrease on the thermal stability was observed, probably due to a decrease in the aromatic content. UP3, however, presents two significant mass losses at 256 °C and 337 °C. This profile can indicate that the polyester has a heterogeneous composition. The onset temperature (T_{on}) of the fumaric acid is of 248 °C, which is fairly close to the value obtained for the UP3 first step, 255 °C. Despite not being possible to support this hypothesis, it is our belief that the first step corresponds to a possible sub product of the polycondensation reaction between FA and the other monomers. This assumption is in agreement with the ¹H NMR final molar %, being UP3 the polyesters with the higher percentage of FA (Table 1).

Table 4. TGA of UPs ($T_{x\%}$: temperature at x% mass loss; T_{on} : extrapolated onset temperature).

Polyesters	$T_{5\%} / ^\circ\text{C}$	$T_{10\%} / ^\circ\text{C}$	$T_{on} / ^\circ\text{C}$
UP1	320.63	344.80	355.70
UP2	289.41	326.73	339.21
UP3	228.28	249.64	255.96; 336.85
UP4	199.45	262.92	342.06
UP5	240.42	295.57	328.49
UP6	308.86	339.67	350.04

Figure 7B comprises a low temperature region, making clear that UP4, UP5 and UP6 formulations have similar mass loss profiles, which is explained by their comparable structures. These results also suggest that the stability of the UPs increases with the number of carbons in the main chain. For UP6, which contains SeBA in its structure, the stability is similar to the more stable UP1. However, this is not valid for temperatures below 330 °C. At lower temperatures (see Figure 7B) UP1 shows a less stable behaviour when compared with UP6. Nevertheless, in general, UP1 appears to be the most stable formulation, with the main mass loss stage starting at 320 °C.

**Figure 7.** A. TG curves of the synthesized UPs obtained at a heating rate of $10^\circ\text{C}\cdot\text{min}^{-1}$ and B. detailed view within the mass loss range up to 10%.

The thermal characterization of the UPs was extended by using the MDSC (see SI, Figure S4). The identified thermal events correspond to the glass transition temperature, T_g , of the UPs. According to Table 2.5, the UPs revealed similar MDSC profiles, having T_g values between 8.9 and -39.94 °C. Except for UP1, the other UPs showed only one transition. The dynamic mechanical results expressed as loss tangent ($\tan\delta$) as a function of temperature are shown in Figure 8. The UPs were submitted to two frequencies of 1 and 10 Hz (Figure 8 includes the values at 1 Hz as a representative result). DMTA, in

Chapter II

multifrequency analysis, allows distinguishing between frequency dependent and nondependent thermal events. Molecular relaxations such as α (or glass transitions), are always frequency dependent.

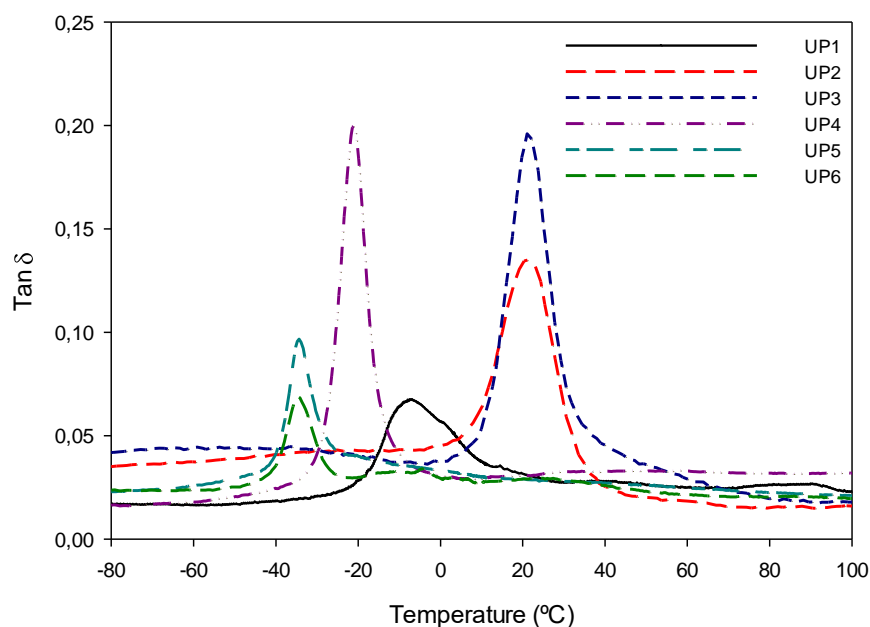


Figure 8. Loss function ($\tan\delta$) versus temperature for the synthesized UPs.

Table 5. Glass transition temperatures obtained from DMTA and MDSC techniques.

Polyesters	T_g (°C)		Tan δ (máx)
	DMTA	MDSC	
UP1	-7.30	-28.11; 8.9	0.07
UP2	18.00	-2.48	0.12
UP3	21.10	-2.9	0.20
UP4	-21.13	-22.22	0.20
UP5	-34.38	-37.49	0.10
UP6	-35.05	-39.94	0.07

Figure 8 shows the $\tan\delta$ traces for all synthesized UPs. The peak observed in the curves corresponds to the glass transition temperature (T_g), whose values are summarized in Table 5. As indicated above, UP1, UP2 and UP3 differ only in the percentages of monomers. The T_g values of UP2 and UP3 are similar (18 and 21 °C) and higher than the obtained values for the biobased UPs. This fact is explained by the high amount of unsaturated monomer incorporated into UP1 and UP2 formulations (see Table 1) and also because the polymer chains of these formulations are much more rigid. Therefore, a higher energy is necessary to allow the mobility of the UP2 and UP3 chains. Although UP2 and

3D Printing of New Biobased Unsaturated Polyesters by Microstereo-thermal-lithography

UP3 have similar T_g , the UP3 shows a higher ratio of loss and storage energies (Table 5). The study of the mechanical properties by DMTA of UPs is scarcely reported in the literature with the exception of the UPRs, which were extensively studied [11, 21, 41-43]. Therefore, it is not possible to establish a comparison of our UP results with other reported values.

According to Table 5, the T_g values obtained by MDSC were in agreement with the values obtained in DMTA for the polymers UP4 to UP6. The obtained T_g values for the aromatic based formulations were quite different for both the techniques. The differences observed between T_g values determined by MDSC and DMTA can be ascribed to differences in the principles used to determine the T_g [44]. The aliphatic polyesters showed negative T_g values in opposition to the positive values obtained for the IA based formulations. Despite the differences in the biobased formulations, the T_g for UP4 to UP6 was very similar, with values ranging between -21 and -35 °C. UP4, UP5 and UP6 showed lower T_g values. This fact can be explained by the absence of rigid aromatic ring in their structure, which results in much easier movements of the polymer backbone. Table 5 also reveals that for UP4, UP5 and UP6, an increase of the carbons in the main chain (from de diacid) results in a decrease of the T_g value, which was expected, since for longer chains, higher mobility is achieved. In Table 5, it is also presented the maximum of $\tan\delta$ curve. Thus, the values of maximum of this curve reveal that UP3 and UP4 are the polyesters with the highest capacity to dissipate energy. In sum, all the UPs reveal similar profiles, except for UP1, that showed two distinct transitions (MDSC technique).

4.4 Cell viability

The application of UPRs for the biomedical field requires the preparation of crosslinked material from synthesized UPs (UPRs). The crosslinking process consists in the use of St and a photo initiator. The biological tests were carried out for three UPs (UP4 to UP6). For the tests, 37% (w/w) of St and 2 to 5% (w/w) of the photo initiator, Irgacure 651 [44], were used. After photo polymerization (UV light of 253.7 nm, for a period time not exceeding 15 minutes), the obtained films were translucent and with clean, soft and flexible surfaces. Before viability tests and to eliminate films acidity they were washed with EtOH for 3-4 h, dried in vacuum at room temperature and finally placed in an oven at 50 °C for a few hours. Figure 9 show that there are no considerable differences on the cell viability of the tested biobased UPRs, being UPR5 the less biocompatible, nevertheless with a value near 80% of cell viability. The *Alamar Blue* assay suggested that the cell viability was in the range of 77-98% for all the tested UPRs, showing no statistically significant differences. Therefore,

the biobased polyesters synthesized in this work proved to be suitable for application in biomedical fields.

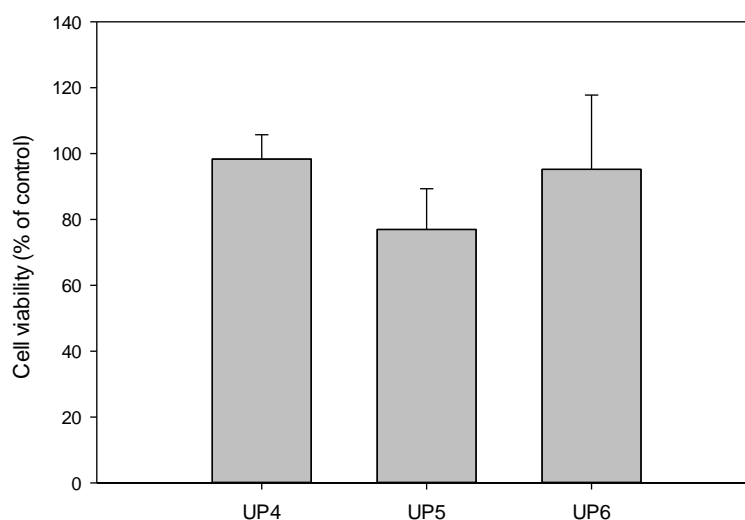


Figure 9. Effect of different UPR on cell viability. The statistical analysis (one-way ANOVA) indicates that there is not a significant difference between the different conditions.

4.5 Scaffolds Fabrication and Characterization

At this stage, only the UV light was used to promote the scaffolds fabrication. Several biobased scaffolds (Scf4-Scf6) with different specifications were fabricated. The times of curing varied between 25 and 60 seconds using St as crosslinking agent [8]. However, HEMA was also used as (UM) unsaturated monomer in this work considering its intrinsic biocompatibility [45]. Figure 10 shows the 3D scaffolds prepared by μ STLG using HEMA as crosslinking agent. The resulting 3D structures presented distinct geometries and very homogeneous surfaces. Also, the obtained results suggest the possibility of producing biobased 3D scaffolds by just applying to the UP/HEMA mixture an UV irradiation for 45 seconds (2 layers and a total thickness of 0.2 mm), in the presence of the biocompatible photo initiator Irgacure 651, 5% (w/w). It was found that depending on the ratio UP/HEMA the time of cure can range from 25 to 60 seconds to afford a complete crosslinking network without the need of further post-cure.

These 3D structures are the first reported structures obtained with this new apparatus using new photo-sensitive materials. These new UPs showed very promising results for TE applications. Further studies are being performed in order to combine UV and IR radiations as well as in the development of a multi-vat system [2, 5], so the fabrication of multi-materials may be a possibility in stereolithography (SLA).

3D Printing of New Biobased Unsaturated Polyesters by Microstereo-thermal-lithography

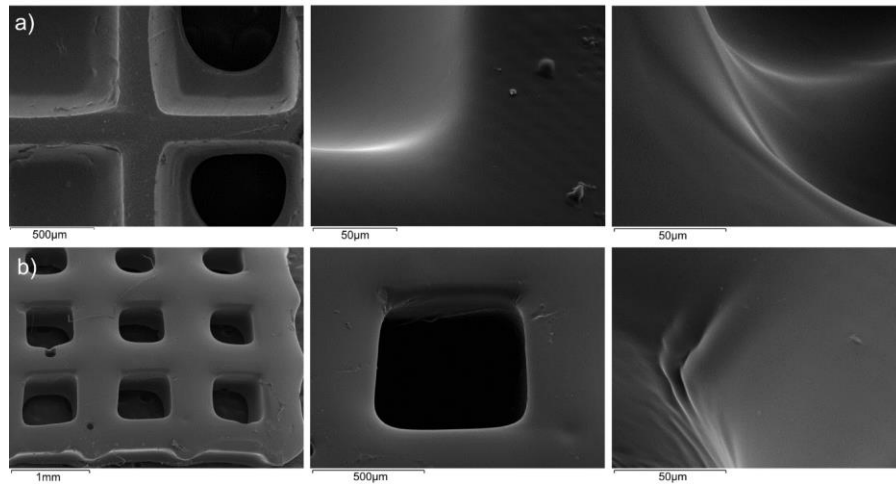


Figure 10. SEM pictures of the scaffolds obtained by μ STLG. **A.** Scf5 based on UP5/St, with different curing times and **B.** Scf4, based on UP4/HEMA formulation.

The roughness is known to have a critical role for cell adhesion and proliferation on the surface of the 3D scaffolds [46, 47], determining the cell-matrix interactions [3]. Previous analysis done by SEM (Figure 10) revealed several difficulties to draw any conclusion regarding this matter. Even for higher magnification, it was impossible to detect irregularities on the surfaces.

To overcome this issue, IFM analysis was performed (Figure 11) and the average roughness values (S_a) are summarized in Table 6. Aiming to compare the different scaffolds using the same conditions, a similar area of the scaffold was selected to be analysed. According to IFM results, all the scaffolds exhibited micro-roughness [48] showing values between 284 nm and 1.65 μ m: micro-roughness is widely reported in the literature for allowing cell growth and differentiation [48].

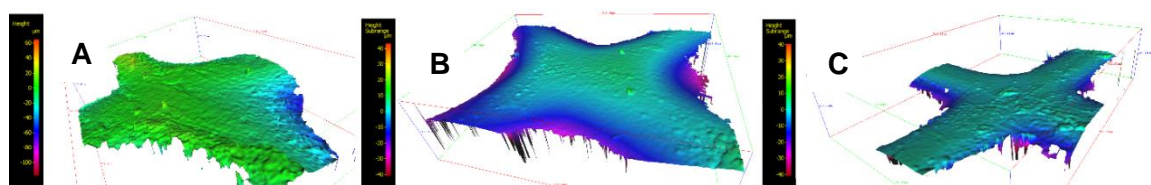


Figure 11. IFM images of 3D scaffolds: **A.** Scf4/HEMA (60 seconds, 1 layer), **B.** Scf5/HEMA (28.5 seconds, 2 layers) and **C.** Scf6/HEMA (28.5 sec, 1 layer).

Table 6. Surface roughness of some of the developed 3D scaffolds.

Scaffolds	UM	Number of layers	Time of cure (sec)	Sa
Scf4	HEMA	1	60	518.43 nm
Scf5	HEMA	2	28	283.69 nm
Scf6	HEMA	1	28	1.649 μ m

5. Conclusions

New biobased unsaturated polyesters were successfully synthesized *via* bulk polycondensation. The success of the polymerization was confirmed through ^1H NMR, ATR-FTIR and MALDI-TOF analysis. An extensive study of the structure properties of the obtained polymers was performed. According to the thermal and mechanical results, the UPs showed a good thermal stability, being UP1, UP5 and UP6 the most stable. Their thermal stability was quite similar, with onset temperature values ranging from 328.49 to 355.70 °C. The thermal properties of the UPs were analysed by DSC, MDSC and DMTA techniques, allowing the determination of the glass transition temperature. This temperature of the biobased UPs were relatively low (-21 to -35 °C). It was found a slight decrease of T_g with the increasing of the number of carbons in the main chain, which is explained by the enhancement of the chain mobility. The results confirm that the replacement of IA with SuCA, AA or SeBA in the formulation did not reduce the thermal stability of the UPs. Also, the rheological behaviour of the biobased materials plays an important role. The biobased polyesters showed proper viscosities to be applied in the μ STLG equipment. The cell viability data also suggested that synthesized UPR are good candidates to the development of new biocompatible and biobased polyesters structures. The extensive characterization points out that the UPs properties match the μ STLG requirements. These data were confirmed by the SEM and IFM results, showing very promising 3D structures, with very accurate geometries and presenting some nano-roughness, which is a very important parameter to promote cell adhesion and proliferation. The successful fabrication of the scaffolds confirms that the system can be used to fabricate 3D structures with complex micro-architectures.

6. References

1. Kruth, J.P., M.C. Leu, and T. Nakagawa, *Progress in additive manufacturing and rapid prototyping*. Cirp Annals 1998 - Manufacturing Technology, Vol 47/2/1998 - Annals of the International Institution for Production Engineering Research, ed. N. Alberti, et al. 1998, 3001 Bern: Hallwag Publishers. 525-540.
2. Melchels, F.P.W., et al., *Additive manufacturing of tissues and organs*. Progress in Polymer Science, 2012. **37**(8): p. 1079-1104.
3. Yeong, W.Y., et al., *Rapid prototyping in tissue engineering: challenges and potential*. Trends in Biotechnology, 2004. **22**(12): p. 643-652.
4. Bartolo, P.J. and G. Mitchell, *Stereo-thermal-lithography: a new principle for rapid prototyping*. Rapid Prototyping Journal, 2003. **9**(3): p. 150-156.
5. Bártolo, P.J., *Stereolithography Processes*, in *Stereolithography: Materials, Processes and Applications*. Springer, Editor. 2011, Springer: New York. p. 1-36.
6. Melchels, F.P.W., J. Feijen, and D.W. Grijpma, *A review on stereolithography and its applications in biomedical engineering*. Biomaterials, 2010. **31**(24): p. 6121-6130.
7. *Unsaturated polyester compositions*. 1973, UNION CARBIDE CORP,US: United States.
8. John Scheirs, T.E.L., *Modern Polyesters: Chemistry and Technology of Polyesters and Copolyesters*. Scheirs Polymer Science. Vol. 10. 2003, Chichester, West Sussex, England: John Wiley & Sons. 788.
9. Lu, M.G., M.J. Shim, and S.W. Kim, *Curing behavior of an unsaturated polyester system analyzed by Avrami equation*. Thermochimica Acta, 1998. **323**(1-2): p. 37-42.
10. Martin E. Rogers, T.E.L., *Synthetic methods in step-growth polymers*. 2003, New Jersey: Wiley-IEEE. 605
11. Worzakowska, M., *Chemical Modification of Unsaturated Polyesters Influence of Polyester's Structure on Thermal and Viscoelastic Properties of Low Styrene Content Copolymers*. Journal of Applied Polymer Science, 2009. **114**(2): p. 720-731.
12. Alkskas, I.A., B.A. El-Gnidi, and F. Azam, *Synthesis and Characterization of New Unsaturated Polyesters Containing Cyclopentapyrazoline Moiety in the Main Chain*. Journal of Applied Polymer Science, 2010. **115**(6): p. 3727-3736.
13. Alemdar, N., A.T. Erciyes, and N. Bicak, *Preparation of unsaturated polyesters using boric acid as mild catalyst and their sulfonated derivatives as new family of degradable polymer surfactants*. Polymer, 2010. **51**(22): p. 5044-5050.
14. Guo, W.X., et al., *New unsaturated polyesters as injectable drug carriers*. Polymer Degradation and Stability, 2007. **92**(3): p. 407-413.
15. Irfan, M.H., *Polyesters in the construction industry*, in *Chemistry and Technology of Thermosetting Polymers in Construction Applications*, S.S.B.M. Dordrecht, Editor. 1998. p. 230-239
16. Matynia, T., M. Worzakowska, and W. Tamawski, *Synthesis of unsaturated polyesters of increased solubility in styrene*. Journal of Applied Polymer Science, 2006. **101**(5): p. 3143-3150.

Chapter II

17. Sanchez, E.M.S., C.A.C. Zavaglia, and M.I. Felisberti, *Unsaturated polyester resins: influence of the styrene concentration on the miscibility and mechanical properties*. Polymer, 2000. **41**(2): p. 765-769.
18. Jasinska, L. and C.E. Koning, *Unsaturated, Biobased Polyesters and Their Cross-Linking via Radical Copolymerization*. Journal of Polymer Science Part a-Polymer Chemistry, 2010. **48**(13): p. 2885-2895.
19. Tawfik, S.Y., *Preparation and characterization of some new unsaturated polyesters based on 3,6-bis(methoxymethyl)urene*. Journal of Applied Polymer Science, 2001. **81**(14): p. 3388-3398.
20. Barrett, D.G., et al., *One-Step Syntheses of Photocurable Polyesters Based on a Renewable Resource*. Macromolecules, 2010. **43**(23): p. 9660-9667.
21. Nebioglu, A. and M.D. Soucek, *Investigation of the properties of UV-curing acrylate-terminated unsaturated polyester coatings by utilizing an experimental design methodology*. Journal of Coatings Technology and Research, 2007. **4**(4): p. 425-433.
22. Najafi, F. and M.N. Sarbolouki, *Synthesis and characterization of block copolymers from aromatic diols, fumaric acid, sebacic acid and PEG*. Journal of Applied Polymer Science, 2003. **90**(9): p. 2358-2363.
23. Jasinska, L. and C.E. Koning, *Waterborne polyesters partially based on renewable resources*. Journal of Polymer Science Part A: Polymer Chemistry, 2010. **48**(24): p. 5907-5915.
24. Takenouchi, S., et al., *Effects of geometric structure in unsaturated aliphatic polyesters on their biodegradability*. Polymer Journal, 2001. **33**(10): p. 746-753.
25. Cherian, A.B. and E.T. Thachil, *Modification of unsaturated polyesters using polyethylene glycol*. Plastics Rubber and Composites, 2007. **36**(3): p. 128-133.
26. Grobelny, J., *Nmr-study of maleate (cis)-fumarate (trans) isomerism in unsaturated polyesters and related-compounds*. Polymer, 1995. **36**(22): p. 4215-4222.
27. Grobelny, J. and A. Kotas, *compositional sequence distribution in unsaturated polyesters as revealed by c-13 nmr-spectroscopy*. Polymer, 1995. **36**(7): p. 1363-1374.
28. Organization, I.S., *Biological evaluation of medical devices. , in Part 5. Tests for cytotoxicity: In vitro methods*. 2009, AAMI: Geneva, Switzerland. p. 50.
29. Faneca, H., A. Faustino, and M.C. Pedroso de Lima, *Synergistic antitumoral effect of vinblastine and HSV-Tk/GCV gene therapy mediated by albumin-associated cationic liposomes*. Journal of Controlled Release, 2008. **126**(2): p. 175-184.
30. Pereira, R.F.B., Paulo J. , *Recent Advances in Additive Biomanufacturing*, in *Comprehensive Materials Processing*, M.S.J. Hashmi, Editor. 2014, Elsevier. p. 265-284.
31. Bechthold, I., et al., *Succinic Acid: A New Platform Chemical for Biobased Polymers from Renewable Resources*. Chemical Engineering & Technology, 2008. **31**(5): p. 647-654.
32. Edlund, U. and A.C. Albertsson, *Polyesters based on diacid monomers*. Advanced Drug Delivery Reviews, 2003. **55**(4): p. 585-609.
33. Ma, J., et al., *The copolymerization reactivity of diols with 2,5-furandicarboxylic acid for furan-based copolyester materials*. Journal of Materials Chemistry, 2012. **22**(8): p. 3457-3461.

3D Printing of New Biobased Unsaturated Polyesters by Microstereo-thermal-lithography

34. Stevens, M.P., *Polymer chemistry: an introduction*. 3rd ed. 1999, New York: Oxford University Press, Inc.
35. Shaw, M.T., *Introduction to Polymer Rheology*. 2012, New Jersey: John Wiley & Sons.
36. Han, C.D. and K.-W. Lem, *Chemorheology of thermosetting resins. I. The chemorheology and curing kinetics of unsaturated polyester resin*. *Journal of Applied Polymer Science*, 1983. **28**(10): p. 3155-3183.
37. de la Caba, K., et al., *Kinetic and rheological studies of an unsaturated polyester cured with different catalyst amounts*. *Polymer*, 1996. **37**(2): p. 275-280.
38. Lee, S.S., A. Luciani, and J.-A.E. Månson, *A rheological characterisation technique for fast UV-curable systems*. *Progress in Organic Coatings*, 2000. **38**(3-4): p. 193-197.
39. Coates, J., *Interpretation of Infrared Spectra, A Practical Approach*, in *Encyclopedia of Analytical Chemistry*, R.A. Meyers, Editor. 2000, John Wiley & Sons Ltd: Chichester. p. 10815–10837.
40. Stuart, B., *Polymer Analysis*. 2002, Chichester: John Wiley & Sons Ltd.
41. Nebioglu, A. and M.D. Soucek, *Microgel formation and thermo-mechanical properties of UV-curing unsaturated polyester acrylates*. *Journal of Applied Polymer Science*, 2008. **107**(4): p. 2364-2374.
42. Mironi-Harpaz, I., et al., *Curing of styrene-free unsaturated polyester alkyd: synthesis, characterization and simulation*. *Polymer International*, 2010. **59**(6): p. 836-841.
43. Vilas, J.L., et al., *Unsaturated polyester resins cure: Kinetic, rheologic, and mechanical dynamical analysis. II. The glass transition in the mechanical dynamical spectrum of polyester networks*. *Journal of Polymer Science Part B-Polymer Physics*, 2001. **39**(1): p. 146-152.
44. Lu, S. and K.S. Anseth, *Photopolymerization of multilaminated poly(HEMA) hydrogels for controlled release* *Journal of Controlled Release* 1999. **57**(3): p. 10.
45. Kejlová, K., et al., *Hydrophilic polymers—biocompatibility testing in vitro*. *Toxicology in Vitro*, 2005. **19**(7): p. 957-962.
46. Boyan, B.D., et al., *Role of material surfaces in regulating bone and cartilage cell response*. *Biomaterials*, 1996. **17**(2): p. 137-146.
47. Anselme, K., A. Ponche, and M. Bigerelle, *Relative influence of surface topography and surface chemistry on cell response to bone implant materials. Part 2: biological aspects*. *Proceedings of the Institution of Mechanical Engineers Part H-Journal of Engineering in Medicine*, 2010. **224**(H12): p. 1487-1507.
48. Hsin-I Chang, Y.W., *Cell Responses to Surface and Architecture of Tissue Engineering Scaffolds*, in *Regenerative Medicine and Tissue Engineering -Cells and Biomaterials*, P.D. Eberli, Editor. 2011. p. 569-588.

Supplementary Information

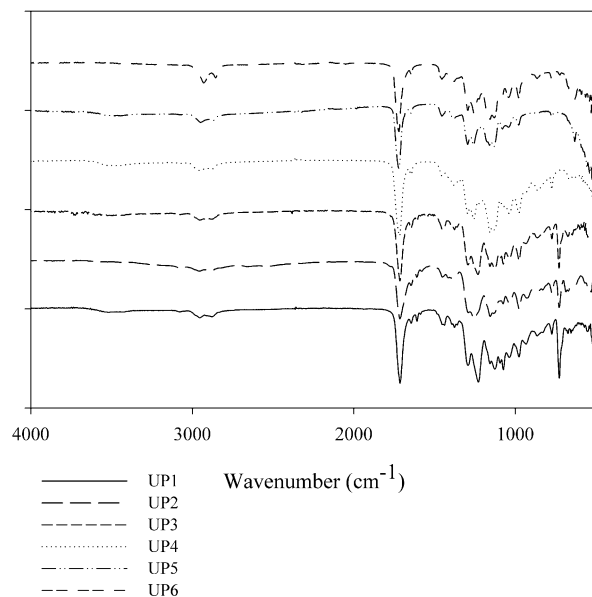


Figure S1. ATR-FTIR spectra for the developed UPs.

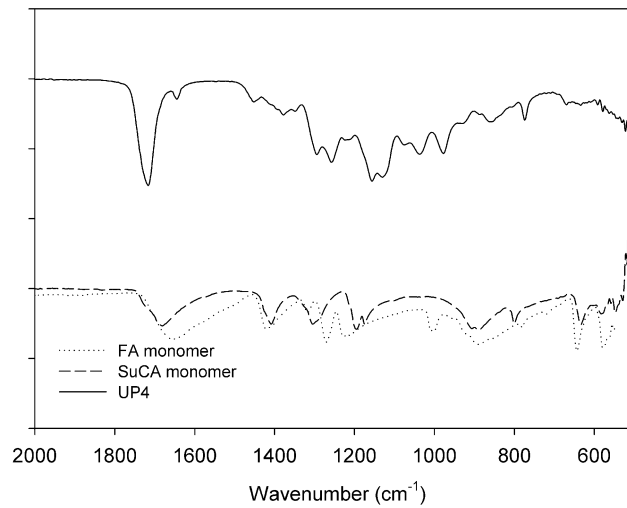


Figure S2. ATR-FTIR spectra of UP4 and respective diacid monomers.

3D Printing of New Biobased Unsaturated Polyesters by Microstereo-thermal-lithography

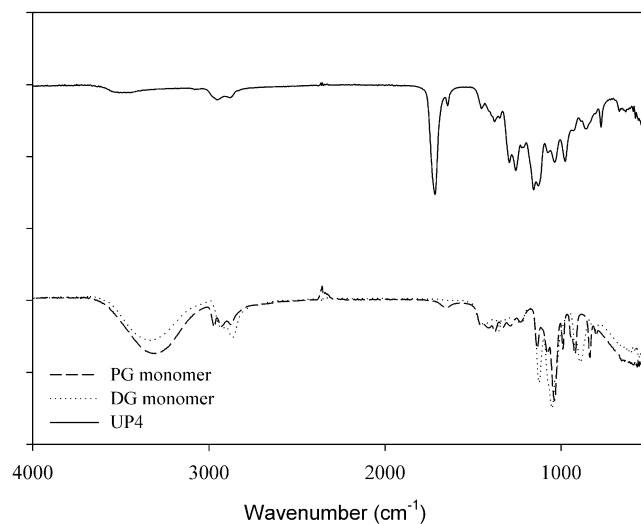


Figure S3. ATR-FTIR spectra of UP4 and respective glycol monomers.

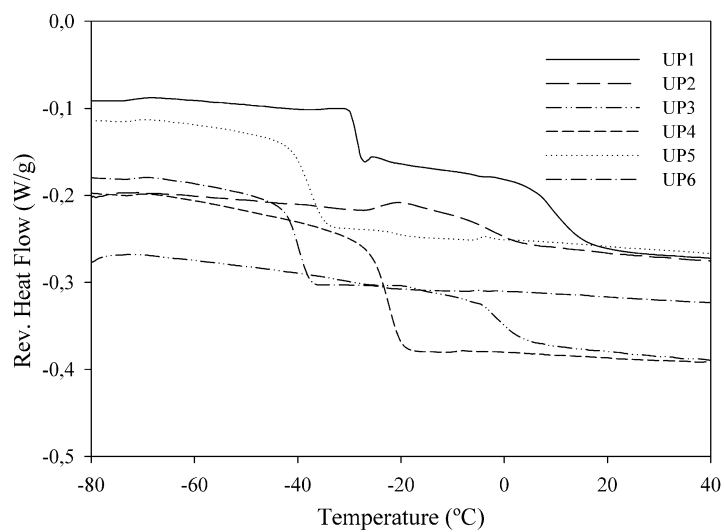


Figure S4. MDSC curves for the developed UPs. The polymers were tested in the temperature range -90 to 50 °C.

Table S1. MALDI-TOF possible combinations, from A to E, for UP5.

<i>Populations (A to E)</i>	<i>Possible Combinations (*)</i>								
	$(AA)_n+(PG)_p-(H_2O)_y$	$(AA)_n+(DEG)_q-(H_2O)_y$	$(FA)_m+(PG)_p-(H_2O)_y$	$(FA)_m+(DEG)_q-(H_2O)_y$	$(AA)_n+(FA)_m+(PG)_p-(H_2O)_y$	$(AA)_n+(FA)_m+(DEG)_q-(H_2O)_y$	$(AA)_n+(PG)_p+(DEG)_q-(H_2O)_y$	$(FA)_m+(PG)_p+(DEG)_q-(H_2O)_y$	$(AA)_n+(FA)_m+(PG)_p+(DEG)_q-(H_2O)_y$
-	A	A	A	A	A	A	A	A	A
B	-	B	B	B	B	B	B	-	B
C	C	C	C	C	C	C	-	-	C
-	-	D	-	D	-	-	D	-	D
-	E	-	-	E	E	-	-	-	E

(*) DP between 1 and 3 were considered for the possible combinations.

CHAPTER III

Novel Biobased Unsaturated Polyester Resins prepared by Thermal crosslinking and μ STLG

1. ABSTRACT	97
2. INTRODUCTION	97
3. MATERIALS AND METHODS.....	98
3.1 MATERIALS	98
3.2 SYNTHESIS AND CROSSLINKING OF UNSATURATED POLYESTERS RESINS (UPRs).....	98
3.3 MICROSTEREO-THERMAL-LITHOGRAPHY OF THE BIOBASED UPRs	99
3.4 VISCOSITY MEASUREMENTS	99
3.5 THERMAL AND MECHANICAL ANALYSIS OF UPRs	99
3.6 SCAFFOLDS MORPHOLOGY AND TOPOGRAPHY	100
3.7 TENSILE TESTS	100
3.8 WETTABILITY OF UPRs	100
3.9 GEL CONTENT DETERMINATION	100
3.10 CELL VIABILITIES TESTS	100
4. RESULTS AND DISCUSSION.....	101
4.1. RHEOLOGY OF UPS.....	102
4.2 THERMAL CROSSLINKING OF UPS	103
4.3 CONTACT ANGLE MEASUREMENTS.....	104
4.4 THERMAL AND MECHANICAL ANALYSIS OF UPRs	105
4.5 3D SCAFFOLDS BY μ STLG AND CHARACTERIZATION	108
4.6 TOPOGRAPHIC ANALYSIS	109
4.7 CELL CULTURING.....	111
5. CONCLUSIONS	112
6. REFERENCES	112
SUPPLEMENTARY INFORMATION.....	116

1. Abstract

Additive Manufacturing (AM) technologies are an effective route to fabricate tailor made scaffolds for tissue engineering and regenerative medicine, being microstereo-thermal-lithography (μ STLG) one of the most promising techniques to produce high quality 3D structures. Here, we report the crosslinking studies of biobased unsaturated polyesters (UPs), using thermal and μ STLG crosslinking processes. The resulting resins were fully characterized in terms of chemical, thermal and mechanical properties. Gel content determination, water contact angles (WCA), topography and morphology analysis by atomic force microscopy (AFM) and scanning electron microscopy (SEM) were also performed. The results suggest that the synthesized resins have promising characteristics for μ STLG. The *in vitro* cytotoxicity tests carried out with 3T3-L1 cell lines showed that the materials prepared by μ STLG presented higher cellular viability when compared with the thermally crosslinked materials. The cellular viability was 60% and this can be tentatively attributed to the acidic character presented by the materials.

2. Introduction

The stereolithography (SLA) technology allows the production of highly complex and accurate 3D scaffolds, due to a precise control over micro and macro-scale characteristics. Indeed, this technology is one of the few available with ability to produce scaffolds with accuracies in the range of the cell size [1, 2]. Several authors have reported the fabrication of scaffolds by SLA, using polypropylene fumarate (PPF) [3], poly(D,L-lactide)-methacrylate [4], hydroxyapatite [5, 6], coumarin copolymers [7], among others. However, the range of materials available nowadays for SLA is very scarce due to several material requirements related with the operation of the technique. SLA methods require the use of photo curing polymers, with low viscosity and high curing rates.

An improved SLA technique called microstereo-thermal-lithography (μ STLG), was used in this work to develop 3D scaffolds based on biobased UP recently reported by our research group [8]. There are several advantages on fabricating micro-scaffolds such as the improvement of the mechanical properties which ultimately leads to a better cell adhesion [9]. The formulations revealed to have two of the most important characteristics for being used in μ STLG: suitable viscosity and fast curing rates [10].

These UPs were synthesized by bulk polycondensation using biobased monomers such as: succinic, adipic and sebacic acids. Fumaric acid (FA) was used as the source of double bonds to promote further crosslinking reactions with selected unsaturated monomers (UMs). The optimized conditions for processing involved a curing time between 25-60 seconds to afford 3D structures with controlled geometry and surfaces with micro-

roughness [8]. Styrene (St) is the most used UM for UP crosslinking due to the interesting mechanical and thermal properties of the resulting UPR. However, the toxicity of St turns its substitution by another UM highly desirable. In this line, its replacement by 2-hydroxyethyl methacrylate (HEMA), *N*-vinyl-2-pyrrolidone (NVP) or acrylic acid (AcA) is a suitable approach, as these monomers have been widely used in the preparation of polymeric structures directed to biomedical fields [11]. Crosslinking studies of new UPRs using HEMA were also tested in the μ STLG. In this context, the biobased UPs were crosslinked with St (for comparison purposes) and HEMA by thermal crosslinking or μ STLG. The UPRs were characterised in terms of chemical composition, topography and thermal/mechanical behaviour. The gel content, water contact angles (WCA) and cell viability were also assessed.

3. Materials and Methods

3.1 Materials

Succinic acid (SuCA, 99%), adipic acid (AA, 99.6%), sebacic acid (SeBA, 94.5%), diethylene glycol (DEG, 99%), propylene glycol (PG, 99%), potassium hydroxide (90%), *N*-vinyl-2-pyrrolidinone (NVP), acrylic acid (AcA), tetrahydrofuran (THF, >95%) and photo initiator 2,2-dimethoxy-1,2-diphenylethan-1-one (Irgacure 651[®], 99%) were purchased from Sigma-Aldrich and used as received. Benzoyl peroxide (BPO, 97%) was ordered from TCI Europe. Styrene (>99%) and 2-hydroxyethyl methacrylate (HEMA, 97%) were purchased from Acros Organics. Hydroquinone (99%) was purchased from Analar. Ethanol (96%) and sodium azide (99%) were purchased from Panreac and phenolphthalein (99%) from Riedel-de Haën.

3.2 Synthesis and Crosslinking of Unsaturated Polyesters Resins (UPRs)

The UPs were prepared by bulk polycondensation following a procedure reported elsewhere [8]. Briefly, diacids, glycols and hydroquinone (0.02 % of the monomers total weight) were charged into a four-necked glass reactor, equipped with a mechanical stirrer, a nitrogen inlet and a condenser connected to a receiver flask. The reactor was heated at 190–200 °C, and further raised to 220 °C. The end of the reaction was determined when the acid value (AV), determined according to standard ASTM 109-01, reached a constant value. In a second step, the UPRs were prepared through both thermal and μ STLG processes. For thermal crosslinking, benzoyl peroxide (BPO) was used as the radical initiator at a concentration of 1% (w/w). The UM was used in a percentage of 37% (w/w) which is a standard value used in the UPRs engineering area. The mixtures were

Novel Biobased Unsaturated Polyester Resins prepared by Thermal crosslinking and μ STLG

transferred to Teflon moulds (4 cm x 2.5 cm x 0.2 cm). The moulds were placed in an oven at 80 °C for 24 h. No post-cure was performed. After crosslinking, the films were removed from the moulds and stored at room temperature.

3.3 Microstereo-thermal-lithography of the Biobased UPRs

3-D scaffolds were prepared by means of μ STLG. The UP and the UMs were loaded into the reservoir and were then exposed to the UV light, for 60 seconds. The different scaffolds were constructed with the same shape. The dimensions were 0.125 mm of thickness and a diameter of 0.6 cm. The μ STLG system is equipped with a mercury lamp of 350 W as a light source (Mercury arc lamp sources, Oriel 66942). Optical fibers, projection and focal lenses irradiate a UV-DMD and an IR-DMD. A dichroic mirror captures the images projected on DMD (1024 x 768 pixels, 14mm in size), combining them into a single image that is transferred to the liquid polymer. The equipment also includes a multi-vat system. The vertical displacement of the platform is held by a positioned uniaxial MYCOSIS Translation Stage VT-80 which allows vertical increments of 1 μ m, at a speed ranging between 0.001 and 20 mm/s. After fabrication, the scaffolds were removed with a razor blade and washed several times with EtOH, to remove possible unreacted precursors.

3.4 Viscosity measurements

The viscosity was measured using a controlled stress rheometer Haake, model RS1. The geometry used was a plate/plate system PP20 (titanium for the rotating part and stainless steel for the stationary part). The UPs were dissolved in the selected monomers and the measurements were taken at 25 °C. The samples were analysed according to the following parameters: shear rate of 100 sec^{-1} ; temperature of 25°C; and UM at 37% (w/w). All measurements were made in triplicate

3.5 Thermal and Mechanical analysis of UPRs

The thermal stability of UPRs was evaluated in the range of ca. 25-600 °C, in a TA Instruments Q500 thermogravimetric analyzer (thermobalance sensitivity: 0.1 μ g) at a heating rate of 10 °C \cdot min $^{-1}$ and under a dry nitrogen purge flow of 100 mL \cdot min $^{-1}$. Universal Analysis 2000 software was used to determine onset temperature (T_{on}) and temperatures of specific weight loss, 5% and 10% ($T_{5\%}$ and $T_{10\%}$).

DMTA analyses were performed in a Tritec 2000 DMA equipment and the UPRs were analysed in the dual cantilever bending geometry. The tests were carried out from -150 °C to 200 °C, in a multifrequency mode (1 Hz and 10 Hz), with a standard heating rate of 5 °C min $^{-1}$.

3.6 Scaffolds morphology and topography

The morphology of the processed scaffolds was observed by means of scanning electron microscopy (SEM) (MEV)/EDS, JEOL, model JSM-5310, at an accelerating voltage of 10 kV. The topography of the polymers was evaluated by atomic force microscopy (AFM) using a NanoScopeIII a model from Digital Instruments operating in tapping mode. AFM images were taken over scanning areas of $10 \times 10 \mu\text{m}^2$.

3.7 Tensile tests

The different samples were immersed in physiological solution, at 37 °C. Tensile tests were carried out on wet specimens with a width (w) of 12.5 mm and a thickness (t) in the range of 2.0 - 2.4 mm. The grip-to-grip distance (l_0) (i.e. gauge length) was 10 mm. All the tests were performed at a rate of 1 mm/min using an INSTRON 5566 testing machine. Tensile modulus, maximum stress and maximum strain were evaluated.

3.8 Wettability of UPRs

Water contact angle (WCA) tests were performed on air-facing surfaces of UPRs using the sessile drop method at room temperature in an OCA 20 contact angle measurement unit from Dataphysics, equipped with a Hamilton syringe (500 μL). Deionized distilled water was dropped onto the surface of the selected UPRs and the measurements were performed at room temperature. The data obtained represents the mean values of at least five independent measurements.

3.9 Gel content determination

The gel content of the crosslinked UPs was determined by Soxhlet extraction, using tetrahydrofuran (THF) as solvent. The samples were first weighted and then extracted with THF for 8 h. The films were dried under vacuum until constant weight:

$$\text{Gel content (\%)} = \frac{W_f}{W_0} \times 100 \quad (3)$$

where W_0 is the initial weight and W_f is the weight of the UPRs after extraction.

3.10 Cell viabilities tests

For cell viability tests the UPs were crosslinked with the UM (37% (w/w)). The cell viabilities of the photo (fabricated in μSTLG , with 5% (w/w) of Irgacure 651[®] and irradiated for 60 seconds) and thermally (BPO 1% (w/w), at 80 °C for 24 h) crosslinked polyesters were

Novel Biobased Unsaturated Polyester Resins prepared by Thermal crosslinking and μ STLG

evaluated. Before any cell assays, the UPRs were treated, e.g., refluxed in ethanol, for a period not exceeding 2 h, to eliminate the terminal acidic groups. 3T3-L1 cell line (Mouse embryonic fibroblast cell line) were maintained in culture at 37 °C, under 5% CO₂, in Dulbecco's modified Eagle's medium-high glucose (DMEM-HG) (Sigma, MO, USA) supplemented with 10% (v/v) heat-inactivated fetal bovine serum (FBS) (Sigma, MO, USA), penicillin (100U/mL) and streptomycin (100 μ g·mL⁻¹). 3T3-L1 cells grow in monolayer and were detached by treatment with a trypsin solution (0.25%) (Sigma, St. Louis, MO) 30 × 10³ 3T3-L1 cells were seeded in 1 mL of medium in 48-well culture plates 24 h before incubation, to obtain 70 % confluence. The cytotoxicity of the different UPRs was evaluated in 3T3-L1 cell lines by an extraction test according to ISO 10993-5 Standard [12]. Before starting the extraction protocol, UPRs were washed once with an ethanol/PBS (1/1) solution for 5 minutes, and then with PBS for 1 minute. Afterwards, the UPRs were immersed in culture medium (DMEM-HG) at an extraction ratio of 1 ml of DMEM-HG per 1.25 cm² of UPRs surface area and incubated in a humidified atmosphere with 5% carbon dioxide, for 24 h, at 37 °C. The pH of the extraction fluid was corrected to 7.4 and then this medium was sterilized using UV radiation for 30 minutes. 3T3-L1 cells, seeded in 48-well culture plates, were incubated with the extraction fluid for 24 h, and the cell viability was assessed by a modified *Alamar Blue* assay [13]. This assay measures the redox capacity of the cells due to the production of metabolites as a result of cell growth. Briefly, following cells incubation during 24 h with the extraction medium, the medium of each well was replaced with 0.3 ml of DMEM-HG containing 10 % (v/v) of Alamar Blue (0.1 mg/mL in PBS) and, after 1 h of incubation at 37 °C, 170 μ L of the supernatant were collected from each well and transferred to 96-well plates. Then, absorbance at 570 and 600 nm was immediately measured in a SPECTRAMax PLUS 384 spectrophotometer (Molecular Devices, Union City, CA). Cell viability was calculated as a percentage of the control cells (cells not treated with the extraction medium) according to the formula $(A_{570}-A_{600})$ of treated cells $\times 100 / (A_{570}-A_{600})$ of control cells. The data are expressed as the percentage of the untreated control cells (mean \pm standard deviation obtained from n = 4) and are representative of two independent experiments.

4. Results and Discussion

In this chapter, the main purpose was the development of novel UPRs, making use of UPs and replacing St by a less toxic monomer. Therefore, the biobased UPs previously developed [8] were here subject of an extensive crosslinking study. Thermal crosslinking and μ STLG technique were employed to develop the bio resins for biomedical applications. Alongside with the UPRs prepared by μ STLG, thermal crosslinking was made

to evaluate several properties that otherwise will be difficult, such as WCA and AFM, due to the small dimensions of the 3D scaffolds.

4.1. Rheology of UPs

The viscosity is a critical parameter for resins used in SLA processes, which turns the selection of appropriate UMs crucial to obtain UPRs with suitable characteristics. Some authors suggested 0.20 Pa·s as the viscosity limit value of the formulation to be used in μ STLG [14]. A commercial formulation, Crystic[®] 272, containing St exhibited suitable viscosity to be used in SLA process [15]. However, St is highly toxic and is also a potential carcinogenic. In this sense, HEMA, NVP and AcA were selected for rheological studies. The same conditions of analysis (temperature, shear rate and UM concentration) were used for all formulations. Considering the extensive use of St in UPRs formulations, combined with the satisfactory viscosities obtained for SLA process, this UM was used for comparison purposes. Figure 1 and Table 1 summarize the viscosity results obtained for the bio UPs.

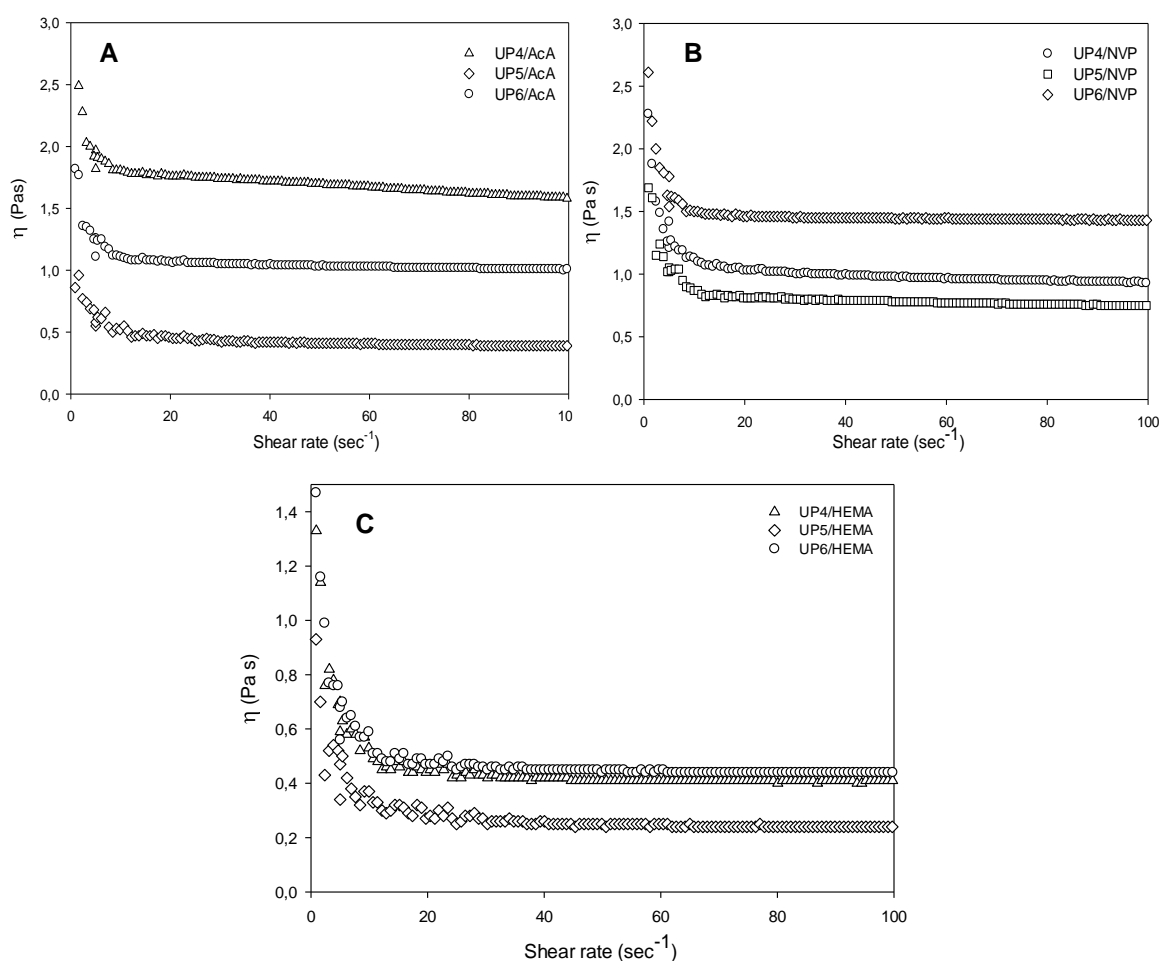


Figure 1. Viscosity versus shear rate for the UP4, UP5 and UP6 formulations using **A.** AcA, **B.** NVP and **C.** HEMA as the UMs.

Table 1. Viscosity values for the different formulations with 37% (w/w) of UMs, at 25 °C and at a shear rate of 100 sec⁻¹.

Formulations	UM	Viscosity (Pa·s)
UP4	HEMA	0.41
UP5		0.24
UP6		0.44
UP4	NVP	0.93
UP5		0.75
UP6		1.43
UP4	AcA	1.58
UP5		0.39
UP6		1.01
UP4	St	0.38
UP5		0.24
UP6		0.58

Above a shear rate of 20 sec⁻¹, the viscosity remains constant for all the samples. The UPs dissolved in HEMA showed the viscosity values closer to the formulations of St ($\eta_{100\text{sec}^{-1}}$ UP4= 0.41 Pa·s; $\eta_{100\text{sec}^{-1}}$ UP5= 0.24 Pa·s; $\eta_{100\text{sec}^{-1}}$ UP6= 0.44 Pa·s). Thus, considering the suitable viscosity observed for the UPs formulations with HEMA and the fact that it is widely used in the preparation of different devices for biomedical applications [16], this monomer was selected for further studies. Although HEMA structure is very different to St structure, both are good solvents for the developed polyesters.

4.2 Thermal Crosslinking of UPs

The thermal crosslinking of UPs was performed *via* a free radical process, involving the reaction between the UM and the internal double bonds of the UP backbone. BPO was chosen as the thermal initiator, since it has been successfully used in the preparation of UPRs directed to biomedical applications [17, 18]. The amount of UM in the formulation was kept in 37 % (w/w). The amount of BPO was set in 1% (w/w) [19, 20].

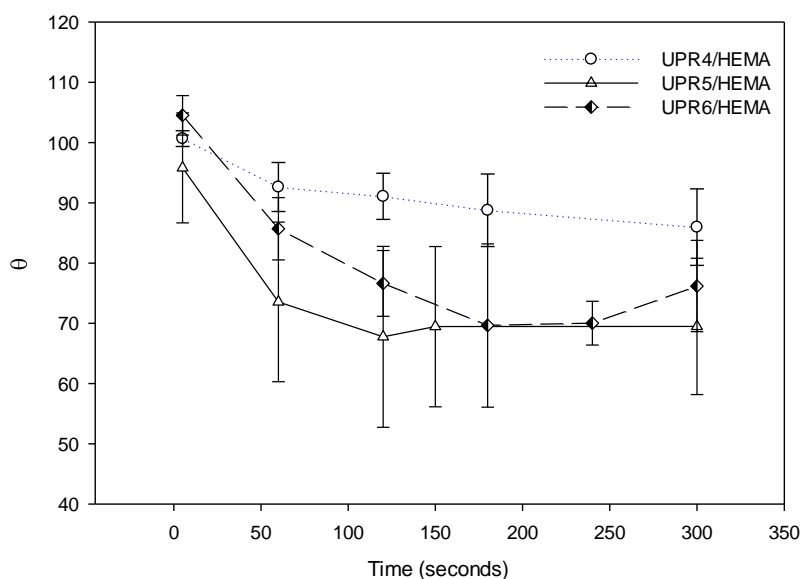
The gel content obtained for the different samples is summarized in Table 2. It is possible to see that in all the formulations tested the soluble fraction is below 15%. According to Table 2 there are no significant differences on gel content of UPs crosslinked with HEMA and UPs crosslinked with St, which suggest the feasibility of using HEMA as UM.

Table 2. Gel content for the bio UPRs prepared with 37% (w/w) of HEMA and St at a final curing temperature of 80 °C.

UPR	Formulation	Gel content %
<i>UPs Thermally crosslinked with HEMA</i>		
UPR4	SuCA (34%)/FA (11%)/PG (40%)/DG (15%)	95.9
UPR5	AA (13%)/FA (13%)/PG (57%)/ DG (17%)	99.8
UPR6	SeBA (18%)/FA (16%)/PG (56%)/DG (20%)	88.8
<i>UPs Thermally crosslinked with Styrene</i>		
UPR4	SuCA (34%)/FA (11%)/PG (40%)/DG (15%)	89.9
UPR5	AA (13%)/FA (13%)/PG (57%)/DG (17%)	97.2
UPR6	SeBA (18%)/FA (16%)/PG (56%)/DG (20%)	98.6

4.3 Contact angle measurements

Contact angle analysis is a common technique to study the wettability of the surfaces. The water contact angles (WCA) were measured for each UPR as an indicator of the hydrophilicity of samples surface. At least five measurements were made for each UPR, in different places of the surfaces. The UPRs analysed were obtained by thermal crosslinking of the UPs with HEMA, in the following conditions: 37% (w/w) of HEMA, 1% (w/w) of BPO, curing temperature of 80 °C, for 24 h. Figure 2 shows the WCA of the different UPRs crosslinked with HEMA expressed in function of time.

**Figure 2.** Dynamic water contact angles of UPRs crosslinked with HEMA determined by the sessile drop method and respective standard deviations.

The initial contact angles were in the same range of values considering the error bars ($\sim 100^\circ$) however, the water droplet spread over the surface, reaching values below 80° (Figure 2). Several tests were carried out and the results were consistent. Also, the results showed the following order: θ UPR5 (AA) $<$ θ UPR6 (SeBA) $<$ θ UPR4 (SuCA). It was expected to have an increase of the contact angle with the increase of carbons in the main chain of the UPs, however, in this case, this is not verified. This is indicative that other factors might affect the hydrophobicity/hydrophilicity of the UPRs. Among such parameters, it is possible to mention the porosity and roughness of the surface [21].

4.4 Thermal and mechanical analysis of UPRs

The thermal behaviour of the studied UPs thermally crosslinked with HEMA are presented in Figure 3. It is possible to observe that the materials degraded in a single stage, corresponding to the degradation of the ester linkages [22, 23]. In Table 3 the onset temperature, T_{on} , (temperature corresponding to the maximum degradation), $T_{5\%}$ and $T_{10\%}$ are presented. All the UPRs are thermally stable up to approximately 250°C . The T_{on} determined for the UPRs are very similar with the values obtained for the respective UPs ($T_{on\ UPR4} = 342.06^\circ\text{C}$; $T_{on\ UPR5} = 328.49^\circ\text{C}$; and $T_{on\ UPR6} = 350.04^\circ\text{C}$). These results are consistent with previous reports on similar materials [24].

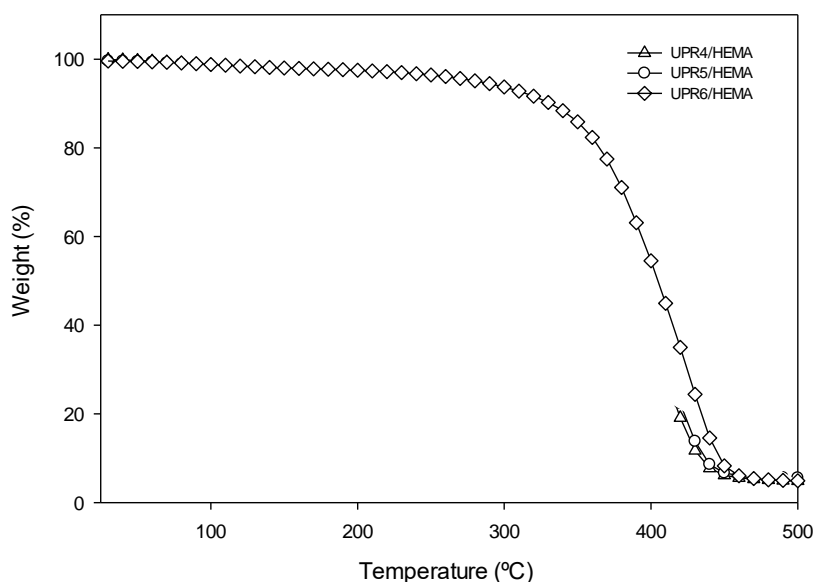
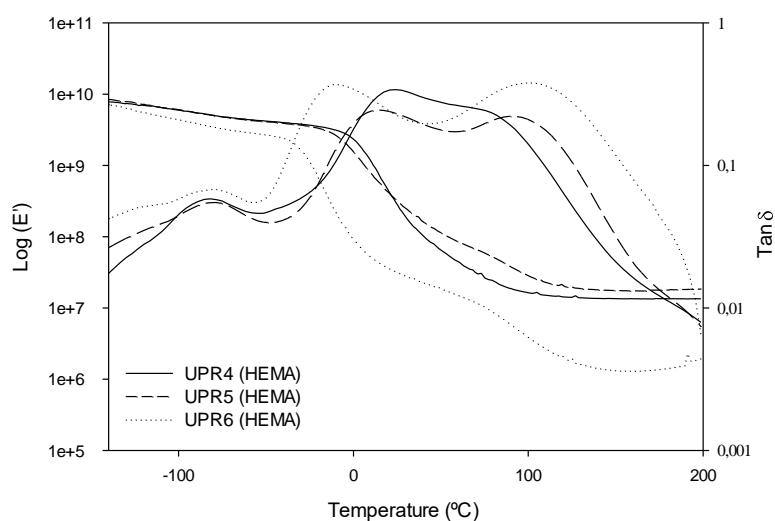


Figure 3. TG curves obtained at a heating rate of $10^\circ\text{C}\cdot\text{min}^{-1}$ of the UPRs thermal crosslinked with BPO 1% (w/w), using 37% (w/w) of HEMA.

Table 3. Degradation temperature ($T_{x\%}$) and onset temperature (T_{on}) for the biobased UPRs.

UPRs/HEMA	$T_{5\%}$ / °C	$T_{10\%}$ / °C	T_{on} / °C
UPR4	253.74	321.02	344.92
UPR5	244.04	308.72	344.73
UPR6	282.54	331.16	364.45

The E' and $\tan \delta$ curves at 1 Hz, for the biobased UPRs are presented in Figure 4. A summary of the data (T_g and E') obtained from the DMTA is summarized in Table 4.

**Figure 4.** E' and $\tan \delta$ traces for biobased UPRs at 1 Hz.**Table 4.** Data obtained from DMTA analysis for UPRs. T_g : glass transition temperature; $E'_{37^\circ\text{C}}$: modulus at 37 °C.

UPRs/HEMA	T_g (°C)	$E'_{37^\circ\text{C}}$ (MPa)
UPR4	25.6; 68.4	114.61
UPR5	11.0; 92.5	190.50
UPR6	-9.3; 101.2	23.68

According to Figure 4 and Table 4, the UPRs presented $\tan \delta$ curves with three distinct peaks, being two of them sensitive to frequency of analysis. The transition detected around -80 °C seems to be independent from the composition of the UPRs and can be assigned to the local motions of the hydroxyl groups in oligo(HEMA) or PHEMA moieties [17].

The other two peaks can be attributed to α transitions, also known as glass transition temperature (T_g). The presence of these two transitions suggests the existence of two immiscible fractions that start the long molecular motions with different energy. The transition appearing at lower temperatures (-9.3 – 25.6 °C) can be tentatively assigned to domains in which the UPs crosslink with themselves or with a small amount of the UM. A

close observation to the values at which such transition occurs shows an increase in the T_g value as the length of the aliphatic chain of the dicarboxylic acid in the UP decreases. The transition appearing at higher temperatures (68.4 – 101.2 °C) can be ascribed to the domains in which the UP is crosslinked with HEMA (see Table 3). For this transition, a relation between the number of carbons in the UPs dicarboxylic acid cannot be drawn. Possibly, these UP-HEMA microdomains have different amounts of HEMA, leading to the differences in the T_g values. Regarding the E' values at 37 °C, it was not possible to establish a direct relation between the composition of the three formulations and the obtained values. Nevertheless, it is possible to observe that the difference in the two T_g values is more accentuated for the UPR6, suggesting a higher degree of heterogeneity in the crosslinked network. This fact might be responsible for the lower E' value of this UPR in comparison with UPR4 and UPR5.

Values of Young's modulus (E), maximum stress (σ_{max}) and maximum strain (ϵ_{max}) were evaluated for the different materials (Table 5) to assess the effect of the composition on the mechanical properties. According to Table 5, the maximum strain obtained, ϵ , was in the range of 0.35 – 0.37 mm.

Table 5. Results from tensile tests for the bio UPRs crosslinked with HEMA for 24 h: Young's modulus (E), maximum stress (σ_{max}) and maximum strain (ϵ_{max}), reported as mean value \pm standard deviation.

UP/UM	E (MPa)	σ_{max} (MPa)	ϵ_{max} (mm/mm)
UPR4/HEMA	20.1 \pm 3.3	2.30 \pm 0.37	0.35 \pm 0.05
UPR5/HEMA	32.0 \pm 4.8	4.32 \pm 0.76	0.37 \pm 0.04
UPR6/HEMA	6.1 \pm 0.7	1.01 \pm 0.16	0.37 \pm 0.05

Regarding the Young's modulus, UPR5 showed a higher rigidity (32.0 MPa) in contrast with UPR6, with 6.1 MPa which is in accordance with the DMTA results (Table 4).

Other authors reported low values of E , in the range of 0.2 and 14 MPa for one-step photo-cured UPs, based on AA and itaconic acid [25]. These low Young's modulus values are related with the amount of diacid in the polyester formulation – high amounts of diacids resulted in more flexible materials and therefore low E . There are several ranges of E values of UPRs described in the literature, since the mechanical properties are strongly dependent on the selected monomers (and respective amounts), and the type of synthesis procedure. Some authors reported high values of E (15.3 x 10² MPa) using the same one-step synthesis procedure with UPs cured with St at room temperature [26], while others reported values of E ranging from 0.02 to 20 MPa [27]. Tang et al. also reported values lower than 1 MPa for Young's modulus and tensile strength [28] for aliphatic polyesters

based on SeBA, glycol and glycerol. Concerning biomedical applications, it is possible to relate the obtained E values of the UPRs with the literature data of human tissues [29]. For instance, for knee articular cartilage E ranges between 2.1 and 11.8 MPa, making feasible the use of these materials in TE. Concerning the final properties of scaffolds (based on UPs crosslinked with HEMA), values between 6 and 32 MPa have been reported, making them suitable for fibrous tissue and cartilage [30], when considering the mechanical properties.

4.5 3D Scaffolds by μ STLG and Characterization

Several formulations were fabricated by μ STLG, based on the bio polyesters UP4, UP5 and UP6 and HEMA. Irgacure 651[®] (5% (w/w)) was used as photo initiator [31] and was selected, due to its known biocompatibility and successful use in SLA techniques [32-34]. With the purpose of evaluating the cell viabilities and adhesion, the shape of the 3D structure by μ STLG was simplified. A 3D image of a round disc was created by CAD and used for μ STLG to create the final product. The curing time was set in 60 seconds for all the formulations. As previously reported, the 3D structures showed very homogenous surfaces. SEM images of the HEMA based scaffolds, fabricated by μ STLG are displayed in Figure 5.

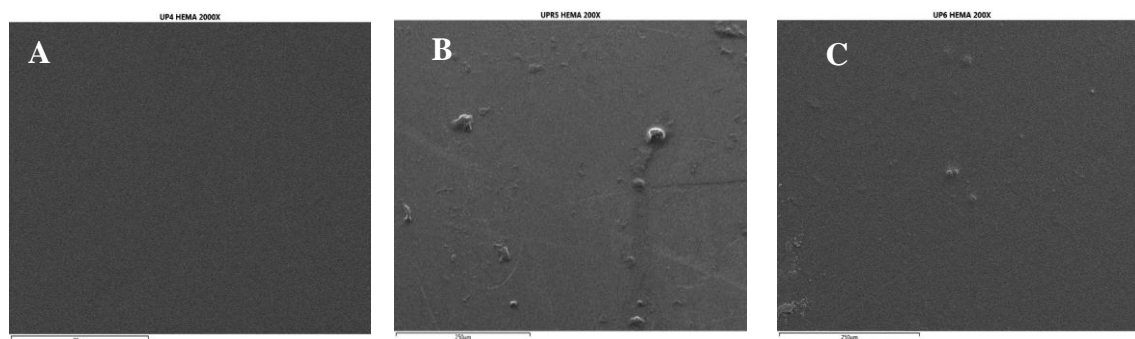


Figure 5. Scanning electron micrographs using microscopy (MEV)/EDS, JEOL, model JSM-5310, at an accelerating voltage of 10 kV of UPR4 (**A**), UPR5 (**B**) and UPR6 (**C**) photo-crosslinked with HEMA (37 % (w/w)) in the μ STLG. The magnifications used were 2000x for **A**, 200x for **B** and 200x for **C**.

As already pointed out, the scaffold shape was a circle with a maximum thickness of 0.125 mm and a diameter of 0.5 mm. The SEM of the 3D structures was carried out for all the samples to evaluate the applicability of this processing technology to the different formulations. According to Figure 5, the 3D structures showed very homogeneous surfaces, suggesting that the materials obtained by stereolithography are characterized by a smooth surface, where no indicators of high levels of surface heterogeneity are detected.

4.6 Topographic analysis

Surface roughness of the UPRs was assessed using AFM in tapping mode, to determine roughness parameters, such as mean surface roughness (Ra). Figure 6 presents the AFM images of the UPR4, UPR5 and UPR6 thermally crosslinked with HEMA. It was not possible to analyse the μ STLG scaffolds since they presented a convex surface, making difficult the acquisition of Ra.

The roughness of the materials plays an important role since it affects the interaction between the surface materials and the cells. Moreover, different type of cells have different interactions with the type of biomaterials surface [35]. On this matter, it is known that osteoblast cells type adhere strongly to more rough surfaces unlike the fibroblast cells, which prefer smoother surfaces [36]. It has also been reported that for fibroblast cells, surface roughness in the order of 10-13 nm showed the best cell adhesion results while increasing nano-roughness to 50 nm or 95 nm significantly decreased fibroblast cell adhesion [37]. For similar Ra, different cell responses can be obtained, as surface patterns and other nanoscopic topologies (grooves, pits) affect cell adhesion and proliferation [38]. Also, smooth surface can have surface irregularities (sharp peaks, for instance) resulting in cell damages [39, 40].

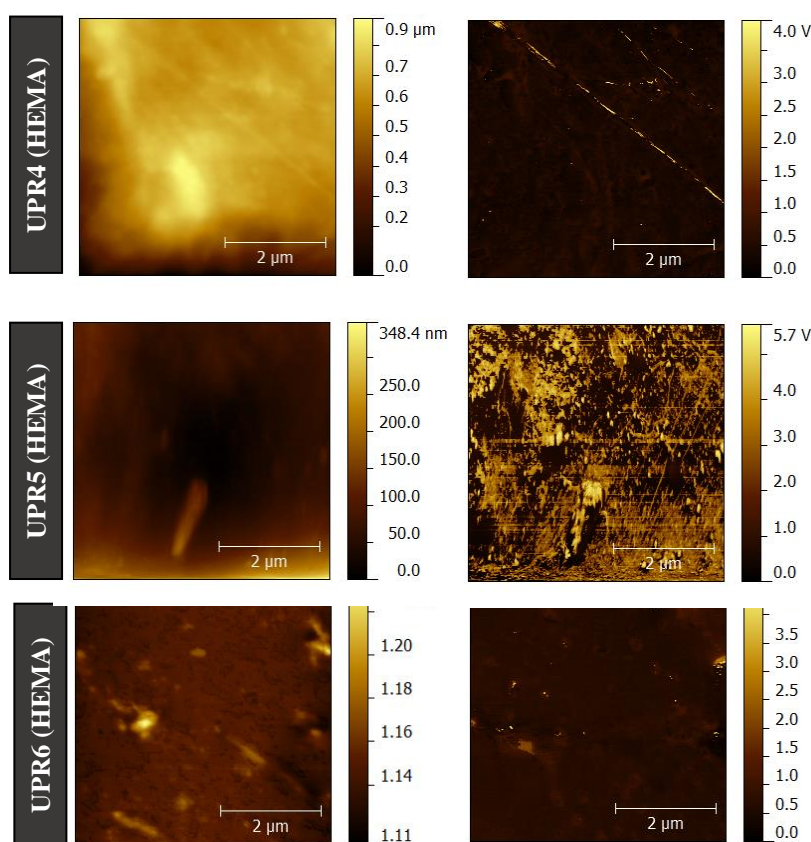
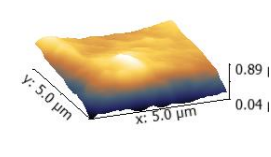
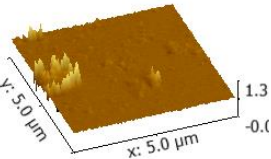
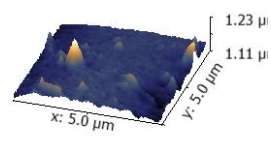


Figure 6. AFM images of UPRs thermally crosslinked with HEMA (37 % w/w). The images at the left correspond to the phase image while the images at our right are topographic images.

According to the topographic and phase images, it is possible to validate the existence of a single phase in the UPRs. The UPRs surface roughness calculated from the plane topography images by using AFM software is shown in Table 6.

Table 6. AFM results for the UPRs thermally crosslinked with HEMA.

UPRs	Ra (nm)	Average (nm)	Skew	Kurtosis	3D view	
Thermal crosslinking, UM 37% w/w	UPR4	115.7	609.8	-1.25	1.13	
	UPR5	31.7	327.9	0.903	1.98	
	UPR6	6.25	34.93	1.67	10.8	

Kurtosis and skewness are statistical properties which provide information about the peaks distribution (measuring in fact the sharpness of the surface profile) and the asymmetric roughness of the surfaces. In general terms, if a skewness moment is negative, the surface is more planar, and valleys are predominant. If the Kurtosis is higher than 3, the surface has more peaks than valleys [41]. Since UPR4(HEMA) skewness have a negative value and the kurtosis is less than 3 for UPR4 (HEMA) and UPR5(HEMA), we can assume that their surface has more valleys than peaks. For UPR6(HEMA), its surface, based on Skew (1.67) and Kurtosis (10.8) values is assumed to have more peaks [42]. According to Table 6, the differences in the scaffolds' morphology are clear. Indeed, the thermally crosslinked polymers showed a large range of Ra, going from 115 nm for UPR4 to 6 nm, for UPR6. Ra affects the wettability behaviour, increasing the wettability of the polymeric surface [43, 44]. The obtained Ra values are in good agreement with the WCA of the UPRs, being UPR4 the polyester with higher WCA and higher Ra. The correlation between surface roughness and wettability can be understood using Wenzel model [45], where an increase of the roughness led to an increase of wettability.

4.7 Cell culturing

Regarding the importance of the interaction between cell-scaffolds interface in tissue engineering, 3T3-L1 cell were seeded in 48-well culture plates containing the thermally crosslinked UPRs and the photo crosslinked UPRs produced by μ STLG. Both cell assays of thermal and photo crosslinked UPRs by μ STLG were performed under the same conditions and the results are presented in Figure 7.

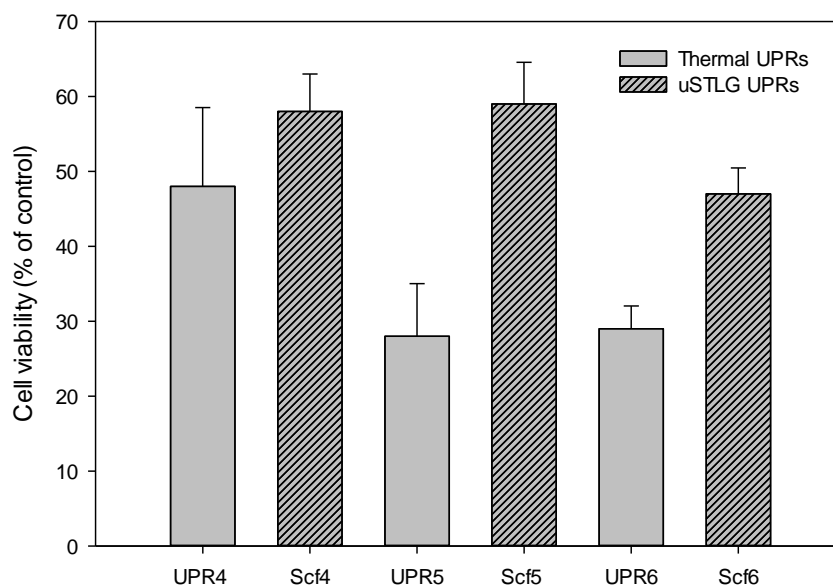


Figure 7. Effect of thermal and photo crosslinked materials on 3T3-L1 cell viability. The data are expressed as percentage of cell viability with respect to the control corresponding to untreated cells (mean \pm SD, obtained from triplicates). The results are representative of at least three independent experiments. The statistical analysis (one-way ANOVA) indicates that there is not a significant difference between the different conditions.

After 48 h of incubation, for the μ STLG UPRs, 50-60% of the cells were viable. In comparison, cell viability significantly decreased for thermally crosslinked UPRs, with the high cell viability (48%), being obtained for UPR4.

Overall, UP4 demonstrated the best results, followed by UP5 formulation. The results observed for UPR6 and Scf6 can be correlated with the gel content – this formulation presented the lowest gel content. This fact is related with the presence of unreacted polyesters, resulting in higher amounts of COOH groups, that ultimately could enhance the acidic character. This is a plausible explanation for its lowest cell viability.

Concerning the two different curing methods, the scaffolds prepared by μ STLG proved to have higher cell viabilities than those observed for the thermal crosslinked UPRs, however this gap is attenuated for the UP4 formulation. The differences observed between these curing methods can be ascribed to the topography of the samples, where UPR4 showed to have a surface with no peaks and with some roughness. Also, fibroblasts, as previously

noted, are very sensitive cells, being this a major reason for the different detected behaviours.

5. Conclusions

An extensive characterization showed that the UPRs obtained by thermal crosslinking showed high gel content values, with the lowest value of 89% for UPR5/HEMA, indicating the success of replacing St by HEMA as the crosslinking agent. The contact angles measurements revealed that the UPRs crosslinked with HEMA have water contact angles between 87 and 69°, which is indicative of their hydrophilic character. Moreover, TGA measurements confirms the UPRs high thermal stability, with an initial decomposition temperature above 244 °C. The DMTA analysis revealed that the UPRs have distinct microdomains (UP-UP and UP-HEMA) within the crosslinked network. The transition at lower temperatures can be ascribed to the motion of the UP-UP microdomain, whereas the transition at higher temperatures can be attributed to the domains composed by UP-HEMA. Topographic analysis also confirms the feasibility of these polyesters for cell support. Finally, UPRs were successfully applied in the μ STLG equipment.

Concerning the UPs processed by μ STLG, cell viabilities of 50-60% were obtained, fact that can be attributed to the acidic character of the samples. However, this disadvantage can be overcome with post treatments that could diminish the acidic character.

6. References

1. Melchels, F.P.W., et al., *Additive manufacturing of tissues and organs*. Progress in Polymer Science, 2012. **37**(8): p. 1079-1104.
2. Tsang, V.L. and S.N. Bhatia, *Three-dimensional tissue fabrication*. Advanced Drug Delivery Reviews, 2004. **56**(11): p. 1635-1647.
3. Kwon, I.K. and T. Matsuda, *Photo-polymerized microarchitectural constructs prepared by microstereolithography (μ SL) using liquid acrylate-end-capped trimethylene carbonate-based prepolymers*. Biomaterials, 2005. **26**(14): p. 1675-1684.
4. Melchels, F.P.W., J. Feijen, and D.W. Grijpma, *A poly(D,L-lactide) resin for the preparation of tissue engineering scaffolds by stereolithography*. Biomaterials, 2009. **30**(23-24): p. 3801-3809.
5. Malayeri, A., et al., *Feasibility of 3D printing and stereolithography for fabrication of custom-shaped poly (lactic acid): hydroxyapatite composite biomaterial scaffolds*. Journal of Tissue Engineering and Regenerative Medicine, 2012. **6**: p. 367-367.

Novel Biobased Unsaturated Polyester Resins prepared by Thermal crosslinking and μ STLG

6. Barry, J.J.A., et al., *In vitro study of hydroxyapatite-based photocurable polymer composites prepared by laser stereolithography and supercritical fluid extraction*. Acta Biomaterialia, 2008. **4**(6): p. 1603-1610.
7. Matsuda, T. and M. Mizutani, *Molecular design of photocurable liquid biodegradable copolymers. 2. Synthesis of coumarin-derivatized oligo(methacrylate)s and photocuring*. Macromolecules, 2000. **33**(3): p. 791-794.
8. Gonçalves, F.A.M.M., et al., *3D printing of new biobased unsaturated polyesters by microstereo-thermal-lithography*. Biofabrication, 2014. **6**(3): p. 035024.
9. Peltola, S.M., et al., *A review of rapid prototyping techniques for tissue engineering purposes*. Annals of Medicine, 2008. **40**(4): p. 268-280.
10. Melchels, F.P.W., J. Feijen, and D.W. Grijpma, *A review on stereolithography and its applications in biomedical engineering*. Biomaterials, 2010. **31**(24): p. 6121-6130.
11. Turunen, M.P.K., et al., *Synthesis, characterization and crosslinking of functional star-shaped poly(ϵ -caprolactone)*. Polymer International, 2002. **51**(1): p. 92-100.
12. Organization, I.S., *Biological evaluation of medical devices. , in Part 5. Tests for cytotoxicity: In vitro methods*. 2009, AAMI: Geneva, Switzerland. p. 50.
13. Faneca, H., A. Faustino, and M.C. Pedroso de Lima, *Synergistic antitumoral effect of vinblastine and HSV-Tk/GCV gene therapy mediated by albumin-associated cationic liposomes*. Journal of Controlled Release, 2008. **126**(2): p. 175-184.
14. Choi, J.W., et al., *Fabrication of 3D biocompatible/biodegradable micro-scaffolds using dynamic mask projection microstereolithography*. Journal of Materials Processing Technology, 2009. **209**(15-16): p. 5494-5503.
15. Bartolo, P.J. and G. Mitchell, *Stereo-thermal-lithography: a new principle for rapid prototyping*. Rapid Prototyping Journal, 2003. **9**(3): p. 150-156.
16. Kejlová, K., et al., *Hydrophilic polymers—biocompatibility testing in vitro*. Toxicology in Vitro, 2005. **19**(7): p. 957-962.
17. Sousa, A.F., et al., *New unsaturated copolyesters based on 2,5-furandicarboxylic acid and their crosslinked derivatives*. Polymer Chemistry, 2016. **7**(5): p. 1049-1058.
18. Fonseca, A.C., et al., *Synthesis of unsaturated polyesters based on renewable monomers: Structure/properties relationship and crosslinking with 2-hydroxyethyl methacrylate*. Reactive and Functional Polymers, 2015. **97**: p. 1-11.
19. Gawdzik, B., T. Matynia, and E. Chmielewska, *Modification of unsaturated polyester resin with bismaleimide*. Journal of Applied Polymer Science, 2001. **82**(8): p. 2003-2007.
20. Suh, D.J., O.O. Park, and K.H. Yoon, *The properties of unsaturated polyester based on the glycolized poly(ethylene terephthalate) with various glycol compositions*. Polymer, 2000. **41**(2): p. 461-466.
21. Stamm, M., *Polymer Surface and Interface Characterization Techniques*, in *Polymer Surfaces and Interfaces*, M. Stamm, Editor. 2008, Springer Berlin Heidelberg. p. 1-16.
22. Lin, Y., et al., *Study on thermal degradation and combustion behavior of flame retardant unsaturated polyester resin modified with a reactive phosphorus containing monomer*. RSC Advances, 2016. **6**(55): p. 49633-49642.
23. Perng, L.H., *Thermal degradation mechanism of poly(ether imide) by stepwise Py–GC/MS*. Journal of Applied Polymer Science, 2001. **79**(7): p. 1151-1161.

24. Jasinska, L. and C.E. Koning, *Unsaturated, biobased polyesters and their cross-linking via radical copolymerization*. Journal of Polymer Science Part A: Polymer Chemistry, 2010. **48**(13): p. 2885-2895.
25. Barrett, D.G., et al., *One-Step Syntheses of Photocurable Polyesters Based on a Renewable Resource*. Macromolecules, 2010. **43**(23): p. 9660-9667.
26. Cherian, B. and E.T. Thachil, *Synthesis of unsaturated polyester resin - Effect of sequence of addition of reactants*. Polymer-Plastics Technology and Engineering, 2005. **44**(5): p. 931-938.
27. Olson, D.A., et al., *Amorphous linear aliphatic polyesters for the facile preparation of tunable rapidly degrading elastomeric devices and delivery vectors*. Journal of the American Chemical Society, 2006. **128**(41): p. 13625-13633.
28. Tang, J., et al., *Synthesis and characterization of elastic aliphatic polyesters from sebacic acid, glycol and glycerol*. European Polymer Journal, 2006. **42**(12): p. 3360-3366.
29. Amsden, B., *Curable, biodegradable elastomers: emerging biomaterials for drug delivery and tissue engineering*. Soft Matter, 2007. **3**(11): p. 1335-1348.
30. Byrne, D.P., et al., *Simulation of tissue differentiation in a scaffold as a function of porosity, Young's modulus and dissolution rate: Application of mechanobiological models in tissue engineering*. Biomaterials, 2007. **28**(36): p. 5544-5554.
31. Williams, C.G., et al., *Variable cytocompatibility of six cell lines with photoinitiators used for polymerizing hydrogels and cell encapsulation*. Biomaterials, 2005. **26**(11): p. 1211-1218.
32. Bartolo, P.J. and J. Gaspar, *Metal filled resin for stereolithography metal part*. Cirp Annals-Manufacturing Technology, 2008. **57**(1): p. 235-238.
33. Bartolo, P.J.D., *Photo-curing modelling: direct irradiation*. International Journal of Advanced Manufacturing Technology, 2007. **32**(5-6): p. 480-491.
34. Matias, J.M., P.J. Bartolo, and A.V. Pontes, *Modeling and Simulation of Photofabrication Processes Using Unsaturated Polyester Resins*. Journal of Applied Polymer Science, 2009. **114**(6): p. 3673-3685.
35. Boyan, B.D., et al., *Role of material surfaces in regulating bone and cartilage cell response*. Biomaterials, 1996. **17**(2): p. 137-146.
36. Xu, C., et al., *In vitro study of human vascular endothelial cell function on materials with various surface roughness*. Journal of Biomedical Materials Research Part A, 2004. **71A**(1): p. 154-161.
37. Le, X., et al., *Engineering a Biocompatible Scaffold with Either Micrometre or Nanometre Scale Surface Topography for Promoting Protein Adsorption and Cellular Response*. International Journal of Biomaterials, 2013. **2013**: p. 16.
38. Ross, A.M., et al., *Physical Aspects of Cell Culture Substrates: Topography, Roughness, and Elasticity*. Small, 2012. **8**(3): p. 336-355.
39. Bacakova, L., et al., *Cell adhesion on artificial materials for tissue engineering*. Physiol Res, 2004. **53**(1): p. S35-45.
40. Yeong, W.Y., et al., *Rapid prototyping in tissue engineering: challenges and potential*. Trends in Biotechnology, 2004. **22**(12): p. 643-652.
41. Sedlaček, M., B. Podgornik, and J. Vižintin, *Correlation between standard roughness parameters skewness and kurtosis and tribological behaviour of contact surfaces*. Tribology International, 2012. **48**: p. 102-112.

Novel Biobased Unsaturated Polyester Resins prepared by Thermal crosslinking and μ STLG

42. Maravi, S., J. Bajpai, and A.K. Bajpai, *Structure and topography of thermally reduced graphene oxide reinforced poly(vinyl alcohol-g-acrylonitrile) films and study of their mechanical and electrical behavior*. Polymer Composites, 2019. **40**(S1): p. E409-E421.
43. Wang, J., et al., *Influence of surface roughness on contact angle hysteresis and spreading work*. Colloid and Polymer Science, 2020. **298**(8): p. 1107-1112.
44. Kasalkova, N.S., et al., *Wettability and Other Surface Properties of Modified Polymers*, in *Wetting and Wettability*. 2015.
45. Wenzel, R.N., *Resistance of solid surfaces to wetting by water*. Industrial & Engineering Chemistry, 1936. **28**(8): p. 988-994.

Supplementary information

Table S1. Results of TGA and DMTA for the biobased UPRs/St.

UPRs/Styrene	$T_{5\%} / ^\circ\text{C}$	$T_{10\%} / ^\circ\text{C}$	$T_{\text{on}} / ^\circ\text{C}$	$T_g / ^\circ\text{C}$	$E_{37^\circ\text{C}} \text{ (MPa)}$
UPR4	216.62	273.00	333.10	60.0	$8.80 \cdot 10^7$
UPR5	259.33	320.18	359.77	55.8	$1.57 \cdot 10^8$
UPR6	284.85	334.20	364.33	39.7	$3.73 \cdot 10^7$

Table S2. Results from tensile tests for the bio UPs crosslinked with styrene: modulus (E), maximum stress (σ_{max}) and maximum strain (ϵ_{max}), reported as mean value \pm standard deviation.

UP/UM	Curing time (h)	E (MPa)	σ_{max} (MPa)	ϵ_{max} (mm/mm)
UPR4(St)	24	54.1 ± 7.5	3.00 ± 0.42	0.22 ± 0.02
UPR5(St)	24	15.3 ± 2.1	1.21 ± 0.22	0.27 ± 0.03
UPR6(St)	24	5.9 ± 0.8	1.10 ± 0.19	0.33 ± 0.05

CHAPTER IV

Fully Biobased Unsaturated Polyesters from Renewable Resources: Synthesis, Characterization and HEMA Crosslinking

1. ABSTRACT	121
2. INTRODUCTION	121
3. MATERIALS AND METHODS	123
3.1 MATERIALS	123
3.2. SYNTHESIS OF UNSATURATED POLYESTERS BY BULK POLYCONDENSATION.....	123
3.3 PREPARATION OF UNSATURATED POLYESTERS RESINS	123
3.4 SIZE EXCLUSION CHROMATOGRAPHY ANALYSIS.....	124
3.5 SPECTROSCOPIC ANALYSIS	124
3.6 THERMAL ANALYSIS OF UPS	125
3.7. WETTABILITY OF UPRs	125
3.8 UPRs TENSILE TESTS	126
4. RESULTS AND DISCUSSION	126
4.1 POLYCONDENSATION OF UPS AND CHEMICAL STRUCTURE IDENTIFICATION.....	126
4.2 THERMAL AND MECHANICAL PROPERTIES OF UPS.....	135
4.3 PREPARATION AND CHARACTERIZATION OF BIO UPRs	137
5. CONCLUSIONS	142
6. REFERENCES	143
SUPPLEMENTARY INFORMATION	146

1. Abstract

The unsaturated polyesters (UPs) have proved to be suitable for AM technologies, producing scaffolds with interesting properties. Herein, we report the development of novel UPs, based in renewable sources – glutaric acid (GA), succinic acid (SuCA), and a variety of glycols, such as isosorbide (IS), through bulk polycondensation, in a two-step synthesis process. By performing the reaction only with three monomers in a two-pot reaction, the synthesis of UP7 and UP8 was accomplished in 8 h. The biobased UPs were thoroughly characterized by ATR-FTIR, ¹H NMR, and MALDI-TOF, confirming the success of the UP synthesis. The UPs exhibited high thermal stability, with an onset temperature (T_{on}) above 350 °C, and glass transition temperatures (T_g) values between -44 and 4 °C. Selected UPs were crosslinked with HEMA, a reactive solvent approved by FDA with attractive merits and extensive uses on biomedical fields, and the results confirmed their good thermal and mechanical performance. The UPs crosslinked with HEMA showed to be thermally more stable than the UPs, with values of T_{on} higher than 400 °C. DMTA also showed high values of T_g , between 17 and 86 °C. The high thermal stability, the proper mechanical properties, the surface hydrophilicity and low reaction times demonstrate the potential of these renewable polyester's resins in a wide range of applications, with a promising applicability in TE.

2. Introduction

A great effort is being placed on the development of polymers based on sustainable resources, with an increase in use in biomedical fields. Herein, glutaric acid (GA) and 1,4:3,6-dianhydro-D-glucitol, also called isosorbide (IS), were some of the selected monomers to develop the new bio UPs (Figure 1A) and improve the performance of the final materials. Succinic acid (SuCA) was still employed to develop new formulations of UPs since it is a key intermediate in the Krebs cycle and is amply used in polyester synthesis. It is produced via anaerobic fermentation but it can also be obtained from *n*-butane *via* oxidation to maleic anhydride and hydrogenation into the final product [1]. This linear aliphatic diacid in combination with other renewable monomers ultimately leads to new biopolymers [2]. Although SuCA is highly reported for the synthesis of polyesters [3-5], the use of GA is yet starting to gain some attention [6-11], with application in biomedical fields and present in patents [12, 13]. This diacid occurs in plant and animal tissues, is non-toxic and can be also used as crosslinking agent [14], and as building block in the production of polyesters and polyamides [9] where several derivatives of GA are used as green solvents, antimicrobial agents, among other applications [9]. The use of

1,4:3,6-dianhydrohexitols (DAH), such as IS, in the preparation of polycondensation products is very well described in the literature [2, 5, 15, 16] being the main reasons its biobased origin, chirality and rigidity [17], leading to products with high thermomechanical resistance. IS has been used as co-monomer in the synthesis of polyesters, namely poly(ethylene terephthalate) (PET) and poly(butylene terephthalate) (PBT), in order to enhance their thermal properties [18]. Produced on a large industrial scale, it can be obtained from starch through hydrolysis to glucose, hydrogenation to sorbitol, and dehydration to the final building block, as schematized in Figure 1B.

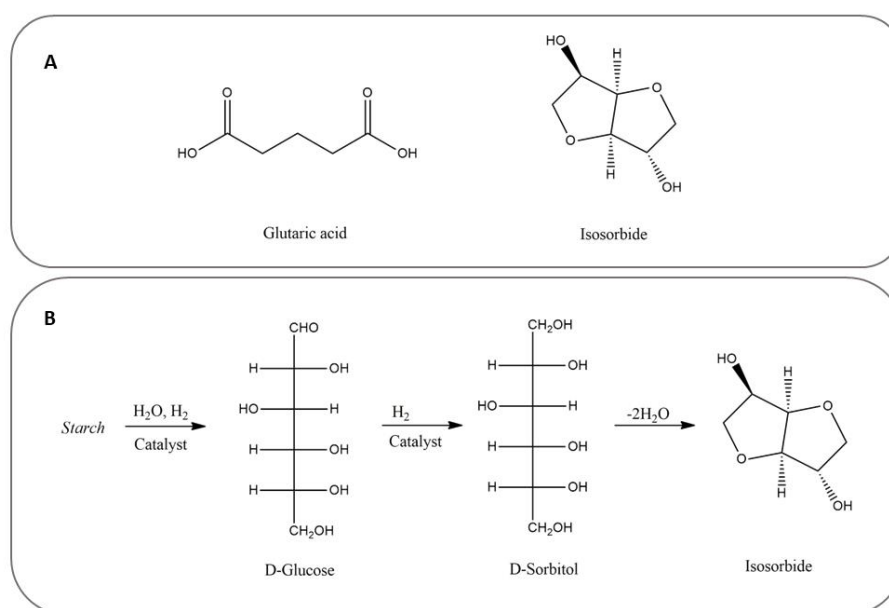


Figure 1.A. Chemical structure of the new diacid and glycol used in bulk polycondensation reactions and **B.** Synthesis of isosorbide from starch, adapted from [1].

It is worth to mention that, besides DEG, all the other monomers described in this chapter and used to prepare the biobased UPs can be obtained from renewable sources [9, 19-23]. Usually, step growth polymerization is performed at very high temperatures (190 – 290 °C) and, without the addition of a catalyst and it could take several hours [24]. Since the previous formulations, described in chapter II and chapter III showed promising results concerning their cell viability, this chapter focuses the synthesis of new UPs using other renewable resources, which can be easily cured with non-toxic monomers. By using a two-step reaction protocol, we aimed to promote a higher incorporation of FA monomer in the formulation and possibly reduce reaction time. The synthesized UPs were fully characterized in terms of chemical (ATR-FTIR, ^1H NMR and MALDI-TOF) and thermomechanical properties (DMTA, DSC). Some of the developed UPs were later cured by radical copolymerization with 2-hydroxyethyl methacrylate (HEMA) and their mechanical and thermal performance evaluated.

3. Materials and Methods

3.1 Materials

Fumaric acid (FA, 99%), isosorbide (IS, 98%), succinic acid ((SuCA, 99%), diethylene glycol (DEG, 99%), 1,2 propylene glycol (PG, 99%), 1,3-propanediol (1,3PG, 98%) and potassium hydroxide (90%) were purchased from Sigma-Aldrich Chemical Company and used as received. Hydroquinone (99%) was purchased from Analar, ethanol (96%) from Panreac, tetrahydrofuran-D (99.5%) from Euriso-top and phenolphthalein from Riedel-de-Haën Allied Signal. 2-Hydroxyethyl methacrylate (HEMA, 98%) and styrene (St, 99%) were purchased from Acros Organics. Glutaric acid (GA, 99%) and benzoyl peroxide (BPO, 97%) were purchased from TCI Europe.

3.2. Synthesis of Unsaturated Polyesters by Bulk Polycondensation

The UPs were prepared by bulk polycondensation. The diacids, the source of double bonds, glycols and hydroquinone (0.02 % of the total weight of fumaric acid) were charged into a four-necked glass reactor, equipped with a mechanical stirrer, a nitrogen inlet and a condenser connected to a receiver flask. The polycondensation synthesis was performed in two steps. First, FA and the diols were charged into the reactor, and the reaction was heated until 160 °C for 1 h. After that, the selected diacid was added to the reactor. The reactor was then heated at 190 °C, and the temperature during reaction was raised no further than 210 °C. When necessary, to drop the acid value (AV), vacuum was applied. The end of the reaction was determined by the attainment of a constant AV value (according to ASTM 109-01).

3.3 Preparation of Unsaturated Polyesters Resins

The UPs were prepared by bulk polycondensation as described in previous work [25]. A second step was performed to obtain a UPR. The polymer networks were prepared through thermal crosslinking, in the presence of BPO as initiator in a concentration of 1 % (w/w). The selected UM was HEMA. The prepared mixture was transferred to Teflon moulds with the following dimensions of 4 x 2.5 x 0.2 cm, which were placed in an oven at 80 °C for 24 h. No post-cure was performed. After the crosslinking, the films were removed from the respective moulds and stored at room temperature.

3.4 Size exclusion chromatography analysis

The chromatographic parameters of the samples were determined using high-performance gel permeation chromatography (HPSEC; Viscotek TDMax) with a differential viscometer (DV), right-angle laser-light scattering (RALLS, Viscotek), low-angle laser-light scattering (LALLS, Viscotek), and refractive-index (RI) detectors. The column set consisted of a PL 10 mm guard column ($50 \times 7.5 \text{ mm}^2$) followed by one Viscotek T200 column ($6 \mu\text{m}$), one MIXED-E PLgel column ($3 \mu\text{m}$), and one MIXED-C PLgel column ($5 \mu\text{m}$). HPLC dual piston pump was set with a flow rate of $1 \text{ mL} \cdot \text{min}^{-1}$. The eluent (THF) was previously filtered through a $0.2 \mu\text{m}$ filter. The system was also equipped with an on-line degasser. The tests were carried out at $30 \text{ }^\circ\text{C}$ using an Elder CH-150 heater. Before the injection ($100 \mu\text{L}$), the samples were filtered through a polytetrafluoroethylene (PTFE) membrane with $0.2 \mu\text{m}$ pore. The system was calibrated with narrow PS standards. Number average (M_n), weight average (M_w) and polydispersity (PDI) of the synthesized polymers were determined by conventional calibration (OmniSEC software version 4.6.1.354).

3.5 Spectroscopic analysis

Attenuated total reflection-FTIR (ATR-FTIR) spectroscopic analysis was carried out with a JASCO FT-IR 4100, equipped with a Golden Gate Single Reflection Diamond ATR. FTIR spectra of the modified scaffolds were obtained in the range $4000\text{--}500 \text{ cm}^{-1}$ at room temperature. Data collection was performed with 4 cm^{-1} spectral resolution and 128 accumulations. The resultant spectra were collected using Spectra Manager FT/IR – 4000-6000 software. ^1H NMR spectra were obtained at room temperature on a Varian Unity 600 MHz Spectrometer using a 3 mm broadband NMR probe, in deuterated tetrahydrofuran (THF- d_8). Tetramethylsilane (TMS) was used as internal reference.

The new biobased UPs were analysed by matrix-assisted laser desorption/ionization-time of flight mass spectrometry (MALDI-TOF MS). The dried-droplet sample preparation technique was used, applying $2 \mu\text{L}$ of 2,5-dihydroxybenzoic acid (DHB) matrix solution ($20 \text{ mg} \cdot \text{mL}^{-1}$ in THF) directly on a MTP AnchorChip™ 800/384 TF MALDI target (Bruker Daltonik, Bremen Germany), and, before drying the matrix solution, $2 \mu\text{L}$ of sample ($20 \text{ mg} \cdot \text{mL}^{-1}$ in THF) were added and allowed to dry at room temperature. External mass calibration was performed with a calibration standard (Bruker Daltonik, Bremen Germany) for the range m/z 700–3000 (9 mass calibrant points): 0.5 mL of calibrant solution and DHB matrix previously mixed in an Eppendorf tube (1:2, v/v) were applied directly on the target and allowed to dry at room temperature. Mass spectra were recorded using an Autoflex III smart beam MALDI-TOF mass spectrometer Bruker Daltonik (Bremen,

Germany), operating in linear positive ion mode. Ions formed upon irradiation by a smart beam nitrogen laser (337nm) using an accelerating potential of 20 kV and a frequency of 200 Hz. Each mass spectrum was produced by averaging 2000 laser shots collected across the whole sample spot surface by rastering in the range m/z 400–3000. The laser irradiance was set to 45–50 % arbitrary units according to the corresponding threshold required for the applied matrix system. Low molecular ion gating was set to 400 Da to remove the ions below this value arising from the matrix and their clusters or other unknown contaminants. All spectra were acquired and treated using the flexControl 3.0 and flexAnalysis 3.0 softwares (Bruker Daltonik), respectively.

3.6 Thermal analysis of UPs

The thermal stability of UPs was evaluated in the range of ca. 25 – 600 °C, in a TA Instruments Q500 thermogravimetric analyzer (thermobalance sensitivity: 0.1 μg) at a heating rate of 10 °C·min⁻¹ and under a dry nitrogen purge flow of 100 mL·min⁻¹.

Modulated Differential Scanning Calorimetry (MDSC) studies were performed within a temperature interval ranging from -80 to 200 °C, in a TA Q100 instrument at a heating rate of 2 °C·min⁻¹ in the temperature modulated mode, and under a nitrogen flow of 50 mL·min⁻¹. Dynamic mechanical thermal analysis (DMTA) were performed in Tritec 2000 DMA equipment at a heating rate of 5 °C·min⁻¹, in the temperature range from -150 °C to 300 °C, with a multi-frequency mode (1 and 10 Hz). The UPs were placed into stainless steel pockets and analysed using a single cantilever bending geometry. The pocket was clamped directly into the DMTA. The UPRs were studied in the dual cantilever bending geometry.

3.7. Wettability of UPRs

Water contact angle tests were performed on air-facing surfaces of UPRs using the sessile drop method at room temperature in an OCA 20 contact angle measurement unit from Dataphysics, equipped with a Hamilton syringe (500 μL). Deionized distilled water was dropped onto the surface of the selected UPRs and the measurements were performed at room temperature. The data obtained represents the mean values of at least three independent measurements.

3.8 UPRs tensile tests

The synthesized biobased UPRs were tested at room temperature, in dry state. Tensile tests were carried out on specimens with a width (w) of 12.5 mm and a thickness (t) in the range of 1.90 - 2.0 mm. The grip-to-grip distance (l_0) (i.e. gauge length) was 10 mm. All the tests were performed at a rate of 1 mm/min using an INSTRON 5566 testing machine. Tensile modulus, maximum stress and maximum strain were evaluated.

4. Results and Discussion

4.1 Polycondensation of UPs and chemical structure identification

The biobased UPs were prepared *via* bulk polycondensation between bio aliphatic acids and the selected glycols. As described previously, FA was used as the source of the double bonds, to promote the subsequent crosslinking reactions. The selected carboxylic acids were succinic acid (SuCA) and glutaric acid (GA), and the used glycols were diethylene glycol (DEG), propylene glycol (PG) and isosorbide (IS). Since in previously synthesized UPs (see Chapter II) the incorporation of the diacids in the biobased UPs was lower than expected, the polycondensation was made in two steps. First, to assure the presence of the double bonds in the final UP, FA along with the glycol were charged into the reactor. After, the GA/SuCA were added to the reaction mixture. Overall, the polycondensation reaction was faster than the previous synthesized UPs, partially due to the number of monomers added to the formulation, combined with the two-step synthesis. Also, the final temperature never exceeded the 210 °C. The formulations developed, along with the reaction conditions, AV value, molecular weight, and polydispersity (\mathcal{D}) are summarized in Table 1 and the structures of the developed materials are presented in Figure 2.

The AV values of commercial UPRs are described to be in the range of 25-50 mg KOH.g⁻¹ [26], and for most cases, that was obtained. Though, it is interesting to notice that some UPs (UP9.2 and UP10) have a very low AV value, even though the time of reaction was not very high. But there are reports of low AV for synthesized UPs in the literature [5]. According to Table 1, the final temperature of the polycondensation reaction was decreased (the previous synthesized UPs showed final temperatures of 220 °C). Also, the synthesis was less time consuming, and for UP7 and UP8, at the end of 8 h of reaction a constant AV was obtained. The resulting viscous polyesters presented a strong orange coloration. For UP9 formulations, the reaction took no more than 14 h, with very low AV for UP9.2. After storage, at room temperature, these formulations became more rigid and with a white coloration. Concerning the formulations UP9.1 and UP10 reaction, both

having the same molar ratio but different diols, a lower AV was expected for UP9.1, since 1,3 PG is more reactive than PG.

Table 1. Synthesis conditions and properties of the UPs prepared from dicarboxylic acids (succinic acid (SA), glutaric acid (GA)) and diethylene glycol (DEG), propylene glycol (PG), 1,3-propanediol (1,3 PG) and fumaric acid (FA) as double bond provider.

UPs	Molar ratio (%)	M _w	M _n	Đ ^b	Reaction Time (h)	Final T. (°C)	AV (mg KOH/g) ^a
UP7	SA/FA/DEG 22/ 24/ 54	7295	12746	1.7	8	190	34
UP8	GA/FA/DEG 20/ 25 / 55	3890	5543	1.4	8	190	26
UP9.1	GA/ FA/1,3 PG 20/ 25 / 55		*		12	210	27
UP9.2	GA/ FA/1,3 PG 20 / 20 / 60		*		12	210	4
UP10	GA/ FA/PG 20/ 25 / 55	1910	4882	2.5	14	210	12
UP11.1	GA/FA/DEG/IS 20/ 25 /45/10	914	1272	1.4	14	190	28
UP11.2	GA/FA/DEG/IS 20/ 25 /25/30	691	1272	1.7	15	190	39

^aAV, acid value; ^b Đ, polydispersity, was determined by SEC, using conventional calibration with polystyrene standards and THF as eluent. * No data since the UPs were not soluble in the eluent.

The formulations containing IS (UP11.1 and UP11.2) showed a more yellowish and amber coloration, being more viscous than the polyesters UP7 and UP8. For the UPs containing IS and presenting a total of four monomers in their composition, the reaction showed to be slower, reaching in some cases a total of 15 h of reaction, which is expected, since this diol is characterized by their low reactivity [17]. IS presents its *exo* and *endo*-oriented hydroxyl groups, where the *endo* position favours the formation of intramolecular hydrogen bonds and consequently, the outcome is a low reactivity during the polycondensation reaction [5]. This explains the low molecular weight observed in Table 1. The structures of the developed materials are presented in Figure 2.

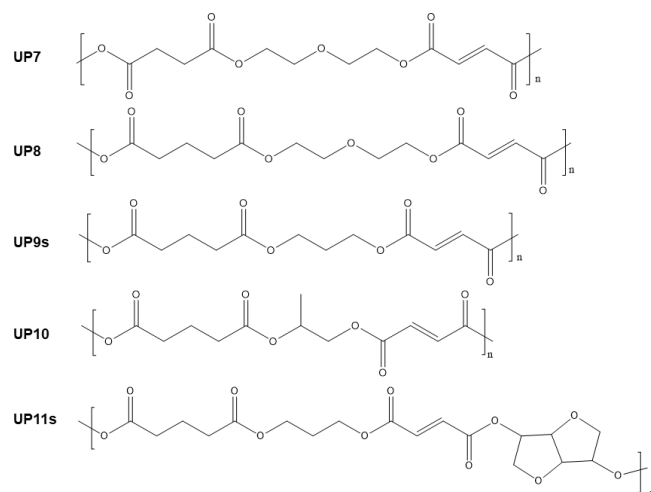


Figure 2. Chemical structure of the synthesized bio unsaturated polyesters UP7 to UP11s.

FTIR spectrum of UPs, presented in Figure 3, showed the bands characteristic of the polyesters, with strong bands ascribed to the carbonyl stretching group characteristic at ca. $1750\text{--}1725\text{ cm}^{-1}$ [27] and also a band in the region $1280\text{--}1240\text{ cm}^{-1}$ related to the stretching vibration of the C-O-C and C-O groups of the same linkage [28].

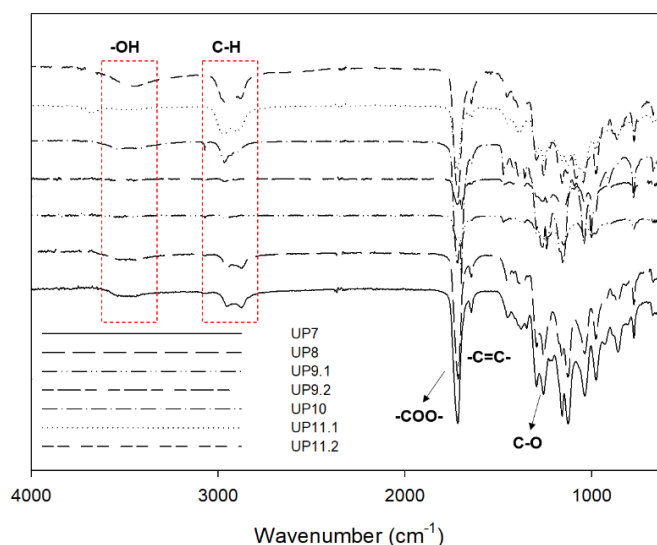


Figure 3. ATR-FTIR spectra of the synthesized UPs.

At $1680\text{--}1600\text{ cm}^{-1}$, the presence of the -C=C- stretching vibration was detected for all the synthesized UPs, indicating the incorporation of FA and the success of the UP synthesis. The bands at ca. $2970\text{--}2950/2880\text{--}2860\text{ cm}^{-1}$ are due to the vibrational modes of the CH stretching. The peaks in the characteristic region $1150\text{--}1050\text{ cm}^{-1}$ can be ascribed to the C-O group, from ether bond. It is also worth to mention the existence of hydroxyl groups, at $3570\text{--}3200\text{ cm}^{-1}$, in the UP11.2 formulation, the one presenting higher amount of IS.

Further insights onto the chemical structure of UPs were obtained by ^1H NMR spectroscopy. Figure 4 to Figure 6 presents the ^1H NMR spectra of the synthesized UPs.

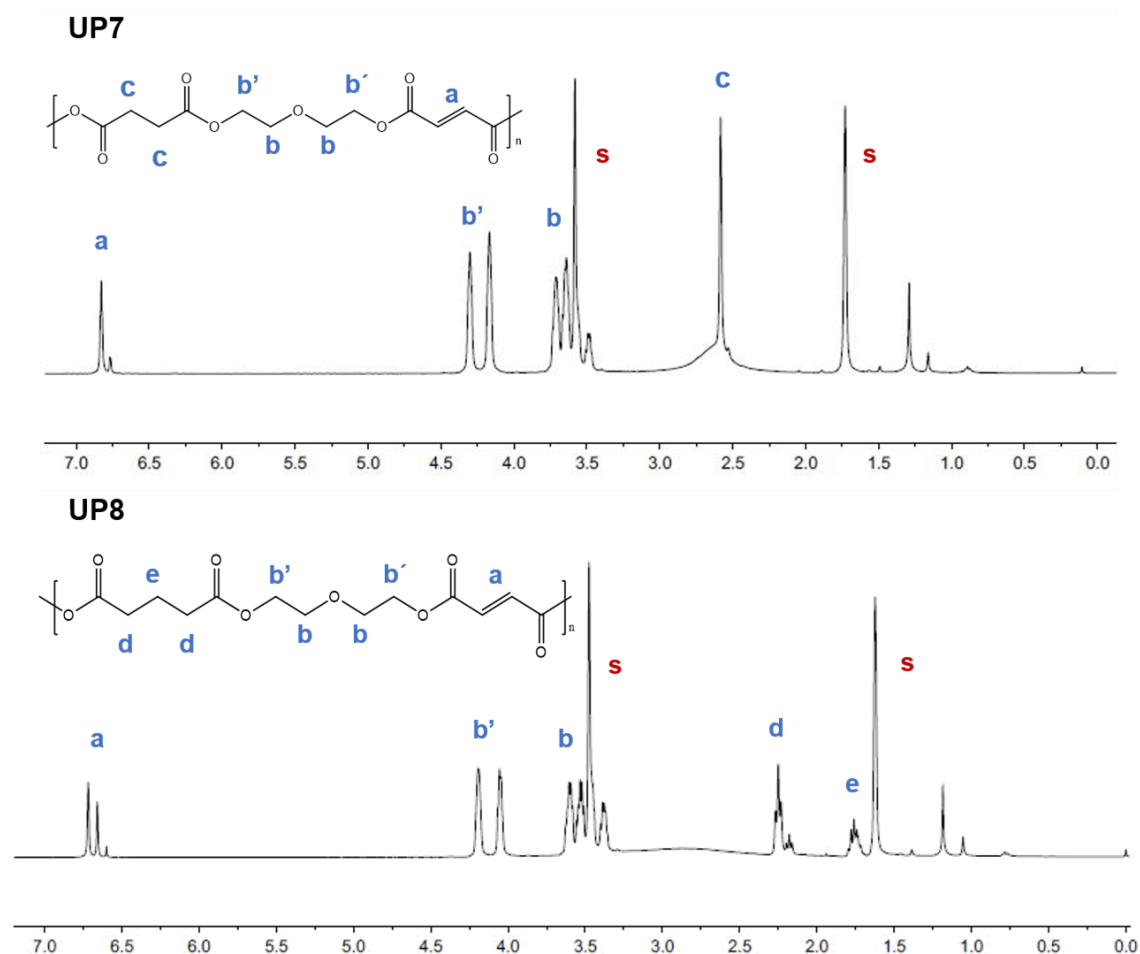


Figure 4. ^1H NMR spectra of the biobased UP7 and UP8, where (s) correspond to the solvent peaks of THF- d_8 .

Figure 4 shows the ^1H NMR spectra of the UPs formulations based on three monomers, UP7 and UP8 with the main difference on the type of diacid used, SA or GA. Considering the two spectra it is possible to identify the protons characteristics of the double bonds of FA moieties (a), located between 6.9 and 6.7 ppm [25, 29, 30]. It also indicates the presence of maleate and fumarate vinyl protons for UP8 formulation. The signals located between 3.71 (b) and 4.45 ppm (b') for UP7 spectrum corresponds to the $-\text{CH}_2$ of the glycol DEG while at 2.58 ppm (c) it is possible to assign to the $-\text{CH}_2$ signals of SuCA. Considering UP8 ^1H NMR spectrum, besides the peaks characteristics of the protons of the glycol and the unsaturated diacid, the protons of $-\text{CH}_2$ of the GA were identified at 2.37-2.34 ppm (d) and 1.88 ppm (e). A peak around 2.5-2 ppm was detected and can be ascribed to unreacted diacid.

For the polyesters UP9 (UP9.1) and UP10, GA and FA were the used dicarboxylic acids, and changes were made concerning the incorporation of different glycols, 1,3-propanediol (UP9) or 1,2-propanediol (UP10), being the respective spectra displayed in Figure 5. The UP9.2 spectrum is presented in SI (see Figure S1), keeping the same designation.

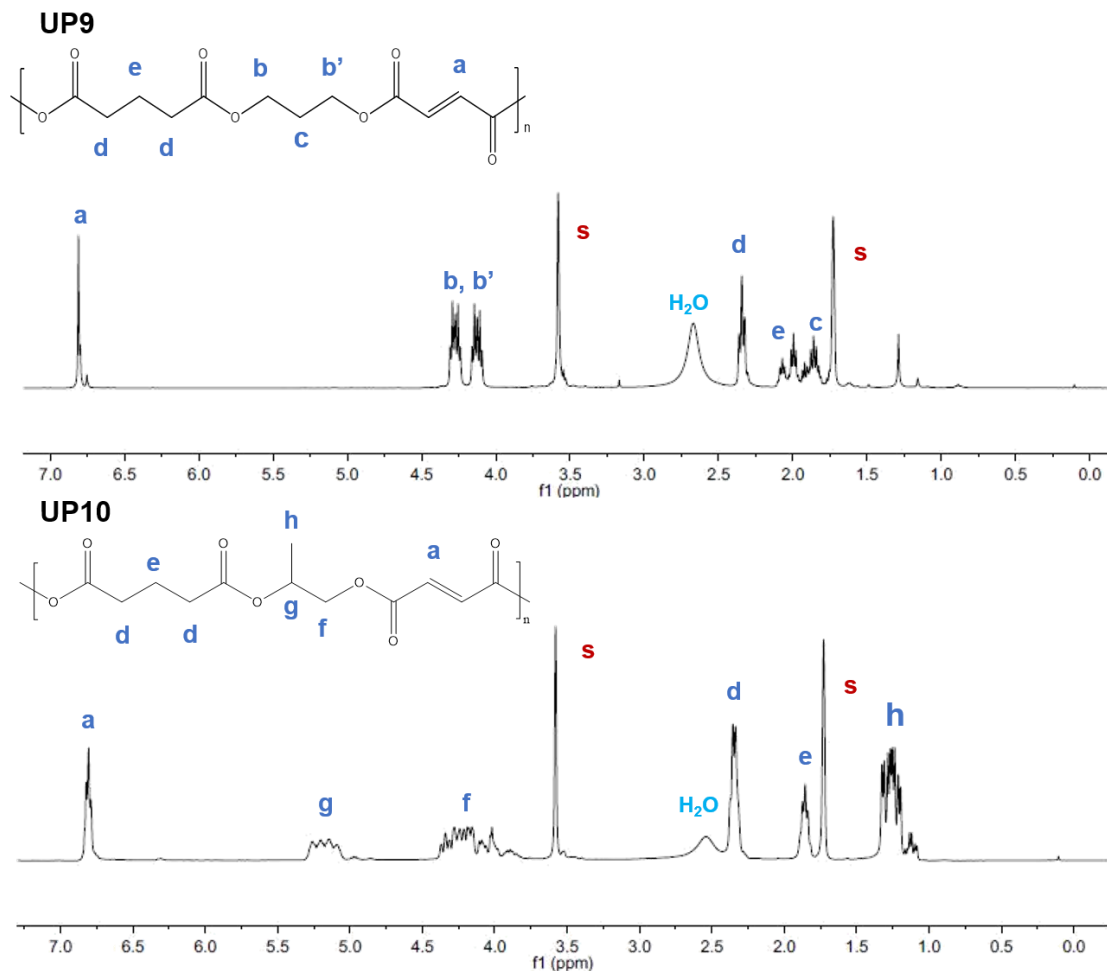


Figure 5. ^1H NMR spectra of UP9.1 and UP10, where (s) correspond to the solvent peaks of $\text{THF-}d_6$.

In both spectra, the signals at 6.81 and 6.75 ppm correspond to the double bonds of FA moieties (a). The protons of diacid GA are identified at 2.34-2.35 ppm (d) and 1.90-2.00 ppm (e) for both formulations. In UP9 spectrum, the identification of the protons of 1,3 PG was made, at 4.31-4.24 ppm, 4.16-4.09 ppm (b, b') and at 1.86 ppm (c), corresponding to the $-\text{OCH}_2-$ and $-\text{CH}_2\text{CH}_2\text{CH}_2-$, respectively. Considering UP10 spectrum, the peaks of the $-\text{CH}_2$ protons of PG are seen at 5.26-5.09 ppm (g) and at 4.37-4.02 ppm (f), while the $-\text{CH}_3$ protons of PG generated a peak at 1.33 ppm (h). ^1H NMR of these formulations indicate the presence of H_2O in the UP, detected around 2.5 ppm.

The formulations UP11s, containing different proportions of IS, were also studied by ^1H NMR and the corresponding spectrum of UP11.1 is displayed in Figure 6. This spectrum

concerns to the polyester UP11.1, the one with lowest incorporation of IS. The remaining UP11.2 spectrum are in SI (Figure S2). As previously reported, the characteristic resonances attributed to the GA were identified at 2.36 ppm (a) and 1.87 ppm (b), while at 6.83 ppm (e) are found the peaks corresponding to the -CH=CH- of the FA. The glycol DEG was also identified at 4.30-4.15 ppm (c) and 3.72-3.64 ppm (d). The incorporation of the glycol IS was also confirmed by ¹H NMR and the peaks ascribed to the IS are easily discerned. The peaks characteristic of IS, from (f) to (k) are signaled in the UP11.1 spectrum ((f, i) 5.24-5.04 ppm, (g) 4.88-4.72 ppm, (j) 4.50-4.39 ppm, (h, k) 3.99-3.86 ppm) [31]. The final molar ratio of the UPs are summarized in Table 2.

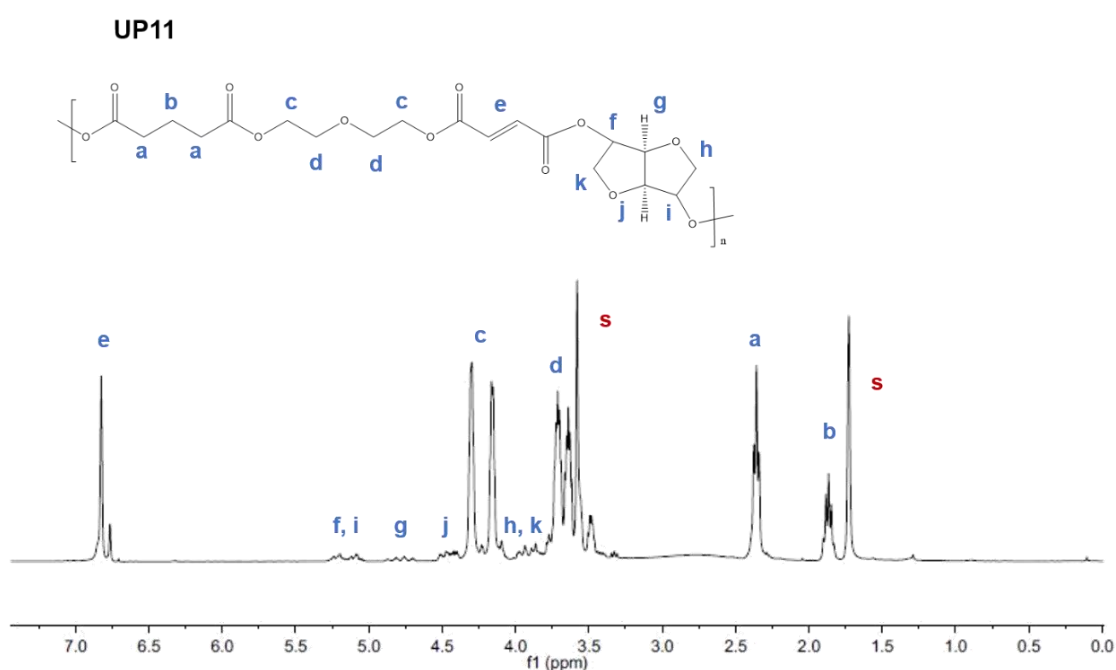


Figure 6. ¹H NMR spectra of UP11.1 where (s) correspond to the solvent peaks of THF- *d*₆.

Table 2. Initial and final molar ratio of the biobased UPs.

UPs	Formulation	Initial Molar ratio (%)	Final Molar ratio (%)
UP7	SA/FA/DEG	22/24/54	42/18/40
UP8	GA/FA/DEG	20/25/55	29/25/46
UP9.1	GA/ FA/1,3PG	20/25/55	27/27/46
UP9.2	GA/ FA/1,3PG	20/20/60	28/24/48
UP10	GA/FA/PG	20/25/55	12/13/75
UP11.1	GA/FA/DEG/IS	20/25/45/10	18/21/48/13
UP11.2	GA/FA/DEG/IS	20/25/25/30	16/18/35/31

Further information concerning the biobased UPs was obtained from MALDI-TOF-MS analysis. MALDI spectra for the selected polyesters UP7 and UP8, both presenting three monomers on their structure and having the lowest reaction times, were analysed and the results are displayed in Figure 7 and Table 3.

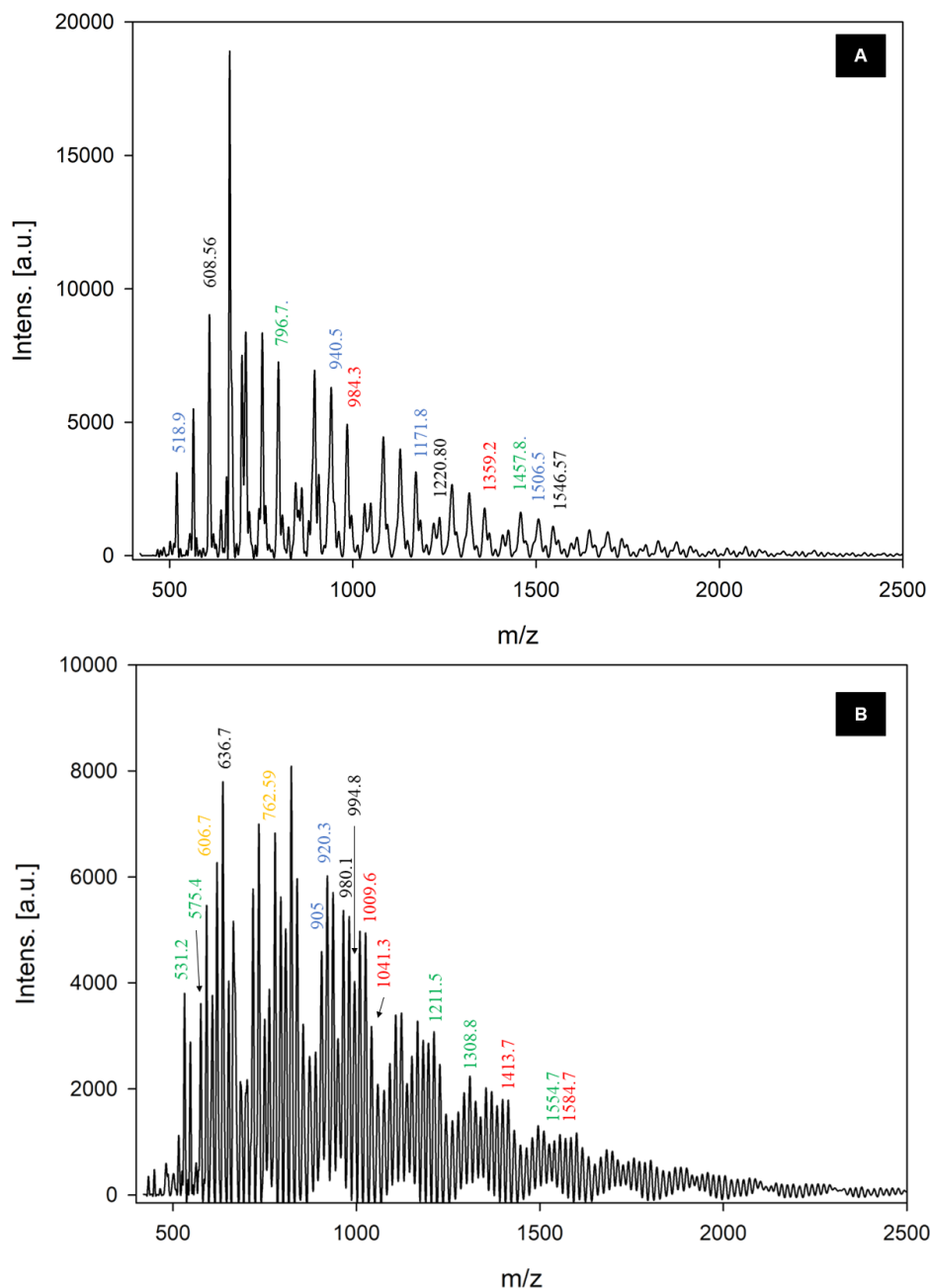
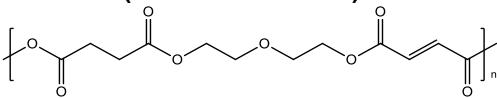


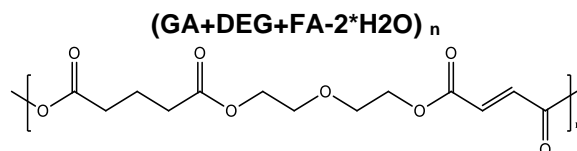
Figure 7. MALDI-TOF-MS in the linear mode (using DHB as matrix) of **A.** UP7 and **B.** UP8, from m/z 400 to 1600. For UP7, the black values identify the $(SA+DEG+FA-2\cdot H_2O)_n$ formulation, the red values correspond to formulation $(SA)_n + (DEG)_p + (FA)_m - (H_2O)_y$, the blue values for $(SA)_n + (DEG)_p - (H_2O)_y$ and green values for $(FA)_m + (DEG)_p - (H_2O)_y$. For UP8, the black values identify the $(GA+DEG+FA-2\cdot H_2O)_n$ formulation, the red values correspond to formulation $(GA)_n + (DEG)_p + (FA)_m - (H_2O)_y$, the blue values for $(GA + DEG - H_2O)_n$, green values for $(GA)_n + (DEG)_p - (H_2O)_y$ and orange values for $(FA)_m + (DEG)_p - (H_2O)_y$.

According to Figure 7A, the spectrum presents different polymer compositions. It was possible to identify some of the MALDI signals, assigned to the monomer composition of the different oligomers, with different degrees of polymerization (DP 1 to 5). The m/z values were, in most cases, associated with the Na^+ or K^+ cations. Based on the MALDI-TOF spectrum, we can easily confirm the existence of several other combinations of monomers, which is expected based on the nature of the step growth polymerization. The same was observed for UP8 (Figure 7B). In Table 3 several other monomer combinations for UP7 and UP8 are listed, where it was possible to assign the peaks to a specific formulation. Formulations such as $(\text{SA})_n+(\text{FA})_m+(\text{DEG})_p-(\text{H}_2\text{O})_y$, $(\text{GA})_n+(\text{FA})_m+(\text{DEG})_q-(\text{H}_2\text{O})_y$, $(\text{GA} + \text{DEG} - \text{H}_2\text{O})_n$ or $(\text{SA} + \text{DEG} - \text{H}_2\text{O})_n$, among others, are presented in Table 3, where the differences between near peaks are usually due to the number of the monomer in the formulation – n , m and p .

Table 3. Relationship between m/z and the chemical structure of UP7 and UP8.

UP7 structure		
$(\text{SA}+\text{DEG}+\text{FA}-2*\text{H}_2\text{O})_n$ 		
Observed mass	Calculated mass	n=
608.560	608.838	1
1220.808	1217.12	4
1546.576	1544.39	5 + $[\text{Na}^+]$
Other monomers combination		
$(\text{SA})_n + (\text{DEG})_p + (\text{FA})_m - (\text{H}_2\text{O})_y$		
984.980	984.289	2
1359.224	1357.36	2
697.887	699.647	1 + $[\text{Na}^+]$
906.568	903.9683	1 + $[\text{K}^+]$
$(\text{SA} + \text{DEG} - \text{H}_2\text{O})_n$		
824.365	824.84	4
640.320	641.62	3
859.975	863.938	4 + $[\text{K}^+]$
$(\text{SA})_n + (\text{DEG})_p - (\text{H}_2\text{O})_y$		
518.882	517.498	1 + $[\text{Na}^+]$
940.477	941.887	3 + $[\text{Na}^+]$
1171.785	1170.337	3 + $[\text{Na}^+]$
1506.556	1506.517	3 + $[\text{Na}^+]$
$(\text{FA})_m + (\text{DEG})_p - (\text{H}_2\text{O})_y$		
796.744	799.958	2 + $[\text{K}^+]$
1457.78	1458.487	3 + $[\text{Na}^+]$

UP8 structure



Observed mass	Calculated mass	n=
636.687	636.62	2
980.072	977.917	3 + [Na ⁺]
1293.155	1296.226	4 + [Na ⁺]
994.781	994.028	3 + [K ⁺]
Other monomers combination		
$(\text{GA})_n + (\text{DEG})_{p+} + (\text{FA})_{m-} - (\text{H}_2\text{O})_y$		
1009.581	1009.00	2
1041.296	1041.10	2
1382.979	1381.38	2
1413.69	1413.48	2
1584.662	1584.63	3+ [Na ⁺]
$(\text{GA} + \text{DEG} - \text{H}_2\text{O})_n$		
905.019	903.947	4+[Na ⁺]
920.325	920.058	4+[K ⁺]
$(\text{GA})_n + (\text{DEG})_p - (\text{H}_2\text{O})_y$		
667.451	668.72	2
793.655	792.96	2
531.249	533.587	1+[Na ⁺]
949.981	948.067	3+[Na ⁺]
1025.093	1026.067	3+[Na ⁺]
1211.528	1212.427	3+[Na ⁺]
1554.691	1554.78	3+[Na ⁺]
575.432	575.698	1+[K ⁺]
964.397	964.178	3+[K ⁺]
1227.58	1228.54	3+[K ⁺]
1308.78	1306.54	3+[K ⁺]
$(\text{FA} + \text{DEG} - \text{H}_2\text{O})_n$		
838.76	839.75	4+[Na ⁺]
855.19	855.86	4+[K ⁺]
$(\text{FA})_m + (\text{DEG})_p - (\text{H}_2\text{O})_y$		
606.67	604.52	2
762.59	760.86	2
778.17	780.76	2
1116.42	1164.28	3+[Na ⁺]
1196.29	1194.13	3+[Na ⁺]
1181.62	1180.39	3+[K ⁺]

The UP11s were not analysed by MALDI-TOF-MS mainly because the probability of side reactions during the bulk polycondensation is very high, leading to the formation of branched structures [5] and making difficult a straightforward analysis of the polyesters.

4.2 Thermal and Mechanical Properties of UPs

Thermal stability of the developed biobased UPs was evaluated by means of TGA. The TGA curves are presented in Figure 8. According to Figure 8, the developed biobased UPs have a good thermal stability under 350 °C. The thermal decomposition of all the bio UPs only reveal a single stage degradation, leaving a final residue of less than 5% at 600 °C. The $T_{5\%}$ and $T_{10\%}$ were also determined, besides the T_{on} (maximum degradation temperature) and the results are listed in Table 4.

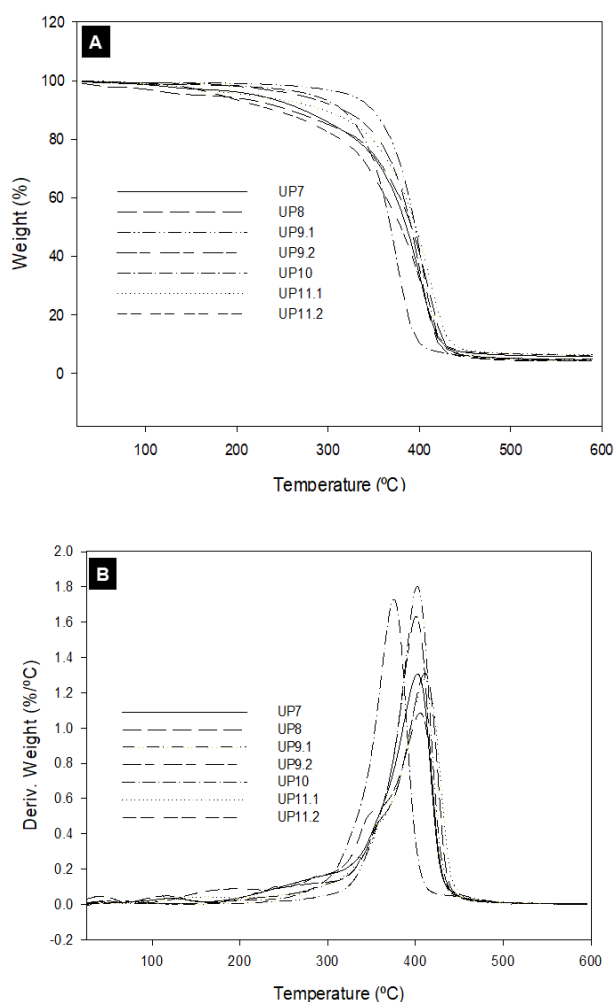


Figure 8. Thermal gravimetric curves of the synthesized UPs, with a heating rate of 5 °C.min⁻¹, in the range of 25 °C to 600 °C.

Table 4. Degradation temperatures ($T_{x\%}$) and onset temperature (T_{on}) of the UPs, obtained from TGA curves.

Polyesters	$T_{5\%}$	$T_{10\%}$	T_{on}
UP7	222.85	272.13	353.88
UP8	164.34	256.54	361.92
UP9.1	325.45	348.92	368.84
UP9.2	268.87	316.95	362.06
UP10	283.68	316.49	341.67
UP11.1	216.20	295.21	365.19
UP11.2	182.66	239.70	345.85

Although the thermoanalytical curves reveal a single degradation stage, the presence of a small shoulder was detected for almost all the bio UPs, which can be ascribed to the degradation of oligomeric segments in an earlier stage. The UPs showed similar T_{on} , with values ranging between 340 and 370 °C, corresponding to the degradation of the ester linkages [32, 33]. However, the $T_{5\%}$ reveals some differences between the formulations. The UP8 started to degrade earlier, when compared with the remaining UPs, even with a T_{on} above 360 °C. This could be ascribed to residual humidity of the polymer. Overall, we can assume that the stability of the polyesters is not greatly affected by the diol length or by the saturated diacid used (SA or GA). Still, the amount of glycol added to the formulation produces changes in the degradation temperature. For UP11s, the increase of IS resulted in a slight decrease of T_{on} ; the same behavior was observed between UP9.1 and UP9.2, considering the percentage of PG added to each formulation.

The thermomechanical properties of bio UPs were studied by DMTA, in a temperature range of -150 to 200 °C. The sensitivity of the $\tan \delta$ peak to the frequency indicates the presence of the α transition, *i.e.*, T_g , which is attributed to the amorphous segment transition from the glassy to the viscoelastic state. The T_g of the UPRs were determined from the maximum of the $\tan \delta$ curve, at the frequency of 1 Hz (Figure S3).

The UPs were also subjected to a MDSC analysis and, in the heat flow curves, only one transition, corresponding to the T_g was found (see Figure S4 for the heat flow curves). This indicates that the UPs have an amorphous character. The values of T_g obtained from both techniques are presented in Table 5.

Table 5. Glass transition temperatures, T_g , obtained from DMTA and MDSC techniques.

Polyesters	T_g (°C)	
	DMTA	MDSC
UP7	-44.3	-35.1
UP8	-36.3	-39.30
UP9.1	-31.6	-36.6
UP9.2	-41.9	-47.6
UP10	3.6	-9.5
UP11.1	-18.2	-25.5
UP11.2	-13.9	-10.7

According to the results obtained from DMTA and MDSC, we can verify that UP7, UP8 and UP9.2 are the UPs with lower T_g , indicating that these formulations are characterized by a higher mobility of the polymeric chains. UP7 and UP8 have similar T_g , which is also expected since the main difference is the saturated diacid used, SA or GA. These diacids have almost the same number of carbons, therefore no significant differences in chain mobility (and therefore in T_g values) were detected. Considering UP8 and UP9.1, the difference between the two polyesters is based on the glycol used, i.e., DEG or 1,3PG and the obtained T_g are extremely similar. For UP9.1 and UP9.2, differing only in the amount of 1.3PG incorporated, 55 and 60%, respectively, UP9.1 showed to be more flexible than UP9.2, with a T_g slightly higher. According also with Table 5, T_g of UP9.1 and UP10 are very different, and the explanation should be related to glycol used. The pendent methyl group in PG should restrain the chain mobility of the UPs [34] which could be a possible explanation for the UP10 higher T_g ,

It is also worth to mention that formulations UP11.1 to UP 11.2 have some of the highest T_g , which is indicative of a more rigid structure. This can be explained by the cyclic structure of one of the diols, which resulted in a decrease of chain mobility and, therefore, a high T_g was obtained. This result is expected – several works reported the use of IS to enhance T_g and modulus of the final UPs [35]. The comparison between UP11.1 and UP11.2 T_g values also corroborates these statements; UP11.2 has a higher amount of IS and consequently, a higher T_g than UP11.1 was observed. The results obtained from the MDSC technique are overall in agreement with the DMTA values.

4.3 Preparation and characterization of Bio UPRs

Considering the above results, some of the developed UPs were selected for the crosslinking studies. UP7 and UP8 showed promising results. However, besides the high thermal stability and proper mechanical behavior, these biobased UPs were prepared in 8

h and with a final temperature of 190 °C. For UP11s, these formulations, although with less mild reaction conditions, the presence of IS are an interesting alternative and therefore the crosslinking studies were also performed for these bio UPRs. Also, considering several literature reports about the use of isosorbide as one of the most promising renewable sources for the preparation of biopolymers, 3D networks of UP11.2, the one with the higher amount of IS were also prepared. UPRs were prepared through thermal crosslinking using BPO (1% (w/w)) as the initiator and HEMA as the crosslinking agent. The prepared mixture was transferred to Teflon moulds, which were placed in an oven at 80 °C for 24 h to yield the UPRs. No post-cure was performed.

The wettability of the bio UPRs was measured along time and the results are summarized in Figure 9, with the water contact angle of the UPRs expressed in function of time. At least three measurements were made for each UPR, in different places of the surface.

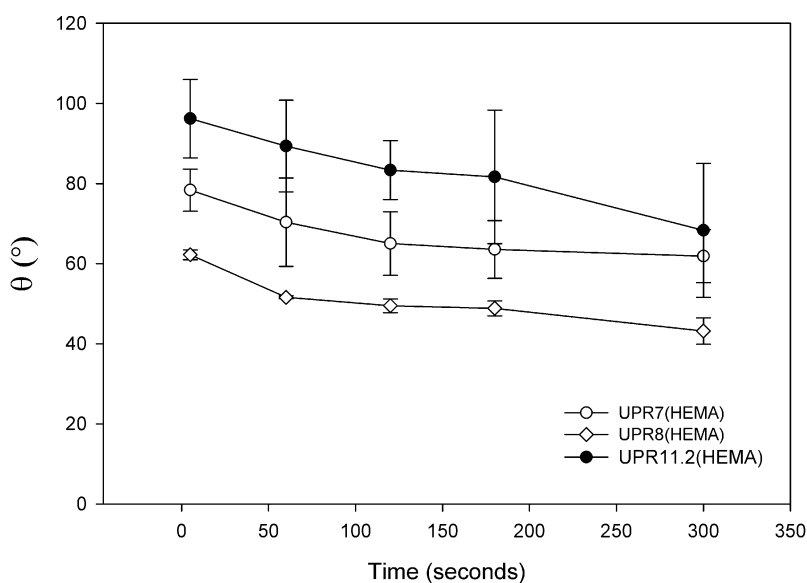


Figure 9. Dynamic water contact angles of UPRs crosslinked with HEMA determined by the sessile drop method and respective standard deviations.

According to the Figure 9, UPR7(HEMA), UPR8(HEMA) present WCA ranging from 60 to 40° after the stabilization (*ca.* 5 min) of the water drop in their surfaces, thus indicating a hydrophilic nature. UPR8(HEMA) is the UPR with low WCA (43°) followed by UPR7(HEMA) (62°). This is explained by the high-water solubility of GA, where diacids containing an odd number of carbons are much more soluble than the even-number carbon diacids [36]. This phenomenon is called the odd-even effect, where due to the molecules conformation and interlayer packaging, the odd-number diacids such as GA, are more soluble [37]. Therefore, the discrepancy between these two relatively similar

formulations can be attributed to the number of carbons present on the diacid used. For UPR11.2 the initial WCA was higher compared with the other two formulations (96°), but decreased considerably after 5 min, reaching a WCA of 68°. The initial WCA of UP is very similar to others reported in the literature, for formulations containing IS and diacids such as SuCA and sebacic acid (SeBA), ranging between 85 and 93° [38]. Other authors characterized PBS copolyesters based on IS and reported WCA between 73 and 51°, depending on the amount of IS incorporated in the polyester formulations [39]. The hydrophilic behavior of HEMA is due to the presence of the hydroxyl group at the end of the monomer [40], promoting hydrogen bond formation, thus leading to UPRs with a hydrophilic character. A quick analysis shows a similar behavior between these formulations and the ones developed on Chapter III. However, the WCA obtained after 300 sec for UP7 and UP8, were considerably lower than the WCA of UP4 to UP6 and clearly more hydrophilic.

The thermal stability of selected UPRs was studied by TGA, in a 25-600 °C range, in a nitrogen atmosphere and the results are presented in Figure 10 and Table 6.

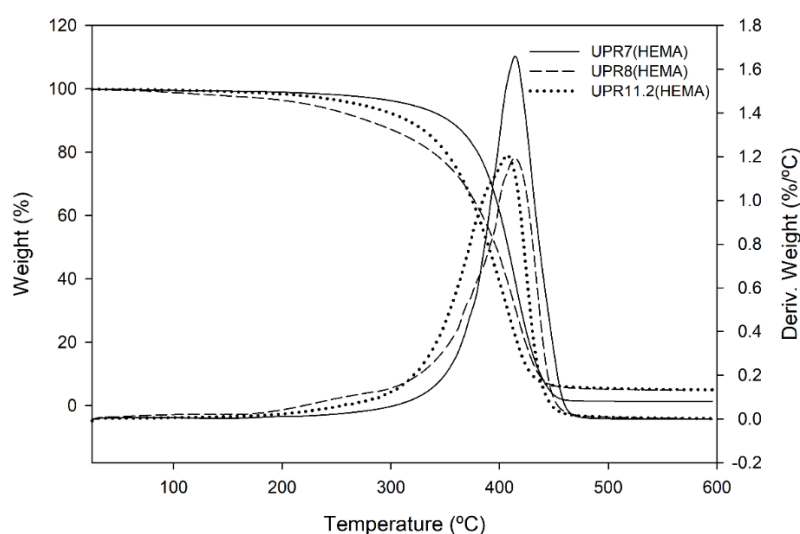


Figure 10. Thermogravimetric curves and respective derivatives of the selected bio UPRs crosslinked with HEMA.

According to Figure 10, all the prepared bio UPRs presented a single degradation stage [41, 42], having a very similar weight loss pattern. As expected, this degradation stage is related with the degradation of the crosslinked network [33] and its indicative of a homogeneous crosslinked UP. Also, the T_{on} increased considerably after the crosslinking of the UPs with HEMA; the UPs T_{on} were over 345-360 °C, while the respective UPRs

were in the range of 405-414 °C, establishing their high thermal stability. Nevertheless, the thermal profile of the UPs and UPRs are quite similar, presenting only one main stage of decomposition, confirmed by DTGA (1st derivative of the TGA curve). Also, these materials leave a final residue of less than 5% for UPR8 and UP11.2, and less than 1% for UPR7, at 600 °C.

Table 6. Degradation temperatures ($T_{x\%}$) and onset temperature (T_{on}) of the selected bio UPRs, obtained from TGA curves.

UPR(HEMA)	$T_{5\%}$	$T_{10\%}$	T_{on}
UPR7	317.55	353.77	413.7
UPR8	225.01	278.74	412.0
UPR11.2	271.50	315.94	405.78

The thermomechanical properties of the crosslinked UPs were also studied by DMTA and the results are presented in Figure 11 and Table 7.

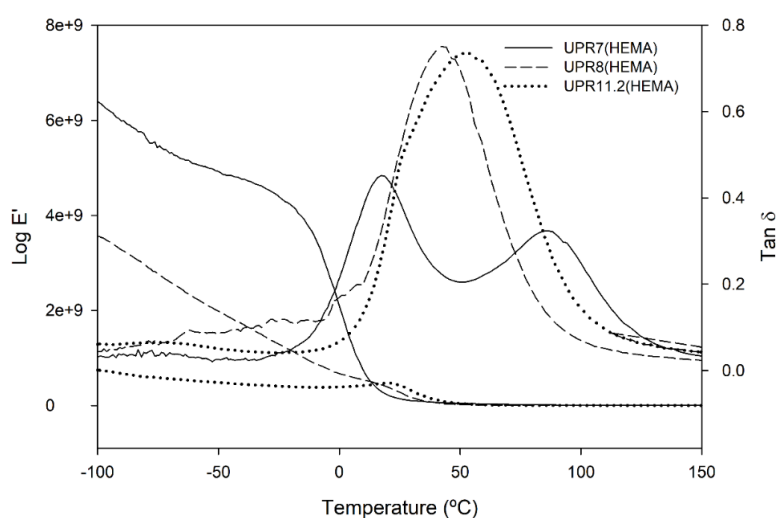


Figure 11. DMTA traces of the selected biobased UPRs in terms of E' and $\tan \delta$.

Figure 11 presents the $\tan \delta$ and E' traces of the crosslinked UPs. At higher temperatures, in the range of 0-100 °C, we can identify the α transition, corresponding to the T_g . While for UPR7, two peaks in $\tan \delta$ are observed, the samples UPR8 and UPR11.2 are characterized by only one α transition, having very similar $\tan \delta_{max}$. Jasinska et al. [5] also reported a single T_g value for isosorbide-based polyesters crosslinked with HEMA, ranging between 83 and 53 °C. The existence of only one α transition is indicative of the UPs-HEMA crosslinking. The two peaks detected for UPR7 are both sensitive to frequency and

can be attributed to the existence of two immiscible parts. While the T_g detected at 17.4 °C is related with the UP-UP crosslinking, or UP with small amounts of HEMA, the T_g at 86 °C can be ascribed to the UP7 crosslinking with HEMA. According to Table 7, the formulation UPR11.2 is the one having the highest storage modulus E' and therefore regarded as the most elastic material; also, it has the highest T_g value, of 53.5 °C as well the highest $\tan \delta_{\max}$ value. Overall, this UPR is characterized by a higher capacity to dissipate energy. It was not expected a great difference between the formulations UPR7 and UPR8, since both have a similar chemical structure, with the main difference being the dicarboxylic acid used (SA or GA). Though, a possible explanation could be ascribed to GA structure and its odd number of carbons. There are reports on the flexibility of GA-based UPs, which could be closely related with GA odd-number carbon structure [43, 44]. The higher elasticity of UPR8 can also be corroborated by the low T_g , of 42.2 °C.

Table 7. Thermomechanical parameters of the prepared bio UPRs obtained from DMTA. T_g : glass transition temperature; E' -37 °C: elastic modulus at 37 °C; E'' 37 °C: loss modulus at 37 °C.

UPR	E' 37 °C (MPa)	E'' 37°C (MPa)	Tan δ (máx)	T_g (°C)
UPR7	72.9	18.7	0.45; 0.32	17.4; 86.4
UPR8	80.7	58.0	0.75	42.2
UPR11.2	169.2	107.7	0.74	53.5

Tensile modulus (E), maximum stress (σ_{\max}) and maximum strain (ε_{\max}) were also determined for the biobased UPRs and the results are displayed in Table 8. Considering the Youngs' modulus, E ranged between 7.5 MPa and 1.3 MPa, with UPR8 having a E value of 1.3 MPa being highly flexible at room temperature (Figure 12).

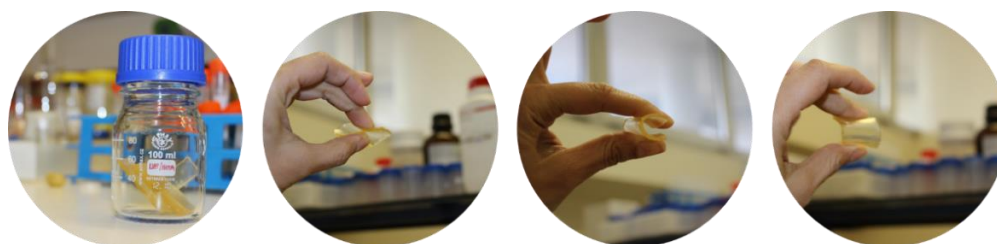


Figure 12. Pictures of biobased UPR8/HEMA and its flexible behavior.

These values are well reported in the literature, matching the prerequisites for application in TE fields [45-47]. Since E clearly depends on the monomers, reaction type and crosslinking agent used, the values of E reported in the literature are very wide-ranging.

Overall, these new biobased UPRs presented a more flexible character and malleability than the previous synthesized materials, making them interesting candidates for articular cartilage [48].

Table 8. Results from UPRs tensile tests: modulus (E), maximum stress (σ_{max}) and maximum strain (ϵ_{max}), reported as mean value \pm standard deviation. The UPRs were crosslinked with HEMA.

UPRs	E (MPa)	σ_{max} (MPa)	ϵ_{max} (mm/mm)
UPR7(HEMA)	7.5 \pm 0.9	1.30 \pm 0.15	0.37 \pm 0.05
UPR8(HEMA)	1.3 \pm 0.2	0.23 \pm 0.03	0.41 \pm 0.07

5. Conclusions

Biobased UPs were prepared with monomers obtained from renewable resources to obtain viable products with suitable properties to be used in tissue engineering fields. UPs based on SA, GA, and diols such as IS, were successfully synthesized by bulk polycondensation, without resorting to toxic solvents and catalysts. Also, the preparation of UPRs using glutaric acid as the diacid is here reported for the first time. The step-growth polymerization leads to amorphous and unsaturated products as expected. It was also possible to reduce the reaction time to 8 to 10 h and the reaction temperature did not exceed the 210 °C. The UPs structures were validated by ATR-FTIR and ¹H NMR. They presented high thermal stability, with decomposition temperatures above 340 °C. Also, T_g was determined by DMTA and MDSC, and the values ranged between -44 and 4 °C, being the value dependent on the composition. The most promising formulations were crosslinked with HEMA and the cured biobased UPs showed they are thermally stable up to 400 °C and with T_g up to 86 °C. GA also brings interesting properties to the final UPRs, with UPR8 having the lowest WCA and T_g . Overall, the UPRs had high thermal and mechanical properties, holding interesting properties with both uses on TE and industrial fields. These polymers with high green content revealed to be promising candidates to the common petroleum based UPRs available in industrial markets but also a green alternative in TE applications.

6. References

1. Fuesl, A., M. Yamamoto, and A. Schneller, 5.03 - *Opportunities in Bio-Based Building Blocks for Polycondensates and Vinyl Polymers*, in *Polymer Science: A Comprehensive Reference*, K.M. Möller, Editor. 2012, Elsevier: Amsterdam. p. 49-70.
2. Noordover, B.A.J., et al., *Co- and terpolyesters based on isosorbide and succinic acid for coating applications: Synthesis and characterization*. *Biomacromolecules*, 2006. **7**(12): p. 3406-3416.
3. Barrett, D.G., et al., *One-Step Syntheses of Photocurable Polyesters Based on a Renewable Resource*. *Macromolecules*, 2010. **43**(23): p. 9660-9667.
4. Tawfik, S.Y., *Preparation and characterization of some new unsaturated polyesters based on 3,6-bis(methoxymethyl)durene*. *Journal of Applied Polymer Science*, 2001. **81**(14): p. 3388-3398.
5. Jasinska, L. and C.E. Koning, *Unsaturated, Biobased Polyesters and Their Cross-Linking via Radical Copolymerization*. *Journal of Polymer Science Part a-Polymer Chemistry*, 2010. **48**(13): p. 2885-2895.
6. Wyatt, V.T. and G.D. Strahan, *Degree of Branching in Hyperbranched Poly(glycerol-co-diacid)s Synthesized in Toluene*. *Polymers*, 2012. **4**(1): p. 396-407.
7. Venkata Nivasu M., T.R.T.a.S.T., *In situ Polymerizable Polyester Polyols for Tissue Sealant Applications: Effect of Choice of Acid and Diol on Sealant Properties*. *Trends Biomater. Artif. Organs*, 2004. **18**(1): p. 52-59.
8. Vera, M., et al., *Synthesis and Characterization of a New Degradable Poly(ester amide) Derived from 6-Amino-1-hexanol and Glutaric Acid*. *Macromolecules*, 2003. **36**(26): p. 9784-9796.
9. Rohles, C.M., et al., *A bio-based route to the carbon-5 chemical glutaric acid and to bionylon-6,5 using metabolically engineered *Corynebacterium glutamicum**. *Green Chemistry*, 2018. **20**(20): p. 4662-4674.
10. Wyatt, V.T., *Effects of swelling on the viscoelastic properties of polyester films made from glycerol and glutaric acid*. *Journal of Applied Polymer Science*, 2012. **126**(5): p. 1784-1793.
11. Stadler, B.M., et al., *Catalytic Approaches to Monomers for Polymers Based on Renewables*. *ACS Catalysis*, 2019. **9**(9): p. 8012-8067.
12. Samuel D. Hilbert, R.L.M., *Copolyester adhesive*. 985, Eastman Kodak Company: Rochester, New York.
13. Vyvoda, J.C., *Glutaric acid based polyester internally plasticized PVC*. 1993, The Geon Company, Independence: Avon Lake, Ohio.
14. Mitra, T., G. Sailakshmi, and A. Gnanamani, *Could glutaric acid (GA) replace glutaraldehyde in the preparation of biocompatible biopolymers with high mechanical and thermal properties?* *Journal of Chemical Sciences*, 2014. **126**(1): p. 127-140.
15. Lomelí-Rodríguez, M., et al., *Synthesis and Characterization of Renewable Polyester Coil Coatings from Biomass-Derived Isosorbide, FDCA, 1,5-Pentanediol, Succinic Acid, and 1,3-Propanediol*. *Polymers*, 2018. **10**(6): p. 600.

Chapter IV

16. Sadler, J.M., et al., *Isosorbide as the structural component of bio-based unsaturated polyesters for use as thermosetting resins*. Carbohydrate polymers, 2014. **100**: p. 97-106.
17. Fenouillot, F., et al., *Polymers from renewable 1,4:3,6-dianhydrohexitols (isosorbide, isomannide and isoidide): A review*. Progress in Polymer Science, 2010. **35**(5): p. 578-622.
18. Bart, A.J.N., et al., *Novel Biomass-Based Polymers: Synthesis, Characterization, and Application*, in *Biobased Monomers, Polymers, and Materials*. 2012, American Chemical Society. p. 281-322.
19. Jiang, M., et al., *Progress of succinic acid production from renewable resources: Metabolic and fermentative strategies*. Bioresource Technology, 2017. **245**: p. 1710-1717.
20. Rose, M. and R. Palkovits, *Isosorbide as a Renewable Platform chemical for Versatile Applications—Quo Vadis?* ChemSusChem, 2012. **5**(1): p. 167-176.
21. Guo, F., et al., *Current advances on biological production of fumaric acid*. Biochemical Engineering Journal, 2020. **153**: p. 107397.
22. Saxena, R.K., et al., *Microbial production and applications of 1,2-propanediol*. Indian Journal of Microbiology, 2010. **50**(1): p. 2-11.
23. Samoilov, V., et al., *Bio-Based Solvents and Gasoline Components From Renewable 2,3-Butanediol and 1,2-Propanediol: Synthesis and Characterization*. Molecules (Basel, Switzerland), 2020. **25**(7): p. 1723.
24. Martin E. Rogers, T.E.L., *Synthetic methods in step-growth polymers*. 2003, New Jersey: Wiley-IEEE. 605
25. Gonçalves, F.A.M.M., et al., *3D printing of new biobased unsaturated polyesters by microstereo-thermal-lithography*. Biofabrication, 2014. **6**(3): p. 035024.
26. John Scheirs, T.E.L., *Modern Polyesters: Chemistry and Technology of Polyesters and Copolyesters*. Scheirs Polymer Science. Vol. 10. 2003, Chichester, West Sussex, England: John Wiley & Sons. 788.
27. Coates, J., *Interpretation of Infrared Spectra, A Practical Approach*, in *Encyclopedia of Analytical Chemistry*, R.A. Meyers, Editor. 2000, John Wiley & Sons Ltd: Chichester. p. 10815–10837.
28. Costa, C., et al., *Going greener: Synthesis of fully biobased unsaturated polyesters for styrene crosslinked resins with enhanced thermomechanical properties*. Express Polymer Letters, 2017. **11**: p. 885-898.
29. Farmer, T.J., et al., *Synthesis of Unsaturated Polyester Resins from Various Bio-Derived Platform Molecules*. Int J Mol Sci, 2015. **16**(7): p. 14912-32.
30. Takenouchi, S., et al., *Effects of Geometric Structure in Unsaturated Aliphatic Polyesters on Their Biodegradability*. Polymer Journal, 2001. **33**: p. 746-753.
31. Noordover, B.A.J., et al., *Co- and Terpolyesters Based on Isosorbide and Succinic Acid for Coating Applications: Synthesis and Characterization*. Biomacromolecules, 2006. **7**(12): p. 3406-3416.
32. Sanchez, E.M.S., C.A.C. Zavaglia, and M.I. Felisberti, *Unsaturated polyester resins: influence of the styrene concentration on the miscibility and mechanical properties*. Polymer, 2000. **41**(2): p. 765-769.

33. Fonseca, A.C., et al., *Synthesis of unsaturated polyesters based on renewable monomers: Structure/properties relationship and crosslinking with 2-hydroxyethyl methacrylate*. *Reactive and Functional Polymers*, 2015. **97**: p. 1-11.
34. Hu, X., et al., *Biodegradable unsaturated polyesters containing 2,3-butanediol for engineering applications: Synthesis, characterization and performances*. *Polymer*, 2016. **84**: p. 343-354.
35. Xu, Y., et al., *Isosorbide as Core Component for Tailoring Biobased Unsaturated Polyester Thermosets for a Wide Structure–Property Window*. *Biomacromolecules*, 2018. **19**(7): p. 3077-3085.
36. Rozaini, M.Z.H. and P. Brimblecombe, *The Odd–Even Behaviour of Dicarboxylic Acids Solubility in the Atmospheric Aerosols*. *Water, Air, and Soil Pollution*, 2009. **198**(1): p. 65-75.
37. Zhang, H., et al., *Identification and Molecular Understanding of the Odd–Even Effect of Dicarboxylic Acids Aqueous Solubility*. *Industrial & Engineering Chemistry Research*, 2013. **52**(51): p. 18458-18465.
38. Park, H.-S., M.-S. Gong, and J.C. Knowles, *Synthesis and biocompatibility properties of polyester containing various diacid based on isosorbide*. *Journal of biomaterials applications*, 2012. **27**(1): p. 99-109.
39. Qi, J., et al., *An investigation of the thermal and (bio)degradability of PBS copolyesters based on isosorbide*. *Polymer Degradation and Stability*, 2019. **160**: p. 229-241.
40. Efron, N. and C. Maldonado-Codina, *7.35 Development of Contact Lenses from a Biomaterial Point of View: Materials, Manufacture, and Clinical Application*, in *Comprehensive Biomaterials II*, P. Ducheyne, Editor. 2017, Elsevier: Oxford. p. 686-714.
41. Lin, Y., et al., *Study on thermal degradation and combustion behavior of flame retardant unsaturated polyester resin modified with a reactive phosphorus containing monomer*. *RSC Advances*, 2016. **6**(55): p. 49633-49642.
42. Perng, L.H., *Thermal degradation mechanism of poly(ether imide) by stepwise Py–GC/MS*. *Journal of Applied Polymer Science*, 2001. **79**(7): p. 1151-1161.
43. Stempfle, F., P. Ortmann, and S. Mecking, *Long-Chain Aliphatic Polymers To Bridge the Gap between Semicrystalline Polyolefins and Traditional Polycondensates*. *Chemical Reviews*, 2016. **116**(7): p. 4597-4641.
44. Kandelbauer, A., et al., *6 - Unsaturated Polyesters and Vinyl Esters*, in *Handbook of Thermoset Plastics (Third Edition)*, H. Dodiuk and S.H. Goodman, Editors. 2014, William Andrew Publishing: Boston. p. 111-172.
45. Sabir, M.I., X. Xu, and L. Li, *A review on biodegradable polymeric materials for bone tissue engineering applications*. *Journal of Materials Science*, 2009. **44**(21): p. 5713-5724.
46. Amsden, B., *Curable, biodegradable elastomers: emerging biomaterials for drug delivery and tissue engineering*. *Soft Matter*, 2007. **3**(11): p. 1335-1348.
47. Byrne, D.P., et al., *Simulation of tissue differentiation in a scaffold as a function of porosity, Young's modulus and dissolution rate: Application of mechanobiological models in tissue engineering*. *Biomaterials*, 2007. **28**(36): p. 5544-5554.
48. Thambyah, A., A. Nather, and J. Goh, *Mechanical properties of articular cartilage covered by the meniscus*. *Osteoarthritis and Cartilage*, 2006. **14**(6): p. 580-588.

Supplementary information

UP9.2

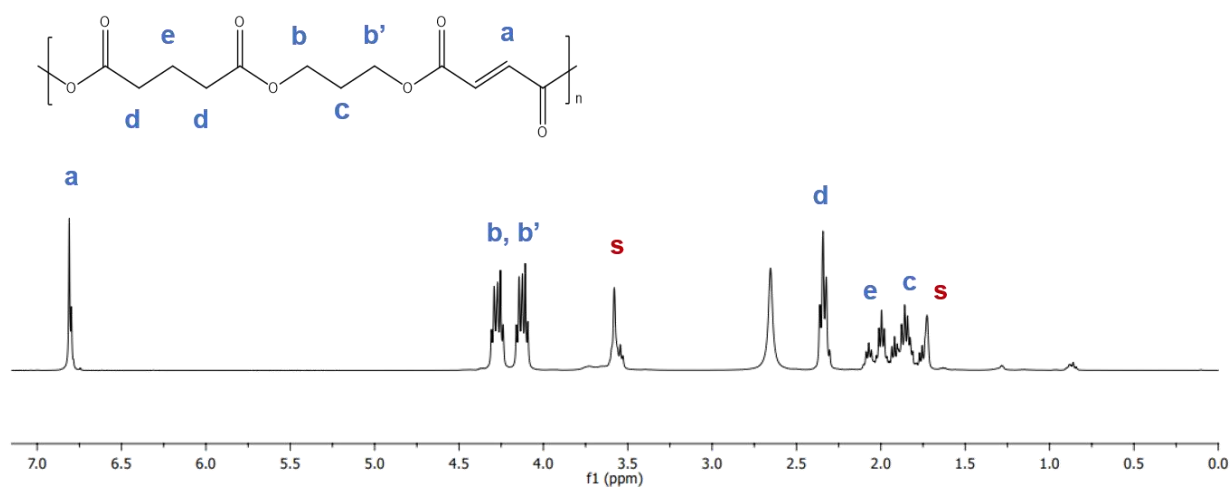


Figure S1. ¹H NMR spectrum of biobased UP9.2, where (s) correspond to the solvent peaks of THF- *d*₈.

UP11.2

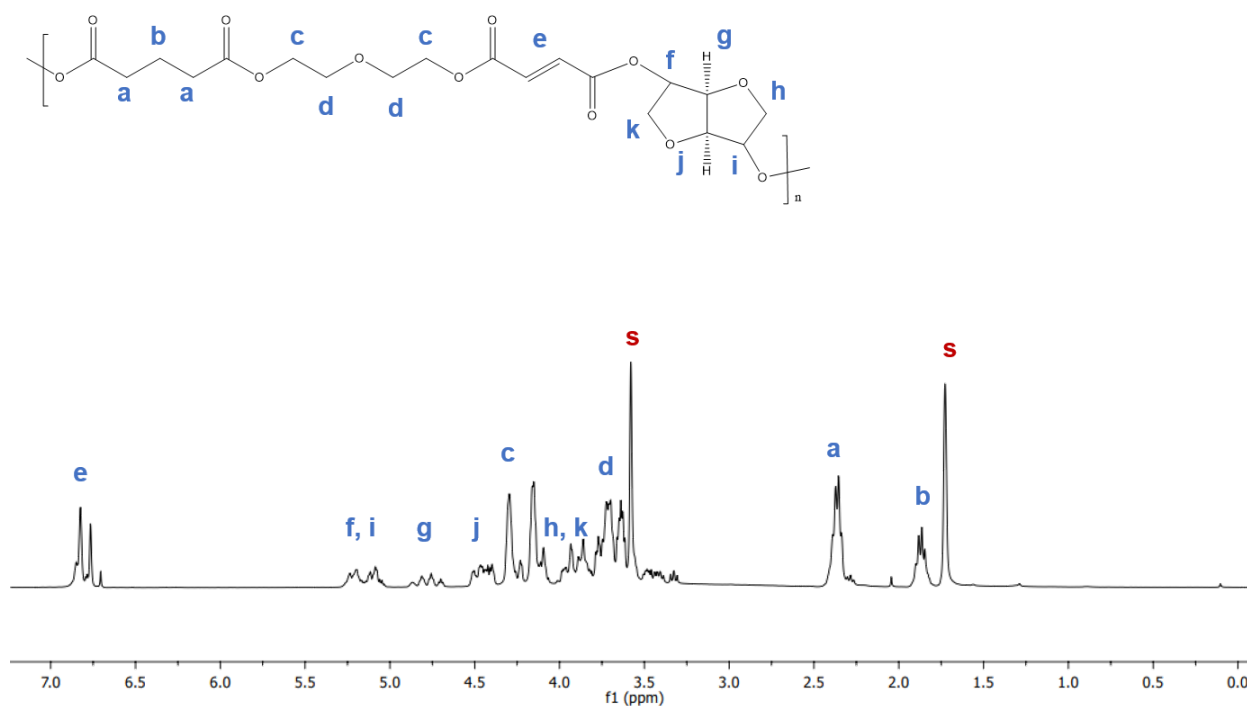


Figure S2. ¹H NMR spectrum of biobased UP11.2 where (s) correspond to the solvent peaks of THF- *d*₈.

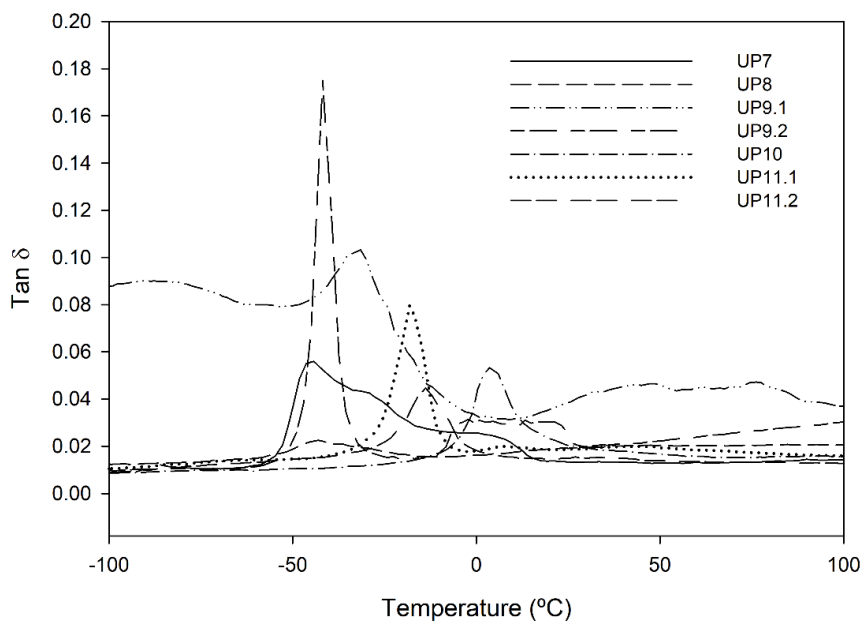


Figure S3. Loss function ($\tan\delta$) versus temperature for the synthesized bio UPs.

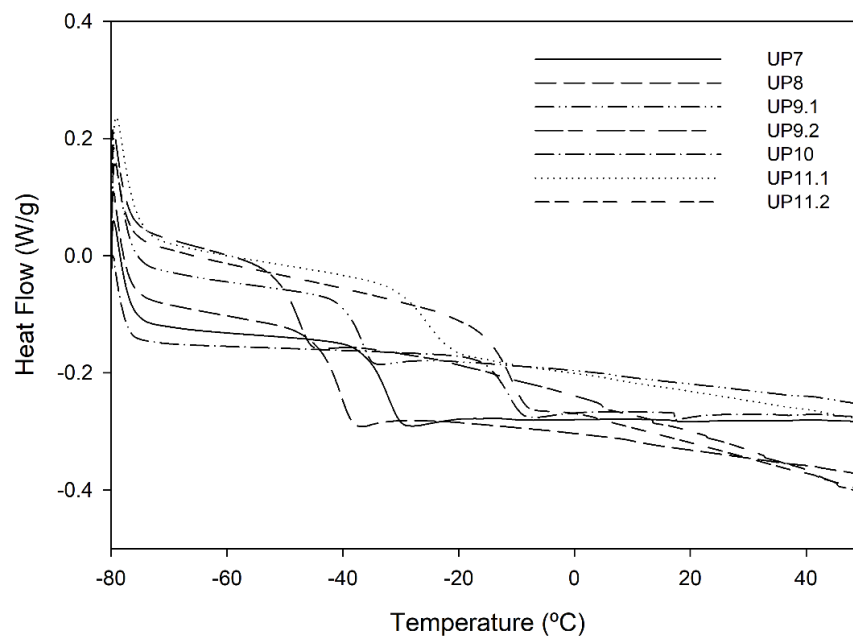


Figure S4. DSC curves from the second heating cycle, for the developed bio UPs. The polymers were tested in the temperature range -80 to 50 °C.

CHAPTER V

A preliminary study: Strategies to improve the biological performance of μ STLG scaffolds

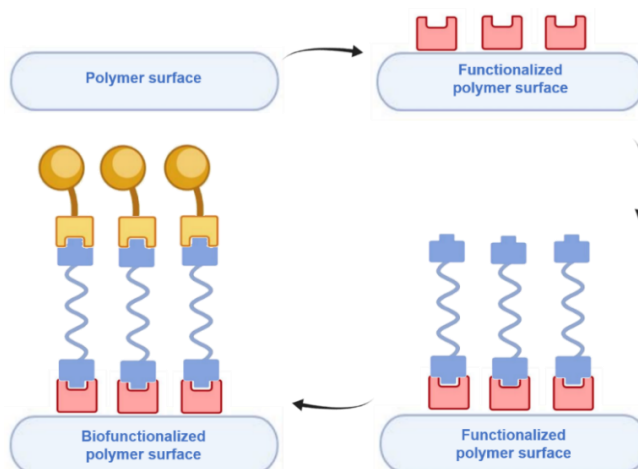
SCAFFOLDS	149
1. ABSTRACT	151
2. INTRODUCTION	151
3. MATERIALS AND METHODS	152
3.1 MATERIALS	152
3.2 MICROSTEREO-THERMAL-LITHOGRAPHY OF THE BIOBASED UPRS	153
3.3 SURFACE MODIFICATION METHODS	153
3.3.1 <i>Ethanol reflux and lysine-ethyl-ester treatment</i>	153
3.3.2 <i>Electrospinning of biopolymers</i>	153
3.3.3 <i>Oxygen plasma treatment</i>	154
3.4 SCAFFOLDS MORPHOLOGY	155
3.5 CELLULAR ASSAYS	155
3.5.1 <i>Sulforhodamine B colorimetric assay for cytotoxicity screening</i>	155
3.5.2 <i>Cell culture</i>	155
3.5.3 <i>Cell viability assays</i>	155
3.5.4 <i>Cell adhesion assays</i>	156
4. RESULTS AND DISCUSSION	157
4.1 SCAFFOLDS ACIDITY	157
4.2 STRATEGIES ADOPTED FOR THE DECREASE OF THE SURFACES' ACIDITY	159
4.2.1 <i>Reflux with EtOH and lysine-ethyl-ester treatment</i>	159
4.2.2. <i>Electrospinning</i>	160
4.2.3. <i>O₂ plasma treatment</i>	163
4.3 CELL ASSAYS	166
5. CONCLUSIONS	168
6. REFERENCES	168
SUPPLEMENTARY INFORMATION	171

1. Abstract

The 3D unsaturated polyesters (UPs) fabricated by μ STLG demonstrated to have high surface acidity, compromising the cell viability. Therefore, in the present work, we report studies of surface treatments of the biobased unsaturated polyester resins (UPRs) to enhance the biocompatibility of the final 3D scaffolds. Several approaches were tested, from simple reflux treatments to O_2 plasma surface modifications. Concerning the reduction of the acid character of the polymeric structures, EtOH reflux and O_2 plasma treatment exhibited the best results. Cytotoxicity assays were performed, for μ STLG scaffolds treated with EtOH for 3 h and, after 48 h of incubation, Scf6 and Scf7 presented cell viabilities of 100%. High cell adhesion of scaffolds surface was also observed, attesting the viability for these materials in tissue engineering (TE).

2. Introduction

The surface modification of biomaterials is one of the most important strategies to enhance their performance (Scheme 1). The surface chemistry plays an important role since the biological interactions with scaffolds occurs at the interfaces. There are several factors that affect the interaction between the biological systems and the scaffolds surface [1].



Scheme 1. Generic scheme of biological surface modification, adapted from [2].

While surface chemistry (surface electric charge and hydrophilicity) and the architecture of scaffolds determine the first interactions occurring between the scaffolds surface and the body fluids and cells [3], other parameters, such as roughness, regulate the adhesion and proliferation of cells [4]. Also, other architectural factors, namely the presence of pores, their interconnectivity, size and distribution determine whether the cells attach or not to the biomaterials' surface. Because most of the pristine synthetic biomaterials do not have the requirements for cell attachment and proliferation, surface modification methods

have been developed to overcome this issue. Several polymers such as: poly(ethylene glycol) (PEG), poly(vinyl alcohol) (PVA), poly(acrylic acid) (PAA), poly(2-hydroxyethyl methacrylate) (HEMA), poly(lactic acid) (PLA), poly(glycolic acid) (PGA), poly(ϵ -caprolactone) (PCL), and poly(propylene fumarate) (PPF), are commonly used in tissue engineering (TE) [1]. Among those, polyesters are widely reported, however they are also well known for their poor hydrophilicity and lack of recognition sites for cell attachment [5, 6].

Different modification strategies can be employed to modify the surface of the biomaterials. Plasma treatment is one of the most used methods to promote the cell adhesion and growth, without changing the bulk properties of the biomaterials [7], [8]. The type of functionalization strongly depends on the gas used (O_2 , N_2 , Ar, CO_2 , NH_3) and other parameters such as time, pressure, and gas flow rate [2, 9]. Another alternative regards the use of electrospinning. It should be mentioned that this technology is an efficient processing method for applications in TE [10] but is usually described as a fabrication method [11] and not as regular “modification” method, such as plasma.

Herein, we report the use of different strategies to reduce the UPRs surface's acidity. With that goal, plasma technology, reflux with ethanol and electrospinning were some of the selected methods to treat the unsaturated polyester resins' (UPRs) surfaces. Regarding electrospinning, different natural polymers – hyaluronic acid (HA), gelatin type A and B – were used to evaluate the influence of electrospun-scaffolds in terms of cell viabilities and cell adhesion. HA is one of the main components of the extracellular matrix of skin and cartilage [12] and it is extremely used in biomedical fields. Same for gelatine, a fully resorbable biopolymer, derived from collagen hydrolysis [13, 14] which is experiencing a rapid growth with a wide range of applicability in TE – as electrospun fibers [15] for bone TE to scaffolds prepared by AM [16]. Cell cytotoxicity and adhesion was also evaluated. *In vitro* adhesion of fibroblasts on treated scaffolds was assessed by means of *Alamar blue* assay and fluorescence microscopy.

3. Materials and Methods

3.1 Materials

Styrene (St, 99%) and 2-hydroxyethyl methacrylate (HEMA, 98%) were purchased from Acros Organics. 2-(*N*-morpholino) ethanesulfonic acid sodium salt (MES), gelatine porcine type A and gelatine bovine skin type B, phosphate buffered saline (PBS) tablets (pH 7.4, 10 mM phosphate, 137 mM sodium, 2.7 mM potassium), L-lysine-ethyl-ester (99%), hyaluronic acid sodium salt from *Streptococcus Equi* (bacterial glycosaminoglycan

polysaccharide) (HA, 99%), dimethylformamide (DMF, 99.8%) and 2,2,2-trifluoroethanol (TFE, 99%) and tetrahydrofuran (THF, >95%) were purchased from Sigma-Aldrich.

3.2 Microstereo-thermal-lithography of the Biobased UPRs

3-D scaffolds were prepared by μ STLG of UPRs based on renewable sources (Table 1). The UPRs were prepared by bulk polycondensation, using the procedure reported elsewhere [17]. The scaffolds (round disc format) were prepared with a diameter of 0.6 cm and a thickness of 0.125 mm. The UPRs and the corresponding unsaturated monomer (UM) were loaded into the reservoir and were exposed to the UV light, for 60 seconds. μ STLG system uses a mercury lamp of 350 W as light source. Optical fibers, projection and focal lenses irradiate a UV-DMD and an IR-DMD [18, 19]. A dichroic mirror captures the images projected on DMD (1024 x 768 pixels, 14 mm in size), combining them into a single image that is transferred to the reactive resin (monomer or oligomers). The equipment also includes a multi-vat system. The vertical displacement of the platform is secured by a uniaxial MYCOSIS Translation Stage VT-80. This positioning system allows vertical increments of 1 μ m, at a speed ranging between 0.001 and 20 mm/s.

Table 1. Scaffolds fabricated by μ STLG and corresponding polyester formulations.

Scaffolds	UM (37% w/w)	Formulation
Scf4	HEMA	SuCA/FA/PG/DEG
Scf5		AA/FA/PG/DEG
Scf6		SeBA/FA/PG/DEG
Scf7		SuCA/FA/DEG

3.3 Surface Modification Methods

3.3.1 Ethanol reflux and lysine-ethyl-ester treatment

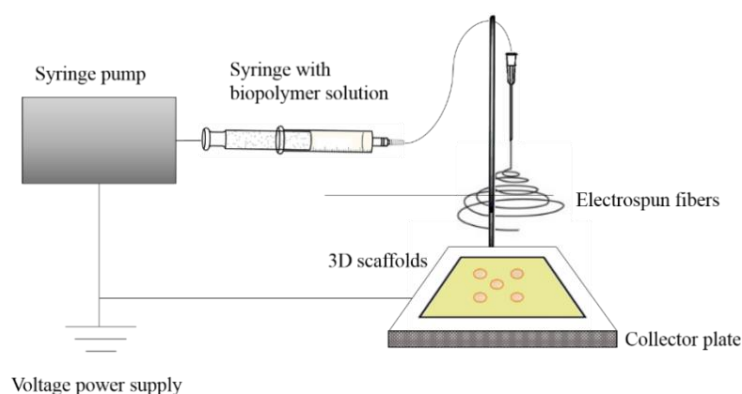
A common reflux setup was used to remove the excess of acidity of the polymeric scaffolds. The reflux with ethanol was performed for 1 h and for 3 h.

For L-lysine-ethyl-ester treatment, the scaffolds were added to a solution of 5 mg of L-lysine-ethyl-ester, dissolved in 1 mL of ethanol and treated overnight, at room temperature.

3.3.2 Electrospinning of biopolymers

The developed 3D scaffolds were layered with different electrospun fibers. Therefore, mixtures of gelatin type A and B, and HA, were electrospun in a homemade electrospinning

set-up mounted in a vertical configuration [20]. The system is composed by a high voltage power supply (SL 10W-300W, Spellman), a syringe pump (NE-1000 Multiphaser, New Era Pump Systems), and a quadrangular copper collector. The mixtures were transferred to a plastic syringe placed in the pump and connected, through a Teflon tube, to a blunted stainless-steel needle, fixed above the collector plate. During electrospinning, a positive high voltage was applied at the tip of a needle and the formed polymeric fibers were collected on a piece of aluminum foil covering the collector plate. The collector was covered with isolating tape, leaving only a small place for the scaffold to be placed, for all the set of experiments. The fibers were directly sprayed for that specific zone. All electrospinning experiments were carried under room conditions. A generic scheme of the used electrospinning apparatus is presented in Scheme 2.



Scheme 2. Schematic representation of the electrospinning apparatus used in the present work. A power supply, a syringe pump and a collector plate constitute the equipment.

3.3.3 Oxygen plasma treatment

The selected scaffolds were treated with oxygen plasma (FEMTO-Low pressure plasma reactor, manufactured by Diemer Electronics) in a stainless-steel chamber 270 mm long by 100 mm wide, in both sides. After the pressure stabilization inside the chamber at 0.6 mbar, a glow discharge plasma was applied, for a period of 3 minutes, using 8 cm from the electrode and at 100 W. The treated samples were immediately immersed in a solution of 10 % (v/v) St/THF, under gentle agitation in a bath at 70 °C. After 4 h, the samples were carefully washed with distilled water. The treated scaffolds were dried until reaching a constant weight and stored for further analysis. All the assays were carried out in triplicate.

3.4 Scaffolds Morphology

The morphology of the scaffolds obtained by μ STLG was observed by scanning electron microscopy (SEM) (MEV)/EDS, JEOL, model JSM-5310, at an accelerating voltage of 10 kV.

3.5 Cellular assays

3.5.1 Sulforhodamine B colorimetric assay for cytotoxicity screening

For sulphorhodamine (SRB) colorimetric assay, 60×10^3 3T3-L1 cells per well were seeded over the treated discs onto 96-well culture plate and incubated for 48 h in 5% CO₂ at 37 °C. Then, 120 μ L of 1% v/v acetic acid in pure methanol were placed in each well of a 96-well plate. After, the plates were placed in the freezer at -20 °C for 1 h. The solution was then removed, and the 96-well plates placed to dry at 37 °C. 50 μ L of SRB solution and 1% v/v acetic acid were added to each well of the dried 96-well plates and allowed to stain at 37 °C for 1 h. The SRB solution was removed by washing the plates with 1% v/v acetic acid, three times, to eliminate unbounded dye. The scaffolds appearance was then recorded, using camera (Canon G10 Wide 52mm) of the microscope (Zein, Axiovert 40C).

3.5.2 Cell culture

3T3-L1 cells (Mouse embryonic fibroblast cell line) and 3T3-L1 cells constitutively expressing the green fluorescence protein (GFP) were maintained in culture at 37 °C, under 5% CO₂, in Dulbecco's modified Eagle's medium-high glucose (DMEM-HG) (Sigma, MO, USA) supplemented with 10% (v/v) heat-inactivated fetal bovine serum (FBS) (Sigma; MO, USA), penicillin (100U/mL) and streptomycin (100U/mL). Cells grow in monolayer and were detached by treatment with a trypsin solution (0.25%) (Sigma, St. Louis, MO).

3.5.3 Cell viability assays

The cytotoxicity of the UPs photopolymerized in the μ STLG, using HEMA as the crosslinking agent, with a concentration of 37% (w/w) was evaluated in the 3T3-L1 cell line (Mouse embryonic fibroblast cell line). For cell viability tests, 30×10^3 3T3-L1 cells were seeded onto 48-well culture plate, 24 h prior to incubation with discs (cells were used at 70 % confluence). The cytotoxicity of the different polymers was evaluated by an extraction test according to ISO 10993-5 Standard [21]. Scaffolds were immersed in cell culture medium (DMEM-HG) (pH = 8.0) at an extraction ratio of 1 mL of DMEM-HG per 1.25 cm²

of polymers surface area and incubated in a humidified atmosphere with 5% CO₂, for 24 h, at 37 °C. 3T3-L1 cells, seeded in 48-well culture plates, were incubated with the extraction fluid for 48 h, and the cell viability was assessed by a modified *Alamar Blue* assay [22]. This assay measures the redox capacity of the cells due to the production of metabolites as a result of cell growth. Briefly, the cell culture medium of each well was replaced with 0.3 mL of DMEM-HG containing 10 % (v/v) of *Alamar Blue* (0.1 mg/mL in PBS) and, after 1 h of incubation at 37 °C, 170 µL of the supernatant were collected from each well and transferred to 96-well plates. The absorbance was measured at 570 and 600 nm in a SPECTRAmax PLUS 384 spectrophotometer (Molecular Devices, Union City, CA). Cell viability was calculated as a percentage of the control cells (cells not treated with the extraction medium) according to the formula $(A_{570}-A_{600})$ of treated cells $\times 100 / (A_{570}-A_{600})$ of control cells. The data are expressed as the percentage of the untreated control cells (mean \pm standard deviation obtained from $n = 3$) and are representative of three independent experiments.

3.5.4 Cell adhesion assays

For fluorescence microscopy assays (cell adhesion tests), 1.80×10^5 3T3-L1 cells per well were seeded over the treated discs onto 96-well culture plate and incubated for 48 h in 5% CO₂ at 37 °C. After 48 h of cell seeding, the discs were washed twice with PBS buffer and nuclear staining was performed with the Hoechst 333258 ($1 \mu\text{g}\cdot\text{mL}^{-1}$) (Invitrogen Life Technologies, Paisley, UK) fluorescent dye for 5 minutes. The microscope observation was performed using PALM MicroBeam equipment (Zeiss, Göttingen, Germany) with LD Plan-Neofluar 40x/0.6 Korr objective at excitation wavelength of 395 nm for GFP (green).

4. Results and Discussion

4.1 Scaffolds acidity

The SRB colorimetric assay is extensively used for *in vitro* cytotoxicity screening, mainly due to its simplicity and sensitivity and was used for cell density determination [23, 24]. This method is based on the measurement of cellular protein content, measuring the ability of the SBR to bind to protein components of cells that have been fixed to tissue-culture plates by trichloroacetic acid (TCA). The samples studied were Scf4, Scf5, Scf6 and Scf7 (scaffolds based on formulations UP4, UP5, UP6 and UP7), obtained from the photo polymerization of UP4, UP5, UP6 and UP7 (see Chapter III and Chapter IV for UP's composition), respectively, by μ STLG, using HEMA as the crosslinking agent (Table 1). According with Figure 1B there is no evidence of cell viability. These experiments suggest that cell death was induced by high levels of acidity, detected by the discoloration of the cell medium, from pink to a yellow coloration.

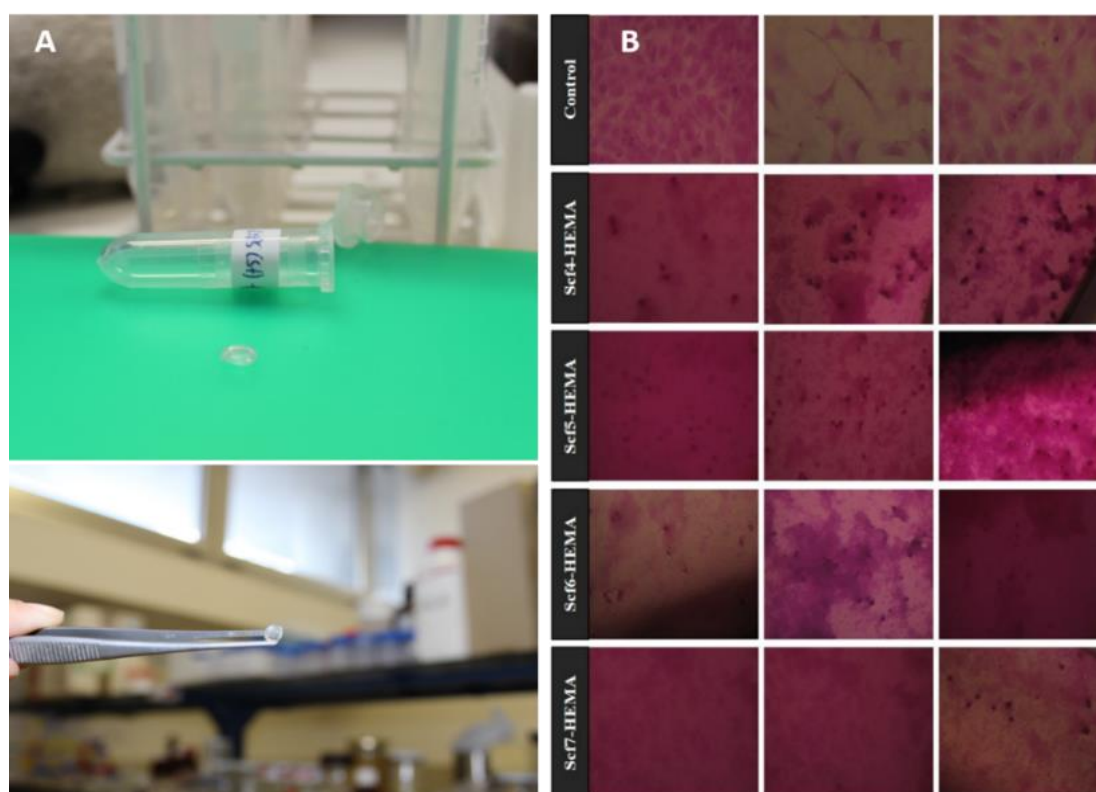


Figure 1. A. The μ STLG scaffolds used in the SRB assay. B. Images of the scaffolds incubated with cells after SRB assay.

The pH of DMEM was monitored by the change of the medium coloration. Except for Scf6, all the samples acidified the cell culture medium, DMEM. The other samples showed high values of acidity, mostly Scf7. Considering the results, the acidity level increases in the

following order: Scf6 < Scf4 < Scf5 < Scf7. Concerning these results, the scaffolds analyzed within this chapter were the ones presenting the highest (Scf6) and the lowest (Scf7) levels of acidity. Another important observation deals with sample Scf6. After 48 h immersed in DMEM, Scf6 shrunk to approximately $\frac{1}{2}$ of the initial diameter (data not shown). This scaffold lost around 28% of weight after 48 h immersed in DMEM. Scf6 and Scf7 were analyzed by SEM analysis to verify changes in their surfaces (Figure 2).

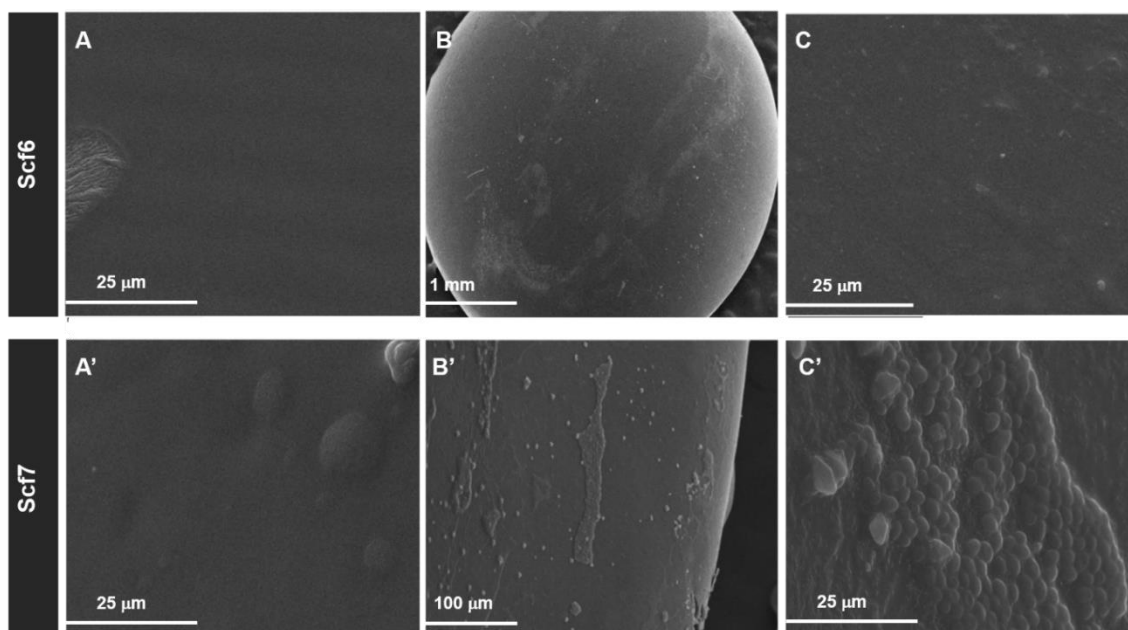


Figure 2. Scanning electron micrographs of the scaffolds Scf6 and Scf7 before (A) and after (B and C) immersion in DMEM medium, using microscopy (MEV)/EDS, JEOL, model JSM-5310, at an accelerating voltage of 10 kV. The magnifications used were 2000x for the controls (A, A'); for scaffolds Scf6, 35x (B) and 2000x (C); and for Scf7, 350x (B') and 2000x (C').

This degradation could be the explanation for the weight loss of the polymer and for no visible changes on the morphology of both Scf6 and Scf7 samples (Figure 2). This phenomena could be explained by the presence of acidic by-products, resulting from hydrolytic breakdown [25]; however this cannot be the explanation since the materials have only been immersed for 48 h. This effect is even more pronounced in nonporous materials, where the acidic by-products are trapped inside the polymer matrix [26]. Another hypothesis deals with the possible hydrolysis of the ester groups. It is well known that aliphatic polyesters, such as PLA and PGA, are characterized by a random bulk hydrolysis occurring in two distinct stages [27, 28]. The hydrolytic cleavage of the ester bonds results in the formation of carboxyl end groups (autocatalytic degradation mechanism). However, and considering the samples size, a reasonable explanation could be the presence of the oligomers entrapped inside the materials. The oligomers near the surface can diffuse out

from the polymer and the outcome is an increase of the acidity of the polyester and therefore the pH change in cell culture medium.

4.2 Strategies adopted for the decrease of the surfaces' acidity

To eliminate the acidity of the scaffolds, those were subject of the following strategies:

- A.** Reflux with EtOH for 1 h or 3 h of the scaffolds.
- B.** Pre-treatment with L-lysine-ethyl-ester, in EtOH.
- C.** Electrospinning (gelatin solution) onto the scaffolds surface, to cover the surface with bio fibers enhancing thus cell affinity.
- D.** Oxygen plasma treatment for 3 min and posterior grafting with 10% (v/v) St/THF, to insert polystyrene (PS) graft onto the scaffold surface.

The methods followed are listed in Table 2.

Table 2. Type of μ STLG scaffolds and respective treatments performed.

Scaffolds	Treatments				
	A		B	C	D
	EtOH reflux 1h	EtOH reflux 3h	Lysine-ether-ester	Electrospinning	O ₂ Plasma
Scf5				✓	
Scf6	✓	✓	✓	✓	✓
Scf7	✓	✓	✓	✓	✓

The selected strategies were chosen mainly by their simplicity, such as reflux with EtOH, or by considering well-known and successful modification methods, such as O₂ plasma treatment [8, 29]. After the treatment of each set of scaffolds, those were placed in cell-culture plates and immersed in culture medium (DMEM) containing a pH indicator (phenol red). To confirm the consistency of the results, the surrounding medium of each scaffold was monitored three times for each of the previous methods.

4.2.1 Reflux with EtOH and lysine-ethyl-ester treatment

As a first approach, the scaffolds were refluxed with EtOH, for 1 h, and dried in vacuum for several days. According to Figure 3, it is visible the color change of the DMEM medium after 24 h and 48 h in the presence of Scf7. The sample Scf7 lowered the pH (ca. 6.8) of the cell culture medium, which turned into a yellowish color. As previously observed, the Scf6 did not acidified the cellular medium.

Considering the treatment with L-lysine-ethyl-ester, (treatment B) a change on pH of DMEM was detected. Like the scaffolds refluxed with EtOH, these pre-treated Scf7 scaffolds, after 48 h immersed in DMEM, led to an acidification of the medium.

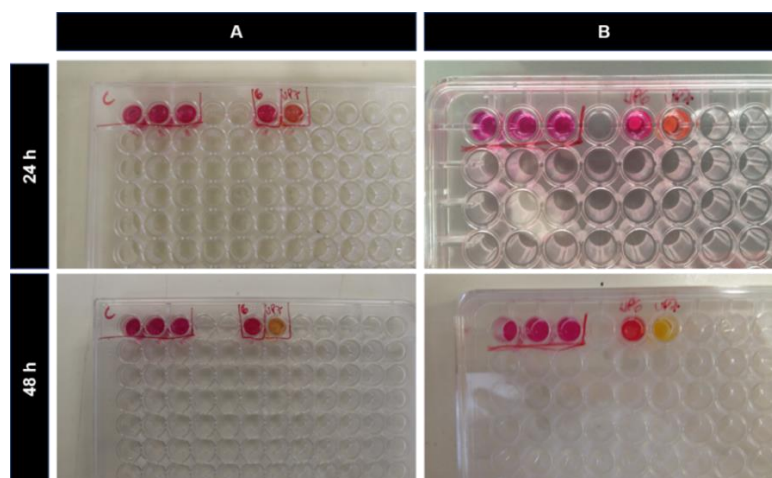


Figure 3. Screening of Scf6 and Scf7 and respective changes on pH medium after **A.** Reflux with EtOH and **B.** Lysine-ethyl-ester treatment, after 24 h and 48 h.

4.2.2. Electrospinning

The use of biobased natural polymers such as proteins, (e.g., gelatin, HA) and polysaccharides (e.g., alginate, chitosan) for the development of biocompatible scaffolds has been extensively explored over the last few years [30-32]. Electrospinning is one of the most used techniques to produce these biobased scaffolds. Commonly electrospinning has applicability in drug delivery systems, TE and polymers reinforcement and or/modification [33] but, to the best of our knowledge, there are no reports on the literature regarding this type of application of electrospun fibers, where the scaffolds is not produced by electrospinning but the technique is used to cover the AM scaffold, thus enhancing the polymer biocharacter. Electrospinning was used to coat the scaffold with biopolymers to enhance the affinity between the biomaterial surface and the cells. It is an alternative where instead of reducing the acidity, we promote the biocharacter of the modified scaffold. For this specific treatment, preliminary studies were performed to attain the best conditions, such as solvent used, polymer concentration, among others. Therefore, instead of using Scf6 and Scf7, other samples were first tested until the optimal electrospinning conditions were achieved. These electrospinning experiments were performed onto the surface of 3D rectangular scaffold with pores, as fabricated in Chapter II. The first experiments were performed on scaffolds Scf5 with controlled porous size to test the electrospinning parameters and were conducted at room temperature and parameters such as the applied voltage, feeding rates, solvent used –

2,2,2-trifluoroethanol (TFE) and dimethylformamide (DMF) – and the tip-to-collector distance are displayed in Table 3 [34, 35]. The concentration of the biopolymer was also controlled, since it influences the fiber morphology [10]. High concentrations of polymer lead to high fiber diameters while high flow rates can result in the presence of beads, structural defects that occur due to the incapacity of the fibers to dry before reaching the collector. The choice of these polymers is based on their natural origin and extensive applicability in TE field and will assure a proper substrate for cells, such as osteoblasts and fibroblasts. The type of produced electrospun fibers is critical since these materials are responsible to provide a good interface between the biomaterial surface and the cells.

Table 3. Composition of the formulations and electrospinning conditions used in the electrospinning method and scaffolds used for this study.

Formulation	[Polymer] (%, w/v)	Solvent	Distance (cm)	Flow Rate (mL/h)	Voltage (kV)	Scaffolds
Gelatin type A	7.5	TFE	11	3; 6	20	
Gelatin type B	7.5	TFE	11	6	20	Scf5
HA	1.5	DMF/H ₂ O	15	3	22	

Since gelatin is a natural polymer and very used in biomedical fields [35-37], two types of this biopolymer were selected: gelatin from porcine skin type A and gelatin from bovine skin type B, which are derived either by partial acid or alkaline hydrolysis, respectively, of animal collagen sources [38]. While more carboxylic acids are present in type A, scaffolds based on gelatin type B showed endothelial cell attachment [39], which is also a one of the reasons of the choice of this biopolymer. However, both gelatines are extremely used in TE and in food, pharmaceutical and cosmetic fields [40].

Scaffolds based on formulation UP5 (AA/FA/PG/DEG) (developed in Chapter II) were used in this study. Scf5 is composed by 2 layers and the time of cure used was between 28 and 37 seconds. The collector was covered with isolating tape, leaving only a small place for the scaffold to be placed, therefore the fibers were directly sprayed for that specific zone. In less than 20 min the scaffolds were completely covered with electrospun fibers of both type of gelatin. The micrographs of electrospun fibers attached to the scaffolds surface are presented in Figure 4. The presence of beads is clearly seen on SEM micrographs of gelatine type B (see also Figure S1 in SI), which is a result of the voltage applied, polymer low rate and capillary-collector distance or even a combination of these three factors.

By observing the scaffold with electrospinning fibers from gelatin type B and gelatin type A, it is quite clear the differences between the fibers. Keeping the parameter such as voltage and flow rate, it was observed that the scaffolds covered with gelatin B provided a

much more uniform-fiber surface than the scaffold with gelatin A fibers. Bovine gelatin solution was filtered before being placed into the electrospinning apparatus, since the prepared gelatin B solution was blurry. This could explain this difference on the fiber's organization and diameters. The scaffolds covered with gelatin B presented a more homogeneous electrospun fibers, with similar diameters. The same was not observed for gelatin A. HA, a polysaccharide present in the extracellular matrix (ECM) was also used in this study. HA plays an important role in cell adhesion, growth and migration, therefore its extensive use in biomedical applications [41, 42]. Thus, HA with a solution concentration fixed at 1.5 w/v%, was dissolved in a DMF-water solution with a volume ratio of DMF to water of 1.5 and the electrospinning experiments were performed. Compared with the gelatines, scaffolds covered with HA showed electrospun fibers with small diameters and the surfaces were not fully covered, even though the conditions used were considered optimal. We must not forget the cost associated with this natural source, making the use of gelatines in this study more appealing. Though, the lack of reproducibility is an issue since the deposition of the fibers on the surface cannot be entirely controlled.

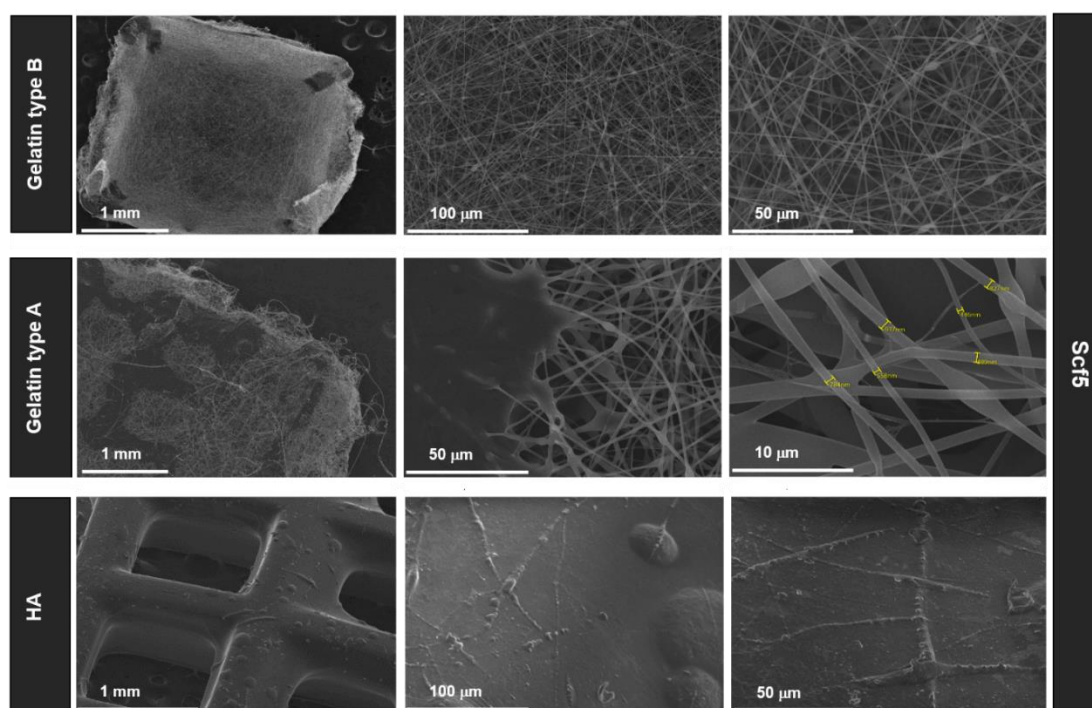


Figure 4. Scanning electron micrographs of the 3D scaffolds, with electrospun fibers of gelatin type A (7.5% w/v, in TFE), type B (7.5% w/v, TFE) and HA (1.5% w/v, DMF/H₂O) at the surface. The magnifications used for the Scf5 modified with gelatin B were 35x, 500x and 1000x; for the modification with gelatin A, 35x, 1000x and 5000x and for Scf5 with HA fibers, 50x, 500x and 1000x.

The results observed strongly suggest the use of gelatin B as the viable solution; besides, other factors such as availability, solubility and costs were also taking into account [40].

Therefore, and according with the results obtained and the conditions tested, the scaffolds Scf6 and Scf7 (discs format) were covered with gelatin type B fibers, the one presenting the most promising results, and were immersed in DMEM medium. The medium coloration was monitored for 48 h (Figure 5) and changes on pH medium were registered. This treatment using the gelatin fibers was not able to reduce the acidity of the scaffolds, which is clearly patent on the pH of cell culture medium displayed in Figure 5.

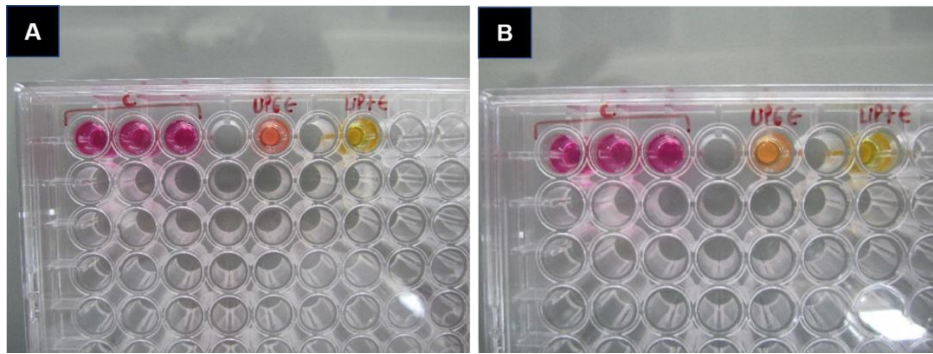


Figure 5. Screening of Scf6 and Scf7 covered with gelatin type B fibers and respective changes on pH medium.

4.2.3. O₂ plasma treatment

The O₂ plasma treatment and posterior grafting of St onto scaffolds surface was also tested at this stage. The grafting of St to the surface was here used as a proof-of-concept to visualize the success or not of the modification. So, to confirm the surface modification, the resulting treated scaffolds Scf6 and Scf7 were analyzed by SEM, as demonstrated in Figure 6.

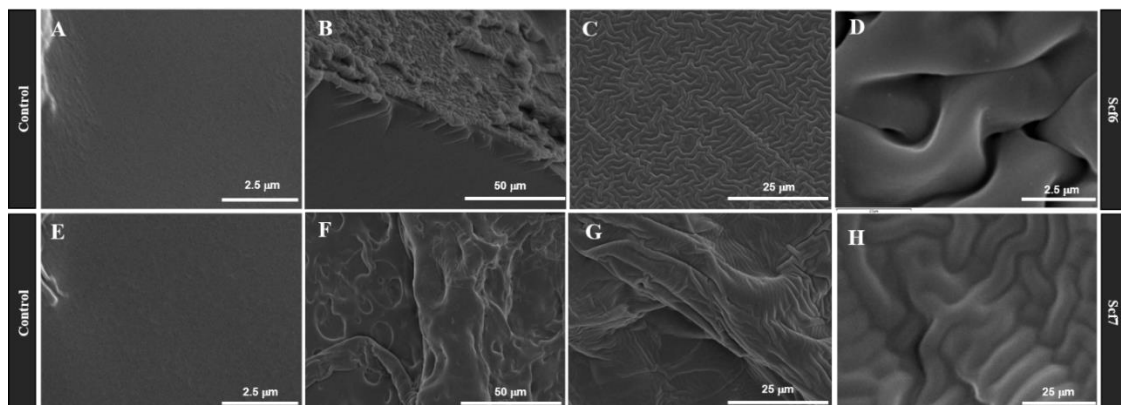


Figure 6. Scanning electron micrographs for the processed Scf6 and Scf7 before (control, A and E) (with magnifications of 15000x) and after modification by O₂ plasma and posterior grafting with St (magnifications of 1000x (B, F), 2000x (C, G) and 15000x (D, H)).

The photos of the scaffolds revealed that the surfaces were successfully modified by O₂ plasma treatment, with posterior grafting with St, resulting in patterned surfaces. These experiments were made in triplicate and the results were found consistent regarding the pattern observed. (Figure S2) Other reports available in the literature suggest the formation of peaks and valleys on the surfaces after O₂ plasma treatments [43]. It was also verified that despite Scf6 having such regular pattern, Scf7 did not showed such a similar level of regularity in terms of pattern. In the three sets of experiments, Scf6 always showed a more defined and organized pattern than Scf7. The O₂ plasma treated scaffolds Scf6 and Scf7 were immersed in DMEM medium and changes in the coloration and pH were monitored for 48 h (Figure 7).

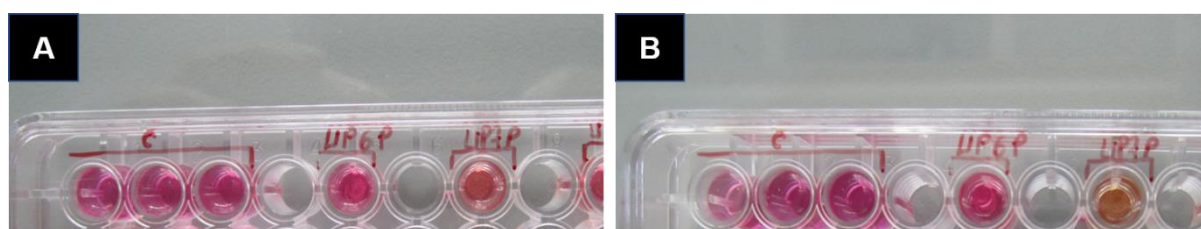
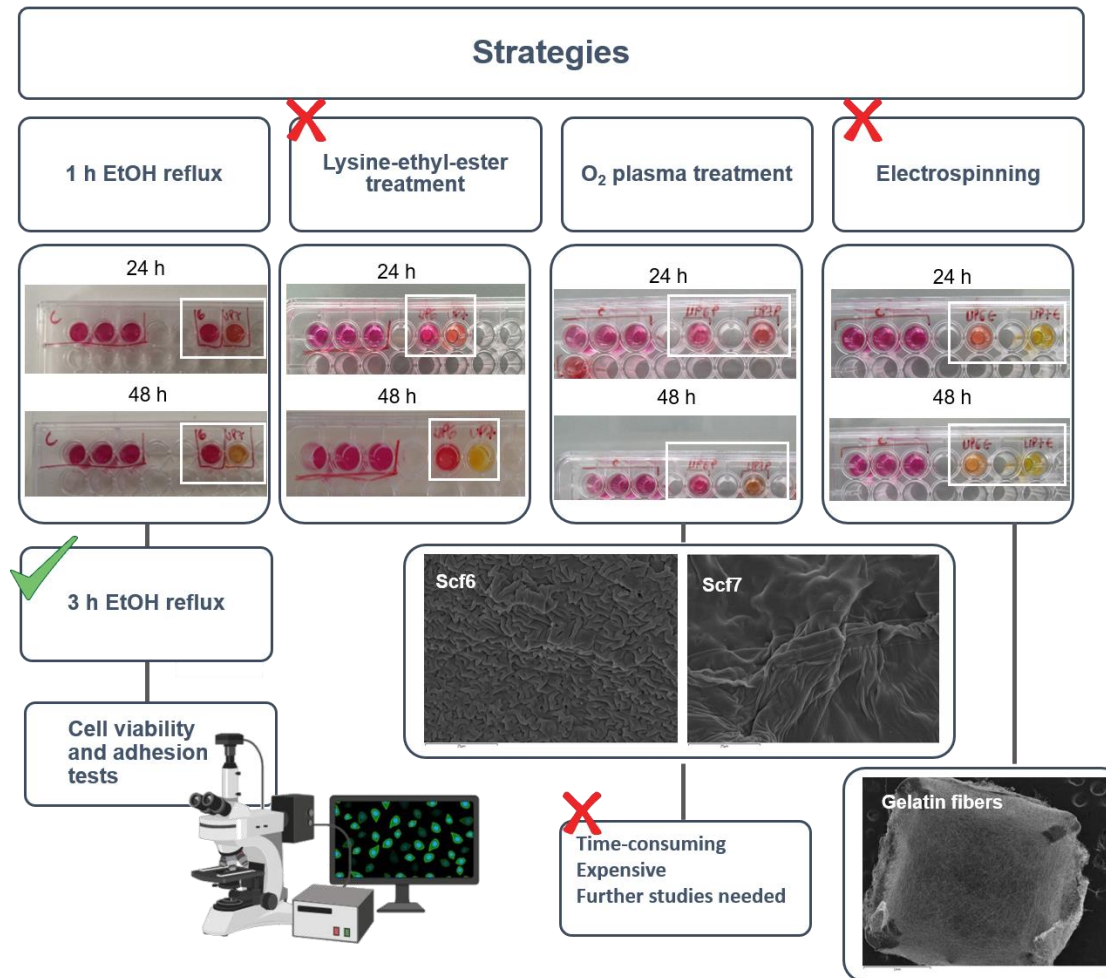


Figure 7. Screening of Scf6 and Scf7 and respective changes on pH medium after O₂ plasma treatment after **A.** 24 h and **B.** 48 h.

After 24 h no significant changes in the pH was detected, however, after 48 h it is clear the low pH of the Scf7. Still, O₂ plasma treatment with posterior grafting with St, seems to offer the most promising results since after 24 h only a slight variation on pH of the cellular medium was observed. However, after 48 h, and like the other applied treatments, a significant change in the pH was detected. This can be related with the previously discussed autocatalytic effect: assuming the presence of the acidic by-products inside the scaffold matrix, with time, and even with pre-treated surfaces, this phenomenon will persist. The graft density could also be a possible explanation for the observed results, since graft density and type of molecule grafted to the surface dictate the performance of the polymer [44]. Regarding the strategies followed to solve the excess of acidity, some treatments were automatically excluded: L-lysine-ethyl-ester and electrospinning of gelatin type B have shown no improvements thus no optimization of the conditions were attempted. On the other hand, and considering time, costs, and outcome, O₂ plasma is a much time-consuming and expensive process than an EtOH reflux. Both methods proved to be enough until 24 h. As a last resource, the time of reflux was extended to 3 h instead the initial 1 h of treatment, which apparently seemed to solve the acidity issue. Thus, the results strongly suggested that EtOH reflux is the best approach to solve the acidity issue. A summary of the strategies followed are displayed on Scheme 3.



Scheme 3. Schematic representation of the strategies followed for the reduction of acidity of the scaffolds and some preliminary results obtained. These preliminary assays were based on surface modifications by EtOH reflux, O₂ plasma and electrospinning. The modified scaffolds were placed into a 48-well plate with 300 μ L per well of the cell culture medium and their acidity was visually evaluated at 24 h and 48 h by change of cell culture medium color. Scanning electron micrographs of some of the modification used are also displayed.

4.3 Cell assays

The cell viabilities and cell adhesion of the selected scaffolds were analyzed. The scaffolds were pre-treated with ethanol, in a reflux system, for 3 h, since this treatment showed to be the most effective procedure to eliminate the high acidity of the scaffolds. The obtained results are displayed in Figure 8.

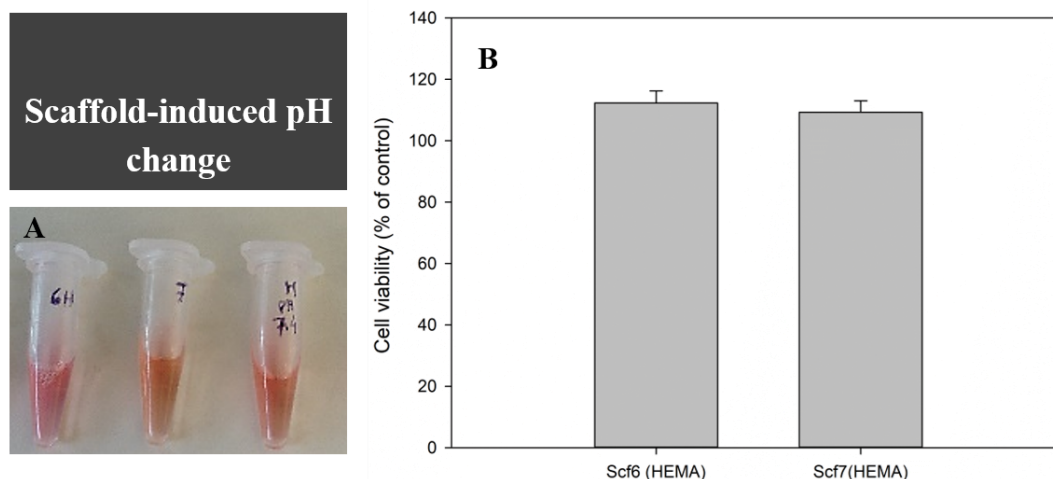


Figure 8. **A.** Differences in the cell culture medium colour after 24 h of incubation with different scaffolds. **B.** Effect of different 3D scaffolds on 3T3-L1 cell viability. The data are expressed as percentage of cell viability with respect to the control corresponding to untreated cells (mean \pm SD, obtained from triplicates). The results are representative of at least three independent experiments. The statistical analysis (one-way ANOVA) indicates that there is not a significant difference between the different conditions.

According to Figure 8, the results suggested that the scaffolds prepared by μ STLG and treated by reflux in EtOH did not decreased cell viability after 48 h, presenting values of 100%. Therefore, we can assume that the reflux treatment was effective. The pH medium of the materials was monitored during the experiment (Figure 8A). The cell adhesion of these scaffolds was also evaluated by microscopy analysis. At this point, some problems arose. First, scaffolds presented some opacity. Second, polymer adsorbed the fluorescent probes tested (Hoechst 333258 and propidium iodide). And third, scaffolds themselves showed some fluorescence for red and blue light. To overcome these problems, 3T3-L1 cells constitutively expressing the green fluorescence protein (GFP) to evaluate the adhesion to the scaffolds were used. The images recorded are displayed in Figure 9.

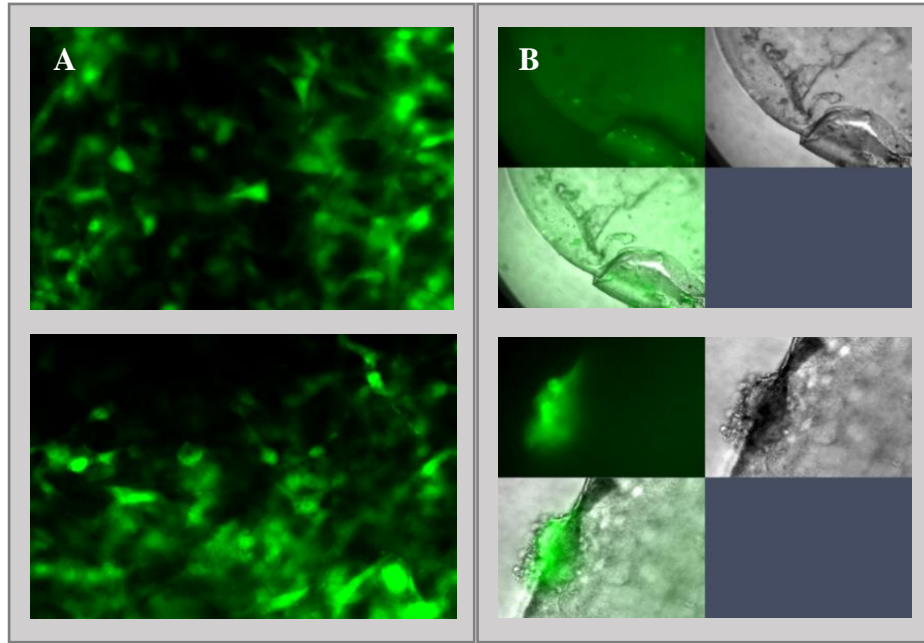


Figure 9. Photo activated localization microscopy images of 3T3-L1 cells on the top of the scaffolds. Cells in absence of any material were used as control (A) and cell adhesion was detected on Scf6 (HEMA) surface (B). Images were captured by microscopy PALM MicroBeam equipment (Zeiss, Göttingen, Germany) with LD Plan-Neofluar 40x/0.6 Korr objective at excitation wavelength of 395 nm for GFP (green).

According to Figure 9, cell adhesion on Scf6 surface was observed. For Scf7, due to its opaque and denser nature it was not possible a proper visualization. By the contrary, Scf6 showed strong evidence of cell adhesion, where a predisposition for the edges of the polymeric material was detected. Nevertheless, some cells at the centre of the scaffolds were also observed though isolated. A great number of cells was observed, indicating that Scf6 (HEMA) supported cell adhesion.

To evaluate the success of the EtOH reflux, thermal crosslinked UPR6/HEMA was also treated, and cell adhesion was observed (Figure S3). UPR6/HEMA showed to be non-toxic to the cells after the EtOH treatment, with high cell viability (116.70%±19.48) after 48 h. Fibroblast cells showed tendency to adhere to the edges of the thermal crosslinked polymers, forming an interconnecting network on these specific sites. Though some cells were observed at the centre of the UPR6, in most cases cells were isolated and disperse in the polymer surface. Overall, these results strongly suggest the viability of the synthesized materials in TE applications.

5. Conclusions

The high potential of the UPs for AM was in jeopardy due to the high levels of acidity. Oxygen plasma treatment, EtOH reflux, among others, were therefore used to overcome such problems and the surface modification of the 3D scaffolds was investigated. Although O₂ plasma treatment and posterior St grafting showed surprising results – SEM results indicate that the scaffolds surfaces were successfully modified –, it was not enough to eliminate the surface acidity; besides it is clearly an expensive and time-consuming technique. On the other hand, by increasing the time of EtOH reflux the problem of acidity was able to be solved, which is patent in the cytotoxicity results and cell adhesion tests. The results suggested that after treated, the scaffolds can be good substrates for cell adhesion also presenting cell viabilities of 100% after 48 h.

6. References

1. Place, E.S., et al., *Synthetic polymer scaffolds for tissue engineering*. Chemical Society Reviews, 2009. **38**(4): p. 1139-1151.
2. Goddard, J.M. and J.H. Hotchkiss, *Polymer surface modification for the attachment of bioactive compounds*. Progress in Polymer Science, 2007. **32**(7): p. 698-725.
3. Liu, X.H. and P.X. Ma, *Polymeric scaffolds for bone tissue engineering*. Annals of Biomedical Engineering, 2004. **32**(3): p. 477-486.
4. Jiao, Y.-P. and F.-Z. Cui, *Surface modification of polyester biomaterials for tissue engineering*. Biomedical Materials, 2007. **2**(4): p. R24-R37.
5. Williams, C.K., *Synthesis of functionalized biodegradable polyesters*. Chemical Society Reviews, 2007. **36**(10): p. 1573-1580.
6. Bikiaris, D., V. Karavelidis, and E. Karavas, *Novel Biodegradable Polyesters. Synthesis and Application as Drug Carriers for the Preparation of Raloxifene HCl Loaded Nanoparticles*. Molecules, 2009. **14**(7): p. 2410-2430.
7. Chu, P.K., et al., *Plasma-surface modification of biomaterials*. Materials Science and Engineering: R: Reports, 2002. **36**(5–6): p. 143-206.
8. Yoshida, S., et al., *Surface modification of polymers by plasma treatments for the enhancement of biocompatibility and controlled drug release*. Surface and Coatings Technology, 2013. **233**: p. 99-107.
9. Vesel, A., et al., *Surface modification of polyester by oxygen- and nitrogen-plasma treatment*. Surface and Interface Analysis, 2008. **40**(11): p. 1444-1453.
10. Sill, T.J. and H.A. von Recum, *Electrospinning: Applications in drug delivery and tissue engineering*. Biomaterials, 2008. **29**(13): p. 1989-2006.
11. Schiffman, J.D. and C.L. Schauer, *A Review: Electrospinning of Biopolymer Nanofibers and their Applications*. Polymer Reviews, 2008. **48**(2): p. 317-352.

12. Velema, J. and D. Kaplan, *Biopolymer-Based Biomaterials as Scaffolds for Tissue Engineering*, in *Tissue Engineering I*, K. Lee and D. Kaplan, Editors. 2006, Springer Berlin Heidelberg. p. 187-238.
13. *Gelatin-Based Biomaterials For Tissue Engineering And Stem Cell Bioengineering*, in *Biomaterials from Nature for Advanced Devices and Therapies*. 2016. p. 37-62.
14. Mari, C.E., et al., *Gelatin as Biomaterial for Tissue Engineering*. Current Pharmaceutical Design, 2017. **23**(24): p. 3567-3584.
15. Ranganathan, S., K. Balagangadharan, and N. Selvamurugan, *Chitosan and gelatin-based electrospun fibers for bone tissue engineering*. International Journal of Biological Macromolecules, 2019. **133**: p. 354-364.
16. Tytgat, L., et al., *Additive manufacturing of photo-crosslinked gelatin scaffolds for adipose tissue engineering*. Acta Biomaterialia, 2019. **94**: p. 340-350.
17. Gonçalves, F.A.M.M., et al., *3D printing of new biobased unsaturated polyesters by microstereo-thermal-lithography*. Biofabrication, 2014. **6**(3): p. 035024.
18. Bartolo, P.J. and G. Mitchell, *Stereo-thermal-lithography: a new principle for rapid prototyping*. Rapid Prototyping Journal, 2003. **9**(3): p. 150-156.
19. Pereira, R.F.B., Paulo J. , *Recent Advances in Additive Biomanufacturing*, in *Comprehensive Materials Processing*, M.S.J. Hashmi, Editor. 2014, Elsevier. p. 265-284.
20. Natu, M.V., H.C. de Sousa, and M.H. Gil, *Effects of drug solubility, state and loading on controlled release in bicomponent electrospun fibers*. International Journal of Pharmaceutics, 2010. **397**(1-2): p. 50-58.
21. Organization, I.S., *Biological evaluation of medical devices. , in Part 5. Tests for cytotoxicity: In vitro methods*. 2009, AAMI: Geneva, Switzerland. p. 50.
22. Faneca, H., A. Faustino, and M.C. Pedroso de Lima, *Synergistic antitumoral effect of vinblastine and HSV-Tk/GCV gene therapy mediated by albumin-associated cationic liposomes*. Journal of Controlled Release, 2008. **126**(2): p. 175-184.
23. Fernández-Carballido, A., et al., *PLGA/PEG-derivative polymeric matrix for drug delivery system applications: Characterization and cell viability studies*. International Journal of Pharmaceutics, 2008. **352**(1): p. 50-57.
24. Assem, Y., et al., *Synthesis of aliphatic biodegradable polyesters nanoparticles as drug carrier for cancer treatment*. Vol. 6. 2016. 032-041.
25. Woodard, L.N. and M.A. Grunlan, *Hydrolytic Degradation and Erosion of Polyester Biomaterials*. ACS Macro Lett, 2018. **7**(8): p. 976-982.
26. Pitt, C.G., et al., *Aliphatic polyesters. I. The degradation of poly(ϵ -caprolactone) in vivo*. Journal of Applied Polymer Science, 1981. **26**(11): p. 3779-3787.
27. Weir, N.A., et al., *Degradation of poly-L-lactide: Part 1: in vitro and in vivo physiological temperature degradation*. Proceedings of the Institution of Mechanical Engineers Part H- Journal of Engineering in Medicine, 2004. **218**(H5): p. 307-319.
28. Li, S., *Hydrolytic degradation characteristics of aliphatic polyesters derived from lactic and glycolic acids*. Journal of Biomedical Materials Research, 1999. **48**(3): p. 342-353.

29. Bu, Y., et al., *Surface Modification of Aliphatic Polyester to Enhance Biocompatibility*. *Frontiers in Bioengineering and Biotechnology*, 2019. **7**: p. 98.
30. Choi, D.J., et al., *Effect of cross-linking on the dimensional stability and biocompatibility of a tailored 3D-bioprinted gelatin scaffold*. *International Journal of Biological Macromolecules*, 2019. **135**: p. 659-667.
31. Soares, R.M.D., et al., *Electrospinning and electrospray of bio-based and natural polymers for biomaterials development*. *Materials Science and Engineering: C*, 2018. **92**: p. 969-982.
32. Akilbekova, D., et al., *Biocompatible scaffolds based on natural polymers for regenerative medicine*. *International Journal of Biological Macromolecules*, 2018. **114**: p. 324-333.
33. Meireles, A.B., et al., *Trends in polymeric electrospun fibers and their use as oral biomaterials*. *Experimental Biology and Medicine*, 2018. **243**(8): p. 665-676.
34. Li, J., et al., *Electrospinning of Hyaluronic Acid (HA) and HA/Gelatin Blends*. *Macromolecular Rapid Communications*, 2006. **27**(2): p. 114-120.
35. Huang, Z.-M., et al., *Electrospinning and mechanical characterization of gelatin nanofibers*. *Polymer*, 2004. **45**(15): p. 5361-5368.
36. Ghasemi-Mobarakeh, L., et al., *Electrospun poly(ϵ -caprolactone)/gelatin nanofibrous scaffolds for nerve tissue engineering*. *Biomaterials*, 2008. **29**(34): p. 4532-4539.
37. Zhang, Y., et al., *Electrospinning of gelatin fibers and gelatin/PCL composite fibrous scaffolds*. *Journal of Biomedical Materials Research Part B: Applied Biomaterials*, 2005. **72B**(1): p. 156-165.
38. Hoque, M.E., et al., *Gelatin Based Scaffolds For Tissue Engineering – A review*. *Polymers Research Journal*, 2015. **9**: p. 15-32.
39. Boccafoschi, F., et al., *Biological Grafts: Surgical Use and Vascular Tissue Engineering Options for Peripheral Vascular Implants*, in *Encyclopedia of Biomedical Engineering*, R. Narayan, Editor. 2019, Elsevier: Oxford. p. 310-321.
40. Bello, A.B., et al., *Engineering and Functionalization of Gelatin Biomaterials: From Cell Culture to Medical Applications*. *Tissue Engineering Part B: Reviews*, 2020. **26**(2): p. 164-180.
41. Luo, Y. and G.D. Prestwich, *Synthesis and Selective Cytotoxicity of a Hyaluronic Acid–Antitumor Bioconjugate*. *Bioconjugate Chemistry*, 1999. **10**(5): p. 755-763.
42. Um, I.C., et al., *Electro-Spinning and Electro-Blowing of Hyaluronic Acid*. *Biomacromolecules*, 2004. **5**(4): p. 1428-1436.
43. Wan, Y., et al., *Characterization of surface property of poly(lactide-co-glycolide) after oxygen plasma treatment*. *Biomaterials*, 2004. **25**(19): p. 4777-4783.
44. Gupta, B., et al., *Plasma-induced graft polymerization of acrylic acid onto poly(ethylene terephthalate) films: characterization and human smooth muscle cell growth on grafted films*. *Biomaterials*, 2002. **23**(3): p. 863-871.

Supplementary Information

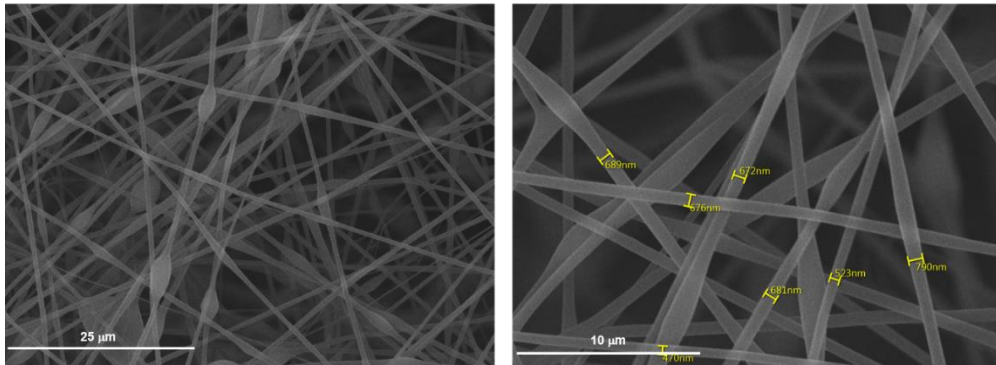


Figure S1. Scanning electron micrographs of the 3D scaffolds, with electrospun fibers of gelatin type B (7.5% w/v, TFE) at the surface. The magnifications used with gelatin B were 2000x and 5000x.

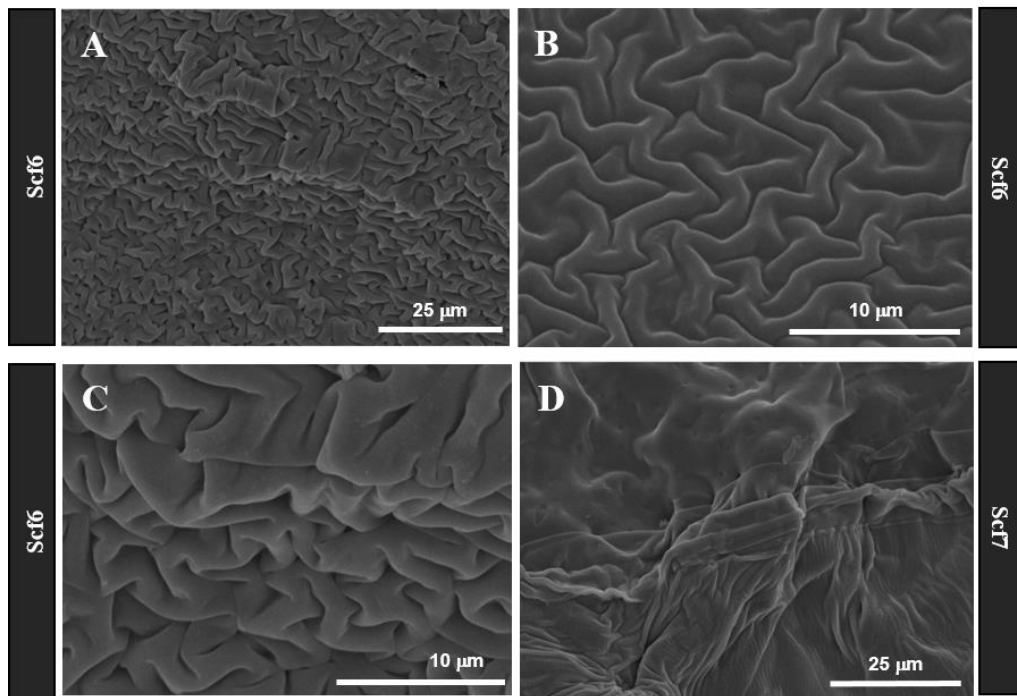


Figure S2. Scanning electron micrographs for the processed Scf6 and Scf7 after modification by O_2 plasma and posterior grafting with St (magnifications of 1500x (A), 5000x (B) and 15000x (C, D) for treated Scf6 and Scf.

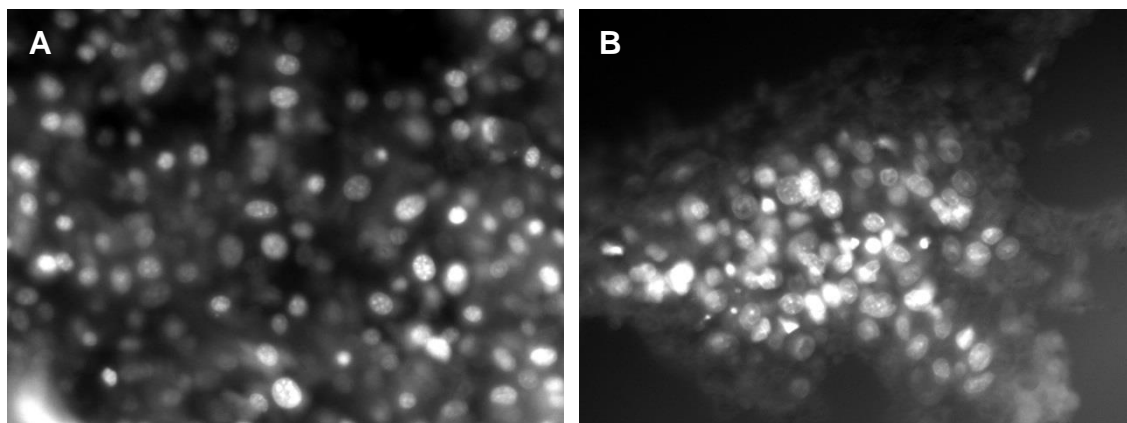


Figure S3. Fluorescence microscopy images of 3T3-L1 fibroblast cells on the biobased UPR6 (HEMA) discs (**B**) by fluorescence microscopy. Cells in absence of any material were used as control (**A**). Cell nuclei were stained by Hoechst 333258. Control cells were seeded directly to the well. Images were captured by microscopy PALM MicroBeam equipment (Zeiss, Göttingen, Germany) with LD Plan-Neofluar 40x/0.6 Korr objective at excitation wavelength of 445 nm for Hoechst (blue).

CHAPTER VI

Concluding Remarks

1. CONCLUSIONS.....	177
2. FURTHER RESEARCH.....	179

1. Conclusions

The development of biobased unsaturated polyesters for tissue engineering application was the goal of this thesis, since these polymers contributed for a remarkable advance in the biomedical fields. These polymers, if presenting a biocompatible character and proper properties, can be a suitable alternative to the toxic polymers commonly used for the fabrication of three-dimensional scaffolds by stereolithographic techniques.

An extensive study on unsaturated polyesters synthesis *via* bulk polycondensation was carried out in the scope of this work. The selection of proper renewable monomers and the ratios between the diacids and glycols for UPs formulations played a key role in terms of the final properties of the polyesters. The resulting oligomers were fully characterized to understand and tailor the properties of the UPs for TE application. In this context, the biobased UPs were tested in the μ STLG equipment resulting in 3D scaffolds with controlled geometry. *In vitro* cytotoxicity tests of the scaffolds were carried out with 3T3-L1 cells confirming the biocompatible character of the scaffolds, even when photocrosslinked with a toxic monomer such as styrene. This was the evidence that these bio polyesters can be used as supporting materials to build complex 3D structures by micro-stereolithography. The present study also constitutes one of the few reports of bio UPs synthesized specifically for AM technologies.

The developed UPs allow to produce biobased resins by additive manufacturing technologies. But at this stage the diluent selected to reduce the viscosity and promote the crosslinking reaction is crucial. The crosslinking studies for the biobased UPs, which aim to understand the behaviour of the final resins and to find suitable monomers for μ STLG, have been carried out. The overall results suggested that there are significant differences between the thermal and the photo crosslinked polymers concerning the final properties. Thermal crosslinked UPs showed high gel content values, with the highest contact angle values of 80° , with a strong tendency to decrease along time. According with the morphological, thermal and mechanical results, the UPRs revealed great possibilities for TE application – the cured polymers presented enough roughness and flexibility for cell attachment, which was demonstrated by the cell adhesion observed on the edges of the polymers.

One of the main problems concerning the step-growth polymerization method employed was the fact that it was time consuming, mainly to the fact that no solvents or catalyst were added to the reaction system. Although the number of reaction parameters decreased, it also contributed to

longer reaction times, at least of 14 h. New formulations were developed with emphasis in new renewable sources, such as glutaric acid and isosorbide, where the number of monomers on the formulations decreased. The resulting outcome of this strategy was: a) polycondensation reaction approximately of 8 hours, for formulations UP7 and UP8; b) final reaction temperatures of 190 °C; c) same possibility of tuning the final properties of UPs by playing with the ratios of the monomers; d) more flexible polymers, one of the pre-requisites for μ STLG. A better understanding of the importance of the type monomers incorporated on the formulation was highlighted. The UPs were, as expected, suitable for the stereolithographic technology. Importantly, these flexible polyesters can be easily applied on several other applications besides AM techniques.

With the development of these bio polyesters, problems related with their application in TE were detected. Surface acidity was one of the main restrictions detected during the development of this work. The identified problem is very similar to those found in polymers with application in biomedical fields, however, pre-treatment at the surface of the UPRs is not an explored area. By the contrary, this work is one of the first reports of the problems that can arise after the scaffold's fabrication, using bio UPs as the starting materials. Independently of the type of crosslinking method used to prepare the resins, the acidity of the resulting polymers was severely high, reducing the changes of cell viability. The surface treatment or surface modification was a potential solution that was tested. Reflux with ethanol, surface modification by oxygen plasma or even the use of electrospinning to "trick" cells response were some of the methods employed at this stage. Although the surface modification of the scaffolds by O₂ plasma was confirmed by SEM, the most effective method to remove the acidity was a much simpler method, such as EtOH reflux. At the end, the treated scaffolds presented cell viabilities close to 100% and cell adhesion. In this context, there is no doubt that this type of polymers can effectively be used as supporting materials for cells in TE applications.

The main achievements and conclusions of this research study can be summarized as follows:

1. Biobased aliphatic unsaturated polyesters were successfully synthesized by bulk polycondensation, leading to polymers presenting high thermal stability and low glass transition temperatures. This polycondensation method led to polymers with low molecular weights therefore with suitable viscosities for application on μ STLG. This was confirmed by the fabrication of 3D scaffolds with accurate geometries and complex micro-architectures. Also, the properties of the materials can be tuned by changing the type and

ratio of monomers used and properties such as polymer flexibility and viscosity can be easily controlled.

2. UPRs were also prepared using biocompatible monomers, such as HEMA. The biobased UPs developed in this work, with no exception, were suitable for μ STLG. This was possible by combining a simple method of synthesis such as bulk polycondensation, with the proper choice of renewable monomers and diluents. The results revealed that by fine tuning the properties of the UPRs, the materials can be used in different applications, specifically in biomedical fields. The adhesion of fibroblasts on the UPRs surfaces confirmed these suppositions.
3. Hardly these polymers can be processable without any pre-treatments. In all the developed formulations, only the sebacic based UP entitled UP6, revealed no need of surface treatment. Therefore, combining AM technologies with surface modification or other type of surface treatments offers a good approach, having as goal the enhancement of scaffolds performance.

2. Further research

Although encouraging, the properties of the synthesized bio UPRs need further investigation concerning the TE application. For that reason, a few tests have to be performed since they will bring a better understanding on the properties of the UPs:

1. Exhaustive study of UPRs degradation, side-by-side with the evaluation of the sub-products toxicity on the biological systems. Although a preliminary study of the hydrolytic degradation of the polyesters was performed, no information about scaffolds degradation was provided in the present work. Also, no evidence of a direct correlation between the starting polyester and the final scaffold properties has yet been established.
2. A full study of the scaffold's characteristics affecting the cell-polymer surface interactions. These includes not only determining the scaffolds porosity, but also an extensive study on the mechanical properties of the UPs, being this one of the major challenges in TE, to mimic the mechanical properties of the ECM.

3. Development of new resins that could add some interesting properties, namely flexibility and mechanical strength, to the final scaffolds. The selection of also renewable unsaturated monomers (vegetable oils such as castor oil, soybean oil and their derivatives such as AESO) or even the modification of known UMs are viable strategies that could enhance biocompatibility and degradability of the 3D scaffolds. The use of other building blocks to prepare new UPs can also be explored.
4. To test the UP formulations having cellular components incorporated into their matrix in the μ STLG equipment. Although challenging, since proper viscosity and cytotoxicity need to be assured, this is one of the major goals envisaging a possible 3D scaffolds product. The incorporation of growth factors that promote cell proliferation, wound healing, or even cellular differentiation will be highly desired. The outcome could be the development of specific scaffolds to treat knee cartilage defects.
5. And finally, *in vivo* assays, to confirm the biocompatibility of the 3D scaffolds produced.

